To the Graduate Council:

I am submitting herewith a dissertation written by Kenneth Nathan Price entitled "Synthetic and Structural Studies on Carbohydrate-Derived Cardioprotective and Anticancer Compounds." I have examined this dissertation for form and content and recommend that it be accepted in partial fulfillment of the requirements for the degree of Doctor of Philosophy, with a major in Chemistry.

David C. Baker

David C. Baker, Major Professor

We have read this dissertation
and recommend its acceptance:

Sir Alexander F.

Georgeta Cabalu

Cynthia B. Peterson

Accepted for the Council:

Carolyn R. Hodges

Associate Vice Chancellor and
Dean of The Graduate School

SYNTHETIC AND STRUCTURAL STUDIES ON CARBOHYDRATE-DERIVED CARDIOPROTECTIVE AND ANTICANCER AGENTS

A Dissertation
Presented for the
Doctor of Philosophy
Degree
The University of Tennessee, Knoxville

Kenneth Nathan Price
August 1997

DEDICATION

This dissertation is dedicated to my parents

Mr. Lester K. Price

and

Mrs. Sara S. Price

for their consistent and unconditional support.

ACKNOWLEDGENTS

First and foremost, I wish to thank my research advisor, Professor David C. Baker, for his invaluable intellectual guidance and support. His consistently high standards, attention to detail, and uncanny ability to cut to the heart of the matter — evident not only in numerous instances of late-night brainstorming on chemistry and project direction, but also during the many occasions of working together on grant proposals and publications, and while traveling together to national and international scientific conferences—have afforded me a rich set of experiences to draw from in my future scientific and personal endeavors. In addition, his unique sense of humor, penetrating insights into numerous day-to-day matters, and creative use of both written and spoken language, made my time in his research group constantly interesting and enjoyable. I also wish to express my gratitude for his first taking a chance on me in 1992 by accepting me for an undergraduate summer research project, and for subsequently going to bat for me the following fall as I sought to begin graduate study in chemistry at UTK.

Among the many past and present members of the Baker research group, I would like to single out the following two people: Sam Victory, for recruiting me into the group and patiently helping me in my first synthetic efforts; and Prashant Deshpande, for providing invaluable guidance in the form of pointers for more efficient bench chemistry, and for bringing me onto the hongconin project. In addition, I would like to thank Steve Johnson, Neil Whittemore, Shijia Yan, and Frank Tagliaferri for their help and friendship

in and out of the lab. Specific thanks also go to the following undergraduates I had the privilege of having as assistants, and who helped synthesize monosaccharide intermediates for me: Sarah Clough, Jonathan Gridley, Mike Peddicord, Ted Davis, and Janet Effler. Elsewhere in the Department of Chemistry at UTK, I wish to thank especially Professor Donald C. Kleinfelter, whose excellent teaching of General and Organic Chemistry sparked my initial interest in chemistry. For external financial support, I am also grateful to the National Science Foundation for a 3-year Pre-Doctoral Fellowship, and to the Hoechst–Celanese Corporation for a $5,000 achievement award.

Finally, although there are too many to mention here, I wish to thank the following friends and family for their personal encouragement, support, and patience: Rick Toerner, Edith Suda, and Les and Sara Price.

ABSTRACT

This dissertation describes synthetic and analytical studies in two areas of carbohydrate chemistry and biochemistry: (1) the use of carbohydrate synthons in the synthesis of the natural product hongconin, and (2) the development of hyaluronic acid oligosaccharides as probes for cancer metastasis.

The natural product hongconin is an isochromanquinoid with demonstrated cardioprotective properties. Described here is a concise methodology for the first enantioselective synthesis of this compound (and analogs) starting from a simple carbohydrate derivative. The novel synthetic strategy represents a significant simplification in synthesizing optically pure isochromanquinoids, and would allow numerous other natural products with similar chemical structures to be conveniently synthesized in an analogous fashion.

A recently discovered process which appears to play a critical role in the metastasis of melanoma cells to the lungs is the binding of the cancer cell's CD44 receptor to hyaluronic acid, a polysaccharide that is synthesized in the plasma membrane and is associated with the host cell's extracellular matrix. The central hypothesis of this study is that metastasis might be prevented by introducing relatively small HA-oligosaccharides that would function as CD44 "metastasis receptor" antagonists. Support for this hypothesis was found in first-generation experiments using enzyme digestion-derived HA oligosaccharides: these compounds were found to virtually prevent the metastasis of B16F10 melanoma cells to the lungs in a murine model. Also described

here is the development of two analytical protocols to characterize these oligosaccharides, namely high-performance anion-exchange chromatography with pulsed amperometric detection and electrospray–ionization mass spectrometry. The utility of the developed methods was highlighted in the discernment of previously unobserved odd-numbered oligosaccharides in the digestion mixtures. Finally, S- and C-linked oligosaccharide intermediates were synthesized with the aim of developing HA mimics with improved *in vivo* stability.

TABLE OF CONTENTS

PART ONE: THE USE OF CHIRAL CARBOHYDRATE SYNTHONS IN THE ENANTIOSELECTIVE SYNTHESIS OF NATURAL PRODUCTS

A Concise, Enantioselective Synthesis of (−)- and (+)-Hongconin

I. Introduction 2
II. Statement of the problem 9
A. Objectives 9
B. Research plan—retrosynthetic analysis 9
C. Significance 15
III. Results and discussion 16
A. Selection of starting materials 16
B. Synthesis of *ent*- and *epi*-hongconin 17
C. Synthesis of (−)-hongconin 20
IV. Conclusions 27
V. Experimental section 28

PART TWO: ANTI-METASTATIC OLIGOSACCHARIDES FROM HYALURONIC ACID

Molecular Probes of Cancer Metastasis—Background, Rationale, Overall Project Design, and Preliminary Biological Evaluations

I. Introduction 37
A. Entry point 39
B. Biological background 38
1. Traditional chemotherapy approaches 38
2. Metastasis 40
3. The HA-CD44 metastatic interaction 40
4. CD44 isoform variability 44
5. Anti-metastasis therapy 47
II. Statement of the problem 48
A. Hypothesis 48
B. Formulation of research questions and project goals 50
1. Biological feasibility 52
2. Chemical structure 53
3. Drug development 55
C. Significance of the proposed studies 55
1. With respect to biomedical science 56

2. With respect to analytical and synthetic oligosaccharide chemistry 59
III. Biological evaluation of hyaluronan oligosaccharides as metastasis inhibitors 61
A. Preliminary considerations 61
1. Potential CD44 and HA side reactions 61
2. Selection of appropriate biological test 64
B. Results and discussion 66
C. Conclusions 70
D. Experimental section 71
1. *In vivo* metastasis model 71
2. Description and justification of the use of animals 71
3. Limiting discomfort and distress 72

Isolation and Characterization of Hyaluronan Oligosaccharides Derived from Digestion with Hyaluronate Lyase and Bovine Testes Hyaluronidase

I. Introduction 73
A. Enzyme digestion-derived HA oligosaccharides 73
B. Electrospray–ionization mass spectrometry 77
C. High-performance anion exchange chromatography 79
II. Statement of the problem 84
A. Objectives 84
B. Research plan 84
C. Significance 85
III. Results and discussion 87
A. Oligosaccharides from HA lyase digestion 87
1. Unexpected oligosaccharides obtained 87
2. Electrospray–ionization mass spectrometry 89
3. High-performance anion-exchange chromatography 97
B. Oligosaccharides from bovine testes hyaluronidase 103
1. Unexpected oligosaccharides obtained 104
2. Electrospray–ionization mass spectrometry 104
3. High-performance anion-exchange chromatography 120
4. Enzyme purity 120
IV. Conclusions 125
V. Experimental Section 128
A. Materials 128
B. Enzyme degradations and preparative column chromatography . . 128
C. High-performance anion-exchange chromatography 129
D. Electrospray–ionization mass spectrometry 130
E. Polyacrylamide gel electrophoresis 131

Chemical Synthesis of Hydrolase-Resistant Hyaluronan Mimics

I. Introduction 132
A. Laboratory probes vs. drug candidates 132
B. Design of hydrolase-resistant HA mimics 133
II. Statement of the problem 139
A. Objectives 139
B. Research plan—retrosynthetic analysis 139
1. Iterative blockwise synthesis 139
2. Synthesis of *S*-disaccharides 140
3. Synthesis of *C*-disaccharides 144
C. Significance 150
III. Results and discussion 153
A. Progress in the synthesis of S-linked oligosaccharides 153
1. Introduction 153
2. Synthesis of an *S*-disaccharide via modified Schmidt chemistry 154
3. Developing a viable protecting group array 164
B. Progress in the synthesis of C-disaccharides 173
1. Attempted synthesis using 4-keto sugars 173
2. Synthesis of a "*C*-disaccharide acceptor" using S_N2 chemistry 175
IV. Conclusions 179
V. Experimental section 180
A. General methods 180
B. Preparation of compounds **37-82** 181

REFERENCES

A Concise, Enantioselective Synthesis of (−)- and (+)-Hongconin 214
Molecular Probes of Cancer Metastasis—Background, Rationale, Overall Project Design, and Preliminary Biological Evaluations 216
Isolation and Characterization of Hyaluronan Oligosaccharides Derived from Digestion with Hyaluronate Lyase and Bovine Testes Hyaluronidase 222
Chemical Synthesis of Hydrolase-Resistant Hyaluronan Mimics 227

APPENDICES

Appendix A. ^{1}H and ^{13}C NMR Spectra of Compounds Involved in the Synthesis of Hongonin and Analogs 232
Appendix B. Negative-ion mode ESIMS spectra and HPAEC traces for selected HA Lyase-derived Oligosaccharides 246

Appendix C. Negative-ion Mode ESIMS Data for BTH-Derived Oligosaccharides dp 4-28 255
Appendix D. ^{1}H and ^{13}C NMR Spectra of Intermediates Involved in the Synthesis of *S*-and *C*-oligosaccharides 274

VITA 310

LIST OF FIGURES

A Concise, Enantioselective Synthesis of (−)- and (+)-Hongconin

Figure 1. The eleutheroids 5

Molecular Probes of Cancer Metastasis—Background, Rationale, Overall Project Design, and Preliminary Biological Evaluations

Figure 1. Interactions between adhesion molecules mediate cancer metastasis 41
Figure 2. Hyaluronic acid 42
Figure 3. The CD44 receptor protein 43
Figure 4. Current model of HA/CD44-mediated cancer metastasis 49
Figure 5. Hypothetical inhibition of metastasis via CD44 receptor antagonism 51
Figure 6. B16F10 Melanoma metastasis model 67
Figure 7. Excised mouse lungs showing inhibition of B16F10 melanoma metastasis by HA oligosaccharides 69

Isolation and Characterization of Hyaluronan Oligosaccharides Derived from Digestion with Hyaluronate Lyase and Bovine Testes Hyaluronidase

Figure 1. HA fragment oligosaccharides derived from enzyme digestion 74
Figure 2. Generation of ions via Electrospray Process 78
Figure 3. Triple-pulse sequence of PAD 82
Figure 4. Gel permeation chromatogram of hyaluronate lyase digest 88
Figure 5. Negative-ion electrospray mass spectrum (A) and MAX ENT-generated MW distribution (B) for 13-mer 94
Figure 6. Negative-ion electrospray mass spectrum (A) and MAX ENT-generated MW distribution (B) for 14-mer. 95
Figure 7. Observed relative intensities of the different charge states of HA lyase-derived oligosaccharides in negative-ion mode ESIMS. . . 96
Figure 8. HPAEC chromatograms for HA oligosaccharides 102
Figure 9. Negative-ion electrospray mass spectrum for 28mer-containing fraction. 105
Figure 10. MAX ENT-generated MW distribution for 28mer-containing fraction. 106
Figure 11. Relative intensities of observed charge states for BTH-derived HA oligosaccharides at CV = 25 V vs. 55-65 V 113

Figure 12. Sodiated trianions of 18-mer (A) and sodiated tetraanions of 28-mer (B). 115
Figure 13. Sodiated trianions of 20-mer. 116
Figure 14. Effect of cone voltage on charge state and signal intensity for 20-, 24- and 28-mer. 119
Figure 15. Polyacrylamide gel electrophoresis of BTH 123

Chemical Synthesis of Hydrolase-Resistant Hyaluronan Mimics

Figure 1. Oligosaccharide structural modifications conferring hydrolase stability. 134
Figure 2. Literature examples of synthesized hydrolase-resistant oligosaccharides. 135
Figure 3. TOCSY ^{1}H NMR spectrum of **55a**. 163
Figure 4. Positive-ion mode ESIMS spectra of **16** and **65**. 165

LIST OF SCHEMES

A Concise, Enantioselective Synthesis of (−)- and (+)-Hongconin

Scheme 1. Importation of carbohydrate center absolute configurations into the C-ring of the isochromanquinoid nucleus. 5
Scheme 2. Postulated biochemical mechanism of action for isochromanquinoids 7
Scheme 3. Synthesis of racemic hongconin by Kraus and co-workers 10
Scheme 4. Synthesis of optically pure isochromanquinone intermediates by Swenton and co-workers 12
Scheme 5. Synthesis of kalafungin and nanaomycin by Tatsuta and co-workers 13
Scheme 6. Proposed retrosynthesis of hongconin (and stereoisomers) 14
Scheme 7. Synthesis of Micheal donors **9a** and **9b** 17
Scheme 8. Synthesis of *ent*-hongconin (**1a**) and 3-*epi*-hongconin (**1b**) 19
Scheme 9. Attempted synthesis of hongconin via epimerization of 3-*epi*-hongconin 21
Scheme 10. Improving the *trans*-stereoselectivity of C-glycosylation 22
Scheme 11. Synthesis of hongconin (**1**) via Michael donor **9c** 24
Scheme 12. Alternative reaction pathways in phthalide annulation reaction 26

Isolation and Characterization of Hyaluronan Oligosaccharides Derived from Digestion with Hyaluronate Lyase and Bovine Testes Hyaluronidase

Scheme 1. Proposed mechanism for sugar oxidation under PAD 82

Chemical Synthesis of Hydrolase-Resistant Hyaluronan Mimics

Scheme 1. Specificities of mammalian hyaluronidases 134
Scheme 2. Candidate hexasaccharide capable of evading mammalian HA-ases 138
Scheme 3. Iterative blockwise synthesis of mixed O-/X- oligomers 141
Scheme 4. Derivation of disaccharide glycosyl donor and acceptor from a common intermediate 142
Scheme 5. Retrosynthetic analysis for *S*-disaccharide **13** 143
Scheme 6. Differential protection requirements for *O*- vs. *S*-oligosaccharide synthesis 145
Scheme 7. Retrosynthetic analysis of *C*-disaccharide **19** 146

Scheme 8. Stereochemical control at C-1' of CH_2-linked disaccharide intermediates 148

Scheme 9. Stereochemical control at C-4 of CH_2-linked disaccharide intermediates 149

Scheme 10. Alternative retrosynthetic analysis of *C*-disaccharide **19** 151

Scheme 11. Synthesis of potential *S*-disaccharide intermediate **15** 155

Scheme 12. Unsuccessful synthesis of *S*-disaccharide via the methodology of Driguez 157

Scheme 13. Revised retrosynthetic analysis for *S*-disaccharide 157

Scheme 14. Synthesis of modified *S*-disaccharide building blocks **45** and **46**. 159

Scheme 15. Synthesis of *S*-disaccharide **16**. 161

Scheme 16. Peripheral Manipulations on *S*-disaccharide **16**. 161

Scheme 17. Synthesis of monosaccharide building blocks for modified *S*-disaccharide **57**. 166

Scheme 18. Synthesis and further manipulations of *S*-disaccharide **57**. 168

Scheme 19. Selection of a new 3-*O*-protecting group for 2-deoxy-2-phthalimido sugars. 170

Scheme 20. Synthesis of diacetate thiol **69a**. 171

Scheme 21. Attempted synthesis of *S*-disaccharide **73** 173

Scheme 22. Attempted Synthesis of β-CH_2NO_2 compound **75b** 174

Scheme 23. Attempted synthesis of 4-branched nitro compound **76** via keto sugar **77**. 174

Scheme 24. Chemistry of nitrile **78**. 176

Scheme 25. Synthesis of *C*-glycoside donors from compound **54** 178

LIST OF TABLES

Isolation and Characterization of Hyaluronan Oligosaccharides Derived from Digestion with Hyaluronate Lyase and Bovine Testes Hyaluronidase

Table 1. Observed vs. predicted ESIMS *m/z* values for HA lyase oligomers 91
Table 2. Literature waveforms used for PAD of carbohydrates.. 98
Table 3. PAD waveform development for HA lyase-derived oligosaccharides. 99
Table 4. HPAEC retention times (min) of HA lyase-derived oligosaccharides 101
Table 5. Observed vs. predicted ESIMS *m/z* values for selected bovine testes hyaluronidase oligomers, dp 4-28 108
Table 6. Cone voltage vs. relative intensity 117
Table 7. HPAEC retention times (min) of BTH-derived oligosaccharides 121

Chemical Synthesis of Hydrolase-Resistant Hyaluronan Mimics

Table 1. Chemical shift (ppm) and coupling constants (Hz) for ring protons of **50**, **51**, and **55a**. 162
Table 2. Development of conditions for synthesis of equatorial nitrile **78**. 177

ABBREVIATIONS AND ACRONYMS

AcOH	Acetic acid
ADMA	Anisaldehyde dimethyl acetal
AIBN	Azobis(isobutyronitrile)
All	Allyl
Bn	Benzyl
BTH	Bovine testes hyaluronidase
CAN	Ammonium cerium(IV) nitrate
ClAc	Chloroacetate
cod	Cyclooctadienyl
CV	Cone voltage
DIBAL-H	Diisobutylaluminum hydride
DBU	1,8-Diazabicyclo[5.4.0]undec-7-ene
DDQ	2,3-Dichloro-5,6-dicyano-1,4-benzoquinone
DEAD	Diethyl azodicarboxylate
DMF	Dimethyl formamide
DMSO	Dimethyl sulfoxide
DP	Degree of polymerization
ECM	Extracellular matrix
EDTA	Ethylenediamine tetraacetate
EI	Electron impact
ESIMS	Electrospray-ionization mass spectrometry
EtOAc	Ethyl acetate
FAB	Fast atom bombardment
HA	Hyaluronic acid
HAL	Hyaluronate lyase
HPAEC	High-performance anion-exchange chromatography
i.v.	Intravenously
LAH	Lithium aluminum hydride
MP	Methoxyphenyl (as a molecular substituent); melting point
MW	Molecular weight
NMR	Nuclear magnetic resonance
NOE	Nuclear Overhauser effect
PAD	Pulsed amperometric detection
PCC	Pyridinium dichromate
PDC	Pyridinium chlorochromate
Phth	Phthalimido
PMBn	*p*-Methoxybenzyl
PPTS	Pyridinium *p*-toluenesulfonate
RDE	Rotating-disc electrode

SAR	Structure–activity relationship
TBDMS	*tert*-Butyldimethylsilyl
Tf	Triflyl (trifluoromethanesulfonyl)
TEA	Triethylamine
TFA	Trifluoroacetic acid
THF	Tetrahydrofuran
TLC	Thin-layer chromatography
TMSOTf	Trimethylsilyl trifluoromethanesulfonate
TOCSY	Totally correlated spectroscopy (also known as HOHAHA)
Tr	Trityl (triphenylmethyl)

PART ONE

THE USE OF CHIRAL CARBOHYDRATE SYNTHONS IN THE ENANTIOSELECTIVE SYNTHESIS OF NATURAL PRODUCTS

A CONCISE, ENANTIOSELECTIVE SYNTHESIS OF (−)- AND (+)-HONGCONIN

I. INTRODUCTION

It is now a well-established fact that chiral pharmaceutical entities are much more desirable than their racemic counterparts. Should the unnecessary enantiomer prove inactive (but devoid of activity altogether), the racemate carries an economic disadvantage in the form of 50 % wasted material. Worse yet, the racemate acquires an additional *pharmacological* disadvantage if the unwanted enantiomer possesses untoward, or even toxic, side effects. Fortunately, synthetic organic chemists have developed many methods to prepare optically pure (or optically enriched) compounds, thus ameliorating such potential problems. These methods include:

- Efficient chiral separation methodologies, such as chiral columns and kinetic resolutions.
- Enantioselective reagents, such as chiral catalysts and chiral auxiliaries.
- Syntheses beginning with or utilizing molecules from the chiral pool.

With respect to the latter class, one need only examine the literature of enantioselective natural product synthesis to understand the important position that carbohydrate starting materials in particular have assumed, with entire monographs having been devoted to the topic.[1] This importance is not surprising, since many natural products, as well as medically desirable synthetic targets, contain implied carbohydrate substructures in their

basic skeletons. Additional advantages accrue from the fact that using a carbohydrate template *automatically* places the synthesis in the 100%-ee category unlike methods involving enantioselective catalysis, enantioselective reagents, and kinetic resolutions with enzymes, which, although greatly improved in recent years, usually yield products with less than 100% ee. Finally, carbohydrates are attractive from an economic vantage point because they are available in large quantities from renewable, organic feedstocks.

The entry-point vision of this project stated in broad terms was thus to develop an efficient, enantioselective synthesis of one or more biologically important molecules using key carbohydrate-derived synthons. In terms of project design, this translated into searching the literature and identifying the "right" target molecule(s). In the interest of balancing both synthetic and medicinal chemistry considerations, our criteria for selecting the target molecule were:

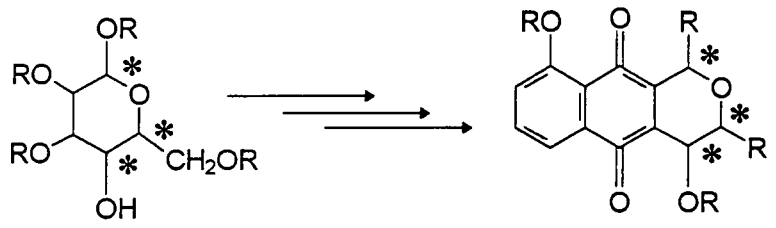
- *Natural Products* — Target compounds should be natural products so that physicochemical data, including optical purity, can be compared to the benchmark data.
- *Established Biological Activity* — The target molecules should have some established biological activity to lend additional value to the material produced and the processes developed.
- *Unexplored Structure–Activity Relationship Information* — Although the compound should have biological activity, it should not already be so well

studied as to make further material and analogs useless; *i.e.*, there should still be unanswered questions that the compounds will help elucidate.

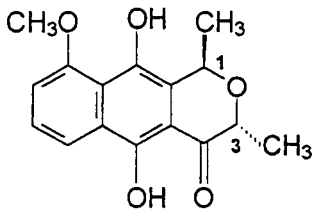
- *Pyranoid Structural Motif* — Perhaps most concretely, we limited our scope to those molecules possessing a specific structural motif: a pyranoid ring with two or more chiral centers.

Based on these constraints, we chose to consider the general class of tricyclic compounds known as the isochromanquinoids. This large class of natural products is represented by such well-established antibiotics and cardioactive agents as the kalafungins and nanaomycins. In addition, their existing syntheses are lengthy (*vide infra*), thus posing an need for further synthetic methodology. In particular, we narrowed our focus to one sub-class of isochromanquinoids: the eleutheroids, which have their historical origin in traditional chinese medicine. The basic strategy we hoped to actualize is shown in Scheme 1, in which the absolute configurations of carbohydrate ring atoms are directly imported into the C-ring of the isochromanquinoid nucleus.

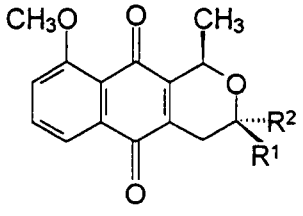
The eleutheroids have a fascinating historical background. The rhizome of the South Chinese herbal plant *Eleutherine americana* Merr. et Heyne (Iridaceae), known as "Hong-Cong" in Chinese, has long been used as a folk remedy for coronary disorders.[2] The eleutheroids, shown in Figure 1, comprise four naphthalene derivatives isolated from the plant's extracts by Chen and co-workers,[3] namely, hongconin (**1**), eleutherine (**2**), isoeleutherine (**3**), and eleutherol (**4**).[4] A formulation containing these four compounds was subsequently demonstrated to increase coronary



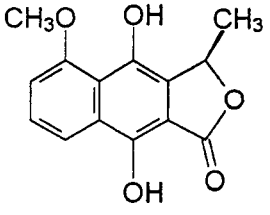
Scheme 1. Importation of carbohydrate center absolute configurations into the C-ring of the isochromanquinoid nucleus.



(-)-Hongconin (**1**)



(+)-Eleutherine (**2**): $R^1 = CH_3$, $R^2 = H$
(-)-Isoeleutherine (**3**): $R^1 = H$, $R^2 = CH_3$

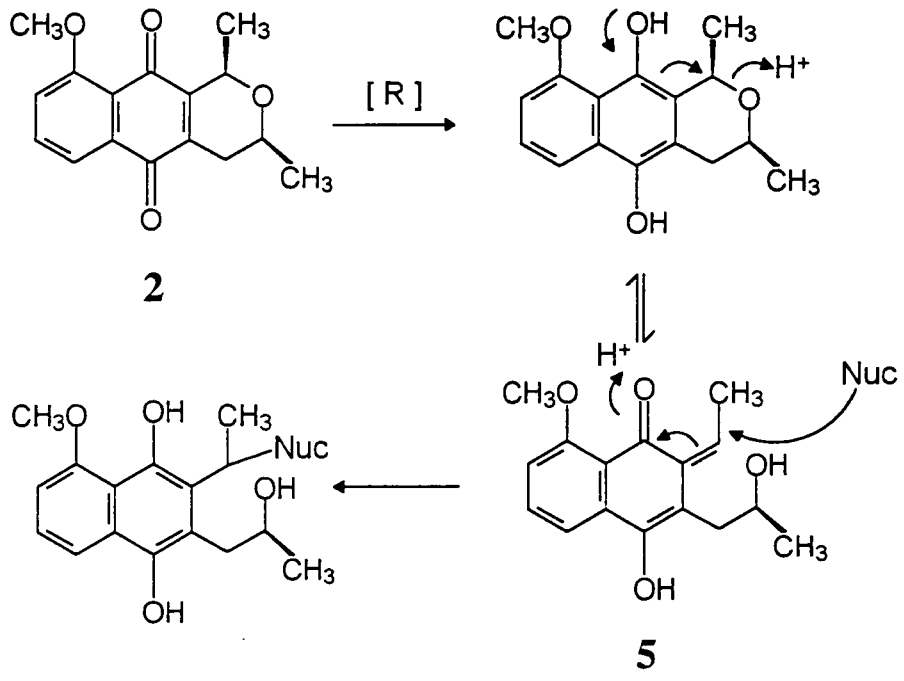


(+)-Eleutherol (**4**)

Figure 1. The eleutheroids

blood flow in isolated guinea pig heart and to exhibit human anti-anginal efficacy approximately equal to that of Persantine (dipyridamol).[3a,5] To the best of our knowledge, the individual abilities of the four agents to confer cardioprotection have yet to be discerned; additional studies are thus needed to clarify this phenomenon and perhaps identify one superior component of the four. Furthermore, the structural similarity of these agents to other well known isochromanquinones, such as kalafungin and the nanaomycins, has suggested other medicinal applications for the eleutherines. The members of this class of antibiotics are thought to function as "bioreductive alkylating agents," whose biochemical mechanism involves *O*-quinone methide-type species capable of alkylating nucleophilic biomolecules,[6] as illustrated in Scheme 2 with the postulated reactions that eleutherine (**2**) might undergo. After *in vivo* reductive activation, enol–keto tautomerization affords the reactive *O*-quinone methide species **5**, which then reacts with a nucleophilic biomolecule such as a protein or nucleic acid residue, with positive or negative biochemical consequences. Hongconin already exists in the same oxidation state as **5** and therefore might serve as an *immediate* bioalkylating agent, in contrast to the rest of the quinone members of the eleutheroids (*i.e.*, **2-4**), which first require *in vivo* reductive activation into their hydroquinone form.

Although the complete structures of compounds **2-4**, including their absolute stereochemistry, are known, only hongconin's *relative* stereochemistry is known. Obviously, there is a strong possibility that hongconin's absolute stereochemistry is the



Scheme 2. Postulated biochemical mechanism of action for isochromanquinoids

one shown arbitrarily in Figure 1, since the four compounds are probably biosynthetically related, and thus share the same absolute stereochemistry at C-1 via a common anabolic intermediate. An enantioselective synthesis would allow the absolute configuration of hongconin to be conclusively defined, which would subsequently clarify the biosynthetic relationship of the eleutheroids. Furthermore, provided that hongconin proved to be a potent cardioactive component, knowing its absolute stereochemical structure would be a key prerequisite for subsequent chiral drug development (either of hongconin itself, or of analogs).

It comes as no surprise then, that hongconin has attracted the interest of synthetic chemists for the reasons stated above and also since an investigation of its medicinal potential will likely require amounts of material in excess of its low natural occurrence. Although hongconin has recently been synthesized in racemic form (*vide infra*), this synthesis is rather lengthy. More efficient—as well as enantiospecific—methods are needed.

II. STATEMENT OF THE PROBLEM

A. Objectives

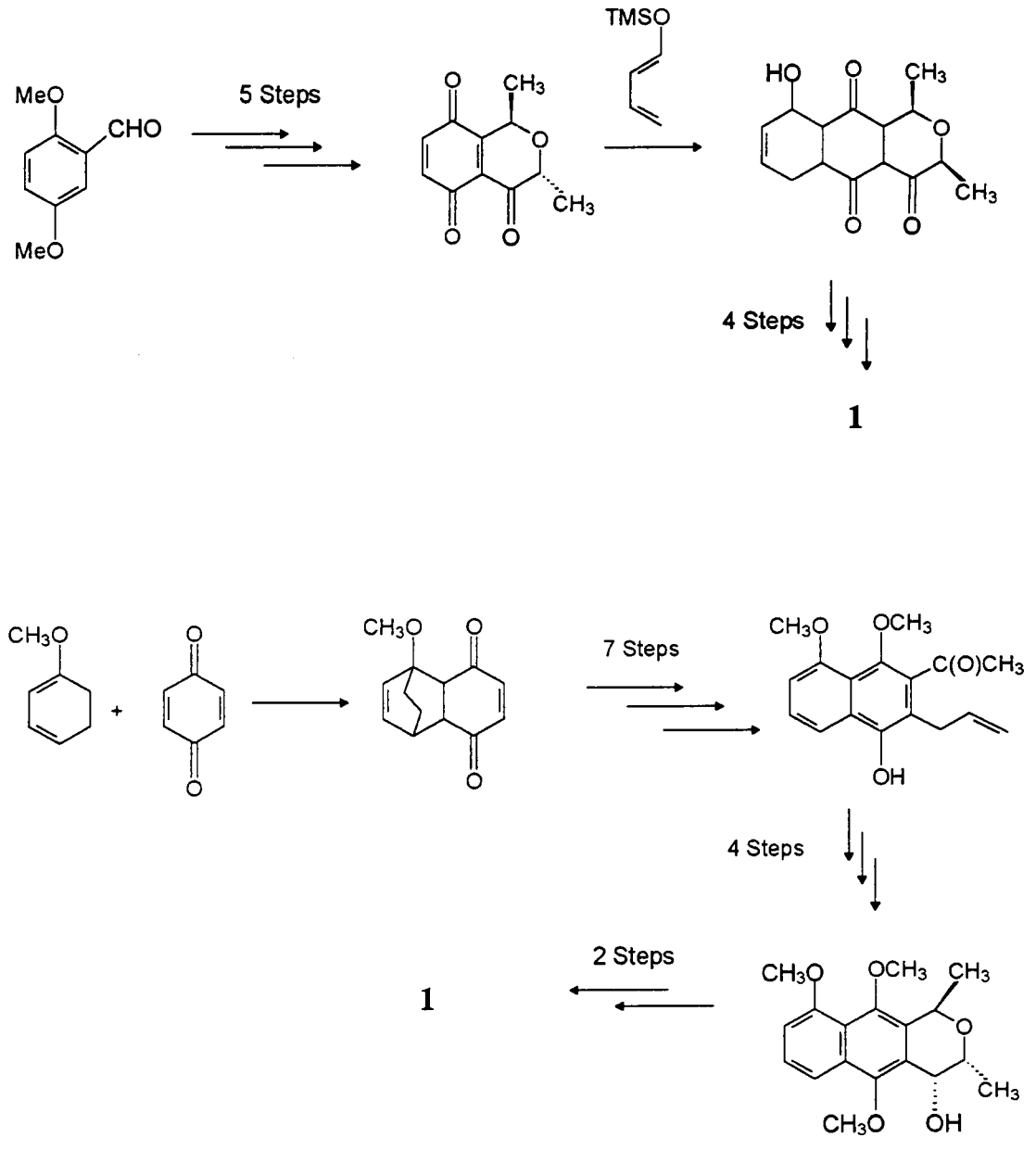
The previously articulated *general* goal of utilizing carbohydrate synthons in the synthesis of an optically pure natural product can now be more precisely focused into two *specific* project goals:

- To synthesize hongconin in its naturally occurring form.
- To establish absolute stereochemical information about the eleutheroids.

B. Research plan—retrosynthetic analysis

In seeking to devise an efficient synthetic scheme, we examined the relevant work already in the literature. There are two racemic syntheses in the literature. Kraus and co-workers recently reported a 10-step racemic synthesis from 2,5-dimethoxy-benzaldehyde which featured a regioselective Diels–Alder reaction to install the naphthalene ring.[7a] Green and co-workers reported a second racemic synthesis in 14 steps from 1-methoxycyclohexa-1,4-diene and benzoquinone.[7b] These two syntheses are summarized in Scheme 3.

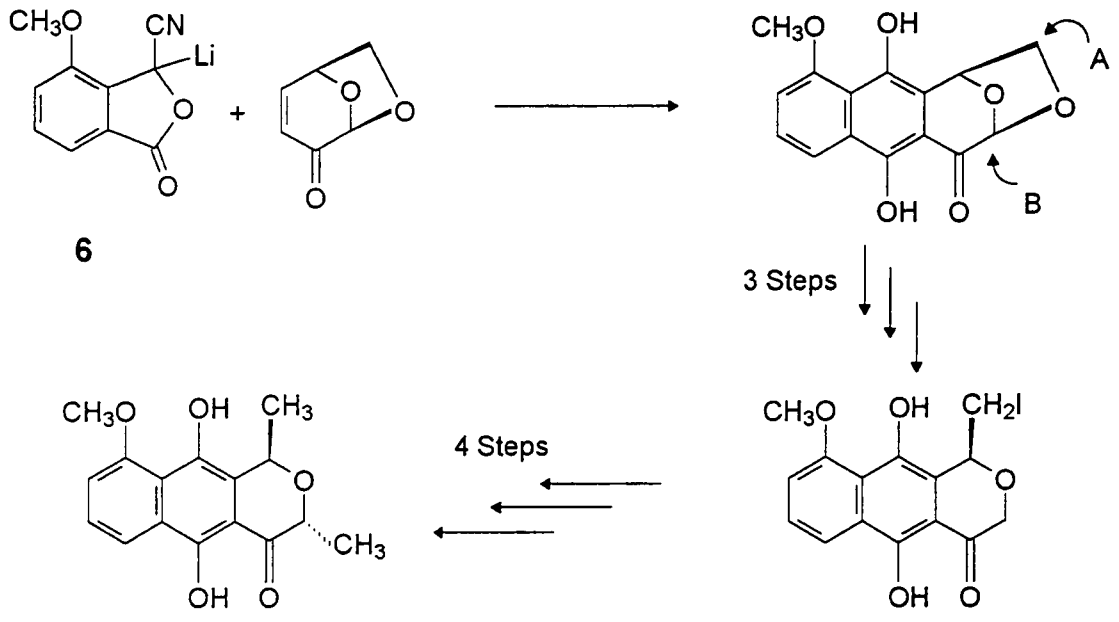
The use of carbohydrates in synthesizing other *optically active* isochromanquinoids has some precedent. Swenton and co-workers had previously disclosed that the well-known and versatile cyanophthalide **6**[8] could react as a Micheal donor with levoglucosenone to provide chiral intermediates *en route* to naphtho[2.3*c*]pyran-5,10-quinone antibiotics. Interestingly, subsequent to our



Scheme 3. Synthesis of racemic hongconin by Kraus and co-workers (upper scheme), and by Green and co-workers (lower scheme)

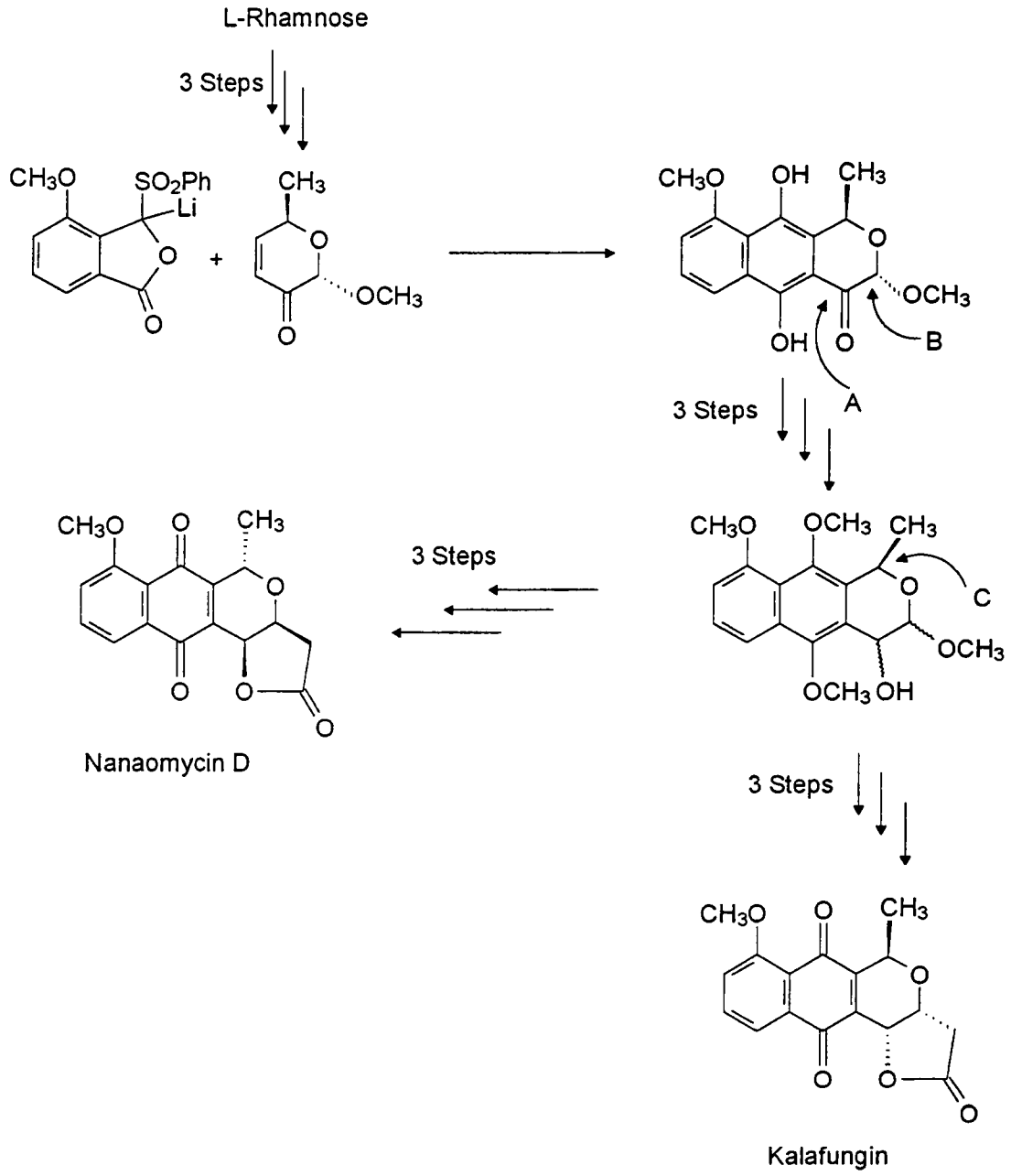
own synthesis of (–)-hongconin (*vide infra*), and in part due to information furnished to them by us, they have recently elaborated one of these intermediates into (–)-hongconin, thus providing a net 8-step synthesis of the natural product (Scheme 4).[9] By similar methodology, Tatsuta and co-workers used an L-rhamnose-derived Michael acceptor in a reaction with the phenylsulphonyl analog of **6** to ultimately afford optically pure kalafungin and nanaomycin D (Scheme 5).[10] As indicated by arrows A, B, and C in Schemes 4 and 5, however, both of these programs required a number of peripheral operations after the coupling step to install or adjust the stereochemistry of the pyran ring substituents in the target compounds, and/or reductively manipulate the oxidation state of the acetal moiety (and/or other carbon centers) remaining from the carbohydrate precursor.

Previous work by Nicolau demonstrated that glycals suffered nucleophilic attack by certain alkyl–metal reagents to afford C-glycosides with defined stereochemistry. We foresaw that the utilization of this advance could allow conversion of the appropriate glycal into a more fully constructed Michael acceptor already possessing hongconin's dimethyl pyran skeleton in its proper stereochemistry and oxidation state, such that its reaction with **6** might provide hongconin directly without further synthetic entanglements. Accordingly, we proposed the retrosynthesis outlined in Scheme 6. After using glycal addition chemistry to afford the requisite dimethylpyran synthon, coupling via phthalide annulation chemistry might immediately afford hongconin. The present study has reduced this strategy to

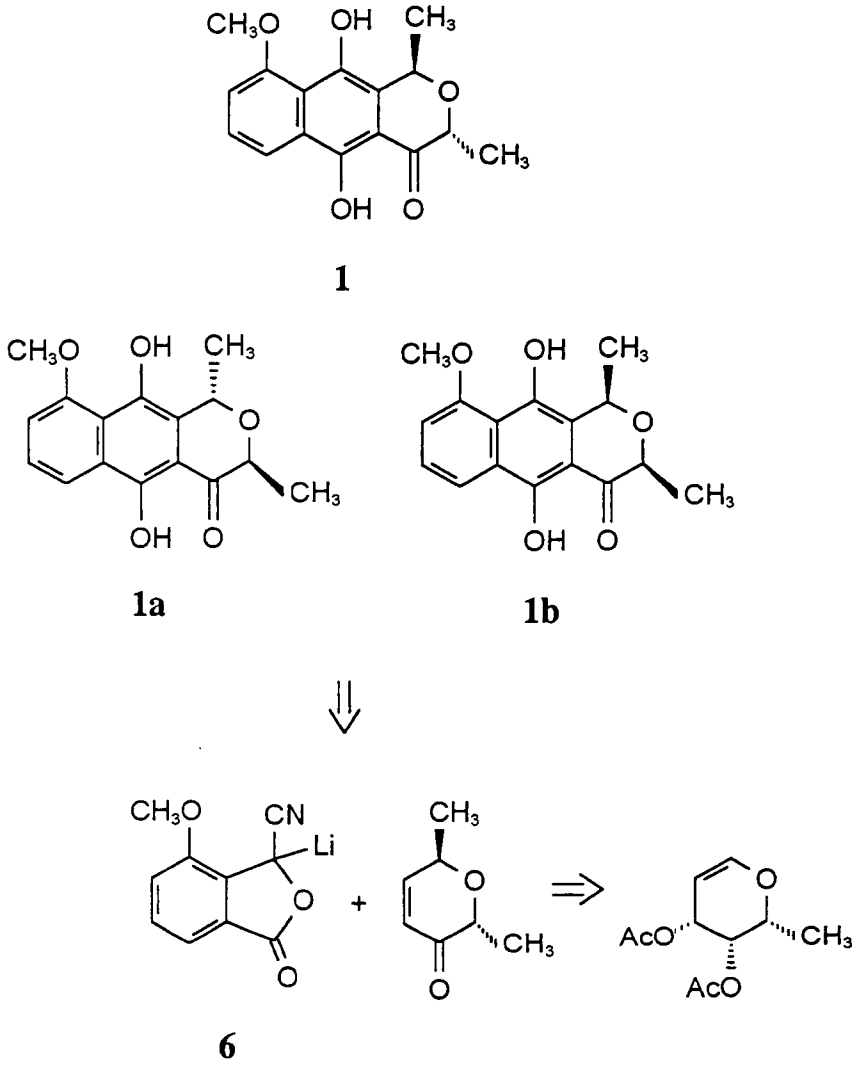


Scheme 4. Synthesis of optically pure isochromanquinone intermediates

by Swenton and co-workers



Scheme 5. Synthesis of kalafungin and nanaomycin by Tatsuta and co-workers



Scheme 6. Proposed retrosynthesis of hongconin (and stereoisomers)

practice via the first enantioselective synthesis of naturally-occurring (–)-hongconin (**1**),[11] a related diastereomer, *iso*-hongconin (**1b**), and *ent*-hongconin (**1a**), as well as elucidating hongconin's previously undetermined absolute configuration.[12]

C. Significance

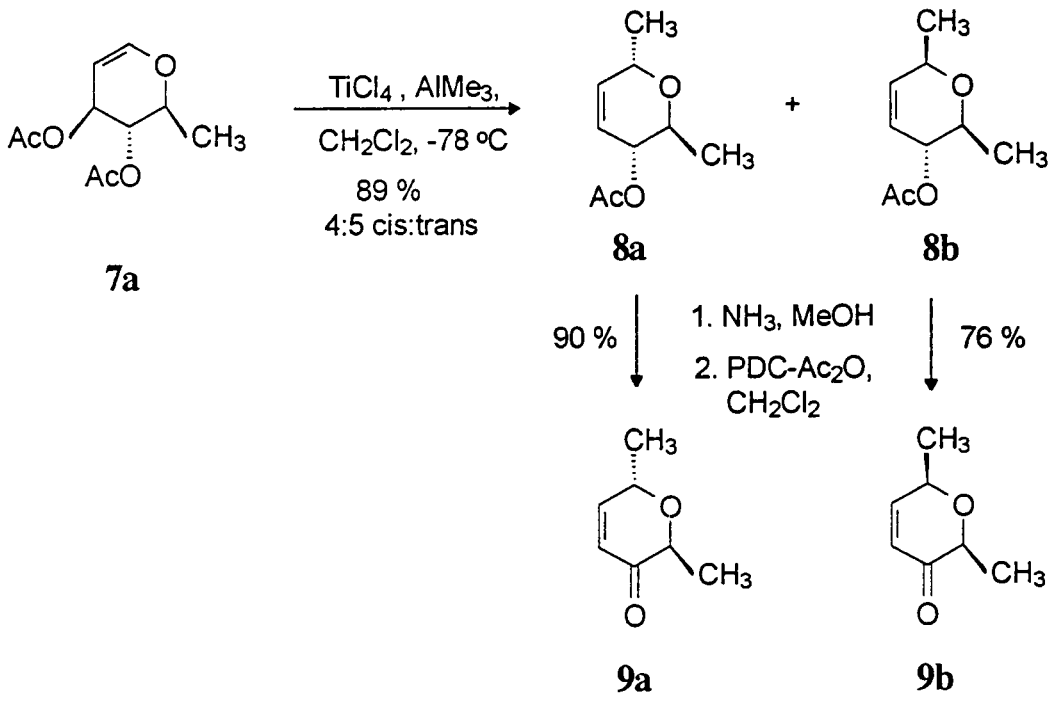
If completed, the proposed synthesis would establish the absolute stereochemistry of hongconin, a potentially useful anti-anginal agent, and establish a convenient preparation of the optically pure natural product and its analogs for biological evaluation.

III. RESULTS AND DISCUSSION

A. Selection of starting materials

At the outset of our enterprise, it was reasonable to extrapolate from the known absolute configurations of the pyran ring substituents in **2**-**4**[4b,c] and assign hongconin's absolute configuration on a provisional basis, since the four compounds are presumed to be biosynthetically related.[3c] Such considerations argue for a methyl group "up" at the 1-position, since that feature is common to **2**-**4** (Figure 1). This rationale was most probably responsible for the uniform adoption in the literature of structure **1** to represent hongconin, even though its absolute configuration had not been experimentally established. The "correct" (*i.e.*, either the D- or the L-) carbohydrate synthon corresponding to the natural product would thus involve D-sugars, as shown in Scheme 6.

We noted, however, that a synthesis of the "wrong" enantiomer would nevertheless be worthwhile since, in the case of some related pyranonaphthoquinone systems, both enantiomers have been isolated and found to be biologically active. For example, nanaomycin D and kalafungin are enantiomers, and the antibiotics granaticin and medermycin have been found in either enantiomeric form.[10] Thus, for the initial exploration into the viability of our synthetic approach, we resorted to considerations of economy and expedience and chose to begin with the commercially available L-sugar, di-*O*-acetyl-L-quinoval (3,4-di-*O*-acetyl-6-deoxy-L-glucal, **7a**, Scheme 7).



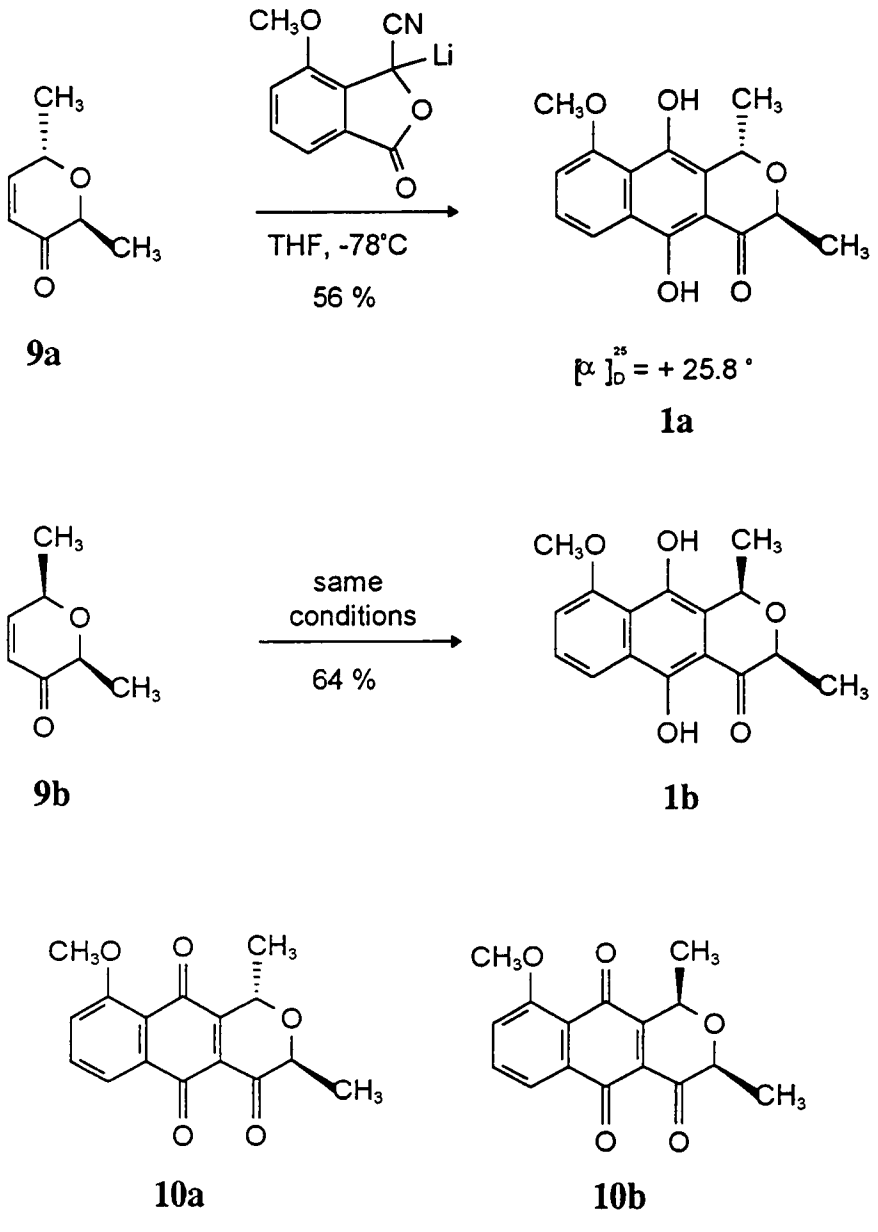
Scheme 7. Synthesis of Micheal donors **9a** and **9b**

B. Synthesis of *ent*- and *epi*-hongconin

Lewis acid-catalyzed C-1 alkylation[13] of **7a** led to a 4:5 mixture of epimers **8a** and **8b** which were easily separated by chromatography. The stereochemistry at C-1 of these two species was assigned tentatively and later confirmed through NOE studies on their respective end-products, and by correlation to published physical data for the natural product. Although we were happy to have a *cis*-compound for purposes of accessing a *cis*-analog of the final compound, the lack of stereoselectivity seemed unattractive since, from the standpoint of developing a concise route to the natural product, the *cis* material is "wasted." Therefore, while carrying through both products in

the meantime, we set as an eventual goal the identification of a way to improve the stereoselctivity of the reaction. This issue is addressed below. In any case, parallel elaboration of acetates **8a** and **8b**, using standard deacetylation and oxidation transformations, afforded the desired Michael acceptors **9a** and **9b**, respectively.

With Michael acceptors **9a-b** in hand, the stage was now set for phthalide annulation coupling which would hopefully produce hongconin, or, in the case of **9b**, a "*cis*" analog of hongconin (Scheme 8). In general, the reaction between **6** and enones **9**, along with ensuing chromatography, occurred most smoothly when **9** was used in slight excess (1.1 equiv). Another problem was encountered in which extended reaction times and/or warming to room temperature produced minor amounts of red side-products, which were identified as the corresponding quinones (*i.e.*, **10a** or **10b**), presumably the result of *in situ* air oxidation of the hydroquinone. In handling these quinones, some epimerization was noted, presumably at C-1. Such epimerizations are well known, for example, as previously reported for the structurally similar **2** and **3**.[4e] In fact, C-1 epimerizations in such systems have even been exploited by Tatsuta as a means of obtaining the desired stereochemistry at that position during a synthesis of kalafungin.[10] In any event, thorough purging of reaction vessels and solvents with nitrogen eliminated the quinones' appearance and facilitated the felicitous conversion of **9a** and **9b** to **1a** and **1b**, respectively. All physical data of synthetic **1a** were identical to that of naturally occurring hongconin, except, unfortunately, for the sign of optical rotation: $[\alpha]_D^{20}$ +25.8 (*c* 1.94, $CHCl_3$)



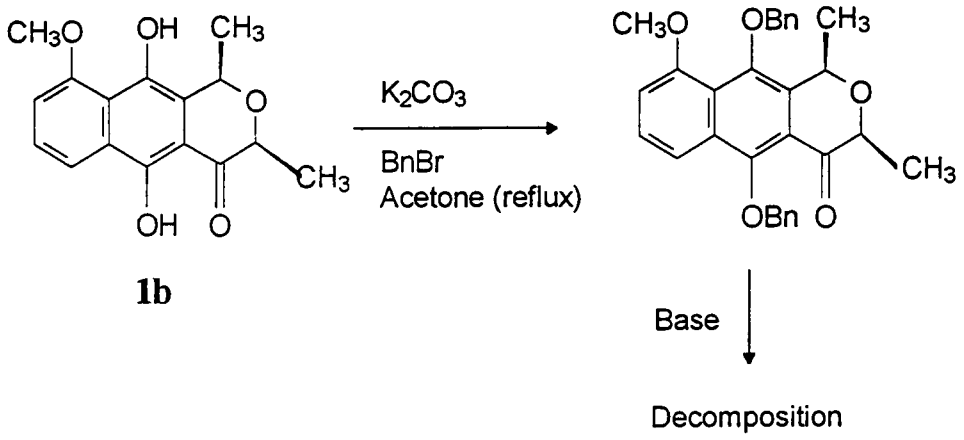
Scheme 8. Synthesis of *ent*-hongconin (**1a**) and 3-*epi*-hongconin (**1b**)

{lit., natural product:[3c] $[\alpha]_D^{20}$ -26.0 (*c* 1.94, $CHCl_3$)}. Compound **1a** is thus the enantiomer of the natural product, whose absolute configuration can thus be represented by structure **1**, as previously suspected.

Since the *cis* compound **1b** differs from (−)-hongconin only in the stereochemical disposition of the 3-methyl group, the prospect of epimerizing C-3 appeared to be a viable route to **1**, even if present as a mixture with remaining **1b**, since we had identified a solvent system capable of separating **1a** and **1b**.[14] Toward this end, a di-*O*-benzyl-protected derivative of **1b** was prepared; however, all attempts to epimerize this species resulted only in decomposition (Scheme 9).

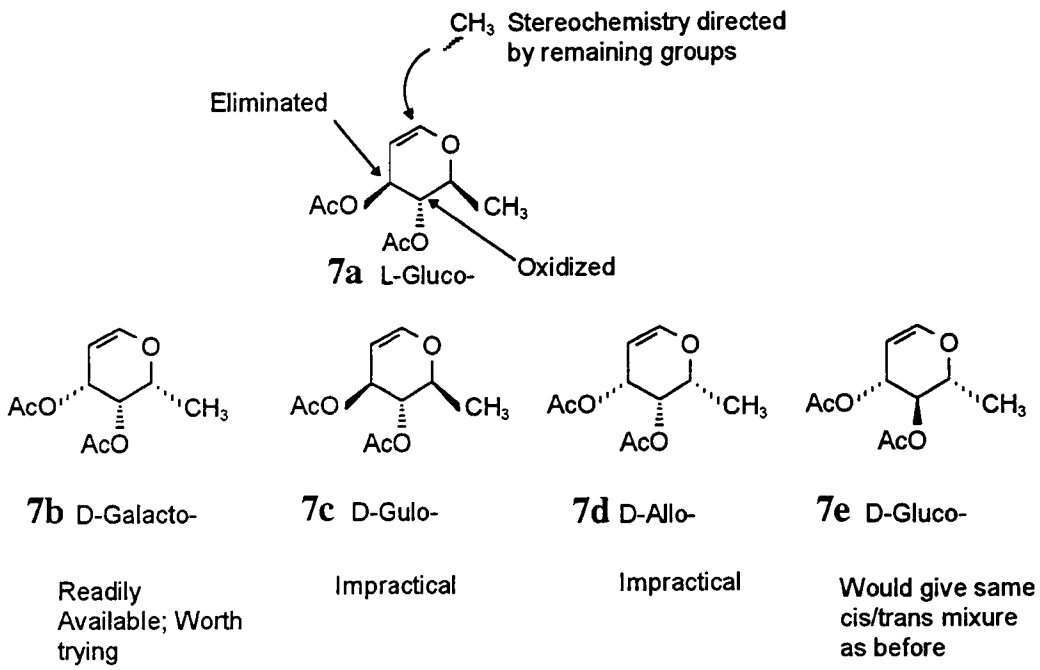
C. Synthesis of (–)-hongconin

Our subsequent recourse to employing the D-isomer of **7a** to obtain **1**, however, was preempted by our finding an improved stereoselective C-1 alkylation to the *trans*-compound, as previously desired, via compound **7b** (See Scheme 10). This finding followed from our analysis of the stereochemistry as follows. First, there are two stereogenic centers of the glycal starting material whose stereochemistry does *not* carry over into the final product: the 3-position is eliminated in the S_N2'-like reaction with $AlMe_3$ and the 4-position is oxidatively destroyed (alcohol to ketone). Only the stereochemistry at C-5 (imparting the "D" configuration) remains and is essential. The C-1 stereochemistry is established in the alkylation reaction via steric and/or coordinating effects of the remaining substituents.



1b

Scheme 9. Attempted synthesis of hongconin via epimerization of 3-*epi*-hongconin

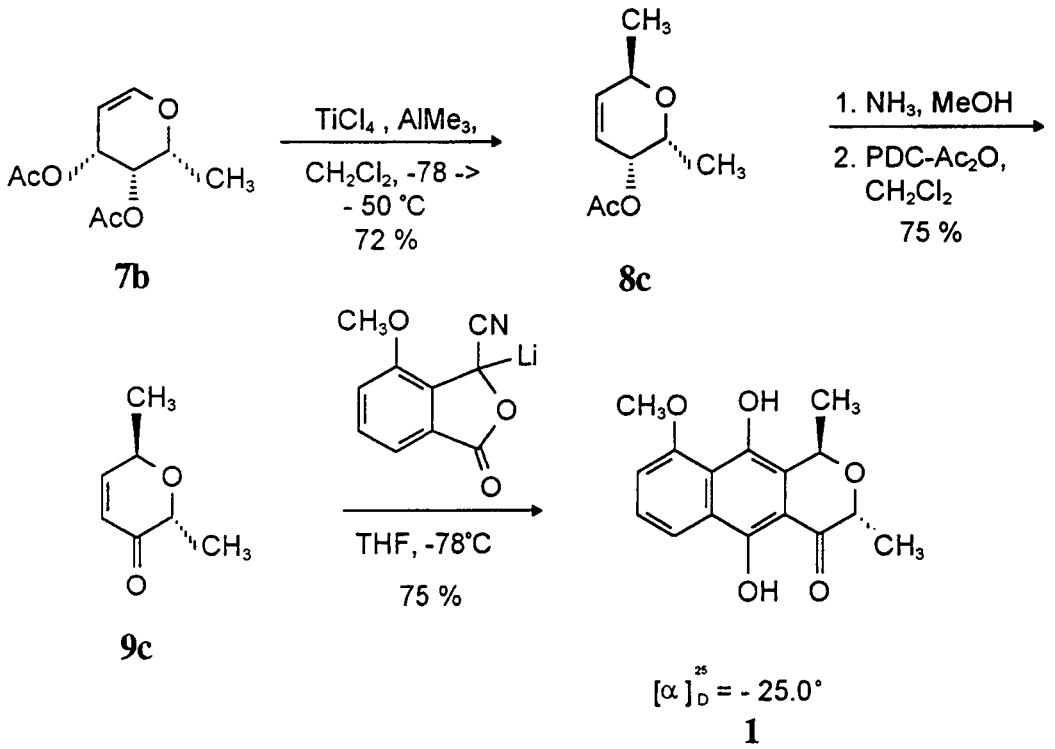


Scheme 10. Improving the *trans*-stereoselectivity of *C*-glycosylation

Obviously, the arrangement of groups in a *gluco*-configuration fails in directing the 1-methyl group into a trans configuration by virtue of the fact that a *cis/trans* mixture results. Therefore, it is logical to consider all possible glycal diastereomers that would also lead to the desired dimethyl product via the "irrelevance" of the 3- and 4-positions' stereochemistry. With two open choices for each of these positions, there are $2^2 = 4$ possiblities. These are represented by the four diastereomers in Scheme 10. The D-*gulo*- and D-*allo*-type glycals **7c** and **7d** are unavailable and would be prohibitively expensive to synthesize. The D-*gluco*-derived glycal (**7e**), again, would merely give the same *cis/trans* mixture as before (since it is the enantiomer of **7a**). However, the D-*galacto* compound **7b** was readily available and was therefore worth investigating.

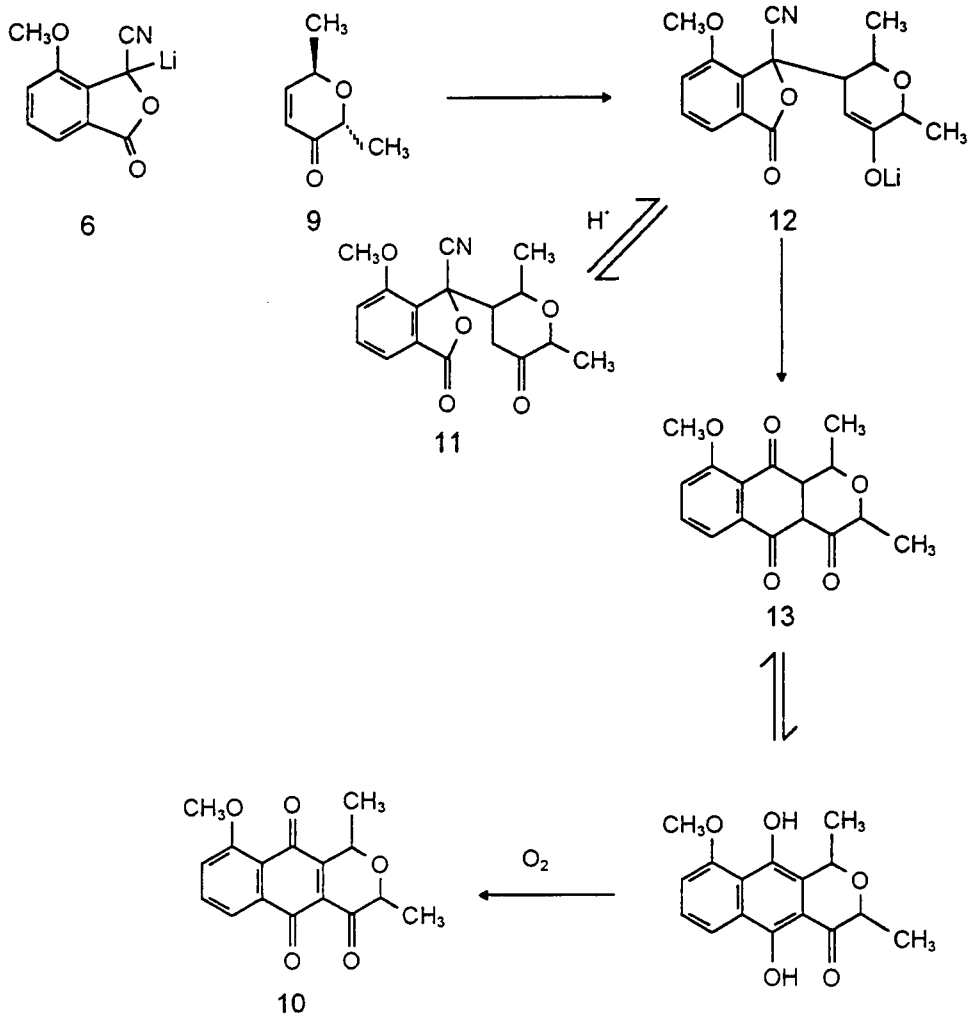
In fact, this compound, namely di-*O*-acetyl-D-fucal (3,4-di-*O*-acetyl-6-deoxy-D-galactal[15]) did, by the action of the same reagents as above, lead exclusively to the *trans*-dimethyl adduct **8c** in moderate yield (Scheme 11). We believe that the hindered β-face of a Lewis acid-chelated intermediate causes nucleophilic addition of Me^- to occur *via* the opposite face of the pyranose ring, thus resulting in the observed *trans* selectivity. Thus, with our improved process in place, the route to naturally occurring hongconin was now a matter of repeating the previously developed chemistry. Processing of **8c** as above led to enone **9c** and finally to synthetic (−)-hongconin, **1**: $[\alpha]_D^{20}$ −25.0 (*c* 1.94, $CHCl_3$).

Although quinone byproducts (encountered in the L-series, as described above) were avoided in this transformation, another interesting finding was made. When the



Scheme 11. Synthesis of hongconin (**1**) via Michael donor **9c**

reaction was quenched prematurely (directly after complete consumption of **6** but prior to complete product formation), high yields of the Micheal adduct intermediate **11** could be isolated (Scheme 12). This compound could be subsequently converted to **1** in near quantitative yield by re-exposure to reaction conditions. Although **11** was converted to **1** upon treatment with *t*-BuOK alone, yields increased when $Na_2S_2O_4$ was included as an antioxidant. (See Experimental Section.) Structures of the type **11** are possible intermediates in reactions between cyanophthalides and Michael acceptors.[16] Compound **11**'s occurrence here was first suspected when the odor of HCN was detected during workup of its conversion to **1**. Its proposed structure was corroborated by its ^{1}H NMR spectrum and decoupling experiments, as well as by ^{13}C NMR, IR, and mass spectral data. (See Experimental Section.) The occurrence of **11** supports the proposed mechanism, and, in conjunction with the finding of the quinone byproducts **10**, generated an understanding of the available reaction pathways shown in Scheme 12. Conjugate addition of **6** to enone **9** produces an intermediate enolate anion **12**. Addition of the nucleophilic α-carbon to the lactone carbon followed by loss of LiCN affords **13**, the diketo tautomer of the final product. Base-catalyzed tautomerization of **13** then furnishes the desired hydroquinone. Alternatively, if anion **12** is protonated at the α-carbon (proton sources include the acidic α-protons of diketo tautomer **13**), observed nitrile **11** is formed. *In situ* oxygen can also oxidize initially formed product to quinone **10**.



Scheme 12. Alternative reaction pathways in phthalide annulation reaction

IV. CONCLUSIONS

In summary, both (+)- and (−)-enantiomers of hongconin, as well as a (+)-*cis*-diastereomer, were enantioselectively synthesized in a parallel fashion in four steps from L-quinoval and D-fucal diacetates, respectively, using a novel combination of *C*-glycoside cyanophthalide annulation chemistry. The synthesis directly establishes the heretofore unknown absolute stereochemistry of (−)-hongconin. Furthermore, the synthesis represents an improvement over the exisiting literature syntheses in two important respects. First, it is substantially shorter than the existing racemic synthesis (4 vs. 9 steps). Second, the employment of *C*-glycoside Michael acceptors, as opposed to their usual *O*-glycoside counterparts, represents a potentially useful simplification of phthalide annulation reactions in synthesizing numerous other such optically pure isochromanquinoids, since it obviates the inconvenience of additional steps late in the synthetic scheme associated with reductive manipulation of a remaining acetal moiety into the desired pyran ring substituent. Finally, in a more general sense, the synthesis augments the existing cases in the literature demonstrating that carbohydrates are convenient chiral synthons for optically active synthetic targets.

V. EXPERIMENTAL SECTION

General Methods. All reactions were monitored by thin-layer chromatography (TLC). Adsorption chromatography was carried out using E. Merck silica gel products: (a) TLC on 0.2 mm aluminum-backed plates, (b) column chromatography using 230–400 mesh silica gel. Visualization of the tlc plates was by 254 nm UV light and by spray–heat development using a *p*-anisaldehyde–sulfuric acid reagent.[17] The solvent systems for adsorption chromatography were A, 8:1 hexanes–ethyl acetate; B, 4:1 hexanes–ethyl acetate; C, dichloromethane; and D, 1:1:1 hexanes–ethyl acetate–dichloromethane. Anhydrous solvents were prepared as follows: dichloromethane was distilled from calcium hydride; THF was refluxed with sodium–benzophenone ketyl and distilled. Reagent *tert*-butanol was distilled from sodium. All reactions were carried out under a nitrogen atmosphere unless otherwise indicated. Solvents were evaporated at aspirator vacuum at about 25 °C unless otherwise indicated. Elemental analyses were furnished by Atlantic Microlab, Inc. of Atlanta, GA. ^{1}H and ^{13}C NMR spectra were determined at 250 MHz and 62.5 MHz, respectively, as ca. 0.1% solutions in chloroform-*d* using a Bruker AM 250 instrument. ^{1}H NMR shifts are reported as δ (ppm) downfield from an internal standard of tetramethylsilane (TMS); multiplicities are first-order values in Hz: s, singlet; bs, broad singlet; d, doublet; t, triplet; bd, broad doublet; dd, doublet of doublets; ddd, doublet of doublet of doublets; dm, doublet of multiplets; dq, doublet of quartets; m, multiplet; bm, broad multiplet. The exchangeable protons of hydroxy groups were determined by deuterium exchange using deuterium oxide. Assigned protons were

determined by decoupling experiments. ^{13}C NMR chemical shifts are reported as δ (ppm) relative to $CDCl_3$ (77.00 ppm) as standard. Optical rotations were measured with a Perkin–Elmer Model 243 automatic polarimeter equipped with sodium and mercury lamps for solutions in a 0.1 dm cell at the indicated temperature. Infrared spectra were obtained on a Perkin–Elmer 710B instrument. The mass spectral analyses were obtained on a VG-instrument at the University of Tennessee.

General Procedure for the Synthesis of Compounds 8. To a solution of the appropriate glycal 7 (1.0 g, 4.66 mmol) in dichloromethane at −78 °C was added dropwise $TiCl_4$ (1.0 M soln in toluene, 5.13 mL, 1.1 equiv) to afford a cloudy yellow–orange mixture which was allowed to stir for 15 min. $AlMe_3$ (2.0 M soln in hexane, 3.5 mL, 1.5 equiv) was then added dropwise, whereupon the reaction mixture immediately turned black. The reaction was allowed to stir at −78 °C for 6 h, at which time it was quenched by the addition of saturated $NaHCO_3$ (10 mL) and allowed to warm to room temperature. The gelatinous mixture was filtered through Celite, washed with brine, dried ($MgSO_4$), concentrated, and submitted to flash chromatography (Solvent A). Careful evaporation of the fractions at 20 °C afforded the appropriate *C*-glycoside [**7a** (1.00 g, 4.67 mmol) → **8a** + **8b** (704 mg, 89% overall); **7b** (1.69 g, 7.90 mmol) → **8c** (830 mg, 72% based on 237 mg of recovered starting material)] as detailed in the following paragraphs.

5-*O*-Acetyl-2,6-anhydro-1,3,4,7-tetradeoxy-L-*arabino*-hept-3-enitol (8a). Beginning with **7a**, **8a** was obtained as a volatile oil containing a small amount of

hexanes (as shown by ^{1}H NMR spectroscopy): $[\alpha]_D^{20}$ -133.0 (*c* 1.0, $CHCl_3$); R_f = 0.35 (Solvent B); ^{1}H NMR ($CDCl_3$): δ 1.17 (d, 3H, *J* = 6.54 Hz, -CH_3-7), 1.22 (d, 3H, *J* = 6.8 Hz, -CH_3-1), 2.02 (s, 3H, -OC(O)CH_3), 3.85 (dq, 1H, *J* = 4.76 Hz, *J* = 6.49 Hz, H-6), 4.25 (m, 1H, H-2), 4.81 (bm, 1H, H-5), 5.67 (dm, 1H, *J* = 10.27 Hz, H-4), 5.82 (dm, 1H, *J* = 10.28 Hz, H-3); ^{13}C NMR ($CDCl_3$): δ16.82, 19.52, 21.07, 66.12, 68.31, 69.46, 122.17, 135.12, 170.54.; Anal. Calcd for $C_9H_{14}O_3 \cdot 0.08\ C_6H_{14}$: C, 64.24; H, 8.96. Found C, 64.28; H, 8.95.

3-*O*-Acetyl-2,6-anhydro-1,4,5,7-tetradeoxy-D-*ribo*-hept-4-enitol (8b).

Beginning with **7a**, **8b** was obtained as a volatile oil: $[\alpha]_D^{20}$ -175.0 (*c* 1.0, $CHCl_3$); R_f = 0.45 (Solvent B); ^{1}H NMR ($CDCl_3$): δ 1.11 (d, 3H, *J* = 6.81 Hz, -CH_3), 1.14 (d, 3H, *J* = 5.92 Hz, -CH_3), 1.99 (s, 3H, OC(O)CH_3), 3.45 (m, 1H, H-2), 4.37 (m, 1H, H-6), 4.97 (bd, 1H, *J* = 8.69 Hz, H-3), 5.57 (bd, 1H, *J* = 10.23 Hz, H-4), 5.69 (bd, 1H, *J* = 10.20 Hz, H-5); ^{13}C NMR ($CDCl_3$): δ 18.36, 20.94, 21.06, 70.67, 71.01, 72.26, 124.69, 134.06, 170.28; Anal. Calcd for $C_9H_{14}O_3$: C, 63.51; H, 8.28. Found C, 63.60; H, 8.33.

3-*O*-Acetyl-2,6-anhydro-1,4,5,7-tetradeoxy-D-*arabino*-hept-4-enitol (8c).

Beginning with **7b**, and conducting the addition of $AlMe_3$ and subsequent stirring at -50 °C instead of -78 °C, **8c** was obtained as a volatile oil containing a small amount of water and dichloromethane, as shown by ^{1}H NMR spectroscopy): $[\alpha]_D^{20}$ -406.0 (*c* 1.6, $CHCl_3$); R_f = 0.35 (Solvent B); ^{1}H NMR ($CDCl_3$): δ 1.19 (d, 3H, *J* = 6.44 Hz, -CH_3), 1.25 (d, 3H, *J* = 6.86 Hz, -CH_3), 2.10 (s, 3H, OC(O)CH_3), 4.03 (dm, 1H, *J* = 2.76 Hz, *J* = 6.5 Hz, H-2), 4.43 (q, 1H, *J* = 2.32 Hz, *J* = 6.85 Hz, H-6), 4.98 (dd, 1H, *J* = 2.80 Hz,

J = 4.82 Hz, H-3), 5.86 (ddd, 1H, J = 1.9 Hz, J = 4.96 Hz, J = 7.12 Hz, H-4), 5.98 (dd, 1H, J = 2.95 Hz, J = 10.21 Hz, H-5); ^{13}C NMR ($CDCl_3$): δ 16.10, 18.23, 21.00, 65.48, 66.29, 68.54, 121.84, 136.25, 170.89; Anal. Calcd for $C_9H_{14}O_3 \cdot 0.035\ CH_2Cl_2 \cdot 0.15\ H_2O$: C, 61.61; H, 8.22; Cl, 1.6. Found C, 61.50; H, 8.22, Cl, 1.6.

General Procedure for the Synthesis of Compounds 9. The appropriate acetate **8** (0.400 g, 2.35 mmol) was treated with a saturated ammonia–methanol solution (50 mL) for 24 h at room temperature. After evaporation of solvent, the resulting crude alcohol was redissolved in dichloromethane (50 mL) and treated with PDC (1.00 g, 1.1 equiv). After 15 min of stirring, acetic anhydride (0.18 mL, 0.8 equiv)[18] was added, and the reaction was allowed to stir overnight at room temperature, after which time it was diluted with ether (50 mL) and filtered through Celite. The filtrate was concentrated and submitted to flash chromatography (Solvent C). Careful evaporation of the fractions at 20 °C provided the appropriate enone (75–90%, two steps) described in the following paragraphs.

2,6-anhydro-1,4,5,7-tetradeoxy-L-*threo*-hept-4-en-3-ulose (9a). Beginning with **8a** (400 mg, 2.37 mmol), **9a** (269 mg, 90%) was obtained as a volatile oil: $[\alpha]_{Hg}^{20}$ +2.0 (*c* 1.0, $CHCl_3$); R_f = 0.45 (Solvent B); ^{1}H NMR ($CDCl_3$): δ 1.38 (d, 1H, J = 7.0 Hz, -CH_3-1), 1.40 (d, 1H, J = 7.0 Hz, -CH_3-7), 4.33 (q, 1H, J = 6.95 Hz, H-2), 4.61 (m, 1H, J = 6.96 Hz, H-6), 6.01 (dd, 1H, J = 1.93 Hz, J = 10.37 Hz, H-4), 6.93 (dd, 1H, J = 2.47 Hz, J = 10.43 Hz, H-5); ^{13}C NMR ($CDCl_3$): δ 15.15, 18.70, 65.79, 73.25, 124.53, 151.80, 197.01; HRMS Calcd for $C_7H_{10}O_2$: 126.068. Found 126.068.

2,6-anhydro-1,4,5,7-tetradeoxy-D-*erythro*-hept-4-en-3-ulose (9b). Beginning with **8b** (1.00 g, 5.91 mmol), **9b** (569 mg, 76%) was obtained as a volatile oil: $[\alpha]_{Hg}^{20}$ -3.0 (*c* 1.0, $CHCl_3$); R_f = 0.7 (Solvent C); ^{1}H NMR ($CDCl_3$): δ 1.37 (d, 3H, *J* = 1.47 Hz, $-CH_3$), 1.40 (d, 3H, *J* = 2.09 Hz, $-CH_3$), 4.07 (dq, 1H, *J* = 1.8 Hz, *J* = 6.61 Hz, H-2), 4.50 (m, 1H, H-6), 6.06 (dd, 1H, *J* = 2.46 Hz, *J* = 10.22 Hz, H-5), 6.87 (dd, 1H, *J* = 1.41 Hz, *J* = 10.17 Hz, H-4); ^{13}C NMR ($CDCl_3$): δ 15.30, 20.58, 70.22, 76.68, 126.10, 152.13, 196.80; HRMS Calcd for $C_7H_{10}O_2$: 126.068. Found 126.068.

2,6-anhydro-1,4,5,7-tetradeoxy-D-*threo*-hept-4-en-3-ulose (9c). Beginning with **8c** (403 mg, 2.38 mmol), **9c** (224 mg, 75%) was obtained as a volatile oil: $[\alpha]_D^{20}$ -53.4 (*c* 2.6, $CDCl_3$); ^{1}H NMR, ^{13}C NMR, TLC data identical to that of **9a**; HRMS Calcd for $C_7H_{10}O_2$: 126.068. Found 126.067.

General Procedure for the Synthesis of Compounds 1, 1a, and 1b. To a solution of *t*-BuOH (0.21 mL, 1.1 equiv), LiCl (0.060 g, cat.), and THF (20 mL) at -78 °C was added dropwise *n*-BuLi (2.5 M soln in hexane, 0.87 mL, 1.1 equiv). To this solution was added dropwise a solution of **6** (0.375 g, 1.98 mmol) in THF (10 mL). The resulting yellow solution was allowed to stir for 10 min, whereupon a solution of **9** (0.30 g, 1.1 equiv) in dichloromethane (5 mL) was added dropwise. The reaction was allowed to continue at -78 °C for 4-6 h. Saturated NH_4Cl (25 mL) and ether (25 mL) were then added, and the mixture was allowed to warm to room temperature. After extractions with ether (4 × 20mL), the combined organic layers were washed with brine, dried ($MgSO_4$), concentrated, and submitted to flash chromatography (Solvent A) to

provide the appropriate isochromanhydroquinone (56–75%), as described in the following paragraphs.

(1*S*,3*S*)-(+)-3,4-Dihydro-5,10-dihydroxy-9-methoxy-1,3-dimethyl-1*H*-naphtho[2,3-*c*]pyran-4-one (*ent*-Hongconin, 1a). Beginning with **9a** (150 mg, 0.793 mmol), **1a** (128 mg, 56%) was obtained as a bright yellow powder: $[\alpha]_D^{20}$ +25.8 (*c* 1.94, $CHCl_3$); R_f = 0.5 (Solvent B); ^{1}H NMR ($CDCl_3$): δ 1.52 (d, 3H, *J* = 6.61 Hz, -CH_3), 1.63 (d, 3H, *J* = 6.70 Hz, -CH_3), 4.04 (s, 3H, OCH_3), 4.68 (q, 1H, *J* = 6.58 Hz, H-3), 5.47 (q, 1H, *J* = 6.73 Hz, H-1), 6.98 (d, 1H, *J* = 7.77 Hz, H-8), 7.35 (t, 1H, *J* = 8.05 Hz, H-7), 8.01 (d, 1H, *J* = 8.42 Hz, H-6), 8.94 (s, 1H, ArOH), 12.79 (s, 1H, ArOH); ^{13}C NMR ($CDCl_3$): δ 16.25, 17.36, 56.34, 67.35, 69.44, 107.80, 109.12, 118.05, 119.59, 120.96, 125.36, 125.93, 139.43, 154.35, 155.68, 202.87.

(1*R*,3*S*)-(+)-3,4-Dihydro-5,10-dihydroxy-9-methoxy-1,3-dimethyl-1*H*-naphtho[2,3-*c*]pyran-4-one (*iso*-Hongconin, 1b). Beginning with **9b** (33 mg, 0.174 mmol), **1b** (32 mg, 64%) was obtained as a bright yellow powder: $[\alpha]_D^{20}$ +207.0 (*c* 1.94, $CHCl_3$); R_f = 0.85 (Solvent C); ^{1}H NMR ($CDCl_3$): δ 1.53 (d, 3H, *J* = 6.58 Hz, -CH_3), 1.77 (d, 3H, *J* = 6.30 Hz, CH_3), 4.06 (s, 3H, OCH_3), 4.26 (q, 1H, *J* = 6.61 Hz, H-3), 5.15 (q, 1H, *J* = 6.28 Hz, H-1), 6.99 (d, 1H, *J* = 7.76 Hz, H-8), 7.37 (t, 1H, *J* = 8.07 Hz, H-7), 8.02 (d, 1H, *J* = 8.37 Hz, H-6), 9.19 (s, 1H, ArOH), 12.69 (s, 1H, ArOH); ^{13}C NMR ($CDCl_3$): δ 15.49, 21.30, 56.42, 71.83, 74.89, 109.06, 109.40, 118.02, 119.74, 120.26, 125.49, 125.98, 141.00, 153.68, 155.68, 159.29, 201.68; HRMS Calcd for $C_{16}H_{16}O_5$: 288.100. Found 288.101.

Quinones 10. These compounds proved difficult to purify and were therefore not fully characterized. Evidence for the assigned structures consist of the following. **10a**: R_f = 0.1 (Solvent B); ^{1}H NMR ($CDCl_3$): δ 1.45 (d, 3H, J = 6.29 Hz, -CH_3), 1.71 (d, 3H, J = 6.76 Hz, -CH_3), 3.79 (q, 1H, J = 6.26 Hz, H-3), 3.95 (s, 3H, -OCH_3), 4.74 (q, 1H, J = 6.69 Hz, H-1), 7.38 (dd, 1H, J = 2.37 Hz, J = 7.15 Hz, H-6), 7.68-7.76 (m, 2H, H-7 and H-8); ^{13}C NMR ($CDCl_3$): δ 15.67, 17.19, 56.61, 66.10, 68.49, 116.50, 117.98, 119.60, 120.05 (2C), 132.57, 135.79 (2C), 186.00, 192.92. **10b**: R_f = 0.1 (Solvent B); ^{1}H NMR ($CDCl_3$): δ 1.39 (d, 3H, J = 6.80 Hz, -CH_3), 1.62 (d, 3H, J = 6.60 Hz, -CH_3), 3.95 (s, 3H, -OCH_3), 4.23 (q, 1H, J = 6.85 Hz, H-3), 4.94 (q, 1H, J = 6.64 Hz, H-1), 7.54 (dd, 1H, J = 0.88 Hz, J = 7.67 Hz, H-6), 7.68-7.76 (m, 2H, H-7 and H-8); MS (*m/z*): 285, 203.

(1*R*,3*R*)-(−)-3,4-Dihydro-5,10-dihydroxy-9-methoxy-1,3-dimethyl-1*H*-naphtho[2,3-*c*]pyran-4-one (Hongconin, 1) and 1-(2,6-dimethyl-5-oxo-tetrahydropyran-3-yl)-7-methoxy-3-oxo-1,3-dihydroisobenzofuran-1-carbonitrile (11). Beginning with **9c** (375 mg, 1.98 mmol), **1** (63 mg, 11%) was directly obtained as a bright yellow powder: $[\alpha]_D^{20}$ −25.0° (*c* 1.94, $CHCl_3$), lit.[2c] $[\alpha]_D$ −26.0° (*c*, 1.94 $CHCl_3$); ^{1}H NMR, ^{13}C NMR, and TLC data identical to that of **1a**. Along with **1** was obtained **11** as colorless crystals after recrystallization from ether–hexanes (400 mg, 70%): ^{1}H NMR ($CDCl_3$): δ 1.08 (d, 3H, J = 6.65 Hz), 1.30 (d, 3H, J = 6.80 Hz), 2.91–3.15 (m, 3H), 3.50–3.54 (m, 1H), 4.03–4.16 (q, 1H, J = 6.77 Hz), 4.03 (s, 3H), 7.28 (d, 1H, J = 7.99 Hz), 7.57 (d, 1H, J = 7.27 Hz), 7.69 (t, 1H, J = 7.87 Hz); ^{13}C

NMR ($CDCl_3$): δ 15.52, 18.96, 36.43, 45.43, 56.38, 66.14, 73.12, 79.12, 114.65, 116.81, 118.31, 127.10, 130.64, 133.95, 154.33, 166.40, 208.94; IR (cm^{-1}, KBr): 1790, 1720; HRMS Calcd for $C_{17}H_{17}O_5N$: 315.111. Found 315.110.

Conversion of 11 to 1. To a solution of compound **11** (50 mg, 0.17 mmol) in THF (8 mL) at −78 °C was added $Na_2S_2O_4$ (10 mg, 0.35 equiv), and *t*-BuOK (10 mg, 0.5 equiv), whereupon the clear solution gradually became bright yellow. After continued stirring at −78 °C, TLC (solvent D) showed the complete conversion of **11** (R_f = 0.4) to **1** (R_f = 0.5). Following workup as described above, compound **1** was obtained (43 mg, 96%).

PART II

ANTI-METASTATIC OLIGOSACCHARIDES FROM HYALURONIC ACID

MOLECULAR PROBES OF CANCER METASTASIS — BACKGROUND, RATIONALE, OVERALL PROJECT DESIGN, AND PRELIMINARY BIOLOGICAL EVALUATIONS

I. INTRODUCTION

A. Entry point

Glycoscience research has exploded in the last 10 years as a result of the discovery that a large proportion of intercellular events are mediated by cell-surface carbohydrates.[1] Two areas in particular, cancer immunotherapy and inflammation, have received a great deal of assistance from synthetic chemists, who have undertaken the total chemical or enzymatic synthesis of cell-surface carbohydrate antigens. The motivation for undertaking the present study was the desire to contribute to the cell-surface carbohydrate research arena by developing a new niche (*i.e.*, a particular biological setting that had not yet received the attention of chemists) in which we could utilize oligosaccharide synthesis as a means toward improving understanding of the relevant biochemical mechanisms of the process, as well as toward developing possible therapeutic agents. Opportunity presented itself in the form of existing collaborations between Professor David C. Baker and cancer biologist Richard L. Cysyk (at the National Cancer Institute) concerning the connection between malignant melanoma and lung cancer. Specifically, these studies had been directed toward understanding cancer-induced hyaluronic acid biosynthesis via nucleoside–nucleotide metabolic and/or signal

transduction pathways *inside* the host cell.[2] It was desired that this research be expanded to include *extracellular* (*i.e.*, cell-surface) carbohydrate-mediated events and therapeutic angles.

A substantial portion of this project's efforts were spent researching the biology and biochemistry of the relevant biological setting for the investigation: assimilating the known science concerning the hyaluronic acid-mediated metastatic phenomenon, articulating this knowledge into a coherent working model, developing a hypothesis regarding the appropriate avenues for pharmacological intervention, assessing the feasibility of the proposed studies, and devising the necessary analytical and synthetic chemistry. This chapter describes how the overall project was developed from existing knowledge in the cancer biology and biochemical literature, and how the project coalesced into three broad research areas. The first of these research areas, preliminary biological screening, including experimental results obtained, is described in Section III of this chapter. Chapters 3 and 4 define the more detailed technical aspects of the two remaining arms of the project, and report the experimental results obtained.

B. Biological background

1. Traditional chemotherapy approaches

The chemotherapy of cancer has traditionally involved cytotoxic compounds that in some way interrupt one or more phases of the cell cycle. Tied in with the oncogenic event itself, this "cell-cycle approach," through the use of cytotoxic agents, has been the

mainstay of cancer chemotherapy. Successes, especially with soft-tissue and hematological cancers, have been impressive, and a plethora of antitumor compounds are now available to the oncologist.[3] Mechanism-based, targeted approaches to cancer chemotherapy have for over three decades attracted the attention of researchers. Both antimetabolites and drugs that act on DNA have received most attention, and these two drug types comprise most of the chemotherapeutic agents in use today.

Cancer as a disease is characterized by (1) uncontrolled cell growth, (2) a lack of cell differentiation, (3) invasion of other neighboring tissues, and (4) metastasis: the ability to establish new foci at sites remote from the primary neoplastic growth.[4] Cell-cycle drugs principally target the growth phenomenon. While either surgery or radiation can be an effective means for eliminating cancer at the primary site, failure to effect a cure in the patient most invariably is due to the presence of numerous micrometastases at remote sites. Chemotherapy, used in combination with surgery and radiation, has established itself as the traditional method of eliminating these micrometastatic colonies. However, a severe limitation in cancer chemotherapy is the fact that both antimetabolites and DNA-active drugs must, by their very mode of action, show toxicity toward normal cells. It is perhaps impossible to dissect the two activities apart, as normal cells and cancer cells share common nucleic acid pathways. Nonetheless, drugs having undesirable general cytotoxicities have become the mainstay of today's cancer chemotherapy.

2. Metastasis

Perhaps the defining element of cancer, and one having the well-deserved status of being the most life-threatening aspect of the disease, is the metastasis of tumor cells. The fixture of a cancer cell in a new site remote from the primary one is a multi-step process requiring that cell to have the capacity to perform the following: (1) loosen its adhesion to its original (primary tumor cell) neighbors, (2) migrate through other tissues to reach a blood vessel, (3) cross the basal lamina and endothelium of that blood vessel to enter circulation, (4) adhere to the endothelial wall in a new organ or tissue, (5) extravasate by crossing the basal lamina, and (6) migrate through the surrounding tissue to reach its ultimate colonization foothold.[5] Interactions between adhesive molecules on the cancer cell and on structural elements of the host now appear to be the molecular mechanisms by which these processes occur,[6] and the actual participants in several specific systems have been identified. Technically, these interactions fall into either scenario depicted in Figure 1. For example, human gastric carcinoma cells during step (4) display sialyl Lewis^x-containing carbohydrates on their surfaces which interact specifically with E-selectin proteins on liver cells[7] (*cf.* case II, a carbohydrate–protein binding event). A specific case of step (5) is represented by a protein–protein interaction between $\alpha_6\beta_4$ integrins on the tumor cell surface and laminin, a major component of the basal lamina.[8] (*cf.* case I)

3. The HA–CD44 metastatic interaction

Another recently discovered such interaction which appears to perform a critical

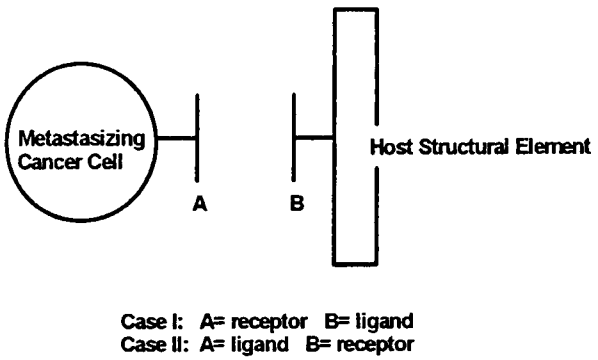


Figure 1. Interactions between adhesion molecules mediate cancer metastasis

role in the metastatic process is the interaction between the cancer cell CD44 receptor and hyaluronan (HA), a heteropolysaccharide of the host's extracellular matrix (ECM). This interaction mediates the translocation of the tumor cell during stages (2) and/or (6) above and constitutes a process of "cellular gluing" and/or "tracking" that is essential to the metastatic event. The HA–CD44 interaction constitutes the biochemical focus for the present studies.

Hyaluronan (HA, also referred to as hyaluronic acid) is a ubiquitous high MW polysaccharide (specifically, a glycosaminoglycan) that is synthesized in the plasma membrane and is associated with the host cell's extracellular matrix.[9] Its chemical structure is composed of a repeating disaccharide unit in which D-glucuronic acid is linked to the 3-position of *N*-acetyl-D-glucosamine, *i.e.* [β-D-GlcNAc(1→4)β-D-GlcA(1→3)]$_n$. Figure 2 shows the chemical structure of HA. HA's physical properties,

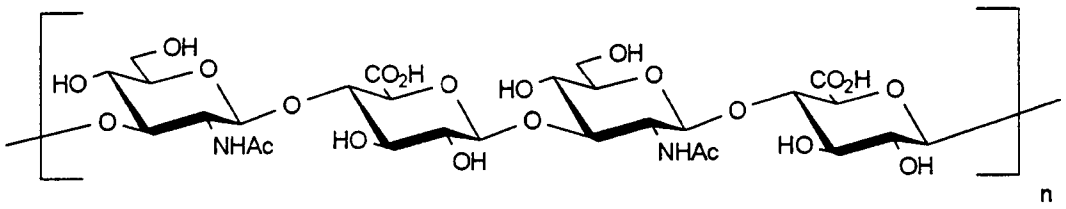
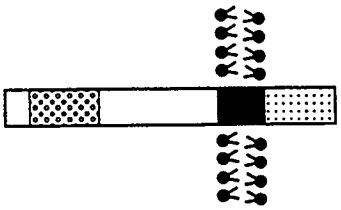


Figure 2. Hyaluronic acid

as well as its nontoxicity, have resulted in its being developed for numerous biomedical applications, such as eye tissue replacement, antiadhesive (for post-surgery), drug delivery, and anticancer applications.

The CD44 (CD = "cluster of differentiation") receptor protein, shown schematically in Figure 3, is a 75–120 KDa MW hyaluronic acid-binding protein expressed on the surface of a wide variety of cells (*e.g.*, leukocytes, fibroblasts, glial, Schwann, muscle, epithelial, and kidney cells). This cell-surface protein serves numerous biochemical functions, including angiogenesis, the binding of lymphocytes to endothelial venules during extravasation, macrophage aggregation, and general cell–ECM adhesion mechanisms. CD44 has also recently been found to play important roles in cancer metastasis, as discussed below.

The discovery that an interaction between HA and CD44 mediates a step in the metastatic sequence unfolded gradually and is still not completely understood. Early on, several lines of evidence indicated that HA facilitates tumor cell migration. As HA is



Amino acid sequence [13]

```
  1  MDKFWWHAAW GLCLVPLSLA↓ QIDLNITCRF AGVFHVEKNG RYSISRTEAA
                *                                          *
 51  DLCKAFNSTL PTMAQMEKAL SIGFETCRYG FIEGHVVIPR IHPNSICAAN
               *           *
101  NTGVYILTSN TSQYDTYCFN ASAPPEEDCT SVTDLPNAFD GPITITIVNR

151  DGTRYVQKGE YRTNPEDIYP SNPTDDDVSS GSSSERSSTS GGYIFYTFST

201  VHPIPDEDSP WITDSTDRIP ATRDQDTFHP SGGSHTTHGS ESDGHSHGSQ
         *
251  EGGANTTSGP IRTPQIPEWL IILASLLALA LILAVCIAVN SRRS
```

Domain structure

1–20	Signal sequence
31–121	Link
269–289	Transmembrane domain

Six potential N-linked glycosylation sites.

Alternatively, spliced variants are generated by the insertion of either a single exon, or a combination of exons, after residue 222.

Figure 3. The CD44 receptor protein (Adapted from Ref. 16)

synthesized in the plasma membrane and is extruded into the extracellular space, it becomes highly hydrated and expands the intercellular space, thus facilitating cell movement along HA-enriched tracks in the expanded space.[10] Carcinomas are usually associated with the production of large quantities of HA, located primarily at the interface of the tumor and the surrounding normal tissue,[11] and malignant tumors express high levels of HA-binding receptors.[12] Several lines of evidence go further by implicating the involvement of one protein in particular—CD44—in HA-mediated metastasis. Hart and co-workers demonstrated that melanoma cells expressing high amounts of CD44 show increased cell motility and increased metastatic potential compared to the same cell types that expressed low amounts of the receptor.[13] The connection between high CD44 levels and tumor-cell migration with respect to HA, and not some other ligand, has been described by Stamenkovitch[14] and Turley.[15] This distinction is important because CD44 also has binding regions for several fibrous proteins such as fibronectin and laminin; however, CD44's HA-binding activity is its most important interaction with a ligand.[16] It should also be mentioned here that CD44 is a normal component of healthy organisms, and it functions in a number of biochemical processes, as enumerated above.

4. CD44 isoform variability

Furthermore, due to the mechanism of variable splicing during transcription, CD44 is actually expressed as any of a number of isoforms that can vary significantly from one tissue to another. That metastasizing cancer cells modify and overexpress

CD44 for their own purposes was first confirmed by Günthert, Zöller, and co-workers, who identified and sequenced a novel "metastasis-promoting" splice variant of CD44, CD44V, from rat cancer cell lines. Their studies compared two cell lines, metastatic vs. nonmetastatic, of rat pancreatic carcinoma cells. Healthy animals injected with the nonmetastatic cells developed only a local tumor and remained healthy after excision of the tumor, while those injected with the metastatic cells developed metastases to the lungs and lymph nodes. CD44V was found to be expressed exclusively by the metastasizing tumor cells; normal rat tissues and even the nonmetastatic tumor cells expressed ordinary forms of CD44. The "metastasis-conferring" status of CD44V was fully earned in the remarkable finding that when the non-metastasizing cell lines were transfected with the CD44V-encoding genes, they began to overexpress CD44V and exhibited full metastatic behavior upon injection into healthy rats.[17]

With respect to the present studies, the subject of CD44 isoforms and their relation to metastasis warranted further investigation, since it appeared to be a potential snag in HA oligosaccharide-based drug selectivity (*vide infra*). The mechanism whereby HA binds to the CD44 receptor is indeed complex, and little is known about the steps in the binding activity. It should be pointed out that, while the CD44V isoform mentioned above is indeed involved in binding HA, the binding of HA to a particular isoform such as CD44V is not a prerequisite for antimetastatic activity. (Note: An isoform is defined as a variant that arises via a specific genetic alteration, either from different genes or from differently processed RNA transcripts from a single gene. Post-transcriptional

modifications, including phosphorylation, cell-surface modifications, and the like do not produce what are defined as isoforms.)

All CD44 isoforms appear to have the potential for binding to HA; however, most often the site(s) involved are "turned off" or "deactivated." Studies have demonstrated that "activation" of CD44 into a state capable of recognizing and binding HA is a part of the malignant transformation. The conclusion warranted by these studies, which are more fully discussed below in Section III.A.1., is that HA oligosaccharides intended as CD44 receptor antagonists for purposes of metastasis inhibition do not need to have structural features allowing them to distinguish between "metastatic" vs. "non-metastatic" CD44 in order to exhibit "selectivity."

5. Antimetastasis therapy

A potentially useful therapeutic approach has been investigated on the lines of the CD44V receptor by Zöller and co-workers.[18] These workers have developed monoclonal antibodies specific for CD44V and have demonstrated that injection of these antibodies, along with injection of metastatic melanoma cells, resulted in a significantly delayed onset of metastasis. Similar results have been found with a human melanoma cell line.[19] Furthermore, the antibodies were shown to completely inhibit the binding of the tumor cells to HA *in vitro*, thus confirming that there is an all-important CD44–HA binding taking place.

Complementing this work are studies on tumor-associated HA by Knudsen and

co-workers,[20] studies on general CD44 function by Underhill and co-workers,[21] studies on HA–cell interactions during embryogenesis by Toole and co-workers,[22] and recent studies by Cysyk and co-workers[23] on tumor cell–stromal cell interactions and HA biosynthesis.

II. STATEMENT OF THE PROBLEM

A. Hypothesis

The following questions prompted our planning: What can now be done to contribute to HA/CD44-mediated metastasis research? How can a "compound-based" or drug design-based approach be applied to develop a therapeutic agent? To facilitate our own thinking, we began by assimilating all the work described in the preceding section (since these reports had not been the subject of a review article), and summarized it by picturing the schematic metastasis model depicted in Figure 4. The scenario is as follows. Migrating cancer cells release paracrine growth factors that induce host cells in adjacent stroma to produce increased amounts of extracellular HA. The cancer cells then make use of their CD44 receptors to bind to and migrate along the newly synthesized HA tracks into new tissues, spawning metastases.

Although it has not been addressed anywhere in the literature, it seemed obvious that one possible approach would be to determine if small oligosaccharide molecules could be used as competitive inhibitors for CD44 receptor sites. This became our central hypothesis:

METASTASIS INHIBITION VIA CD44 RECEPTOR ANTAGONISM:

→If HA polysaccharide strands are used as "tracks" for cancer cell migration, then small HA oligosaccharide molecules should inhibit the binding to these tracks, thus blocking metastasis.

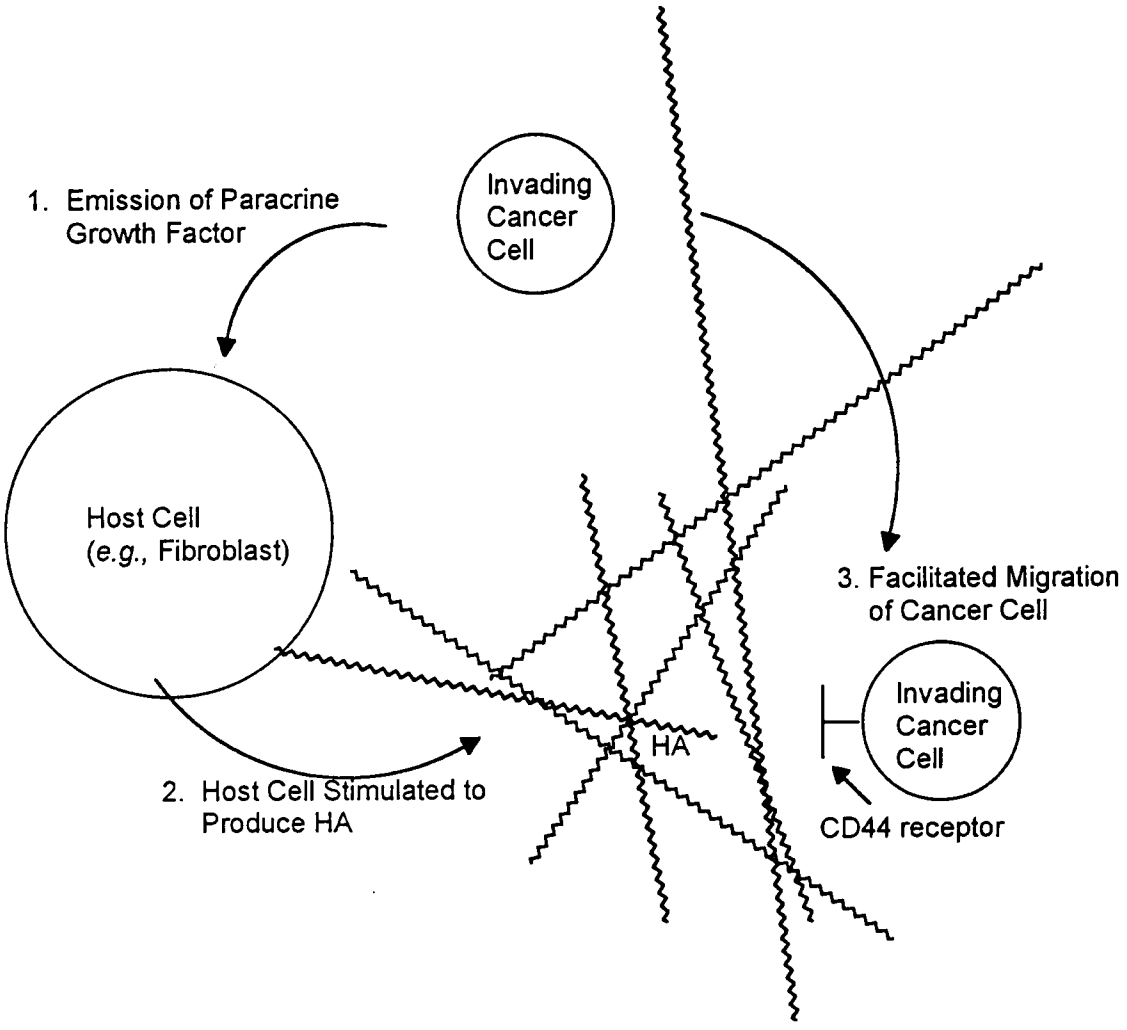


Figure 4. Current model of HA/CD44-mediated cancer metastasis

Figure 5 illustrates this pictorially by showing what might happen if the original metastasis scenario (*cf.* Figure 4) is amended by the introduction of small HA oligosaccharide molecules. We propose that these oligosaccharides might out-compete extracellular matrix HA for the limited number of CD44 receptor binding sites, with the result that cancer cells can no longer anchor themselves to and migrate along HA tracks into new tissues.

Although simplistic, we noted that this hypothesis was not outlandish. Interestingly, there was literature precedent for the general idea of inhibiting metastasis via substituting a fragment motif for the larger (natural) biopolymer ligand of a metastasis-involved receptor. Studies by Humphries, Gehlsen, and Kumagai, which in essence are "peptide-based" analogs of the present approach, focused on integrin–protein interactions, making use of defined tripeptide sequences[24] or cyclic peptides[25] as small molecule mimics for the natural fibronectin protein ligand. In all cases, the reduction in B16F10 melanoma metastasis in a murine model was dramatic. Hopefully, similar results could be obtained in our carbohydrate-based studies.

B. Formulation of research questions and project goals

Stated in broad terms, the goal of this project was to develop oligosaccharide probes to better understand the HA–CD44 metastasis interaction and to possibly function as antimetastasis drug candidates or leads.

In the course of analyzing the HA–CD44 literature, we also identified three major

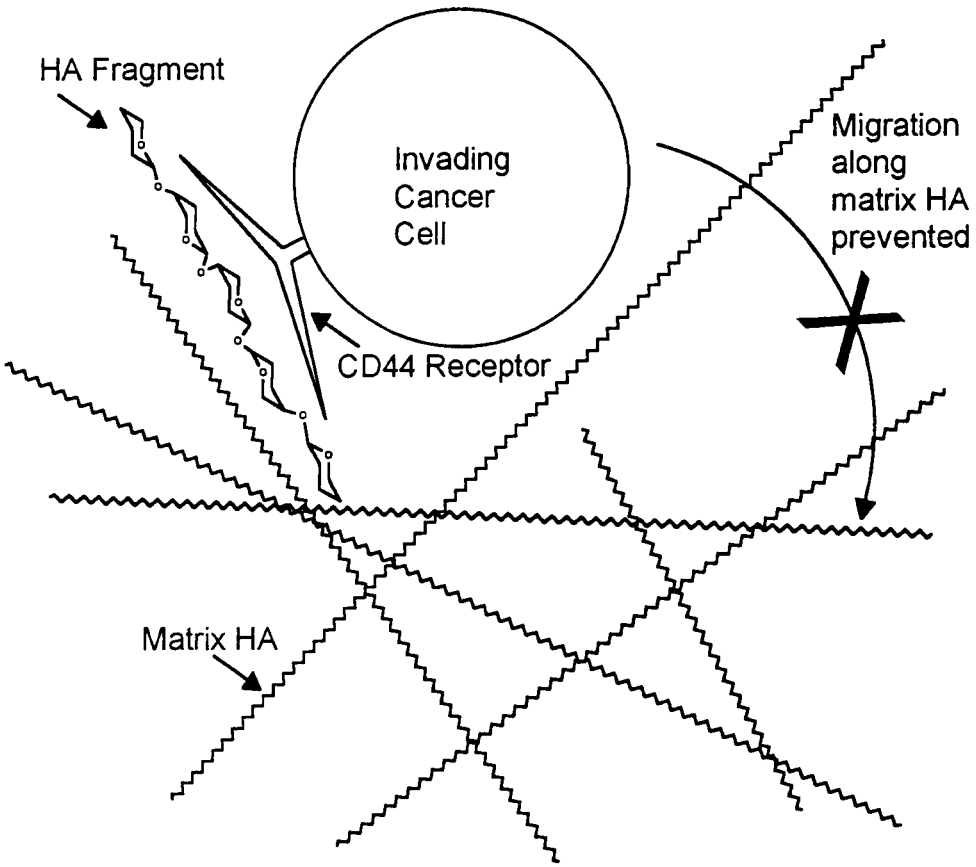


Figure 5. Hypothetical inhibition of metastasis via CD44 receptor antagonism

areas in which crucial information was lacking. These knowledge gaps implied groups of specific research questions that in turn generated the three basic thrusts of our project, summarized as follows:

- *Biological Feasibility Questions* — Will HA oligosaccharides *actually work* as metastasis inhibitors?
- *Materials Questions* — What is known about HA Oligosaccharide Structure?
- *Drug Development Questions* — Even if HA oligomers are active, can a real drug ever be developed from the idea?

This section discusses the development of these research questions and goals. As mentioned in section I.A., these three points are outlined here in general terms only. The science is fully elaborated with more extensive technical details in section III of this chapter, and in Chapters 3 and 4.

1. Biological feasibility

The crucial question, of course, is one of biological feasibility. Although the basic model is supported in the literature, there are many details about the question of the HA–CD44 metastasis model that are not well understood. Is "metastasis inhibition via CD44 receptor antagonism" a sound hypothesis? In other words, will the oligosaccharides actually work in the manner we think they will? Furthermore, it must

be remembered that there are other cancerous and noncancerous functions of HA and CD44 besides metastasis mediation. How will these be affected by the introduction of extraneous HA oligosaccharides? Will there be negative side effects? Finally, there is the issue of CD44 isoform variability. Is there a particular isoform of the protein responsible for metastatic behavior? Must the HA oligosaccharide agent distinguish between cancerous and noncancerous CD44 isoforms? We resisted the temptation to be discouraged by these possible scenarios in which the compounds would not be active, and decided to first attempt to obtain empirical evidence that the approach would work. As the initial biological evaluation would have to include all these factors, *in vitro* assays examining only isolated variables were ruled out in favor of an *in vivo* whole animal (mouse) model that was already available through collaborators at the National Cancer Institute (NCI). Thus:

GOAL #1: To determine the viability of the metastasis inhibition hypothesis through first-generation probes in a *whole animal model.*

→Biological studies in conjunction with the NCI

2. Chemical structure

The second major issue involved the selection of which particular HA oligosaccharides to use as probes. The fastest way to get HA oligomers is by enzyme degradation of high molecular weight HA (not by synthetic means). Via this route, access to oligosaccharides dp 4–30 is achieved using digestion and chromatographic procedures in the literature. Several enzymes that are routinely used to degrade HA are

available (see Chapter 3 for details). Hyaluronate lyase (EC 4.2.2.1, from *Streptomyces hyalurolyticus*) is the most widely used. The first stage of the project would utilize this enzyme. Later stages could expand into the use of other enzymes. Structure–activity relationships are expected to emerge from the B16F10 murine melanoma studies (Goal #1 above) that will serve to guide further work on enzymatic cleavage. Enzymatic cleavage conditions will be varied to produce those ranges of dp that show maximum biological activity.

Questions begin to crop up with regard to the chemical structures of these enzymes' digestion products. Despite the current widespread interest in HA, enzyme-derived HA oligosaccharides have not been satisfactorily characterized: their use has been reported frequently in the literature for the past 20 years, yet the studies have continued to rely on the characterization in the early papers that used colorimetric methods. Clearly, it is absolutely essential to have *precise structural data on the compounds being investigated* if meaningful biological correlation with structure is desired. It became clear that an analytical arm to the project would have to be developed. Fortunately, two of the newest and most powerful analytical tools in carbohydrate chemistry were available to us: an electrospray-ionization mass spectrometer, and a Dionex high-performance anion-exchange chromatography system with pulsed amperometric detection. Thus:

GOAL #2: To prepare, isolate, and *characterize* HA oligos derived from enzyme degradation of polysaccharide HA.

→Digestion, preparative separation:

stage one: hyaluronate lyase

stage two: testicular and leech hyaluronidases

→Characterization: Dionex HPAEC-PAD, Electrospray-ionization MS

3. Drug development

Finally, the third set of questions concerns practical aspects of using the HA oligosaccharides as antimetastasis drugs. That is, even if the HA oligosaccharides prove to inhibit or prevent metastasis in laboratory animals, can a *real drug* ever be developed from the idea? The chief problem is that HA oligosaccharides are unstable in the human body. There are specific enzymes, hyaluronidases, that rapidly hydrolyze the glycosidic bonds, with the result that their *in vivo* half-life might be only a few minutes. This circumstance renders them poor drug candidates. Fortunately, there are several types of structural modifications that can be made to an oligosaccharide that make it resistant to such hydrolase action. Thus:

GOAL #3: (If warranted by the successful outcome of biological tests) To design and synthesize *physiologically stable* HA-oligosaccharide analogs.

→Convergent synthesis is desirable should oligomers dp > 5 needed.

C. Significance of the proposed studies

In order to justify embarking on a project of this magnitude, it is necessary to

examine it in the context of existing science to ascertain its novelty and significance.

1. With respect to biomedical science

The present project, namely the probing of antimetastatic activity with oligosaccharides derived from HA with the aim of developing small, stablilized molecules that will bind to CD44, occupies a unique and significant niche in biomedical science for the following reasons:

- There are no existing studies demonstrating a small-molecule carbohydrate inhibition of metastasis.
- Crucial knowledge about the molecular basis of metastasis would be gained, and a promising drug lead might be uncovered that can complement existing clinical treatments by focusing on metastasis rather than on tumor eradication.
- The therapeutic approach is different than traditional chemotherapy "cell-kill" methods: the chemical agents would *modify the behavior* of cancer cells rather than killing them.
- Intervention is at the cell-surface level: chemical agents are not required to cross cell membrane or disrupt cellular metabolic pathways, thus avoiding common toxicity and delivery problems.
- There is currently an intense interest in the HA–CD44 phenomenon in general; probing the interaction at the molecular level would complement existing work.

To date, we have found no studies in metastasis involving specific HA-derived compounds. One paper describes a study of the binding of an HA-hexamer,[26] derived from HA by a hyaluronidase of testicular origin, and showed that binding to CD44 was competitive with HA; however, the antimetastatic activity was not determined.

The proposed studies of metastasis inhibition via a small-molecule pharmacological intervention at the cell surface stand in sharp contrast to traditional medicinal chemistry approaches in cancer chemotherapy that are focused on poisoning the internal workings of the cell (the cell cycle) via cytotoxic agents. The approach would be refreshingly novel, since—by involving essentially only cell-*surface* phenomena—it would avoid the formidable common problems of dose-limiting toxicity and drug delivery through the cell membrane.

Heretofore, therapies designed to prevent clinical metastasis with tumor–ligand adhesion blocking agents have not been developed, in part due to the presumption that, invariably, micrometastases are already present at the time of diagnosis. However, recent studies suggest that a successful approach might be to target individuals at high risk for certain types of cancer and "immunize" them by filling up cancer cell adhesion receptors with ligand-mimic drugs.[27] One could envision a therapeutic approach that would involve either surgical removal or radiation therapy on the primary tumor, followed by a treatment with a CD44 antagonist that would, in cases of highly metastatic tumors, prevent metastasis. In cases of highly metastatic forms of cancer, a metastasis inhibitor could prolong life, especially in cases where the primary tumor is untreatable.

Such an approach using non-HA type compounds as ligand-mimicking drugs to effectively block cancer-cell adhesion has been suggested for patients at high risk of metastasis.[28] In any case, a detailed investigation into finding a potent CD44 receptor antagonist is sufficiently warranted by the need to more fully understand molecular mechanisms of cancer metastasis, and by the likely prospect that future clinical developments will eventually ensure a niche for such a compound in the arsenal of efficacious anticancer drugs.

There has recently appeared a plethora of peer-reviewed biological papers on HA–CD44 binding, indicating that this interaction has aroused a considerable interest in the biomedical research community. The year 1996 alone saw several review articles devoted to this topic, most notably those of Sy, Knudson, and Entwistle.[29] We were particularly heartened by the congruence of Entwistle's arguments with the aims and scope of our own proposal on probing CD44–HA metastatic interactions: "The elucidation of the molecular mechanisms regulating HA-mediated events will not only contribute greatly to our understanding of a variety of disease processes, but will also offer many new avenues of therapeutic intervention." As discussed earlier, the phenomenon of CD44's existence in a number of isoforms is still not well understood and has the potential of raising legitimate questions as to the viability of our proposed studies. In addition to the points enumerated above, which we believe show that our approach is anything but disqualified by the existence of multiple isoforms, several studies have continued to support these points by showing that metastatic CD44 is

indeed activated to bind to HA and is often a key development in the malignant transformation of cells.[30] The interest in cancer-related CD44–HA interactions is broad and not merely limited to the particular scenario of the melanoma–lung locale focused upon by our biological model. For example, in the last year a number of reports have provided evidence that HA–CD44 binding is involved in several different types of neoplastic growths such as pancreatic,[31] ovarian,[32] breast,[33] colon,[34] prostate,[35] and brain[36] cancers. HA has also found other applications in cancer treatment as a drug-delivery agent,[37] and hyaluronidases have been found to have uses in anticancer therapy as well.[38] Clearly, the broad spectrum of the HA–CD44 phenomenon adds significance to our proposed work of probing the interaction at the molecular level.

2. With respect to analytical and synthetic oligosaccharide chemistry

In addition to these biomedical considerations, the outlined strategy of implementing extensive chemical methods of structure elucidation and synthesis represent novel and significant advances in their own right:

- The analysis of HA via HPAEC-PAD or ESIMS has not yet been reported, and the developed methods would be potentially useful for the general field of glycosaminoglycan analysis.
- Convergent syntheses of hydrolytically stable oligosaccharides of the type evisioned herein (*vide infra*) have not yet been reported, and would be potentially useful in oligosaccharide synthesis in general.

These latter two points are discussed in greater detail in Chapters 3 and 4, respectively.

Finally, this project offers significant opportunities for rewarding spinoff work, which might become the main focus of later projects, or which might replace a failed effort in part of the planned research. Several possibilities come to mind:

- Development of stabilized, fluorescent tagged oligosaccharides for probing the activated CD44 receptor. These much needed probes would be developed along the lines of work in related areas, for example, with a fluorescent tag used to probe cell-surface glycoprotein interactions.[39]
- Work toward stabilizing the natural oligosaccharides from the enzyme digests of HA. A similar effort, for example, of van Beockel, Petitou, and co-workers (at Organon and Sanofi) in the heparin field has produced[40] what may become a small-molecule replacement for heparin.[41]
- Expansion into other cancer areas. With knowledge that other tumor systems may have suitable "activated" CD44 receptors, it would be logical to expand into these areas. Ovarian and prostate cancer, for example, might be prime targets for this type of research. The "wait and watch" approach to prostate cancer among the elderly could be a possible area for useful adjunct therapy with a nontoxic antimetastatic drug.

III. BIOLOGICAL EVALUATION OF HYALURONAN OLIGOSACCHARIDES AS METASTASIS INHIBITORS

A. Preliminary considerations

1. Potential CD44 and HA side reactions

It remained to be proven by experiment that the compounds would actually inhibit metastasis. There are several reasons why it is important to establish at an early stage in this project that possible "side reactions" of HA fragments will not prevent metastasis inhibition. These reasons include the biochemical involvement of HA and CD44 in other cellular events and the matter of CD44 isoform heterogeneity, which will now be discussed in detail.

As pointed out in Section I.B., CD44 is present to varying degrees on a wide variety of cells, such as leukocytes, fibroblasts, glial, Schwann, muscle, epithelial, and kidney cells.[42] In addition to a role in cancer metastasis, the various isoforms of CD44 are involved in other biological functions, such as angiogenesis, receptor-mediated HA degradation, the binding of lymphocytes to endothelial venules during extravasation, HA-dependent macrophage aggregation, and general cell–ECM adhesion.[43] Problems associated with angiogenesis are a particularly worrisome prospect, since angiogenesis is a facilitating factor in tumor growth. West and co-workers have reported that HA fragments 8–50 saccharide units in length actually *stimulate* angiogenesis,[44] probably through an indirect activation of macrophages, neutrophils, or other cell types, although

the mechanism is not well understood. It is thus possible that the introduced HA oligosaccharides might have a cancer-promoting effect rather than an antimetastatic effect.

Another issue with uncertain repercussions is the phenomenon of CD44 receptor-mediated HA degradation. This process, which has been experimentally confirmed by Underhill,[45] Orkin,[46] and co-workers through studies on chick embryo and SV-3T3 fibroblasts, vascular tissue cells, and macrophages, is thought to occur as follows: CD44 binds a strand of HA, after which it is endocytosed, transferred to a lysosome, and degraded by acid hydrolases. Underhill even speculates that this process might also be part of the mechanism by which tumor cells migrate through an HA matrix. However, the size requirements that govern which small HA-oligosaccharides are degraded, and/or which inhibit the degradation of larger HA strands are not well understood.[47]

The subject of CD44 isoforms and their relation to metastasis aroused our concern, since on first appraisal it appeared to be a potential snag in HA oligosaccharide-based drug selectivity. For example, perhaps Günthert's CD44V isoform is exclusively the "metastatic CD44 isoform." A viable drug candidate, such as the intended HA oligosaccharides, would thus need to distinguish "normal (*i.e.*, non-cancerous)" HA isoforms from "metastatic HA" isoforms in order for it to have "selectivity." However, upon closer investigation of the literature, we found that several recent studies on HA–CD44 binding disqualified such an objection. First, while the CD44V isoform mentioned above is indeed involved in binding HA, the binding of HA to a particular

isoform such as CD44V is not a prerequisite for antimetastatic activity. All CD44 isoforms appear to have the potential for binding to HA; however, most often the site(s) involved are "turned off" or "deactivated." Studies have demonstrated that "activation" of CD44 into a state capable of recognizing and binding HA is a part of the malignant transformation. For example, cells displaying CD44, but not capable of binding HA, were treated with phorbol esters (known tumor promoters) and subsequently developed the ability to bind HA. The cellular-based events thought to be responsible for this change are either (1) phosphorylation of certain cytoplasmic subunits of CD44 or (2) particular cell-surface aggregation effects of CD44.[48] Most remarkable is the recent finding by Günthert and co-workers that metastatic cancer cells previously binding to HA can develop the ability to dissociate from HA by shedding their CD44 receptors![49] The result of this research is that one can conceptually partition CD44 isoforms into "activated" vs. "inactivated" with respect to HA binding, which is essentially independent of minor protein differences associated with isoform variation. Thus, the proposition that *CD44V exclusively* should be the proper target for study and SAR is invalid. The "metastasis receptor" is not a particular HA-binding site of a particular isoform; it is simply an HA binding site on an "activated" CD44 molecule. In short, selectivity depends on activation of CD44 receptor binding to HA, not on purported differences in the binding motifs of the proteins. Nevertheless, the question of CD44 isoforms is still not fully understood, and might hold other unforeseen problems.

Finally, the initial screenings could provide information about the minimum

length of oligosaccharides required for CD44 recognition by the specific cancer cell types to be used in this study,[50] and thus required for a potential antagonist. Despite its having been widely reported in the literature that CD44 requires a minimum hexasaccharide domain for recognition, those results have been obtained by the study of a few particular cell types[51] and may not necessarily be general.

As warranted by the reasons discussed above, then, it is important to establish at an early stage in this project that possible "side reactions" of HA fragments or isoform-related problems will not outweigh or interfere with the inhibition of cancer metastasis to such an extent as to result in an observed lack of metastasis inhibition, a promotion of metastasis, or an occurrence of undesirable side effects. The objective of the present studies was to demonstrate, through a whole animal *in vivo* model, that HA oligosaccharides can in fact inhibit metastasis.

2. Selection of appropriate biological test

Careful consideration needed to be given to the particular cancer model being used. Primarily, a simplified, rapid system for determining lead candidates was needed. There are several *in vitro* methods used in the literature to evaluate various aspects of the HA oligosaccharides' effect(s) on CD44-bearing cancer cells. Such types of tests are often invaluable in giving specific details about the mechanism by which an observed effect occurs. For example, to determine whether or not the oligosaccharides interfere with cell movement, the Boyden *in vitro* cell invasion assay with Matrigel as the

basement membrane could be used.[52] To determine the degree that the small HA oligosaccharides compete with native high-MW HA for the CD44 receptor, experiments developed by Toole, Underhill, and Knudsen,[53] could be used: the cells are first treated with [^{3}H]-HA , after which they are exposed to varying concentrations of oligosaccharide which "compete off" a fraction of the initially bound native ligand. Radioactivity monitoring then allows this fraction to be calculated, providing a %-inhibition figure.

As outlined above however, there are numerous other factors at work. Suppose an *in vitro* assay shows that HA does inhibit the invasiveness of cells. By isolating this effect, the positive result does not reflect other *in vivo* factors which might outweigh, negate, or inhibit that process. This potential scenario led to our selection of the primary screen being used, namely, the *in vivo* lung metastasis model using intravenously (i.v.) implanted B16F10 melanoma cells. B16F10 melanoma cells can be grown both *in vitro* (prior to injection) and *in vivo* in the mouse. When injected i.v. into the mouse, they metastasize directly to the lung, thus allowing an *in vivo* assessment of antimetastatic activity with a drug substance. Oligosaccharides would be evaluated for their ability to alter the formation of lung tumors in mice following i.v. injection of B16F10 melanoma cells, and for their ability to extend the life-span of mice inoculated with B16F10 cells. This system is a very manageable one that is known to give reliable and reproducible results. Furthermore, it is a valid choice since the B16F10 cells *do* express CD44 and have been shown by experiment to bind HA. Finally, the model is so well established

and credible that data derived from it are readily accepted in the scientific community, and easily compared with data from numerous other studies done on the same system.

The *in vitro* tests mentioned above are planned, subsequent to the completion of the *in vivo* tests. However, further discussion of this subject is beyond the scope of this dissertation.

B. Results and discussion

Biological evaluations of all HA oligosaccharides were conducted in the Biochemistry Section, Laboratory of Medicinal Chemistry at The National Cancer Institute, Bethesda, MD under the direction of Dr. Richard L. Cysyk.

Individual oligosaccharides, as well as mixtures of oligosaccharides, crude digests of HA, and high-molecular-weight HA itself, were all evaluated according to the same procedure, as illustrated schematically in Figure 6. In the control set of experiments (shown in the first line), the cells were injected into the tail vein as usual with no treatment with HA. In the second set of experiments, the cells were first pre-incubated with HA oligomers. After 10 days, the lungs of both sets of animals were excised and examined for metastatic colonies.

It was anticipated that a reduction in metastasis would be observed in the mice whose B16F10 cells had been pre-treated with HA oligosaccharides. In the event, not only did pre-treatment with HA reduce metastasis: there was a near-total absence of metastatic colonies in the lungs of the mice receiving the HA oligosaccharide pre-treated

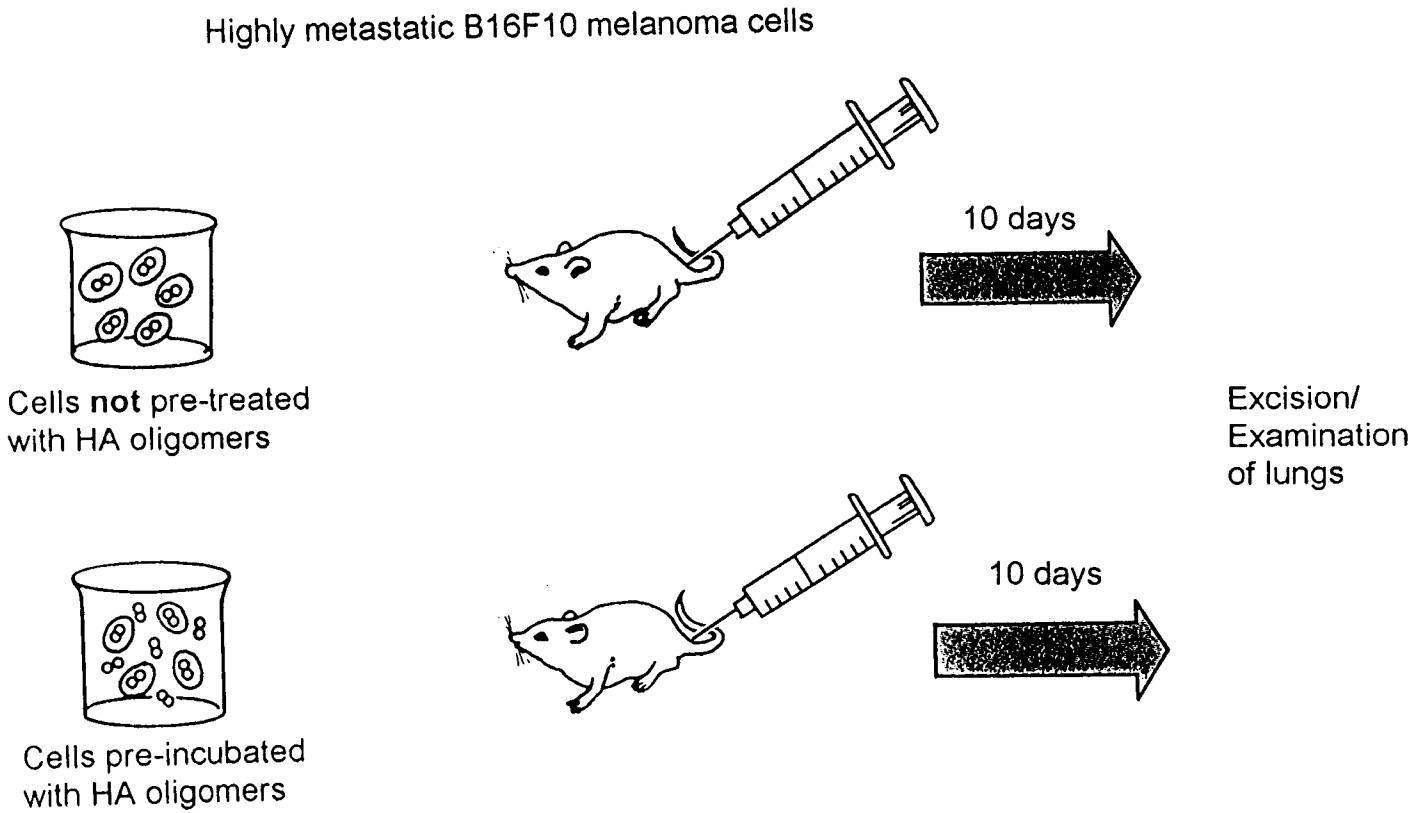


Figure 6. B16F10 Melanoma metastasis model

B16F10 cells. Figure 7 shows a typical set of results. The left panel, A, shows the lungs excised from the treated mice, where there are only about six or fewer metastatic sites observed. Panel B shows lungs of untreated mice, where the lungs are literally speckled with 400–500 sites/lung.

The experiments have been repeated with identical results using a variety of controls. For example, B16F10 cell viability was checked in the presence of HA oligosaccharides, as well as in the presence column effluent, buffers, etc. Experiments using double and triple the amount of oligosaccharides (up to 3 mg/mL) were carried out to identify possible toxic effects of the digest on the melanoma cells, and no toxicity was found (as determined by cell viability assays). A similar experiment with high-MW HA itself (1 mg/mL) shows an antimetastatic effect; however, the fact that the purified (gel-permeation chromatography) oligosaccharides (free of high-MW HA) are active as metastasis inhibitors indicates that a relatively small molecule can function as an antimetastatic probe, which is essential to our proposed research. Work is ongoing to determine structure–activity relationships (SARs) among the oligosaccharides (activity vs. dp). Preliminary studies indicate that activity sets in with the 8-mer (*i.e.*, oligomers smaller than dp 8 are only weakly active).

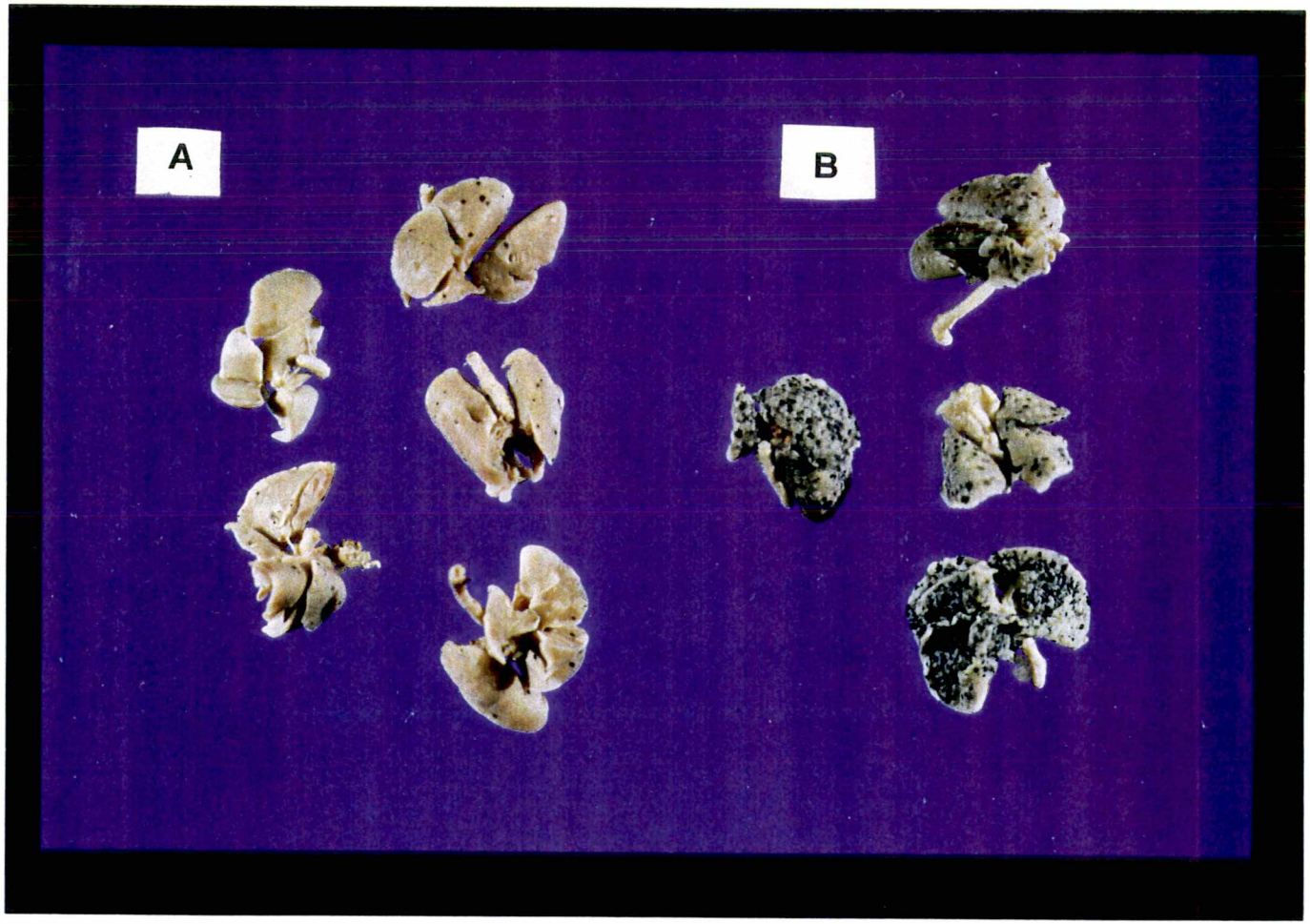


Figure 7. Excised mouse lungs showing inhibition of B16F10 melanoma metastasis by HA oligosaccharides

C. Conclusions

Oligosaccharides derived from HA by hyaluronate lyase degradation show a profound antimetastatic effect on B16F10 melanoma as shown by the *in vivo* murine model. The mechanism for the effect is undoubtedly complex and, in a sense, a biochemical black box. While it is still premature to conclude that the hypothesized "CD44 receptor antagonism by HA oligosaccharides" is the precise mechanism which accounts for the observed inhibition of metastasis, the results provide strong evidence that the stated hypothesis is a viable explanation, and provides ample justification for our continuing efforts in the analytical and synthetic arenas.

D. Experimental Section

1. *In vivo* metastasis model.

B16F10 cells, maintained in log-phase culture, were removed from flasks with EDTA, washed, and incubated with or without HA oligosaccharides (in a concentration of 1 mg/mL). Into the tail vein of each mouse was then injected a total of 2.5×10^5 cells (in 0.2 mL). After 10 days, the mice were anesthetized with an intraperitoneal injection of chloral hydrate and sacrificed by cervical dislocation. The lungs were removed and placed in a preservative/fixative. Discrete colonies of metastasized B16F10 melanoma were counted using a dissecting microscope.

2. Description and justification of the use of animals.

The animals used were CDF_1 male mice, 20–25 g. Animals were used because they provide the available model for tumor invasion and metastasis. The B16F10 melanoma grows well in CDF_1 mice and metastasizes specifically to the lungs. There is no appropriate *in vitro* model that can provide metastatic data as significantly as the B16F10 *in vivo* model. The number of mice (25/week, 25 experiments) is the fewest that can provide statistically significant results. The NIH animal facility is under the supervision of a veterinarian. The facility is an approved facility and operates fully within approved guidelines. All work with vertebrate animals was approved by the NIH's Animal Care Committee under Protocol No. LBC-005, approved 6/18/95. The Animal Welfare Assurance No. is A-999.

3. Limiting discomfort and distress.

To prevent pain and discomfort to the animals, they were anesthetized with chloral hydrate prior to sacrifice by cervical dislocation. Lungs were removed after death of the animal. This method is consistent with the recommendations of the Panel on Euthanasia of the American Veterinary Medical Association.

ISOLATION AND CHARACTERIZATION OF HYALURONAN OLIGOSACCHARIDES DERIVED FROM DIGESTION WITH HYALURONATE LYASE (EC 4.2.2.1) AND BOVINE TESTES HYALURONIDASE (EC 3.2.1.35)

I. INTRODUCTION

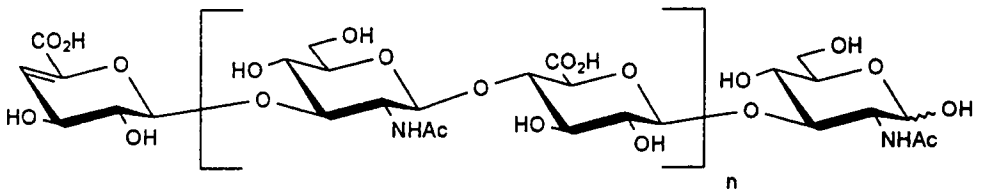
A. Enzyme digestion-derived HA oligosaccharides

As rationalized in the preceding chapter, we chose to employ oligosaccharides derived from digestion of HA with various hyaluronidases. A closer look at the available HA-degrading enzymes is now appropriate. The chief ones are:

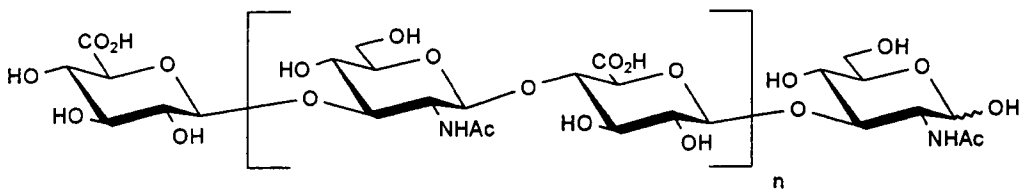
- Hyaluronate lyase (HAL, EC 4.2.2.1, from *Streptomyces hyalurolyticus*)
- Hyaluronidase (BTH, EC 3.2.1.35, from bovine testes)
- Hyaluronidase (EC 3.2.1.36, from leech heads)

The present studies focused on hyaluronate lyase and its resulting oligosaccharides. In addition, later work was extended to HA fragments from bovines testes hyaluronidase. Leech head hyaluronidase is not addressed.

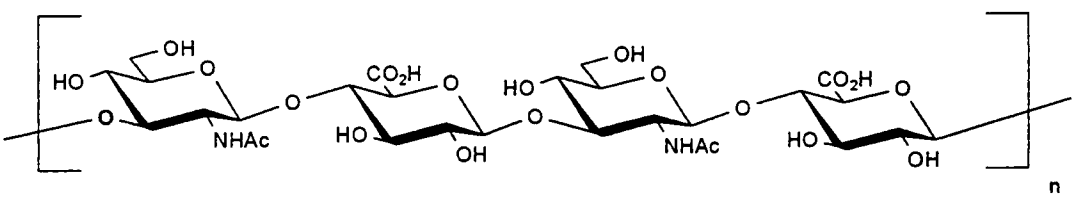
Figure 1 shows the general structure of HAL- and BTH-derived fragments (**1** and **2**, respectively) alongside the structure of native HA (**3**). As heretofore described in the literature, hyaluronate lyase is an *endo*-hexosaminidase, producing even-numbered



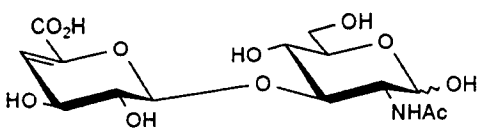
1



2



3



4

Figure 1. HA fragment oligosaccharides derived from enzyme digestion

fragments of structure $^{\Delta 4,5}$ β-D-GlcA(1→3) [β-D-GlcNAc (1→4)-β-D-GlcA]$_n$(1→3)β-D-GlcNAc (**1**).[1] This enzyme is perhaps the one used most often to afford fragments of HA since its eliminase activity introduces an α,β-unsaturated carboxylic acid moiety at the nonreducing end, thus providing oligomers with a convenient UV chromophore.[2] It should be noted that this enzyme is distinct from other, more obscure HA lyases that have been isolated from *streptococcal*[3] or *staphalococcal*[4] microbes. Bovine testes hyaluronidase is also considered to be an *endo*-hexosaminidase, but differs from HAL in that it is a true hydrolase, and thus does not introduce the double bond. The products thus have a nonreducing *saturated* D-glucuronic acid terminus: β-D-GlcA-(1→3)-[β-D-GlcNAc-(1→4)-β-D-GlcA]$_n$-β-D-GlcNAc (**2**). Digestion procedures and preparative-scale oligosaccharide purification protocols for these enzymes are adequately documented in the literature.[5]

Despite their frequent use in the biochemical literature, however, we found that these digestion products have not been rigorously characterized. In the case of HAL, the oligomers were studied primarily by Linker and co-workers,[6] who characterized them via UV and chemical analysis (*e.g.*, comparison of the extent of Br_2 and H_2 consumption vs. glucosamine content after hydrolysis). Later studies by Shimada and Matsumura used UV measurements in conjunction with Morgan–Elson, carbazole, and thiobarbituric acid assays (to determine total uronic acid and/or glucosamine content).[7] The smallest oligomer reported to be produced is the tetramer, and the remaining oligomers consisted of successive even-numbered oligosaccharides. It should be noted that, although the

unsaturated HA disaccharide **4** (Figure 1) has been characterized by NMR methods,[8] this entity (which is commercially available) is actually obtained from chondroitinases, not from HAL. The BTH products were studied primarily by Meyer and co-workers, who characterized them via Morgan–Elson assays,[9] and later by Rodén and co-workers, who used viscometric methods to estimate the average MW's of isolated oligosaccharide fractions.[10] A later report provides NMR studies on the tetrasaccharide.[11] Interestingly, the numerous biochemical and cell biological studies that use these oligosaccharides have continued to rely on these assignments without further augmentation using newer available analytical methods. Clearly, if meaningful SAR information is going to be derived from the biological evaluation of these compounds, it is necessary to have the more rigorous structural characterization that is now possible. In addition to these obvious considerations dictated by our biological studies, the desire to characterize these compounds by more modern methods was further prompted by our isolation of unpredicted oligomers from the reaction mixture (*vide infra*). These factors introduced a degree of uncertainty which, with respect to the dramatic antimetastasis experiments described in Chapter 2, placed us in the uncomfortable position of having to essentially say "we have some extremely potent antimetastasis compounds, but we don't know exactly what they are." Thus, a major focus of the project became the precise characterization of these compounds by modern analytical methods. These studies are the subject of this chapter.

B. Electrospray–ionization mass spectrometry

Electrospray–ionization mass spectrometry (ESIMS) has emerged in the last few years as a powerful new tool for carbohydrate analysis.[12] In contrast to more traditional MS methods such as fast-atom bombardment (FAB) and electron impact (EI), the electrospray method generates ions in an extremely gentle manner according to the process shown in Figure 2. After a solution containing the analyte is sprayed into a fine mist of droplets, evaporation of solvent results in a shrinking droplet whose increasing concentration of (nonvolatile) ions eventually attains such a high state of repulsive interactions that a "coulombic explosion" occurs in which even finer droplets are produced. Further evaporation results in analyte ions that are effectively de-solvated, thus allowing them to acquire a measurable *m/z*. By circumventing the problem of the normally unattainable high vapor pressure that polar carbohydrate molecules have, the fragile glycosidic bonds (which often do not survive traditional mass spectral conditions) remain intact during the electrospray process.[13] This gentleness has translated into success in visualizing delicate and highly polar biomolecules such as proteins, carbohydrates, and nucleic acids.

Most of the ESIMS studies involving carbohydrates have been conducted on neutral oligosaccharides. In particular, the field of protein glycosylation has benefitted from the resulting data, since molecular weights of complex oligosaccharide–peptide conjugates can be directly observed.[14] Glycosaminoglycans are an important class of heteropolysaccharides that have been eliciting increased attention due to their

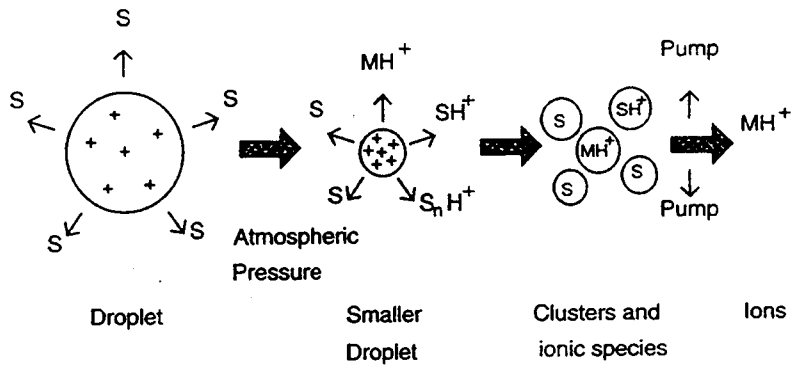


Figure 2. Generation of ions via electrospray process (taken from Reference 13)

involvement in a number of biochemical/medical processes.[15] Some important glycosaminoglycans include heparin, chondroitin sulfate, and hyaluronan. The distinguishing structural characteristics of these carbohydrates are the presence of amino (or acetamido) groups, and the extensive presence of anionic carboxylate and/or sulfate groups. The arrays of anionic groups have caused glycosaminoglycans to be more difficult to characterize than neutral sugars. There are only a few studies on anionic oligosaccharides using ESIMS in the literature.[16] With respect to hyaluronan, the only existing study is that by Zhao and co-workers, who observed ESIMS signals corresponding to covalent complexes between HA *di*saccharide fragments and peptides.[17] In conjunction with these few studies, an application of negative-ion mode ESIMS on larger oligomers would therefore be important in further demonstrating the usefulness of this tool in the area of glycosaminoglycan analysis. As we began our own studies on much larger HA oligos (dp 3–16), Arpino and co-workers reported a study

of small oligogalacturonic acid oligosaccharides (dp 4–7) under negative-ion ESIMS and queried to what extent the sugars would polyanionize as the dp increased to larger values than those they studied: "It would be interesting to verify whether the number of negative charges also increases with increasing dp values, as is the case for peptides with an increasing number of basic residues."[18] Our studies on much larger anionic oligosaccharides shed light on this matter.

C. High-performance anion-exchange chromatography

In conjunction with the mass spectral characterization, we sought to develop a convenient screening protocol to assess the identity and purity of fractions from our preparative scale gel-filtration chromatography of HA digests. The requisite method should also be suited for use in the work planned with BTH, whose digest products do not possess the convenient α,β-unsaturated acid UV chromophore. There are serveral problems associated with detecting non UV-active sugars. Methods utilizing low wavelength cells to detect the $-CO_2^-$ group absorption often suffer from interference from other groups, and inordinately limit the choice of buffer eluents (which typically employ acetate or formate salts). Refractive index is also used, but its well known capriciousness can pose significant experimental delays and snags. Cowman and co-workers have used chemical analysis of fractions (via the carbazole and modified Morgan–Elson procedures) to generate a chromatogram for the preparative chromatography of BTH-derived oligosaccharides.[19] With respect to HA in particular, a

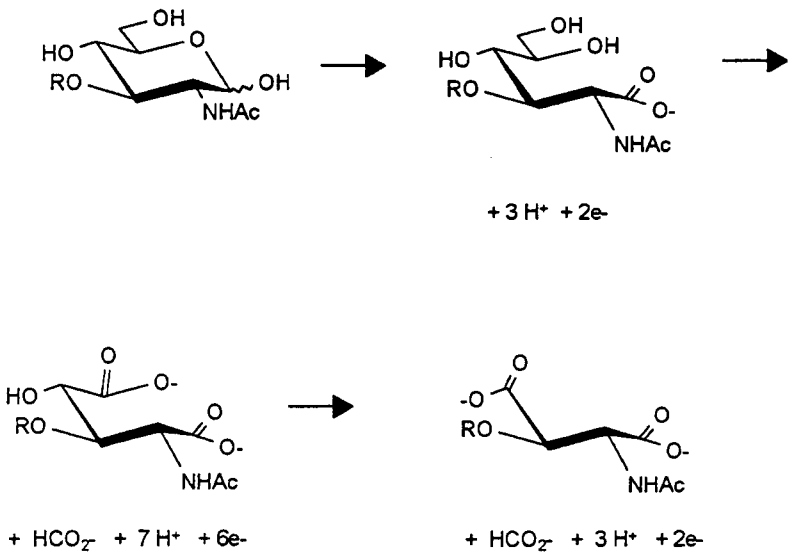
protein-binding assay for screening column fractions has been developed by Orvisky and co-workers,[20] but its use is restricted to facilities authorized to handle ^{125}I radioisotope-labeled materials. For the present studies, high-performance anion-exchange chromatography with pulsed amperometric detection (HPAEC-PAD) seemed the logical option, owing to its well-known excellent sensitivity and resolution, as well as its convenience and reliability.[21] Typically the method allows for the detection of analytes at the nano- or picogram level. Furthermore, it would ideally solve two problems at once:

- Its non-dependence on UV means that it would apply to any HA type we could need (not just eliminase-derived oligomers).
- Its extreme sensitivity prevents wasting valuable carbohydrate material, since only minute amounts are required, and might also allow us to directly sample preparative column fractions where analyte is typically present in very low concentration.

As with ESIMS, neutral oligosaccharides are far more well studied than acidic oligosaccharides; nevertheless, several reports have documented progress in this area.[22] Studies on HA oligosaccharides in particular have not yet been reported. There are several problems to be solved in applying HPAEC-PAD to the analysis of HA oligosaccharides. First, the typically used high pH conditions cause the materials to be strongly retained on the stationary phase with resulting long retention times and or decomposition mechanisms. Furthermore, it is widely known that optimal electrochemical waveform parameters vary widely with sugar used and are often tedious

to identify.[23] The chromatographer is often impeded by the exasperating failure by many authors to report specific electrochemical parameters in their published studies.[24] At this point, it is helpful to consider the PAD process in greater detail. The oxidation mechanism of sugars at the gold electrode in alkaline media has been developed by Johnson. Note that although the elution conditions developed here are conducted using neutral pH eluents (as discussed below) the analyte-containing eluate is mixed post-column with 400 mM NaOH just prior to the detection chamber, so that detection itself occurs at high pH. Scheme 1 details the proposed mechanism for sugar oxidation, in which carbohydrate C-1 (acetal/aldehyde oxidation state) and C-6 (primary alcohol) groups are oxidatively cleaved with the production of formate. Unfortunately, these reactions result in extensive fouling of the electrode, because the species shown in Scheme 1 (as well as free-radical intermediates, not shown) irreversibly adsorb to the gold surface.

The triple-pulse sequence of PAD was thus developed to solve this problem. The electrode cycles through a sequence of three potentials, as shown in Figure 3. During E_1, the sugar is oxidized via the reactions discussed above, during which time the current is integrated (t_{int}), after a short delay (t_{del}). A much higher potential E_2 is then applied for a period of time (t_{ox}) in order to oxidatively clean the electrode, during which oxidative desorption of carbonaceous species and formation of surface oxides occur. This is followed by a third potential E_3 (during t_{red}) which reductively converts the surface oxide to pristine metal, thus regenerating the electrode. An examination of the



Scheme 1. Proposed mechanism for sugar oxidation under PAD

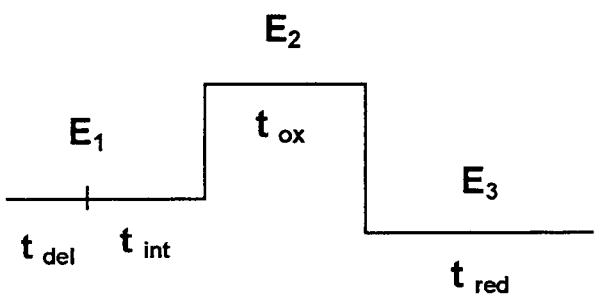


Figure 3. Triple-pulse sequence of PAD

generalized waveform reveals four time variables and three potential variables. As the optimal response of a particular sugar is a function of all these parameters which vary independently, one can easily see why waveform identification is often difficult, with the well known result that a extensive trial and error method based on multiple injections with manual adjustments of each waveform parameter is required.[25] LaCourse has developed a systematic way to identify a waveform using an algorithm of successive rotating-disc electrode (RDE) measurements to nail down the optimal parameters;[26] however, this method still requires a number of steps. Moreover, the RDE experiments are themselves difficult to conduct and do not guarantee that a satisfactory waveform will be identified. In any case, either by this or by the trial and error method, the anticipated difficulties should not occlude the identification of a satisfactory set of detection parameters.

II. STATEMENT OF THE PROBLEM

A. Objectives

The goals of this phase of the project can now be stated as follows:

- To conduct the digest and separate the oligomers on a preparative scale via existing literature protocols utilizing gel-permeation chromatography.
- To develop ESIMS and HPAEC-PAD protocols for characterizing HA-type oligosaccharides.
- To use these methods to characterize the individual HAL- and BTH-derived HA oligomers.

B. Research Plan

In the first stage of the project, digestion with HAL will be used since its UV chromophore affords an advantage in the identification and quantitation of compound present. BTH will then be used in the second stage. By varying the length of hydrolysis, the dp of the oligosaccharides will be varied. The oligosaccharides will be characterized by ESIMS and HPAEC-PAD and will then be evaluated for their HA-binding and antimetastatic behavior using the B16F10 murine melanoma metastasis screen, either as individual components or as mixtures. Using feedback from the biological studies, the enzymatic degradations will be adjusted to produce the oligosaccharides that show most activity.

Identification of the proper electrochemical "integrated amperometry" waveform

will be conducted by trial and error starting from presumably close waveforms for similar compounds reported in the literature. In order to force a more rapid elution of the highly retained carboxylated sugars, and also in light of Hicks' recent observations that sugars having 2-acetamido-groups with an adjacent glycosidic linkage from the 3-position are unstable in the high pH conditions normally used in HPAEC,[27] eluent buffers at lower pH levels, as reported by Hotchkiss, will be used.[28]

C. Significance

As discussed in the previous sections, numerous recent studies have established HA as an increasingly important and promising bioactive polysaccharide. Furthermore, as a result of its unique physicochemical properties, HA is also finding use in drug delivery, antiadhesive, ophthamalic tissue replacement, and osteoarthritis therapy applications.[29] Thus, not only with respect to the CD44 metastasis investigations outlined herein but also for HA's roles in cancer in general, as well as for noncancer applications, there is a clear need for HA fragments of precisely defined MW and end-group identity for use as biological probes in more extensive investigations of these processes. The lack of precise molecular characterization in the literature to date renders the studies in this chapter timely and significant.

An attendant benefit of the ESIMS and HPAEC-PAD studies is that they could function as a rapid screening method for the preparative-scale chromatography of enzyme digest-derived oligosaccharides. Fractions from preparative columns could be

directly sampled via HPAEC, and the observed retention times could be correlated to MS-confirmed MWs, allowing the assessment of both fraction purity and component identity. This would be an improvement of existing methods.

Finally, the developed HPLC and ESIMS conditions could potentially be applied to facilitate the analysis of other glycosaminoglycans, whose analysis by these methods is often difficult.

III. RESULTS AND DISCUSSION

A. Oligosaccharides from HA lyase digestion

1. Unexpected oligosaccharides obtained

As explained above, previous reports on the enzyme's regiospecificity led us to expect a series of even-numbered hyaluronan fragments from the HA lyase digestion. However, as shown in Figure 4, the UV trace of our preparative gel-filtration chromatography column suggested the presence of two series: the series of expected even-numbered oligomer products resulting from glucosaminidase cleavage (larger peaks), and a second series that we suspected to be the intervening odd-numbered oligomers (smaller peaks). In fact, there are four possible arrangements of odd-numbered oligomers (shown here with abbreviated structures, where A = GlcNAc, U = GlcA, and an asterisk indicates a 4,5-unsaturated moiety in the indicated residue):

$$*A\text{-}[U\text{-}A]_n\text{-}U\text{-}A \quad (5)$$

$$U\text{-}[A\text{-}U]_n\text{-}A\text{-}U \quad (6)$$

$$A\text{-}[U\text{-}A]_n\text{-}U\text{-}A \quad (7)$$

$$*U\text{-}[A\text{-}U]_n\text{-}A\text{-}U \quad (8)$$

An oligomer with a non-reducing end $^{\Delta 4,5}$ β-D-GlcNAc moiety, **5**, is highly unlikely since the GlcNAc possesses no carboxylic acid group and hence no acidic proton at C-5 to make eliminase cleavage thermodynamically viable. Structures **6** and **7** are unlikely based on the fact that the candidate odd-numbered oligomers possess UV activity. Structure **8** emerges as the most likely candidate. As unambiguously shown by the mass

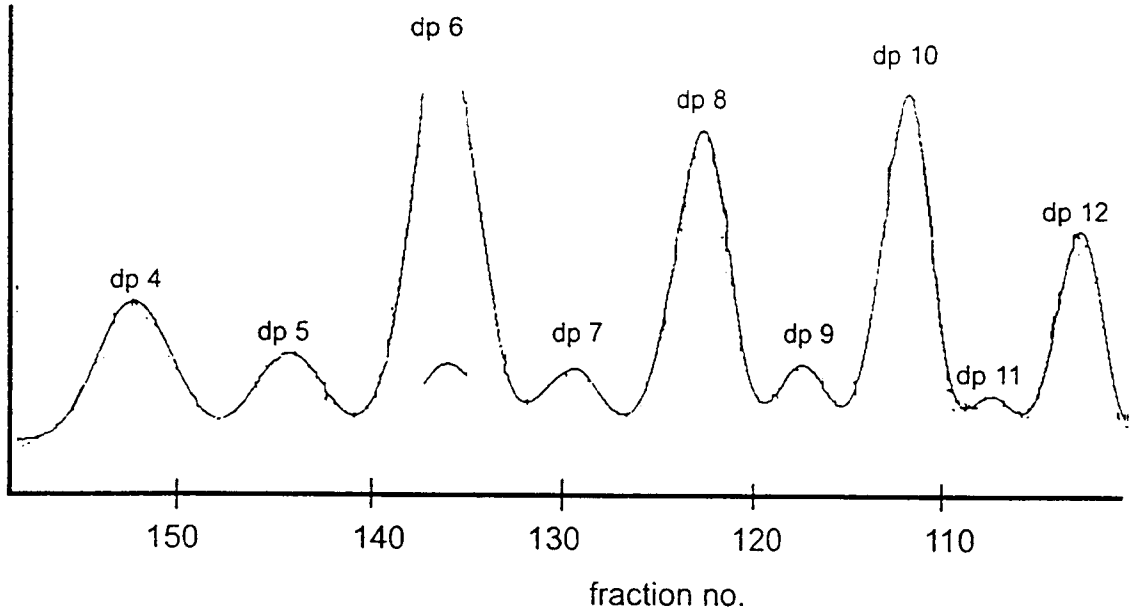


Figure 4. Gel permeation chromatogram of hyaluronate lyase digest.

(BioRad P-30, UV absorbance at 232 nm; fraction volume = 10 mL)

spectral data summarized below, the isolated oligomers do in fact have the structure **8**:

$^{\Delta 4,5}$ β-D-GlcA(1→3)[β-D-GlcNAc(1→4)β-D-GlcA]$_n$.

There are several pathways that might possibly afford such oligomers. One possibility is that a reducing-end GlcAc moiety in an HA oligosaccharide is inherently unstable and suffers chemical hydrolysis. In this way, the expected even-numbered oligomers resulting from HA lyase's known hexosaminidase activity would slowly decompose to give small amounts of the observed odd-numbered oligomers. If, on the other hand, the odd-numbered oligomers do in fact arise from a true enzymatic cleavage, then some sort of glucuronidase activity must be present. This activity could be assigned

either to a secondary glucuronidase activity of hyaluronate lyase itself, or to maverick hydrolase impurities in the enzyme preparation (used as purchased from Sigma), such as *endo-* or *exo*-glucuronidases.

The presence of the 2-mer and 3-mer among the data deserves some comment. As noted in the literature, HA lyase produces a tetrasaccharide as the smallest product, which conforms to our observations in general. However, we found that extremely long reaction times (3–5 days, vs. normal reaction times of 1–3 h) did indeed afford a small amount of the 3-mer, along with the major products of 4-, 6-, and 8-mer. The 2-mer is commercially available, but, as noted above, is the result of digestion with chondroitinase, not HA lyase.

2. Electrospray–ionization mass spectrometry

As noted above, there has been some question in the literature as to the extent of polyanionization to be expected from larger acidic oligosaccharides, and the degree to which this would complicate spectral interpretation. This study indicates that such multiply charged anions predominate in the spectra of the larger oligomers, thus conveniently compressing the observed $(M - nH)^{n-}$ signals into the *m/z* 300–1100 range. In fact, this phenomenon allows one to calculate a "fingerprint" set of *m/z* ratios for each oligomer and to compare that to the observed spectrum. The calculated values are such that confusion of a species with those of half or double its MW is avoided due to key nonduplicated values.

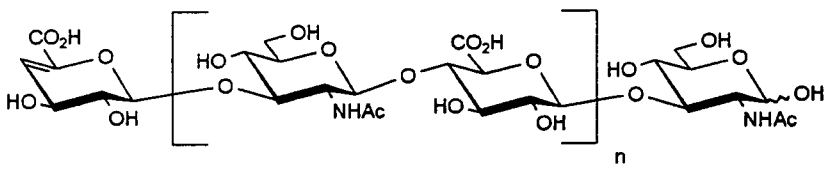
Actual *m/z* values thus obtained agreed with the calculated values and permitted a

correct assignment of MW. Table 1 summarizes the data for the entire sequence of oligomers. The assigned MWs were also in agreement with a MW value extrapolated from the raw data by the MAX ENT (see Experimental Section) program. Figures 5 and 6 show representative observed spectra along with MAX ENT-generated MW distributions for the 13-mer and 14-mer. Each of these is shown by the MAX ENT analysis to contain minor impurities of lower oligomers. The data for the entire sequence of oligomers may be found in Appendix B. As evident from the data, a particular compound will not have observed signals for all possible anionic forms; rather, the distribution will tend to cluster in a small range of charge states. Thus, as shown graphically for the entire sequence in Figure 7, the smaller oligomers exist predominantly as the mono- or dianion, whereas larger ones, such as the 12–14-mers exist mainly as the pentaanion, and finally the 16-mer exists chiefly as the hexaanion. (It should be noted that charge-distribution envelopes presented in Figure 3 were observed at cone voltage = 25 V. At higher cone voltages, *e.g.*, 40 V, the envelope for any particular *n*-mer is shifted somewhat to lower charge-states. This effect is explored systematically in the next section.) Moreover, the data clearly show that the anionic oligosaccharides obey a logical and expected pattern of behavior, and are thus readily analyzable by electrospray methods. This phenomenon should also apply to the numerous other important carboxylated and/or sulfated glycosaminoglycan oligosaccharides, whose characterization is often difficult.

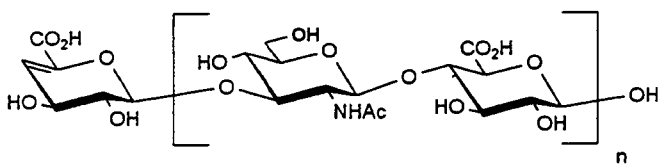
Table 1. Observed vs. predicted ESIMS *m/z* values

for HA lyase oligomers[a]

Predicted Even-Numbered Oligomers



Novel Odd-Numbered Oligomers



Oligomer (No. CO_2^- groups)	**Observed *m/z***	**Relative Intensity (%)[b]**	**Possible Ions (charge) Predicted *m/z***
2-mer [c] (1)	378.2	100	(-1) 378.2
3-mer (2)	554.1	81	(-1) 554.1
	276.6	100	(-2) 276.5
4-mer (2)	757.3	9	(-1) 757.2
	378.2	100	(-2) 378.1
5-mer (3)	933.3	3	(-1) 933.2
	466.1	100	(-2) 466.1

[a] All measurements were taken with capillary and cone voltages at 2.5 kV and 25 V, respectively, as indicated in the experimental section.
[b] Normalized by assigning the predominant signal to 100 %.
[c] Not a product of HA lyase digestion (see discussion above). Obtained from Sigma Chemical Co.
[d] — Indicates ion not observed.

Table 1, continued

Oligomer (No. CO_2^- groups)	Observed *m/z*	Relative Intensity (%)[b]	Possible Ions (charge) Predicted *m/z*
6-mer (3)	—[d]	—	(-1) 1136.3
	567.9	95	(-2) 567.6
	378.3	100	(-3) 378.1
7-mer (4)	—	—	(-1) 1312.3
	655.6	28	(-2) 655.6
	437.0	100	(-3) 436.7
	—	—	(-4) 327.3
8-mer (4)	—	—	(-1) 1515.4
	757.2	20	(-2) 757.2
	504.5	100	(-3) 504.4
	378.2	20	(-4) 378.1
9-mer (5)	—	—	(-1) 1691.4
	845.4	6	(-2) 845.2
	563.3	47	(-3) 563.1
	422.3	100	(-4) 422.1
	—	—	(-5) 337.5
10-mer (5)	—	—	(-1) 1894.5
	946.9	6	(-2) 946.7
	631.0	41	(-3) 630.8
	473.1	100	(-4) 472.9
	378.2	6	(-5) 378.1
11-mer (6)	—	—	(-1) 2070.6
	1034.9	3	(-2) 1035.0
	689.6	26	(-3) 689.5
	517.1	100	(-4) 517.0
	413.5	98	(-5) 413.3
	—	—	(-6) 344.2

Table 1, continued

Oligomer (No. CO_2^- groups)	Observed *m/z*	Relative Intensity (%)[b]	Possible Ions (charge) Predicted *m/z*
12-mer (6)	—	—	(-1) 2273.6
	—	—	(-2) 1136.3
	757.4	14	(-3) 757.2
	567.9	83	(-4) 567.7
	454.1	100	(-5) 453.9
	378.2	6	(-6) 378.1
13-mer (7)	—	—	(-1) 2449.7
	—	—	(-2) 1224.3
	816.0	4	(-3) 815.9
	612.1	20	(-4) 611.7
	489.4	100	(-5) 489.1
	407.5	57	(-6) 407.4
	349.0	4	(-7) 349.1
14-mer (7)	—	—	(-1) 2652.9
	—	—	(-2) 1325.9
	883.8	7	(-3) 883.6
	662.6	30	(-4) 662.4
	529.9	100	(-5) 529.7
	441.4	48	(-6) 441.3
	—	—	(-7) 378.1
16-mer (8)	—	—	(-1) 3031.9
	—	—	(-2) 1515.4
	—	—	(-3) 1009.9
	757.5	21	(-4) 757.2
	605.7	63	(-5) 605.6
	504.7	100	(-6) 504.5
	432.4	24	(-7) 432.3
	—	—	(-8) 378.1

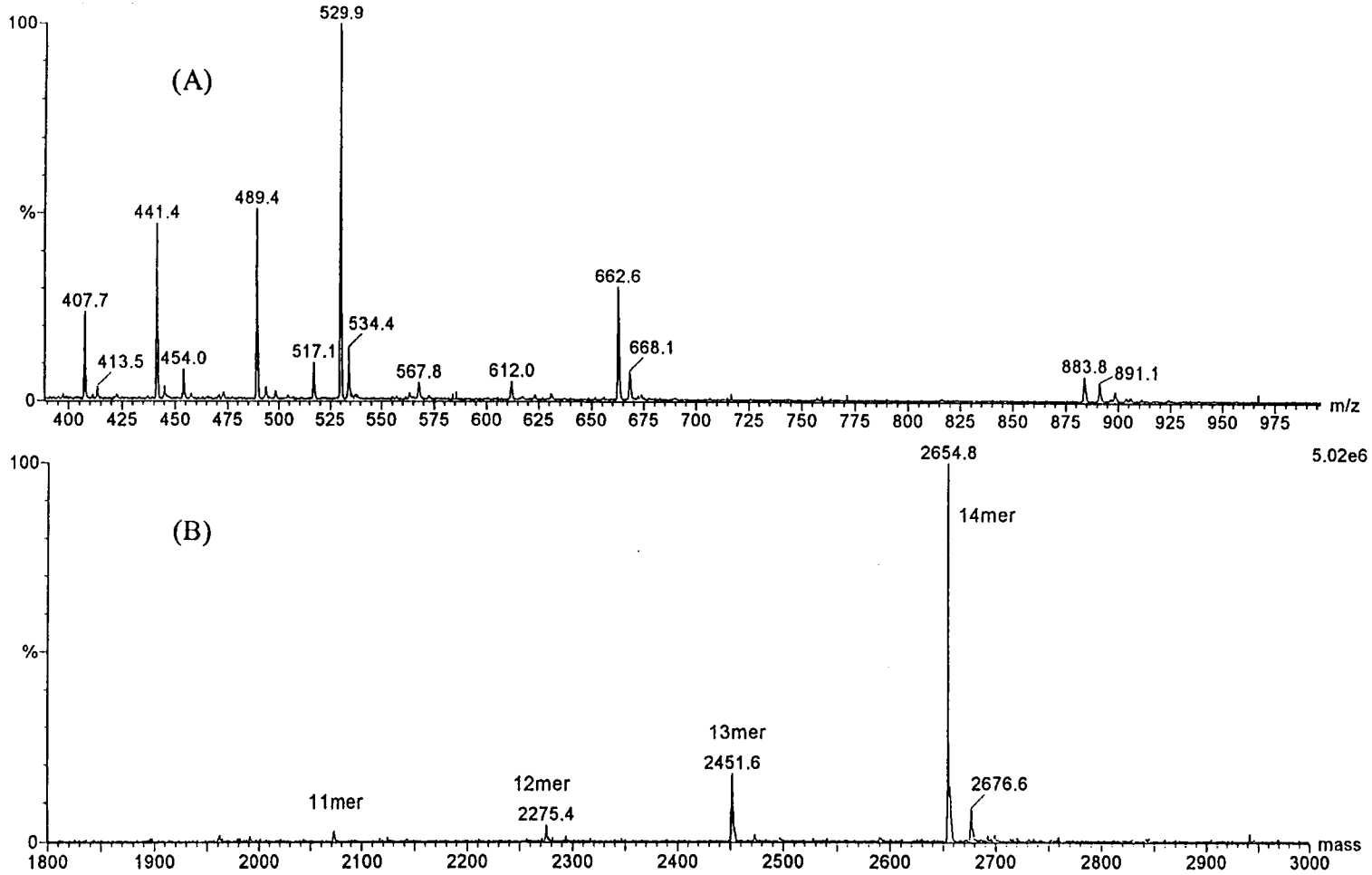


Figure 5. Negative-ion electrospray mass spectrum (A) and MAX ENT-generated MW distribution (B) for 13-mer.

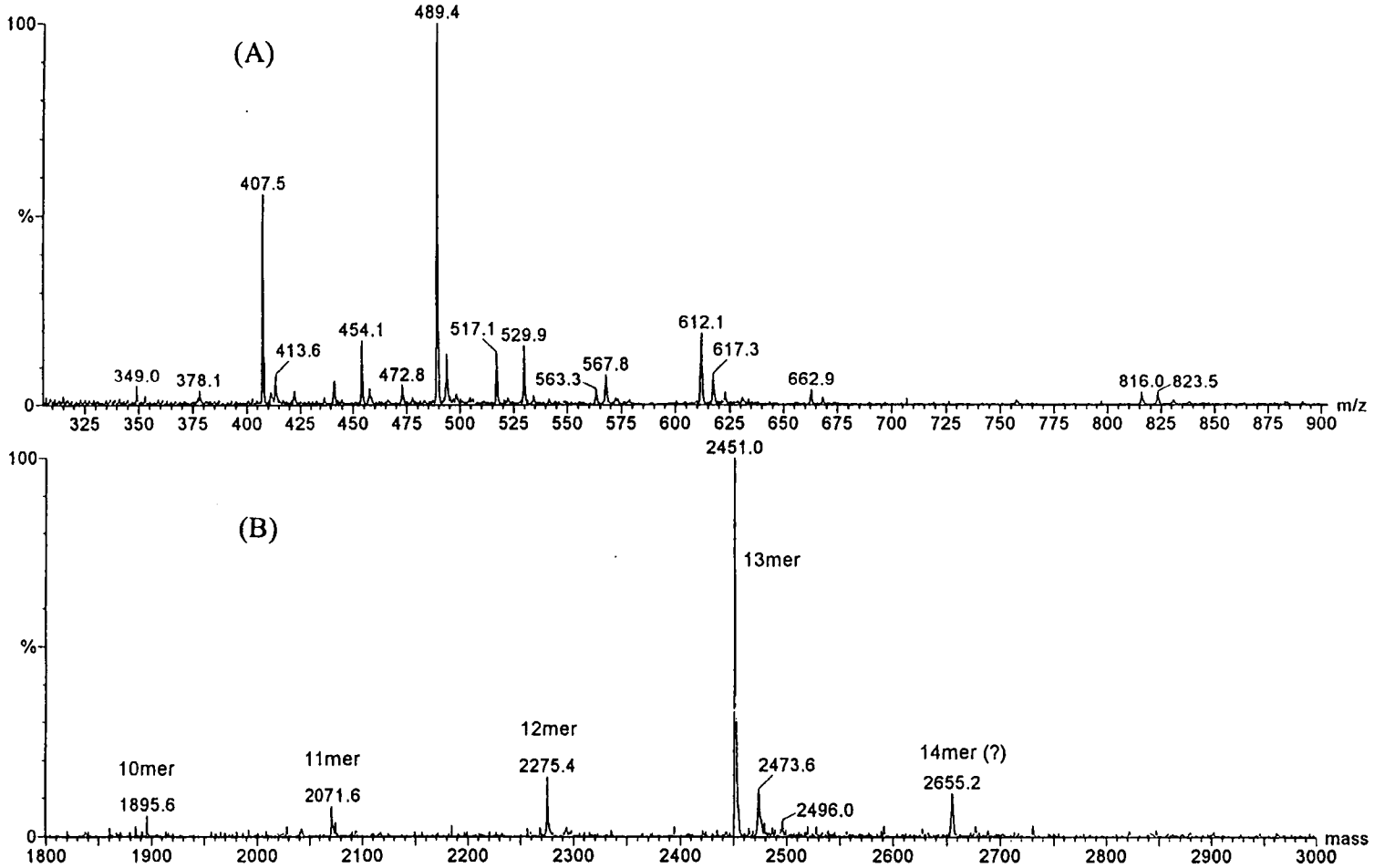


Figure 6. Negative-ion electrospray mass spectrum (A) and MAX ENT-generated MW distribution (B) for 14-mer.

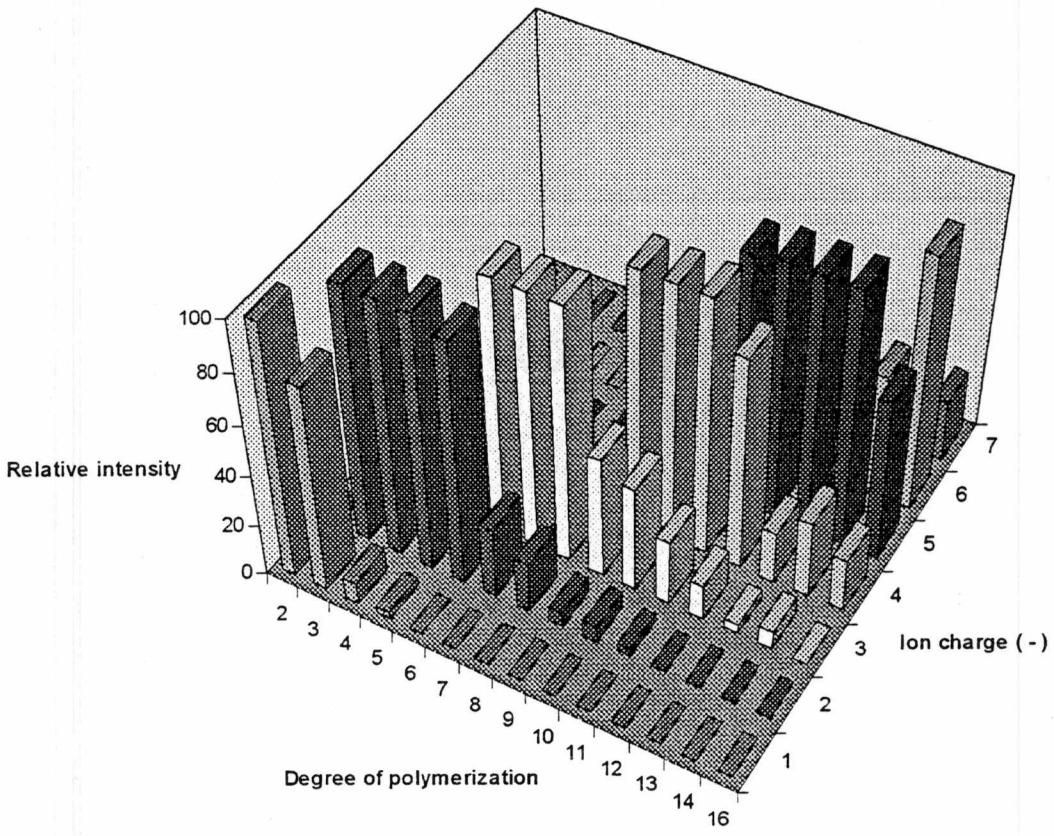


Figure 7. Observed relative intensities of the different charge states of HA lyase-derived oligosaccharides in negative-ion ESIMS.

3. High-performance anion-exchange chromatography

Employment of eluents and PAD waveforms previously used in the literature resulted in no (or very weak) detector response and/or anomalous or irreproducible retention times. Table 2 shows a list of PAD waveforms in the literature[30] that were tried but found to be unsuccessful. Table 3 shows a list of new waveforms that were gradually adjusted to finally develop the waveform optimized for HAL oligomers (waveform 18). Although there was some trial-and-error involved, the individual waveform components were modified according to the following rationale. After several unsuccessful attempts, waveform #4 appeared to be a favorable random "hit." Increasing the duration of oxidation (t_{ox}) and/or regeneration (t_{red}), however, resulted in a loss of signal intensity (entries #5–6). Waveform #4 was then revisited and modified systematically via addition of +100 mV to each potential, while retaining the same durations, according to the rationale by Johnson,[31] which states that lower eluent pHs (relative to the normally used high pH conditions) require increased (*i.e.*, more positive) potentials. This provided an improved waveform (entry #7). Further manipulations were conducted, with two key observations:

- Shortened durations for t_{del} and t_{int} gave improved response.
- E_1 could assume a much lower, and even *negative*, value compared to those in the literature.

These points were applied and fine tuned (bold-faced numbers in Table 3 illustrate this) to finally afford an optimized waveform (#18). This pulse sequence, whose potentials

Table 2. Literature waveforms used for PAD of carbohydrates.

Potentials (E_n , mV) and durations (t_n , ms) of triple pulse sequence.[a]

Type of Sugar (Ref.[b])	E_1	E_2	E_3	t_{del}	t_{int}	t_{ox}	t_{red}
Linear and branched glucose oligomers (30a)	+50	+600	-80	480	n.r.[c]	120	60
Arabino-oligosaccharides (30b)	+50	+750	-150	200	200	190	390
Asialoglycopeptides (30c)	+50	+80	-60	360	n.r.	120	420
Oligogalacturonic acids (30d)	+100	+600	-800	200	100	120	300
Monosaccharides (30e)	+200	+800	-300	240	200	180	360
Unsaturated Oligogalacturonic acids (30f)	+50	+600	-600	480	n.r.	120	60
N-linked Oligosaccharides (30g)	+50	+600	-600	290	220	100	50
Tyraminated oligogalacturonides (30h)	+150	+700	-300	240	240	180	360

[a] Indicated parameters correspond to the time-potential diagram shown in Figure 3, Section I.C.

[b] See reference number 30.

[c] The delay (t_{del}) and integration (t_{int}) times were not discretely indicated; in such cases, "t_{del}" refers to their sum duration.

Table 3. PAD waveform development for HA lyase-derived hyaluronic acid oligosaccharides: Potentials (E_n, mV) and durations (t_n, ms) of triple pulse sequence.[a]

Entry	E_1	E_2	E_3	t_{del}	t_{int}	t_{ox}	t_{red}
1	+100	+600	-800	100	210	120	290
2	+100	+600	-800	370	210	120	290
3	+100	+600	-800	200	200	110	100
4	**+150**	**+700**	**-300**	**240**	**240**	**180**	**360**
5	+150	+800	-500	240	240	400	420
6	+200	+800	-300	240	240	280	360
7	+250	+800	-200	240	240	180	360
8	+200	+750	-250	**240**	**240**	180	360
9	+200	+750	-350	**200**	**200**	180	360
10	+300	+750	-350	**200**	**200**	180	360
11	+200	+750	-350	**150**	**200**	180	360
12	**+150**	+750	-350	**150**	**200**	180	360
13	**+100**	+750	-350	**100**	**150**	180	360
14	**+50**	+750	-350	**100**	**150**	180	360
15	**+50**	+750	-350	**80**	**130**	180	360
16	**-50**	+750	-350	80	130	180	360
17	**-100**	+750	-350	80	130	180	360
18	**-150**	+750	-350	80	130	180	360

[a] Indicated parameters correspond to the time-potential diagram shown in Figure 3, Section I.C.

and durations differ significantly from others reported in the literature, allowed satisfactory detection of the HA oligomers.

As alluded to above, we chose to employ neutral-range operating pHs to force a faster elution of the oligomers and also to avoid decomposition. Although high pH conditions cause acidic oligosaccharides to be strongly retained, they can nevertheless be eluted, albeit at long retention times. Under such conditions, we noted that high pH conditions resulted in apparent decomposition of the oligomers (as indicated by unreproducible retention times, broad humps indicative of decomposition, etc.), thus confirming Hicks' postulation about the base-lability of 3-glycosylated 2-deoxy-2-acetamido sugars. Unfortunately, a gradient elution method suitable for eluting the entire sequence of oligomers was not feasible due to excessive baseline drift caused by the increasing acetate buffer concentration. Recourse was thus made to several different isocratic solvent systems. These, along with standard retention times for the oligomers, are summarized in Table 4. Once compiled and correlated with mass spectral data, the collection of retention times allowed rapid sampling of preparative column fractions. The extreme sensitivity of the PAD, as well as its relative imperviousness to the 250 mM ammonium formate buffer, allowed us to conveniently sample fractions directly from the preparative gel permeation column without desalting or concentrating them. Representative chromatograms in Figure 8 contrast a pure fraction (A), for example, with an overlap fraction (B).

Table 4. HPAEC retention times (min) of HA lyase-derived oligosaccharides.

(at the indicated concentration of acetate (Na^+/H^+), pH 7.5)[a]

Oligomer (No. GlcA residues)	200 mM	280 mM	350 mM	400 mM
2-mer (1)	3.0	—[b]	—	—
3-mer (2)	2.7	—	—	—
4-mer (2)	5.0	3.5	—	—
5-mer (3)	3.7	2.7	—	—
6-mer (3)	11.8	5.6	—	—
7-mer (4)	8.0	3.8	—	—
8-mer (4)	—	10.3	—	—
9-mer (5)	—	6.5	—	—
10-mer (5)	—	21.3	9.1	—
11-mer (6)	—	12.9	5.8	—
12-mer (6)	—	—	15.7	8.1
13-mer (7)	—	—	9.5	5.5
14-mer (7)	—	—	29	13.7
16-mer (8)	—	—	—	22.3

[a] Dionex DX-500 system with CarboPac PA-1 guard precolumn (25 mm × 3 mm) and CarboPac PA-1 column (250 mm × 4 mm); HA oligosaccharide samples (25 μL of solutions approximately 1–50 μg/mL in analyte) eluted at a flow rate of 1.0 mL/min; Acetate eluents obtained by adjusting the system pump to mix the appropriate proportion of a 1.0 M sodium acetate solution (pH 7.5) with deionized water.

[b] — Indicates not measured.

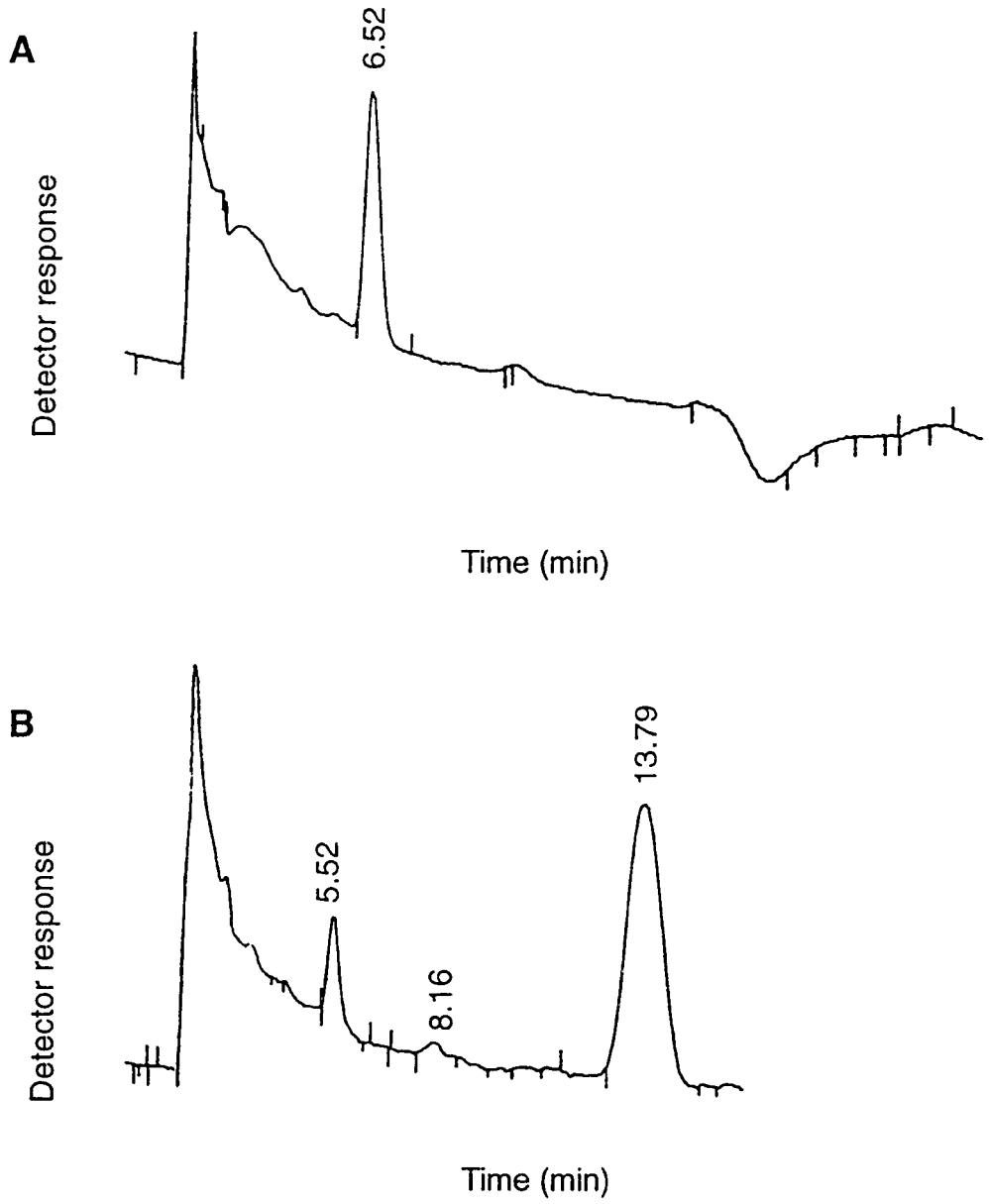


Figure 8. HPAEC chromatograms for HA oligosaccharides (Dionex system, PAD). (A) 9-mer (6.5 min) at 350 mM acetate eluent. (B) 14-mer (13.7 min) at 400 mM acetate eluent, with impurity 13-mer (5.5 min.) and 12-mer (8.1 min) present at approximately 50:6:1, respectively.

Interestingly, we also found that the compounds do *not* elute strictly in order of increasing number of monosaccharide residues; *i.e.*, the additional residue possessed by an odd-numbered species (with respect to its next-lower even-numbered neighbor) serves to *decrease* the retention time, sometimes by a factor of almost 2. Thus, for example, whereas the hexamer elutes at 5.6 min in 280 mM buffer, the heptamer elutes at only 3.8 min. We believe that this phenomenon may be rationalized as follows. In the odd-numbered oligomers, the acidic residues outnumber the neutral residues, whereas in the even-numbered oligomers, the acidic and neutral residues are present in equal numbers. Apparently, then, although there is the usual and expected contribution by increased MW toward increased retention, there also appears to be a counterbalancing contribution *toward increased mobility* by additional glucuronate residues that, overall, outweighs the MW contribution.

B. Oligosaccharides from bovine testes hyaluronidase

In the preceding section, it was shown that multiple degrees of polyanionization generated a fingerprint set of *m/z* values that allowed a convenient and anambiguous MW assignment, and that the observed degrees of polyanionization obeyed a logical and expected trend with respect to increasing MW. Described in this section are continued studies on another series of HA oligomers derived from digestion with BTH encompassing a significantly larger and more biologically interesting mass range (700–5300 Da), thus demonstrating the versatility of negative-ion mode ESIMS in the analysis

of anionic oligosaccharides. Also described are additional details on the significant degree of mutiple sodiation of CO_2^- groups, and the relationship between cone voltage and observed charge state envelopes. HPAEC-PAD protocols developed for the HAL-derived oligosaccharides were also extended without difficulty to the larger MW BTH-derived species.

1. Unexpected oligosaccharides obtained.

HA was digested and subjected to preparative gel-filtration chromatography. Fractions were collected and combined to afford samples with segregated MW ranges (typically 5–6 adjacent oligomers, see below). Subsequent analysis unambiguously confirmed the presence of odd-numbered oligomers having structure β-D-GlcA(1→3)[β-D-GlcNAc(1→4)D-GlcA]$_n$, in addition to the expected even-numbered species. Previous reports on BTH have not noted such oligomers.

2. Electrospray–ionization mass spectrometry.

Analysis on a Micromass VG Quattro II instrument showed (as it had for HA lyase oligomers) that the existence of multiple charge states allowed correlation of an oligomer's observed spectrum with its set of calculated *m/z* values. A representative spectrum for a high-MW fraction is shown in Figure 9. The major peaks correspond to the 28-mer species, with minor peaks also confirming the presence of adjacent oligomers. As before, a theoretical MW distribution extrapolated from the raw data by the MAX ENT program was found to conveniently facilitate the correlation of the observed *m/z* signals to their parent molecules' neutral MW. Figure 10 shows the MAX

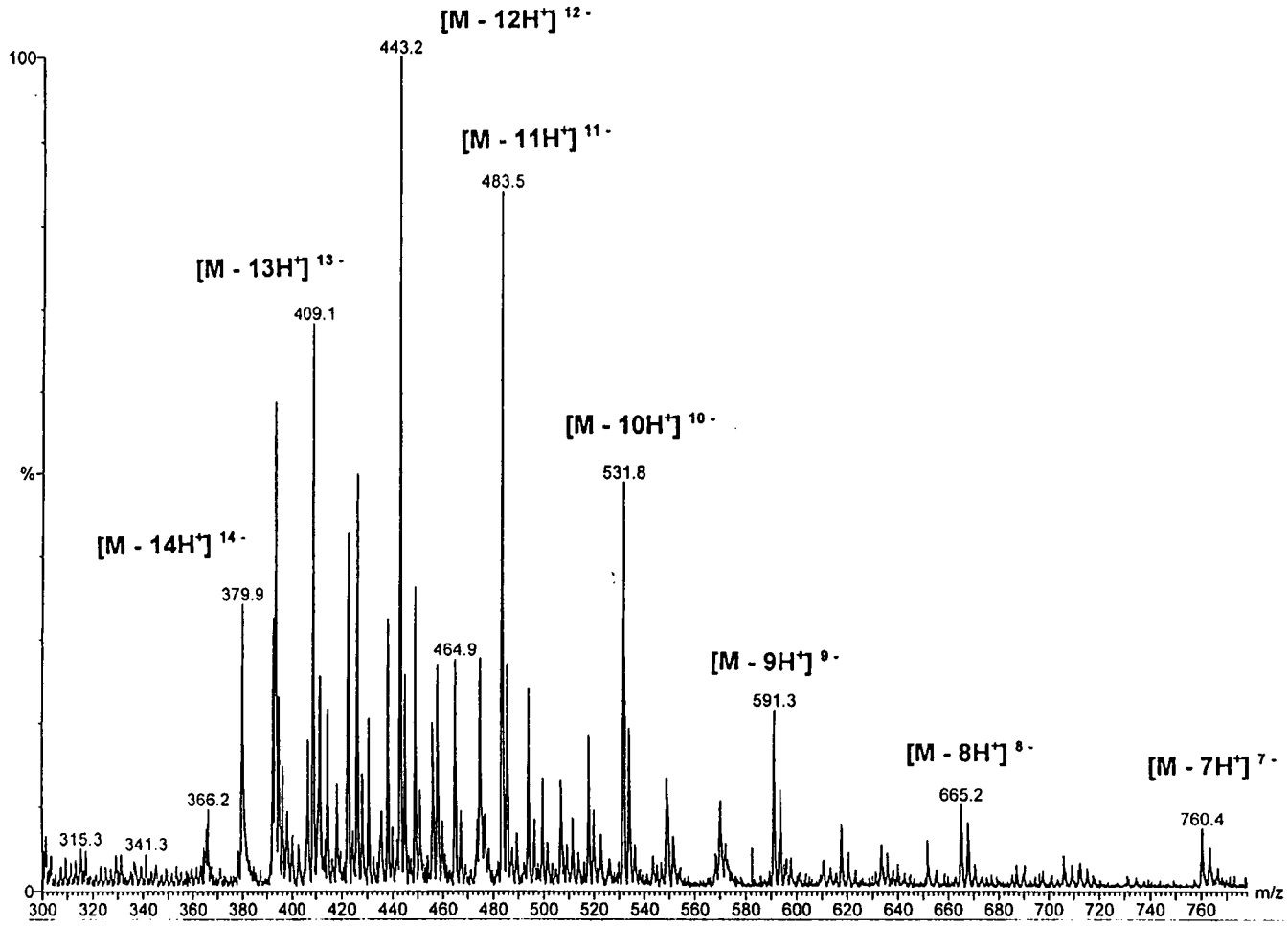


Figure 9. Negative-ion electrospray mass spectrum for 28-mer containing fraction.

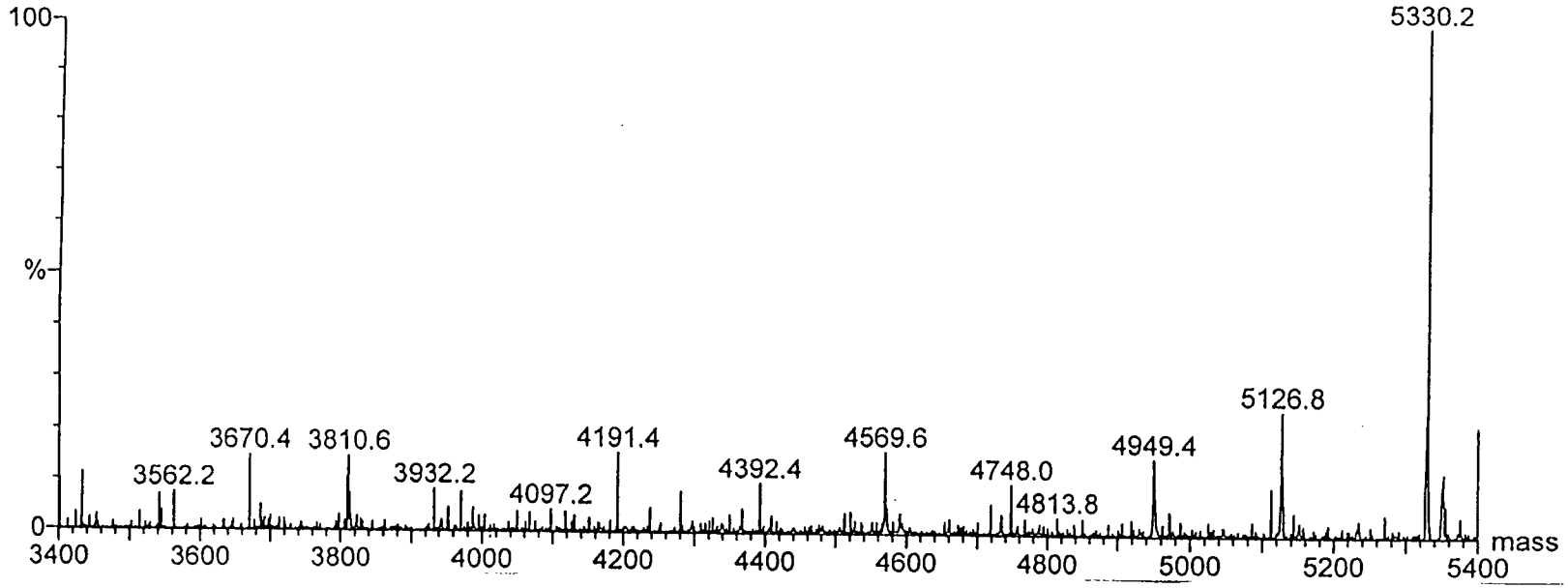


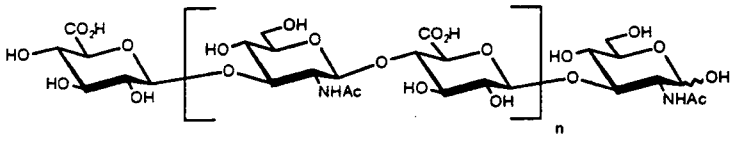
Figure 10. MAX ENT-generated MW distribution for 28mer-containing fraction.

ENT MW distribution generated from the spectrum in Figure 9, translating the major peaks into the MW signal for the 28-mer (*i.e.*, 5330.2), and also extracting and collecting subsets of Figure 9's remaining minor peaks into a clear succession of adjacent oligomers (*i.e.*, the 27-, 26-, 25-, 24-, and 23-mers, at 5126.8, 4949.4, 4748.0, 4569.6, and 4369.6, respectively). The deconvolution of spectral data consisting of superimposed sets of charge state envelopes (plus sodiated variants thereof) illustrates the utility of ESIMS analysis in confirming individual MWs in mixtures of compounds.[32]

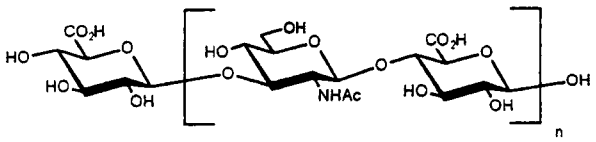
The technique of manipulating cone voltage in order to shift the observed charge state envelopes to desired lower or higher *m/z* is well known in the protein ESIMS literature.[13] Although it has not yet been reported for acidic carbohydrates, we expected that the effect would also be observed in the HA oligomers. Indeed, the effect was clearly observed over the entire range of oligomers for two series of experiments conducted at low (25 V) vs. high (55–65 V) cone voltage. Table 5 shows representative sets of data for five oligomers. Whereas lower cone voltages allowed observation of higher charge state envelopes (lower *m/z*, typically <1000), higher cone voltages shifted the observed charge state envelopes to lower charges, allowing extensive collection of data with *m/z* >1000. The effect is more pronounced in the higher MW oligomers. The tabular data is condensed into the two charts in Figure 11 in order to emphasize the clearly contrasting general trends for the location of predominant charge states under low vs. high cone voltage conditions.

Table 5. Observed vs. predicted ESIMS *m/z* values for selected bovine testes hyaluronidase oligomers, dp 4-28[a]

Predicted Even-Numbered Oligomers



Novel Odd-Numbered Oligomers



Oligomer (No.CO_2^- groups)	Observed signals at CV = 25 V *m/z*	rel. int.	at CV = 55–65 V *m/z*	rel. int.	Assignment [species]	Pred. *m/z*
7-mer	[1332.1]*[b]				[M = 1332.1]	
(4)	—[c]	—	—	—	$[M - H^+]^{1-}$	1331.1
	—	—	664.9	100	$[M - 2H^+]^{2-}$	665.0
	—	—	676.0	76	$[M - 3H^+ + Na^+]^{2-}$	676.0
	—	—	686.9	50	$[M - 4H^+ + 2Na^+]^{2-}$	687.0
	443.0	100	443.0	36	$[M - 3H^+]^{3-}$	443.0
	450.3	3	450.3	13	$[M - 4H^+ + Na^+]^{3-}$	450.4
	332.0	17	332.1	4	$[M - 4H^+]^{4-}$	332.0

[a] This table combines the data of two acquired spectra per sample. Each sample provided data for the predominant even-numbered oligomer present, and for the next-lower odd-numbered oligomer. Observed signals derive from acquisitions at CV = 25 V (*m/z* values and relative intensities shown in columns 3 and 4, respectively) or at CV = 55–65 V (columns 5 and 6). Relative intensities are assigned separately to each individual oligomer, with the predominant peak for that oligomer set as 100 %.

[b] Values marked with an asterisk correspond to the neutral MW extrapolated from the raw data (CV = 25 V series) by the MAX ENT program, and correspond in all cases to within ± 0.06 % of the calculated MW. Distributions extrapolated from the CV = 55–65 V series were found to contain greater error, and are not included.

[c] Indicates signal not observed.

Table 5, continued

Oligomer (No.CO_2^- groups)	Observed signals at CV = 25 V *m/z*	rel. int.	at CV = 55–65 V *m/z*	rel. int.	Assignment [species]	Pred. *m/z*
8-mer	[1534.6]*				[M = 1535.3]	
(4)	—	—	—	—	$[M - H^+]^{1-}$	1534.3
	766.5	11	766.5	87	$[M - 2H^+]^{2-}$	766.6
	777.5	9	777.4	100	$[M - 3H^+ + Na^+]^{2-}$	777.6
	788.5	5	788.5	65	$[M - 4H^+ + 2Na^+]^{2-}$	788.6
	510.7	100	—	—	$[M - 3H^+]^{3-}$	510.8
	518.0	29	—	—	$[M - 4H^+ + Na^+]^{3-}$	518.1
	382.8	56	—	—	$[M - 4H^+]^{4-}$	382.8
17-mer	[3229.2]*				[M = 3228.7]	
(9)	—	—	—	—	$[M - H^+]^{1-}$	3227.7
	—	—	—	—	$[M - 2H^+]^{2-}$	1613.3
	—	—	1075.2	7	$[M - 3H^+]^{3-}$	1075.2
	—	—	1082.6	10	$[M - 4H^+ + Na^+]^{3-}$	1082.6
	—	—	1089.9	9	$[M - 5H^+ + 2Na^+]^{3-}$	1089.9
	—	—	1097.3	9	$[M - 6H^+ + 3Na^+]^{3-}$	1097.2
	—	—	1104.5	7	$[M - 7H^+ + 4Na^+]^{3-}$	1104.5
	806.2	1	806.3	52	$[M - 4H^+]^{4-}$	806.2
	—	—	811.8	67	$[M - 5H^+ + Na^+]^{4-}$	811.7
	—	—	817.2	43	$[M - 6H^+ + 2Na^+]^{4-}$	817.2
	—	—	822.8	29	$[M - 7H^+ + 3Na^+]^{4-}$	822.7
	644.8	2	644.9	100	$[M - 5H^+]^{5-}$	644.7
	649.3	1	649.3	71	$[M - 6H^+ + Na^+]^{5-}$	649.1
	—	—	653.7	27	$[M - 7H^+ + 2Na^+]^{5-}$	653.5
	537.2	6	537.0	8	$[M - 6H^+]^{6-}$	537.1
	540.9	2	—	—	$[M - 7H^+ + Na^+]^{6-}$	540.8
	460.4	47	46	3	$[M - 7H^+]^{7-}$	460.2
	463.5	8	—	—	$[M - 8H^+ + Na^+]^{7-}$	463.4
	402.8	100	—	—	$[M - 8H^+]^{8-}$	402.6
	357.9	7	—	—	$[M - 9H^+]^{9-}$	357.7

Table 5, continued

Oligomer (No.CO_2^- groups)	Observed signals at CV = 25 V *m/z*	rel. int.	at CV = 55–65 V *m/z*	rel. int.	Assignment [species]	Pred. *m/z*
18-mer	[3432.8]*				[M = 3431.9]	
(9)	—	—	—	—	$[M - H^+]^{1-}$	3430.9
	—	—	1714.5	4	$[M - 2H^+]^{2-}$	1714.9
	1143.0	1	1143.0	41	$[M - 3H^+]^{3-}$	1143.0
	1150.5	2	1150.5	71	$[M - 4H^+ + Na^+]^{3-}$	1150.3
	1157.7	2	1157.7	70	$[M - 5H^+ + 2Na^+]^{3-}$	1157.6
	1165.1	1	1165.0	54	$[M - 6H^+ + 3Na^+]^{3-}$	1164.9
	—	—	1172.3	46	$[M - 7H^+ + 4Na^+]^{3-}$	1172.3
	—	—	1179.6	34	$[M - 8H^+ + 5Na^+]^{3-}$	1179.6
	—	—	1187.0	25	$[M - 9H^+ + 6Na^+]^{3-}$	1186.9
	857.1	5	857.1	100	$[M - 4H^+]^{4-}$	857.0
	862.6	6	862.6	93	$[M - 5H^+ + Na^+]^{4-}$	862.5
	868.1	3	868.0	50	$[M - 6H^+ + 2Na^+]^{4-}$	868.0
	873.6	1	873.5	21	$[M - 7H^+ + 3Na^+]^{4-}$	873.5
	685.5	16	685.5	40	$[M - 5H^+]^{5-}$	685.4
	689.9	11	689.9	35	$[M - 6H^+ + Na^+]^{5-}$	689.8
	694.3	3	694.3	8	$[M - 7H^+ + 2Na^+]^{5-}$	694.2
	698.7	1	698.6	6	$[M - 8H^+ + 3Na^+]^{5-}$	698.6
	571.2	37	570.9	8	$[M - 6H^+]^{6-}$	571.0
	574.8	17	—	—	$[M - 7H^+ + Na^+]^{6-}$	574.6
	489.4	83	—	—	$[M - 7H^+]^{7-}$	489.3
	—	—	492.3	4	$[M - 8H^+ + Na^+]^{7-}$	492.4
	428.2	100	—	—	$[M - 8H^+]^{8-}$	428.0
	—	—	—	—	$[M - 9H^+]^{9-}$	380.3

Table 5, continued

Oligomer (No.CO_2^- groups)	Observed signals at CV = 25 V *m/z*	rel. int.	at CV = 55–65 V *m/z*	rel. int.	Assignment [species]	Pred. *m/z*
27-mer	[5126.8]*				[M = 5125.3]	
(14)	—	—	—	—	$[M - H^+]^{1-}$	5124.3
	—	—	—	—	$[M - 2H^+]^{2-}$	2561.7
	—	—	—	—	$[M - 3H^+]^{3-}$	1707.4
	—	—	1280.2	8	$[M - 4H^+]^{4-}$	1280.3
	—	—	1285.6	13	$[M - 5H^+ + Na^+]^{4-}$	1285.8
	—	—	1024.0	20	$[M - 5H^+]^{5-}$	1024.1
	—	—	1028.4	16	$[M - 6H^+ + Na^+]^{5-}$	1028.5
	—	—	1032.8	12	$[M - 7H^+ + 2Na^+]^{5-}$	1032.8
	—	—	853.2	37	$[M - 6H^+]^{6-}$	853.2
	—	—	857.0	68	$[M - 7H^+ + Na^+]^{6-}$	856.9
	—	—	860.5	28	$[M - 8H^+ + 2Na^+]^{6-}$	860.5
	—	—	864.2	13	$[M - 9H^+ + 3Na^+]^{6-}$	864.2
	—	—	731.1	100	$[M - 7H^+]^{7-}$	731.2
	—	—	734.4	90	$[M - 8H^+ + Na^+]^{7-}$	734.3
	—	—	—	—	$[M - 8H^+]^{8-}$	639.7
	568.4	5	—	—	$[M - 9H^+]^{9-}$	568.5
	511.6	14	—	—	$[M - 10H^+]^{10-}$	511.5
	464.9	45	—	—	$[M - 11H^+]^{11-}$	464.9
	426.2	84	—	—	$[M - 12H^+]^{12-}$	426.0
	428.1	21	—	—	$[M - 13H^+ + Na^+]^{12-}$	427.9
	393.4	100	—	—	$[M - 13H^+]^{13-}$	393.2
	365.2	10	—	—	$[M - 14H^+]^{14-}$	365.1

Table 5, continued

Oligomer ($No.CO_2^-$ groups)	Observed signals at CV = 25 V *m/z*	rel. int.	at CV = 55–65 V *m/z*	rel. int.	Assignment [species]	Pred. *m/z*
28-mer	[5330.2]*				[M = 5328.5]	
(14)	—	—	—	—	$[M - H^+]^{1-}$	5327.5
	—	—	—	—	$[M - 2H^+]^{2-}$	2663.3
	—	—	—	—	$[M - 3H^+]^{3-}$	1775.2
	—	—	1331.1	33	$[M - 4H^+]^{4-}$	1331.1
	—	—	1336.6	53	$[M - 5H^+ + Na^+]^{4-}$	1336.6
	—	—	1342.0	70	$[M - 6H^+ + 2Na^+]^{4-}$	1342.1
	—	—	1347.5	55	$[M - 7H^+ + 3Na^+]^{4-}$	1347.6
	—	—	1352.9	37	$[M - 8H^+ + 4Na^+]^{4-}$	1353.1
	—	—	1358.4	30	$[M - 9H^+ + 5Na^+]^{4-}$	1358.6
	—	—	1064.7	41	$[M - 5H^+]^{5-}$	1064.7
	—	—	1069.1	56	$[M - 6H^+ + Na^+]^{5-}$	1069.1
	—	—	1073.5	41	$[M - 7H^+ + 2Na^+]^{5-}$	1073.5
	—	—	1077.7	22	$[M - 8H^+ + 3Na^+]^{5-}$	1077.9
	—	—	887.1	91	$[M - 6H^+]^{6-}$	887.1
	—	—	890.7	97	$[M - 7H^+ + Na^+]^{6-}$	890.7
	—	—	894.4	42	$[M - 8H^+ + 2Na^+]^{6-}$	894.4
	760.4	5	760.6	100	$[M - 7H^+]^{7-}$	760.2
	763.4	4	763.5	78	$[M - 8H^+ + Na^+]^{7-}$	763.4
	665.1	10	664.9	50	$[M - 8H^+]^{8-}$	665.1
	667.8	7	—	—	$[M - 9H^+ + Na^+]^{8-}$	667.8
	670.6	3	670.7	13	$[M - 10H^+ + 2Na^+]^{8-}$	670.6
	591.1	22	—	—	$[M - 9H^+]^{9-}$	591.1
	593.6	11	—	—	$[M - 10H^+ + Na^+]^{9-}$	593.4
	531.9	46	—	—	$[M - 10H^+]^{10-}$	531.8
	534.0	19	—	—	$[M - 11H^+ + Na^+]^{10-}$	534.0
	483.5	80	—	—	$[M - 11H^+]^{11-}$	483.4
	485.5	24	—	—	$[M - 12H^+ + Na^+]^{11-}$	485.4
	443.2	100	—	—	$[M - 12H^+]^{12-}$	443.0
	444.9	23	—	—	$[M - 13H^+ + Na^+]^{12-}$	444.9
	409.0	64	—	—	$[M - 13H^+]^{13-}$	408.9
	—	—	—	—	$[M - 14H^+]^{14-}$	379.6

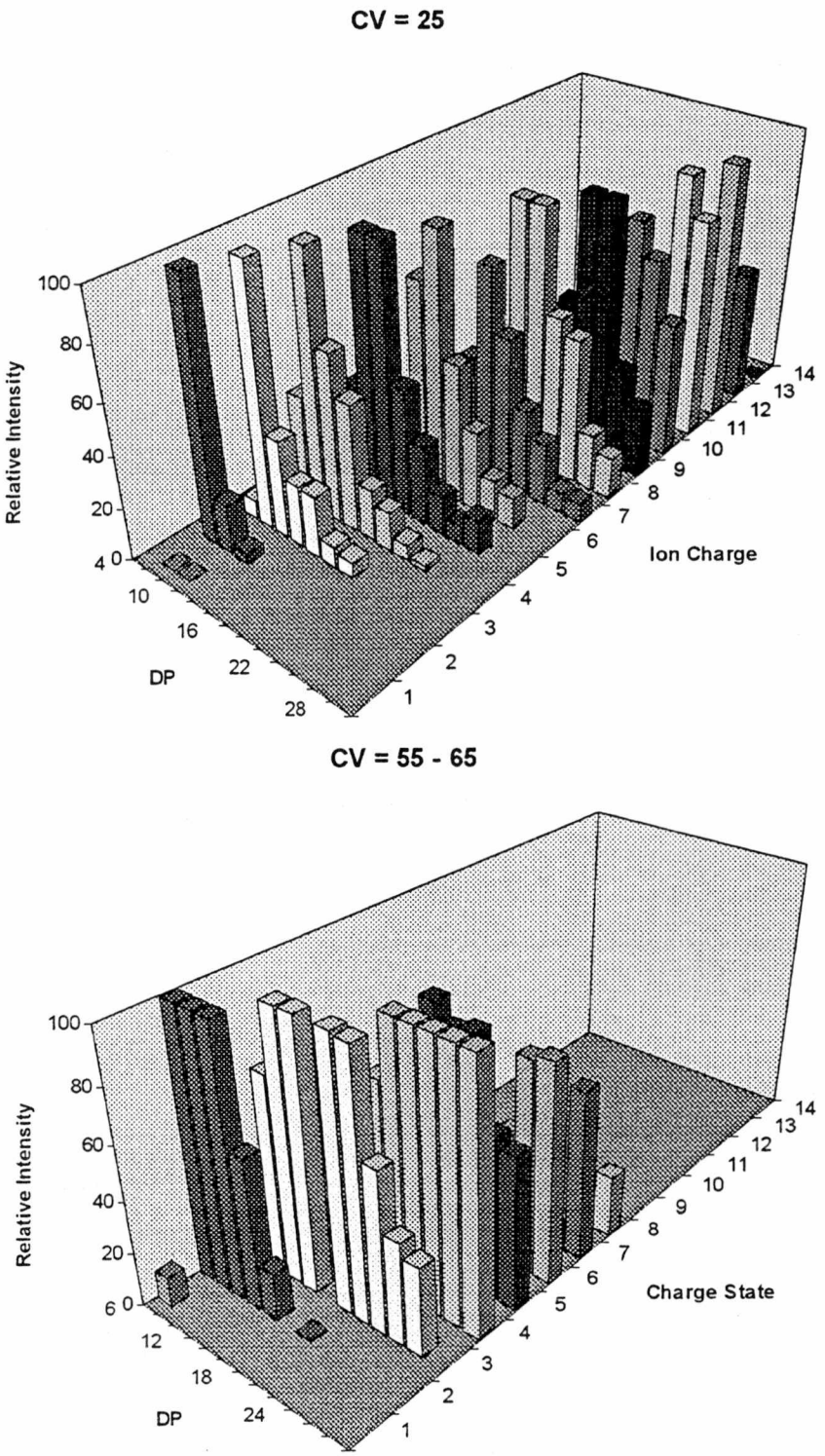


Figure 11. Relative intensities of observed charge states for BTH-derived HA oligosaccharides at CV = 25 V vs. 55–65 V

Another interesting phenomenon apparent from the data in Table 5 is the high affinity of the oligomers' $-CO_2^-$ groups for sodiation. *M/z* values corresponding to various degrees of Na^+-for-H^+ substitution can thus be calculated and correlated with the observed spectra. The remarkably strong affinity of the CO_2^- groups for sodiation expanded the "fingerprint set" of *m/z* values for the larger oligomers to twenty or more values, thus providing a preponderance of data for conclusive MW assignment (of special value for confirming the identity of the odd-numbered oligosaccharides). The use of higher cone voltages (*e.g.*, 55–65 V) was found to be particularly advantageous, with five or more variably sodiated species of a particular charge state > *m/z* 1000 being observed. Spectral examples are shown in Figures 12-13.

In order to explore these phenomena in greater detail, a series of experiments was conducted in which the cone voltage was sytematically varied in 10 V increments for three representative high-MW oligomers (20-, 24-, and 28-mers; see Table 6). In general, a shift in the predominant charge state by one charge unit is accomplished by increasing the cone voltage by 10 V. Although higher cone voltages were useful in extending the observed *m/z* range, there was a clear tradeoff, in that *absolute* signal intensities decreased considerably (presumably due to fragmentation). Figure 14 clearly illustrates both the shifts in charge state envelope distributions and the loss of signal intensity with increasing CV. In addition to the obvious consideration that a proper choice of cone voltage is critical in optimizing signal intensity, the data also highlight the importance of cone voltage selection in the analysis of anionic carbohydrates, insofar as

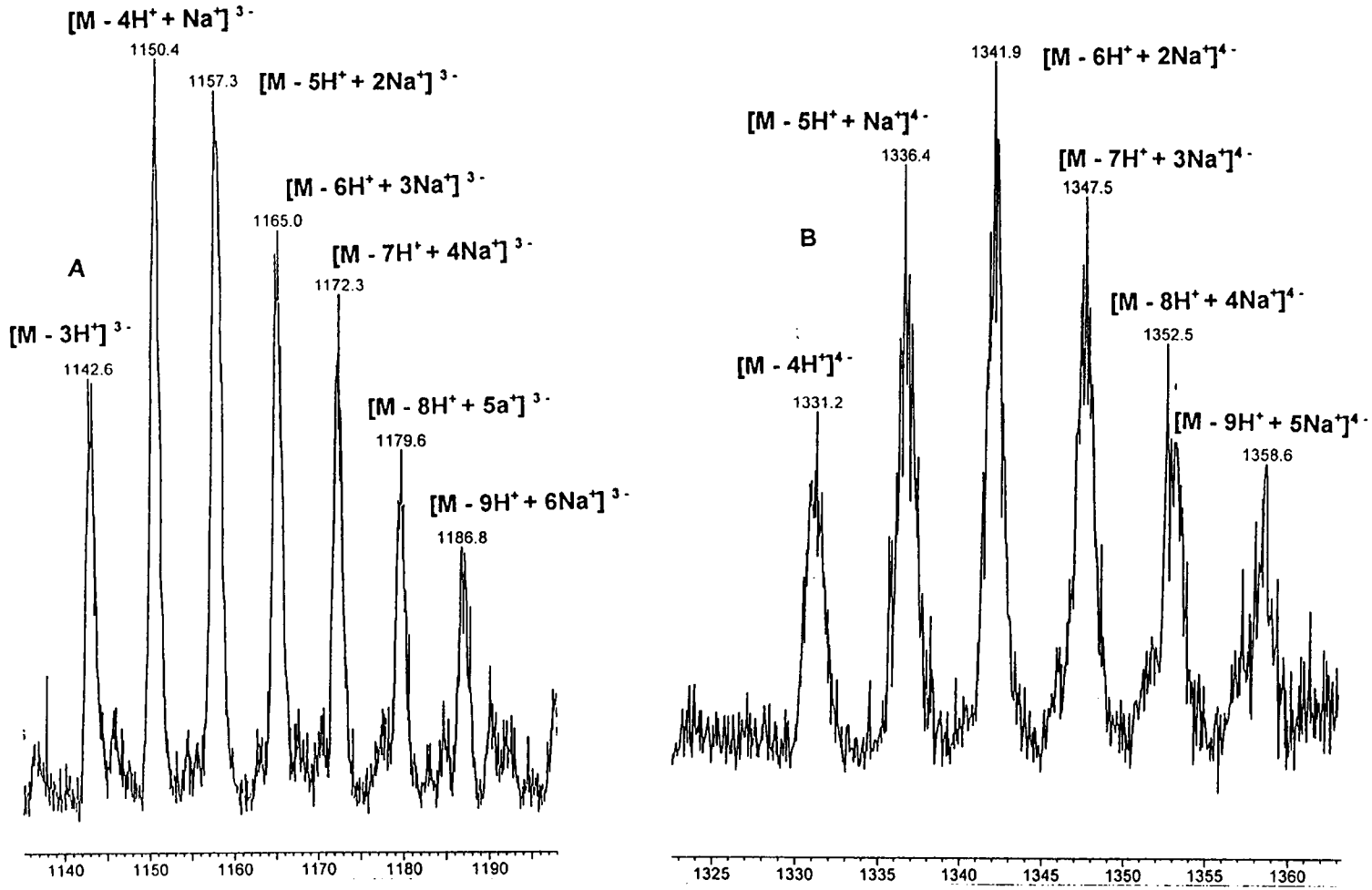


Figure 12. Sodiated trianions of 18-mer (A) and sodiated tetraanions of 28-mer (B).

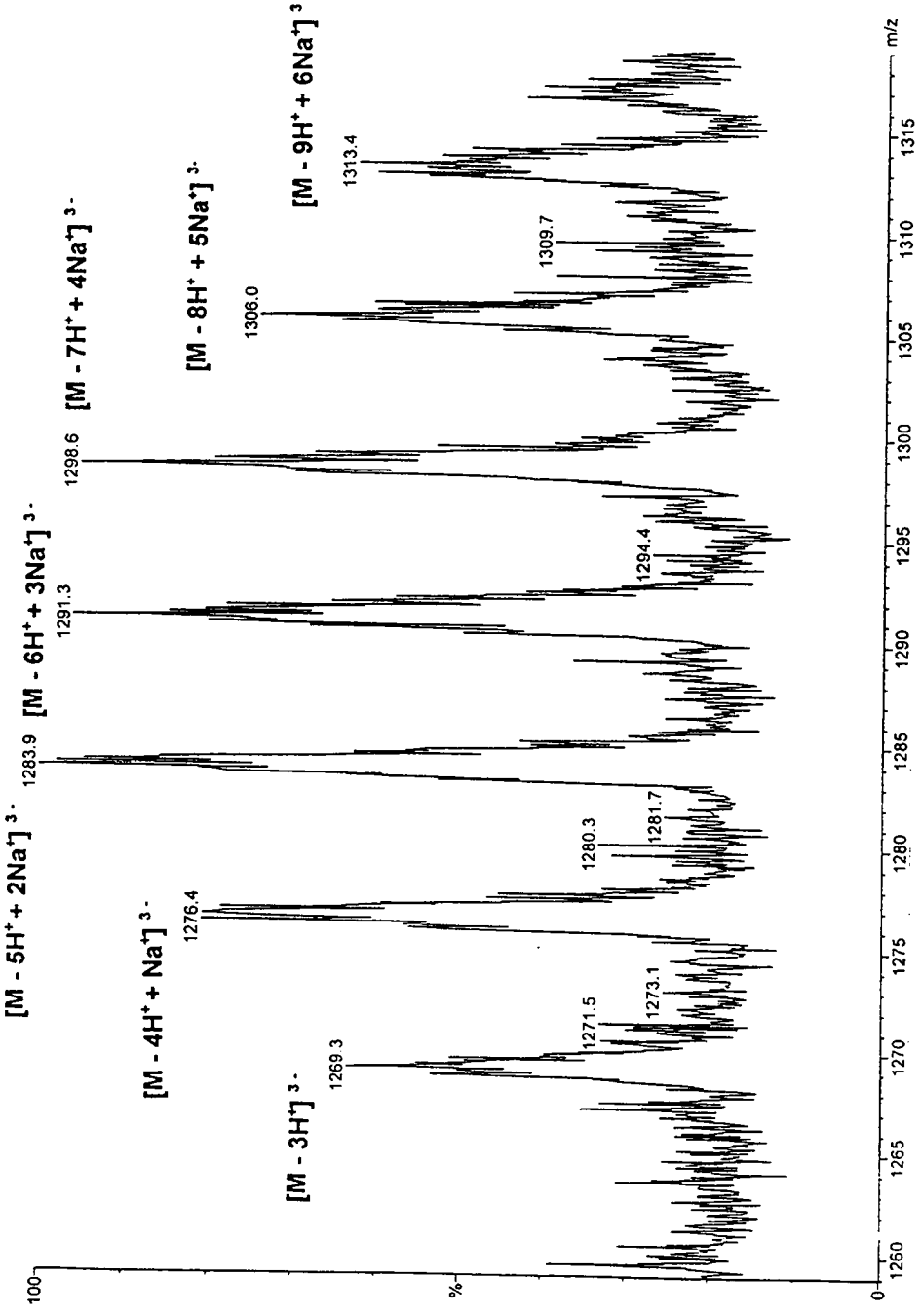


Figure 13. Sodiated trianions of 20-mer.

Table 6. Cone voltage vs. relative intensity[a]

Oligomer	charge state	Relative Intensities at CV = 20V	30V	40	50V	60V	70V	Ramp[b]
20-mer	-1	—[c]	—	—	—	—	—	—
	-2	—	—	—	—	—	—	—
	-3	—	4	8	9	13	12	8
	-4	7	9	14	16	12	4	13
	-5	8	13	21	26	9	—	25
	-6	29	41	38	11	4	—	47
	-7	48	58	14	4	—	—	70
	-8	85	53	—	—	—	—	100
	-9	100	7	—	—	—	—	50
	-10	—	—	—	—	—	—	—
24-mer	-1	—	—	—	—	—	—	—
	-2	—	—	—	—	—	—	—
	-3	—	—	—	1	3	1	1
	-4	—	4	6	8	9	6	9
	-5	5	9	9	14	9	4	13
	-6	10	13	20	18	8	—	21
	-7	17	27	26	6	—	—	31
	-8	30	42	24	—	—	—	51
	-9	51	40	—	—	—	—	71
	-10	100	32	—	—	—	—	87
	-11	75	—	—	—	—	—	20
	-12	28	—	—	—	—	—	6

[a] For each oligomer, relative intensities are normalized with respect to the most intense signal from among all seven of the voltage programs (for all three oligomers, this turned out to be the 12^- charge state under CV = 20V conditions, therefore assigned a value of 100%). The intensity indicated for a given charge state represents the sum of the intensity of the primiary ion (*i.e.*, $[M - nH^+]^{n-}$) plus all observed sodiated variants thereof.

[b] During the scan interval, the cone voltage was programmed to increase as a linear gradient from 20 to 70 V.

[c] Indicates signal(s) not observed.

Table 6, continued

Oligomer	charge state	Relative Intensities at CV = 20V	30V	40	50V	60V	70V	Ramp[b]
28-mer	-1	—	—	—	—	—	—	—
	-2	—	—	—	—	—	—	—
	-3	—	—	—	—	—	—	—
	-4	—	3	7	8	8	9	6
	-5	—	7	8	8	7	6	8
	-6	4	10	9	10	7	3	11
	-7	3	12	16	15	6	1	15
	-8	13	22	23	9	1	1	20
	-9	26	45	15	—	—	—	42
	-10	37	48	5	—	—	—	55
	-11	62	30	1	—	—	—	63
	-12	100	11	5	—	—	—	53
	-13	43	—	—	—	—	—	—
	-14	19	—	—	—	—	—	—

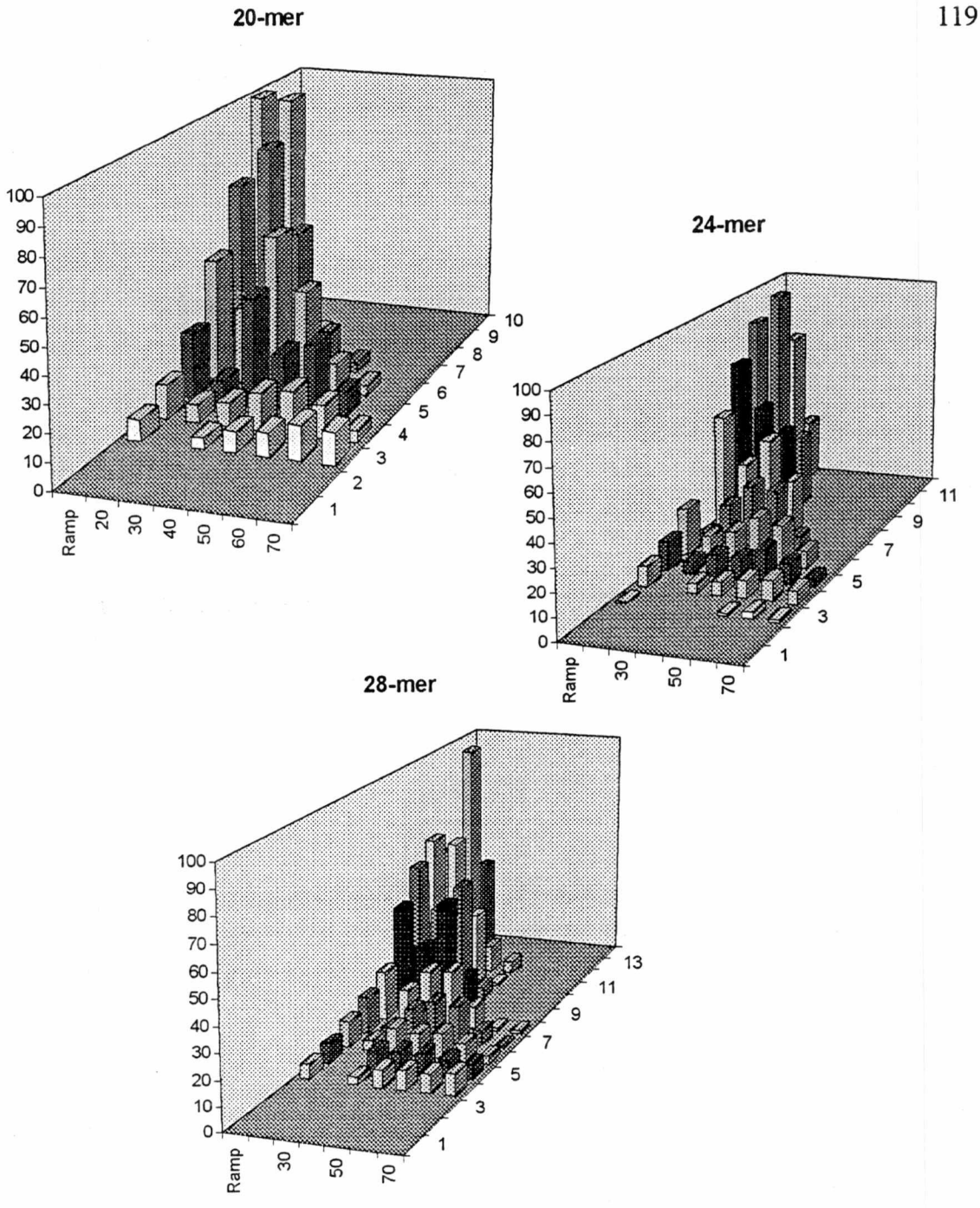


Figure 14. Effect of cone voltage on charge state and signal intensity for 20-, 24- and 28-mer. Z axis = relative intensity; X axis = cone voltage; Y axis = charge state (-).

they tune the observed *m/z* arrays to the desired charge state envelope range.

3. *High-performance anion-exchange chromatography*

Using the elution and electrochemical detection conditions developed for hyaluronic acid oligomers in section A.3.,[1] the BTH-derived oligosaccharides were analyzed via isocratic elution as shown in Table 7. A similar zig-zag effect, in which odd-numbered oligomers exhibit *faster* retention times with respect to their next-*lower* adjacent even-numbered oligomers, was observed as was the case with the HA lyase-derived oligomers. Once correlated to ESIMS-confirmed MWs, the observed retention times then allowed the convenient identification of oligosaccharide components, as well as their relative amounts. Thus, preparative gel-filtration column fractions could be directly screened (without desalting or concentration) in order to ascertain component identity and purity.

4. *Enzyme purity*

As with HAL, we considered several means for the production of the odd-numbered oligomers. One possibility is that a reducing-end GlcNAc moiety in an HA oligosaccharide is inherently unstable and suffers chemical hydrolysis. In this way, the expected even-numbered oligomers resulting from BTH's known hexosaminidase activity might slowly decompose to give small amounts of the observed odd-numbered oligomers, along with free GlcNAc. We have not noticed such decomposition in our routine handling of the compounds over months at a time, however, so this possibility appeared unlikely. If, on the other hand, the odd-numbered oligomers do in fact arise

Table 7. HPAEC retention times (min) of BTH-derived HA oligosaccharides.[a]

(at the indicated concentration of acetate eluent, pH 7.5)

Assignment	180 mM	260 mM	350 mM	400 mM	500 mM
4-mer	3.8	—[b]			
5-mer	3.0	—			
6-mer	8.2	4.2	2.9		
7-mer	7.8	3.7	2.5		
8-mer	27.0	7.8	3.8	3.0	
9-mer		—	3.3	2.5	
10-mer	—	—	5.5	3.7	
11-mer			4.6	3.4	
12-mer		—	8.0	5.2	
13-mer			7.2	4.4	
14-mer			—	7.5	
15-mer				6.2	
16-mer				11.5	—
17-mer				9.3	—
18-mer				18.6	4.9
19-mer				14.5	4.0
20-mer				—	6.0

[a] Dionex DX-500 system with CarboPac PA-1 guard precolumn (25 mm × 3 mm) and CarboPac PA-1 column (250 mm × 4 mm); HA oligosaccharide samples (25 μL of solutions approximately 1–50 μg/mL in analyte) eluted at a flow rate of 1.0 mL/min; Acetate eluents obtained by adjusting the system pump to mix the appropriate proportion of a 1.0 M sodium acetate solution (pH 7.5) with deionized water.

[b] — Indicates not measured.

Table 7, cont.

Assignment	180 mM	260 mM	350 mM	400 mM	500 mM
21-mer					5.0
22-mer				—	7.9
23-mer					6.4
24-mer				—	10.3
25-mer					8.4
26-mer				—	13.9
27-mer					11.3
28-mer				—	19.2

from a true enzymatic cleavage, then some sort of glucuronidase activity, assigned either to a secondary *glucuronidase* activity of BTH itself, or to extraneous glucuronidase impurities in the enzyme preparation (used as purchased from Sigma), must be present. The former possiblity appeared remote, since BTH has been the subject of numerous studies in the literature, and no such activity has previously been noted. As an initial effort to probe the latter possibility, we subjected BTH as purchased to polyacrylamide gel electrophoresis and found that the protein exhibited multiple bands (Figure 15). Based on previous reports, we expected a single band at 61,000 Da for the pure BTH protein.[33] However, numerous other bands, including a major band at ca. 30,000 Da, were also observed. As our concerns were confined primarily to issues of separation and structure elucidation, an extensive investigation into this matter was deemed

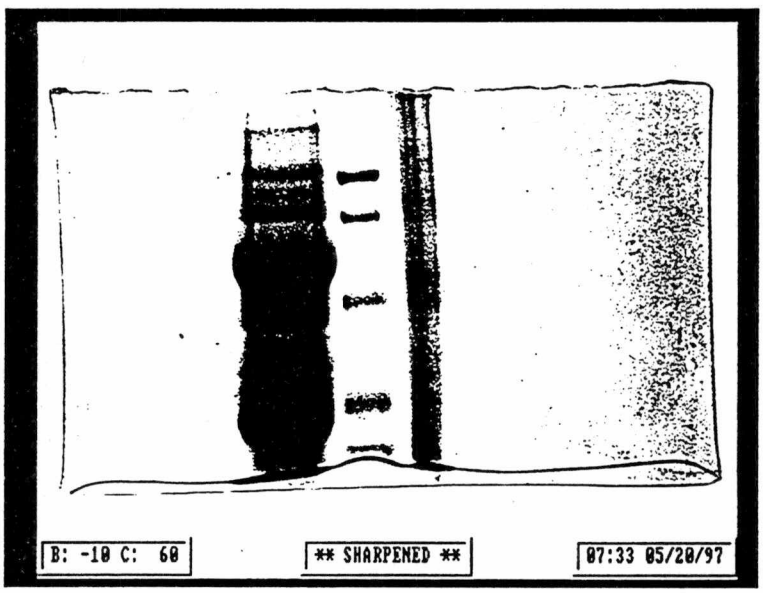


Figure 15. Polyacrylamide gel electrophoresis of BTH. BTH, left lane; MW standards (28.3, 33.5, 46.9, 80.8, 104.0 kDa), right lane.

beyond the scope of the present study. Nonetheless, the limited data warrant the conclusion that, among the possible causes, an impurity with glucuronidase activity is most likely responsible for the production of the odd-numbered oligomers. Although extraneous protein impurities are expected (and usually immaterial) for normal usage of such enzymes, the presence of enzymes with competing and/or unwanted activities on the substrate in question is a significant infringement on their utilization for producing well-defined oligosaccharide fragments for biological evaluation.

As HAL is also well studied in the literature, the production of odd-numbered oligomers in that case is also likely to be attributable to the presence of extraneous hydrolase impurities in the purchased preparation.

IV. CONCLUSIONS

Hyaluronan was degraded with hyaluronate lyase (EC 4.2.2.1) and bovine testes hyaluronidase (EC 3.2.1.35), and the resulting oligosaccharides up to dp 16 (for HAL) and 28 (for BTH) were characterized by ESIMS and HPAEC–PAD. In both cases, minor but significant amounts of novel and unexpected odd-numbered oligomers were also isolated and characterized in addition to the expected even-numbered oligosaccharides.

The developed methods are the first reported applications of ESIMS and HPAEC–PAD to hyaluronan oligosaccharides. In a more general sense, the studies demonstrate the usefulness of both ESIMS and HPAEC–PAD in the analysis of anionic glycosaminoglycan-type oligosaccharides in general and provide experimental parameters that could facilitate the extension of these methods to carbohydrate examples that might prove difficult using existing literature conditions. In the case of ESIMS, an existing literature question with regard to the polyanionization of acidic oligosaccharides has been answered. As shown by the facile extension of the methods developed with the HAL oligomers to the much larger BTH-derived oligosaccharides, increasing MW does *not* seem to diminish the ability of *m/z* data to confirm analyte MW, so the method should be amenable to other glycosaminoglycan-type oligosaccharides of comparable and higher MW. With respect to the behavior of the acidic oligomers under negative-ion mode electrospray, we observed that the extensive sodiation of carbohydrate carboxylate groups afforded numerous additional *m/z* data points to corroborate

assigned structures, and also described a logical and expected relationship between cone voltage and observed charge state envelopes, concluding that optimization of cone voltage is critical in both maximizing signal intensity and in selecting the desired charge state window for such compounds. In the case of HPAEC–PAD, the electrochemical waveform developed is significantly different from published waveforms, especially in the integration potential and durations. An occurrence in which the neutral pH acetate eluent causes odd- and even-numbered oligomers to elute in a staggered pattern with respect to the number of monosaccharide residues was also uncovered. With standard retention times correlated to mass spectral data, the combination of HPAEC-ESIMS methods furnished the desired means of directly screening fractions from preparative chromatography, a well known and tedious obstacle in carbohydrate separations.

The finding of unexpected reaction products in conjunction with the demonstrated impurity of the enzyme suggest that the digestion mixtures of these and other glycosaminoglycan-degrading enzymes would benefit from more detailed study utilizing sensitive methods such the ones developed here, and should be noted by researchers using the commercially available enzyme preparations to afford supposedly well defined glycosaminoglycan oligosaccharide fragments for biological evaluation.

Finally, the preceding work has established clear structural characterization of hyaluronate lyase and bovine testes hyaluronidase-derived HA oligosaccharides previously lacking in the literature. As the biomedical significance of such carbohydrates continues to become more recognized, the characterization provides a better foundation

for structure–activity relationships, including the SAR for the metastasis inhibition studies described herein.

V. EXPERIMENTAL SECTION

A. Materials

Hyaluronate lyase, and bovine testes hyaluronidase were purchased from Sigma Chemical Co. (St. Louis, MO). Sodium hyaluronate was either purchased from Sigma Chemical Co. or received as a gift from Genzyme Corp. (Boston, MA). Enzyme-derived samples were either prepared as described below, or were obtained pre-prepared (also by the procedure below) from the laboratory of Dr. Richard Cysyk at the National Cancer Institute. Water was deionized and filtered using a Barnstead Nanopure 550 system.

B. Enzyme degradations and preparative column chromatography

For the HAL digestions, 50 mg of sodium hyaluronate was suspended in 10 mL of aqueous buffer (200 mM in NaCl, and 50 mM in NaOAc, pH 6.0) and the mixture stirred overnight at 0°C resulting in a clear solution to which HA lyase (1000 units) was added, and stirring continued at 37 °C. Aliquots (50 μL) were periodically removed and monitored at 232 nm on a Shimadzu 2101PC spectrophotometer until absorbance began to level off (ca. 2–4 h). The mixture was then boiled for 10 min, diluted with 10 mL of water, and lyophilized. To afford a mixture containing the 3-mer, digestions were conducted and purified as above except that the reaction time was 3–5 days.

For the BTH digestions, 50 mg of sodium hyaluronate was suspended in 10 mL of aqueous buffer (200 mM in NaCl, and 50 mM in NaOAc, pH 6.0), and the mixture

was stirred overnight at 0°C, resulting in a clear solution to which BTH (1000 units) was added. Stirring was then continued at 37 °C for 3 h, after which time the reaction was boiled for 10 min, and lyophilized.

In both cases, the resulting white powder was redissolved in 250 mM NH_4HCO_2 and subjected to gel-filtration chromatography (BioGel P-30), using 250 mM NH_4HCO_2 as eluent. Fractions were collected on the basis of UV absorbance (in the case of HAL, either by taking aliquots of individual fractions, whose absorbance values were compiled into a chromatogram, or by use of an ISCO UA-5 flow monitor), or in the case of BTH by the radiolabeled HA-binding protein assay of Orvisky[34] (when conducted in Dr. Cysyk's laboratories) or by Dionex sampling (when conducted at UTK). Pooled fractions were lyophilized five times and analyzed as described below.

C. High-performance anion-exchange chromatography

The analytical system consisted of a Dionex DX-500 system (Sunnyvale, CA) equipped with a CarboPac PA-1 guard precolumn (25 mm × 3 mm), CarboPac PA-1 column (250 mm × 4 mm), and a type II PAD (with gold working electrode and silver/silver hydroxide reference electrode) interfaced to a Hewlett-Packard 3390A integrator. The electrochemical detector was operated in the pulsed amperometric mode at 3 μA sensitivity. The triple pulse sequence used for amperometric detection included the following potentials and durations: E_1 = − 0.15 V (210 ms, integrating from 81-210 ms), E_2 = + 0.75 V (180 ms), E_3 = −0.35 V (360 ms). To facilitate pulsed

amperometric detection and minimize baseline drift, 400 mM NaOH was added post-column at a flow rate of ca. 0.5 mL/min. HA oligosaccharide samples (25 μL of solutions approximately 1–50 μg/mL in analyte) were eluted at a flow rate of 1.0 mL/min. Acetate eluents at the concentrations listed in Table 1 were obtained by adjusting the system pump to mix the appropriate proportion of a 1.0 M sodium acetate solution (pH 7.5) with deionized water.

D. Electrospray–ionization mass spectrometry

Negative-ion electrospray mass spectra were obtained using a Micromass Quattro II triple quadrupole instrument, with a nominal mass range to 4,000 Da. Data acquisition and manipulation were accomplished using the Micromass MassLynx software package, including MAX ENT data analysis software. Sample solutions (approximately 16 μg/mL in 1:1 methanol–water containing 0.3 % triethylamine) were infused at a flow rate of 4 μL/min. Nitrogen was used as the nebulizing (20 L/h) and drying gas (300 l/h) while maintaining the source temperature at 80 °C.

For the HA lyase-derived samples, the following parameters were used. Capillary- and cone voltages were 2.5 kV and 25 V, respectively. Spectra were acquired in multi-channel-acquisition mode from scans encompassing *m/z* 50–1750 at 10 s/scan (and averaging of 10 such scans per spectrum). Reported masses are the averaged value for the isotope cluster.

For the bovine testes hyaluronidase-derived samples, the following parameters

were used. The capillary voltage was set at 2.5 kV and the cone voltage was set at 17–65 V as indicated. Spectra were acquired in multi-channel-acquisition mode from scans encompassing *m/z* 50–1750 as above. Reported masses are the averaged value for the isotope cluster.

E. Polyacrylamide gel electrophoresis

The polyacrylamide gel electrophoresis was conducted by Dr. Baburaj Kannemal in the dept of Biochemistry, UTK, according to described procedures.[34]

CHEMICAL SYNTHESIS OF HYDROLASE-RESISTANT HYALURONAN MIMICS

I. INTRODUCTION

A. Laboratory probes vs. drug candidates

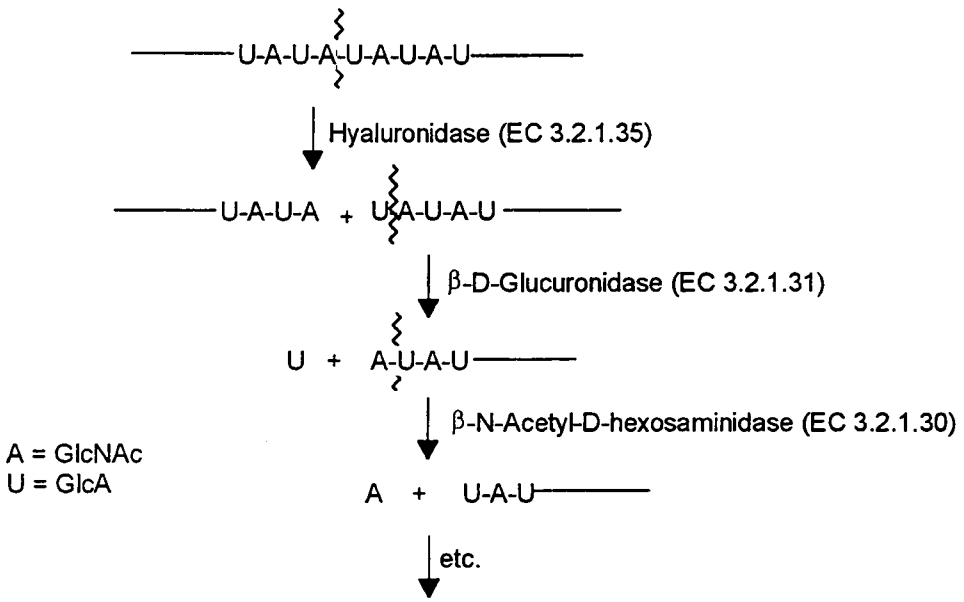
Although useful as laboratory probes for cancer metastasis, the enzyme digest-derived oligomers are not anticipated to be useful as drugs, since they would most likely be cleared rapidly from the bloodstream by the action of hyaluronidases. The *in vivo* half-life of HA (as well as smaller HA oligosaccharides) has been estimated at under 5 minutes.[1] In order to design hydrolase-resistant HA mimics, the biochemistry of mammalian HA degradation must be examined in greater detail.

Hyaluronan is degraded in the local tissues where it is produced, as well as in the lymph nodes and in the liver.[2] Degradation may be initiated by the receptor-mediated process whereby the CD44 receptor binds HA, after which it is endocytosed, transferred to a lysozome, and degraded by acid hydrolases.[3] In addition, degradation pathways via extracellular hyaluronidases are also suspected.[4] It is known in mammals that the degradation of HA is accomplished by the following three enzymes: hyaluronidase (EC 3.2.1.35), β-D-glucuronidase (EC 3.2.1.31), and 2-acetamido-2-deoxy-D-hexosaminidase (EC 3.2.1.30).[5] Their substrate specificities are also known: hyaluronidase is an *endo*-glycosidase specific for a glycosidic bond containing C-1 of a GlcNAc residue, whereas β-D-hexosaminidase and β-D-glucuronidase are *exo*-glycosidases that remove a GlcNAc

or a GlcA residue, respectively, from the nonreducing end of the polymer. Scheme 1 graphically shows these specificities.

B. Design of hydrolase-resistant HA mimics

There are several types of structural modifications that can be incorporated into an oligosaccharide to render it resistant to hydrolase action. As depicted in Figure 1, these can be divided into two general classes (for convenience, several modifications are incorporated into a single structure) . The oligosaccharides representing Class 1 involve structural modifications that offer the *possibility* of rendering resistance. These types of structures still contain the hydrolyzable O-glycosidic bond, but possess substitutions for certain hydroxyl groups with other functional groups such as halogen, hydrogen, methoxy, etc., in such a way as to force the structure to not be recognized by the hydrolyzing enzyme. When planning resistant oligossaccharides of this type, it is difficult to predict whether or not a given substitution will actually turn out to confer resistance: the result must be verified by experiment after synthesis. The first example of this type (Figure 2) is a deoxy analog from Hindsgaul and co-workers (substitute -H for -OH, compound **1**),[6] and the second example is a heparin analog developed by Petitou and co-workers, which subsitutes several hydroxyl groups with methoxy groups (**2**).[7] The oligosaccharides shown in Class 2 (Figure 1), in contrast, involve modifications that render *unequivocal* resistance because the O-glycosidic linkage has been eliminated. These include the *C*- and *S*-oligosaccharides, in which the interglycosidic oxygen atom has been substituted by a CH_2-group (ether linkage, not hydrolyzable by enzymes,[8]



Scheme 1. Specificities of mammalian hyaluronidases

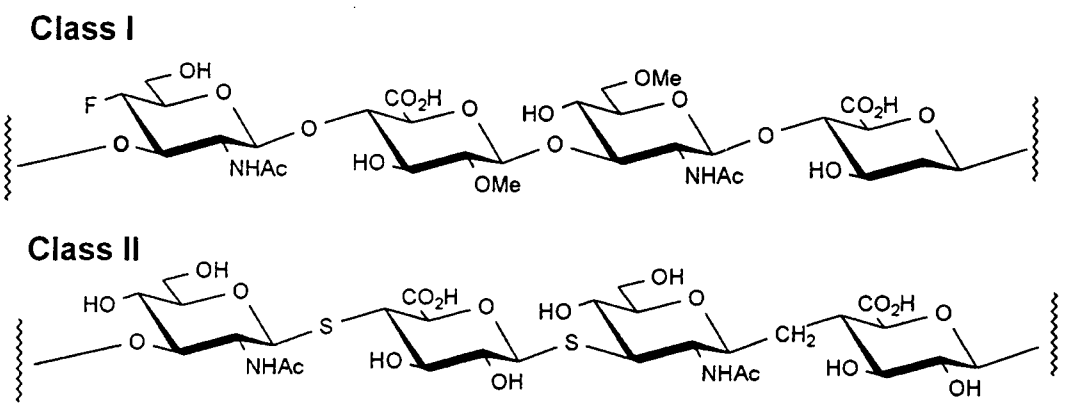


Figure 1. Oligosaccharide structural modifications conferring hydrolase stability

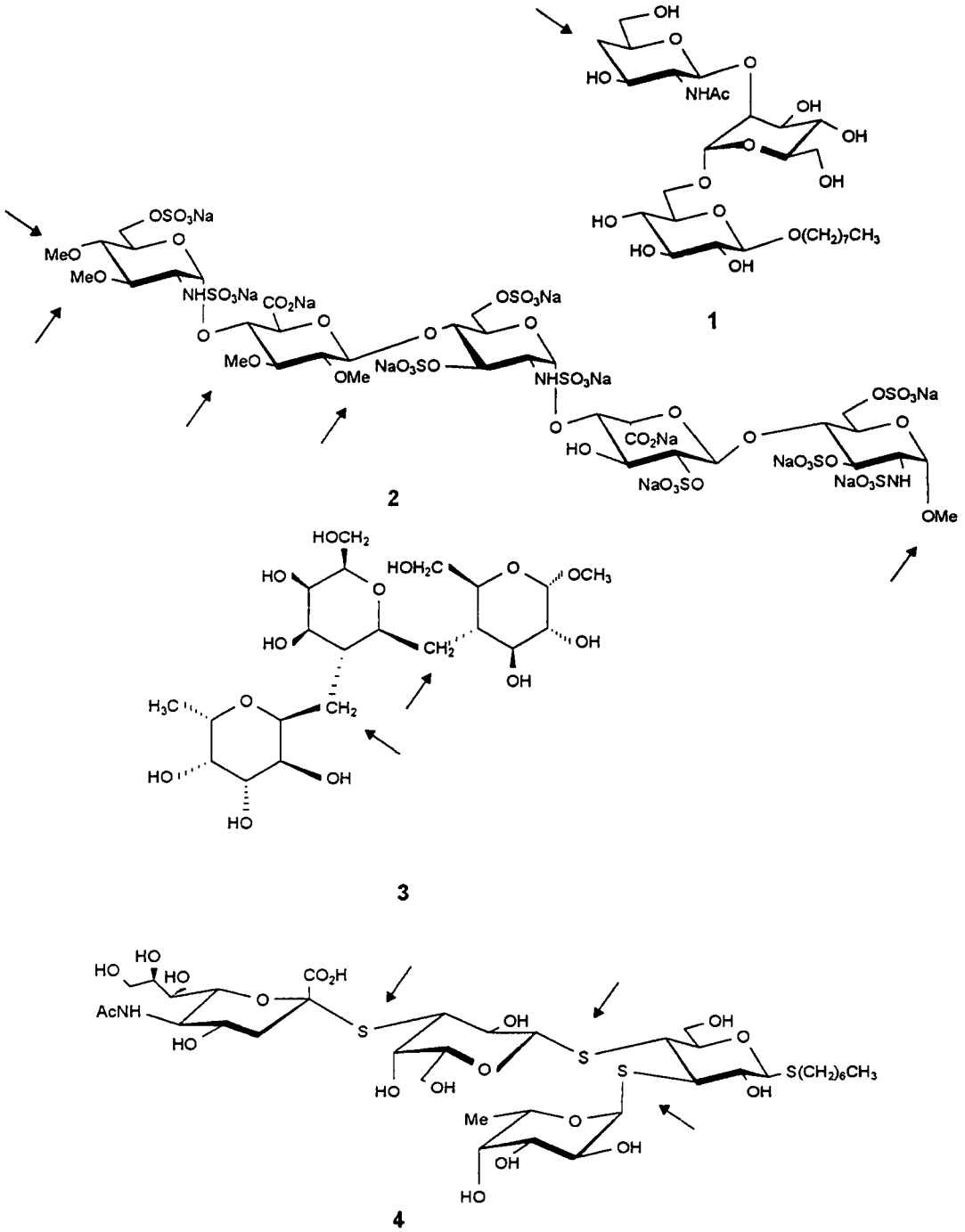


Figure 2. Literature examples of synthesized hydrolase-resistant oligosaccharides

compound **3** in Figure 2) or sulfur atom (thioacetal, for all purposes not hydrolyzable by enzymes,[9] compound **4**), respectively. Class 1 offers greater ease in synthesis but greater uncertainty as to enzyme resistance. Class 2 offers certainty with respect to enzymatic stability, but involves much more complicated chemical synthesis.

In light of recent studies showing that *C*-oligosaccharides are known to conformationally mimic their O-glycoside counterparts,[10] a C-linked analog was selected as the target for the present studies. In addition to the CH_2-linked oligosaccharides, we also decided to consider the S-linked compounds. Perhaps since thioglycosides are so well studied due to their utility as C-1 activator groups in glycosylation reactions,[11] the chemistry of *S*-oligosaccharides is more developed, making these compounds comparatively easier of synthesis than their C-linked counterparts. Nevertheless, *both C*- and *S*-oligosaccharides are difficult to synthesize in absolute terms, and the degree of difficulty increases drastically with the number of sugar units in the target compound. To date, the largest *C*-oligosaccharide is but a *C*-trisaccharide,[12] and the largest *S*-oligosaccharide is but an *S*-tetrasaccharide.[13] Hence, the use of a *C*- or *S*-oligosaccharide of four or more units as a readily available metastasis probe or drug candidate is, at present, out of the question.

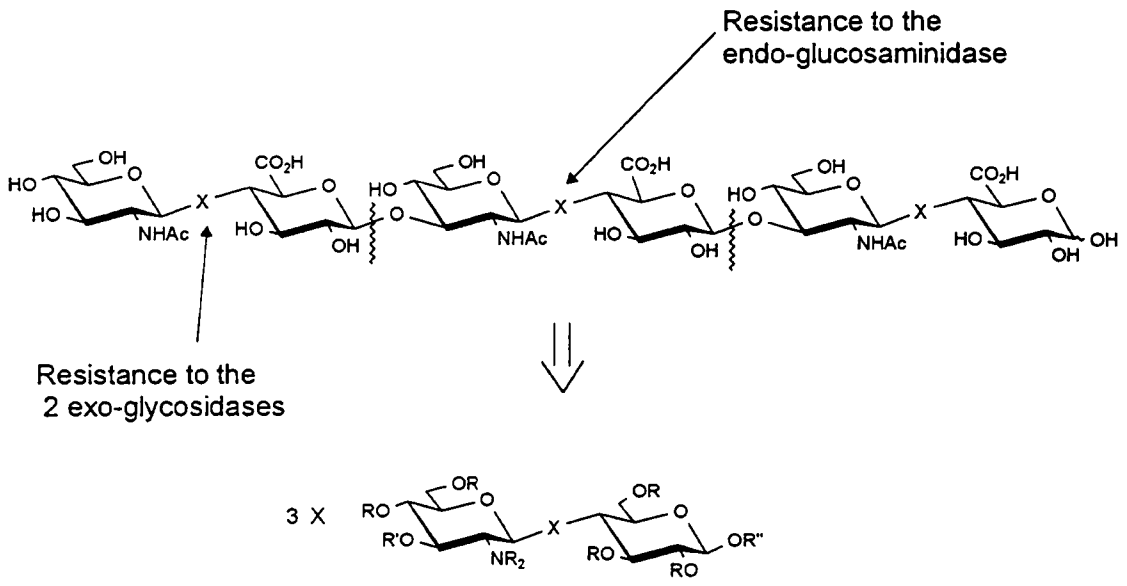
We analyzed the possibilities and chose *not* to synthesize an entirely CH_2/S-linked oligosaccharide. Rather, we would design a "mixed" oligosaccharide that would contain strategically placed CH_2/S-linkages only at those positions in the oligosaccharide where the molecule would be vulnerable to enzymatic hydrolysis. The remaining glycosidic linkages would consist of the usual O-linkages, mainly to facilitate ready synthesis (the

chemistry of O-glycosides is perhaps the most well documented discipline within carbohydrate chemistry[14]). To our knowledge, "mixed" oligosaccharides of this design have not yet appeared in the literature. The known specificities for the three major HA-degrading enzymes (refer back to Scheme 1) require that a hyaluronidase-resistant oligosaccharide must have stabilized linkages at every linkage containing C-1 of a GlcNAc residue and also at the first linkage at the nonreducing end of the oligomer, regardless of the residue. A hexasaccharide candidate satisfying these constraints is shown in Scheme 2, where X = S or CH_2. This sugar is also designed to make it amenable to a convergent, blockwise synthetic approach wherein multiple copies of a single CH_2/S-linked disaccharide are linked *n* times via normal glycosidation techniques to produce oligomers of specified length (either 4, 6, or 8 residues, etc.); *i.e.*, only one type of CH_2/S linkage needs to be constructed. Once the *C/S*-disaccharide has been synthesized, it could be coupled together seqentially using conventional O-glycosylation reactions to afford larger oligomers (*vide infra*).

In summary, the purpose of a "mixed" oligosaccharide, with either S- or CH_2-linkages, is two-fold:

- To confer resistance to degradation by HA-degrading enzymes.
- To facilitate synthesis via a block approach, wherein a single *S/C*-disaccharide is synthesized and linked once, twice, or more times via normal O-glycosidation techniques.

An additional advantage to using a "mixed-link" oligosaccharide might be to minimize the inevitable chain lengthening resulting from multiple insertion of large –S– groups.



Scheme 2. Candidate hexasaccharide capable of evading mammalian HA-ases

II. STATEMENT OF THE PROBLEM

A. Objectives

The synthetic objectives of this project are as follows:

- To synthesize prototype *S*-disaccharides.
- To synthesize a mixed S/O-linked oligosaccharide via blockwise O-glycosylation of *S*-linked disaccharides.
- To synthesize key intermediates for *C*-disaccharide synthesis.

As the synthetic chemistry of *S*-disaccharides is less complicated than that of *C*-disaccharides, efforts would first focus on developing a route to the appropriately protected *S*-disaccharide, followed by elaboration of the disaccharide into larger mixed *S/O*-oligosaccharides. Within the time constraints of the project, the chemistry for key synthons in the synthesis of *C*-disaccharides would be developed concurrently.

B. Research plan—retrosynthetic analysis

1. Iterative blockwise synthesis: construction of O-linkages; common X-disaccharide intermediate

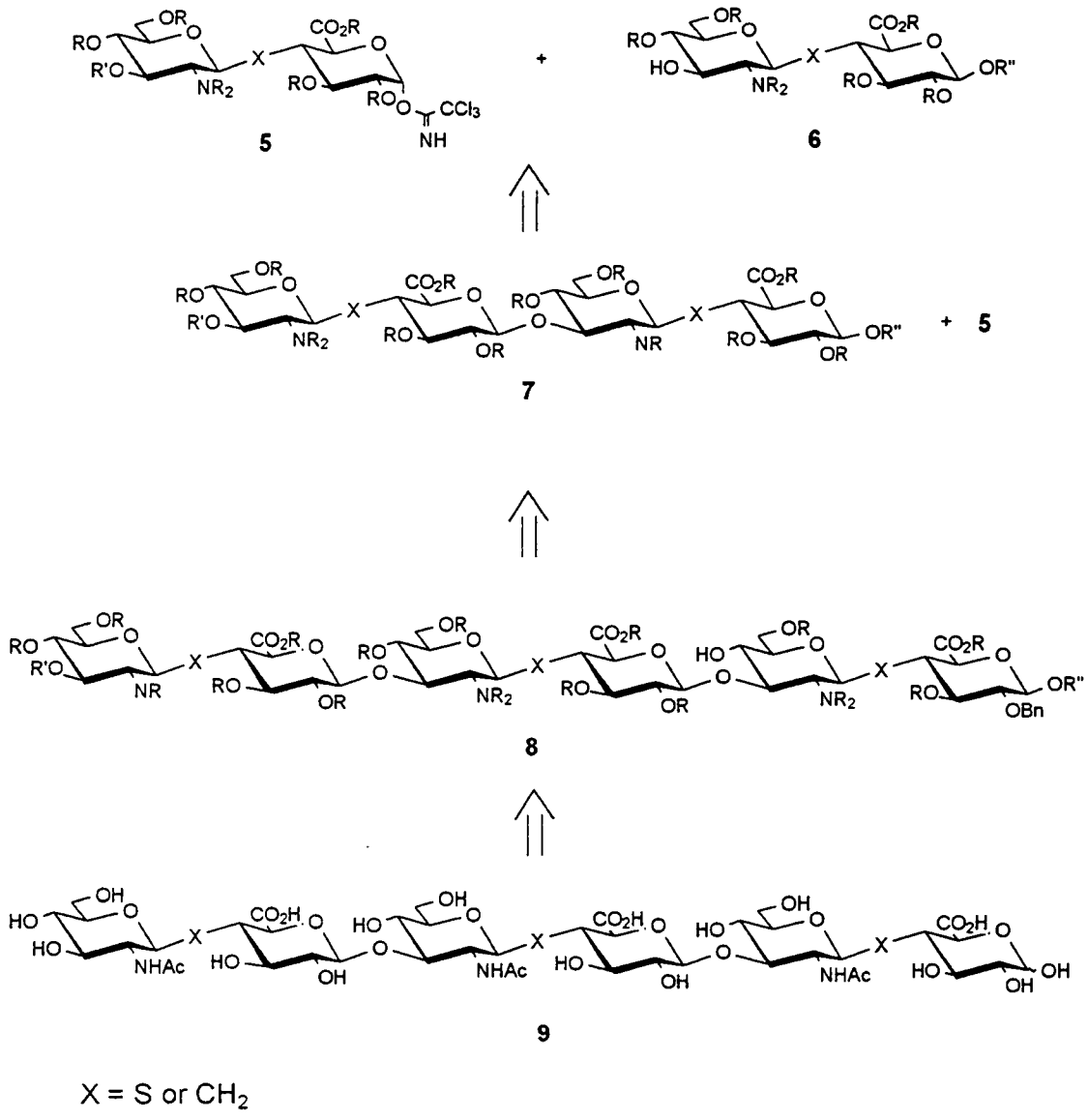
The general success of trichloroacetimidate glycosyl donors[15] as well as their successful employment for β-glycosylations in Ogawa's HA-related oligosaccharide syntheses[16] suggest the use of that methodology in constructing the O-glycosidic linkages of the oligosaccharides targeted in this study. The retrosynthetic analysis begins by envisioning the large-scale construction of the oligosaccharide as accessible through such Schmidt O-glycosylations between pre-synthesized X-linked (or mixed X/O-linked)

oligosaccharide blocks, where X = CH_2 or S. This "iterative blockwise glycosylation protocol," mentioned in Section I.B., is now outlined in Scheme 3. Thus, X-linked disaccharide glycosyl donor **5** is coupled with X-linked disaccharide glycosyl acceptor **6** to afford tetrasaccharide **7**. This tetrasaccharide would then be deprotected at the nonreducing end (via selective removal of R') and resubjected to donor **5** to afford hexasaccharide **8**. Global deprotection would then afford the desired hydrolase-resistant HA mimic **9**. Alternatively, the 3' deprotection and coupling to **5** processes could be repeated an additional one or two times (followed by deprotection) to provide the octa- or decasaccharides, respectively.

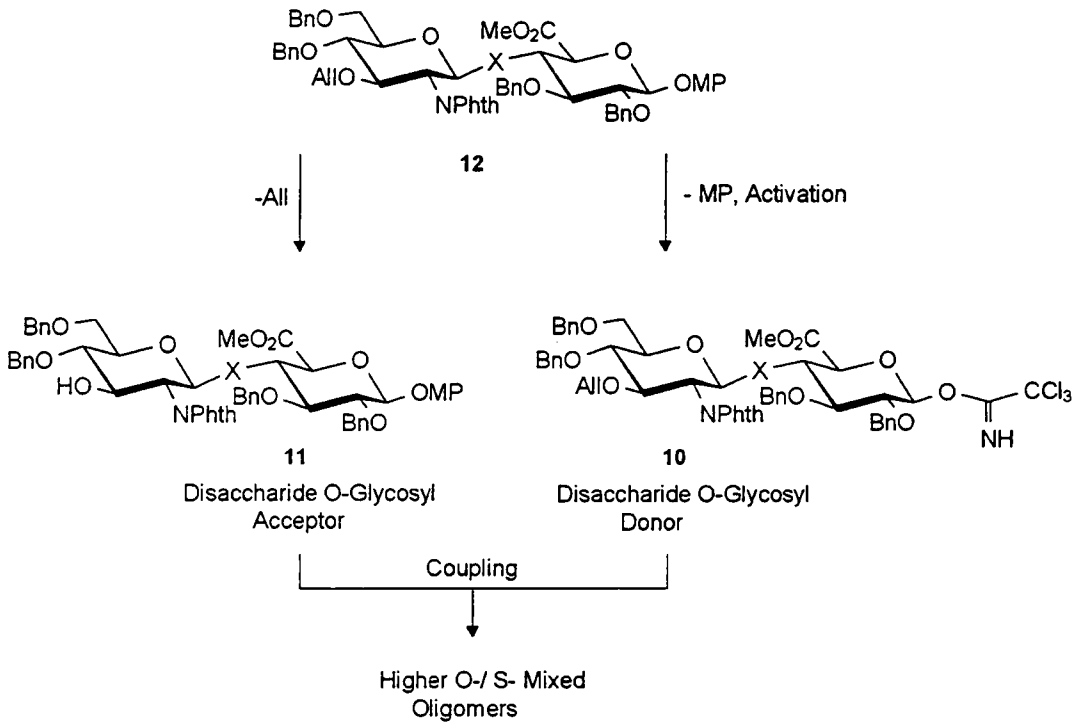
The approach would be made convergent by deriving both **5** and **6** (here shown with specific protecting groups as **10** and **11**, respectively) from a single, completely protected intermediate **12**, shown in Scheme 4. Again, the advantage to this approach is that only one X-linked species needs to be synthesized.

2. Synthesis of S-disaccharides

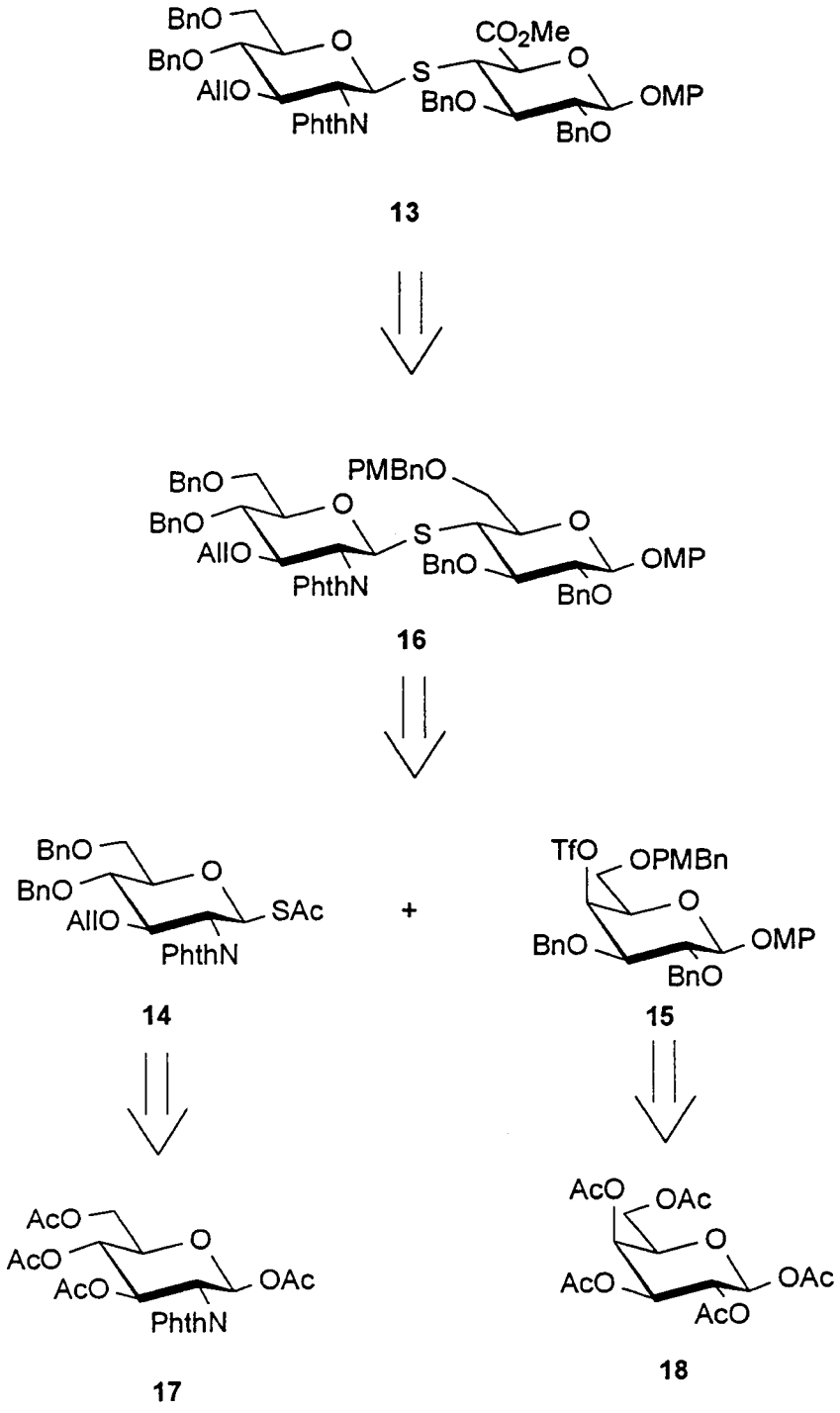
Consideration can now be extended to the synthesis of **13**, the *S*-disaccharide case of **12** (Scheme 5). The first issue concerns the construction of the S-linked structure itself. Fortunately, there is ample precedent in the literature for the synthesis of such species. Based on chemistry developed by Driguez and co-workers,[17] in which a 1-*S*-acetyl-1-thioglycoside (Gly-SAc, **14**) displaces an axial *O*-triflyl group of a second protected carbohydrate moiety (**15**), it was anticipated that the coupling shown in Scheme 5 would afford S-linked disaccharide **16**, a precursor to **13**. Compounds **14**



Scheme 3. Iterative blockwise synthesis of mixed O-/X- oligomers



Scheme 4. Derivation of *di*saccharide glycosyl donor and acceptor from a common intermediate



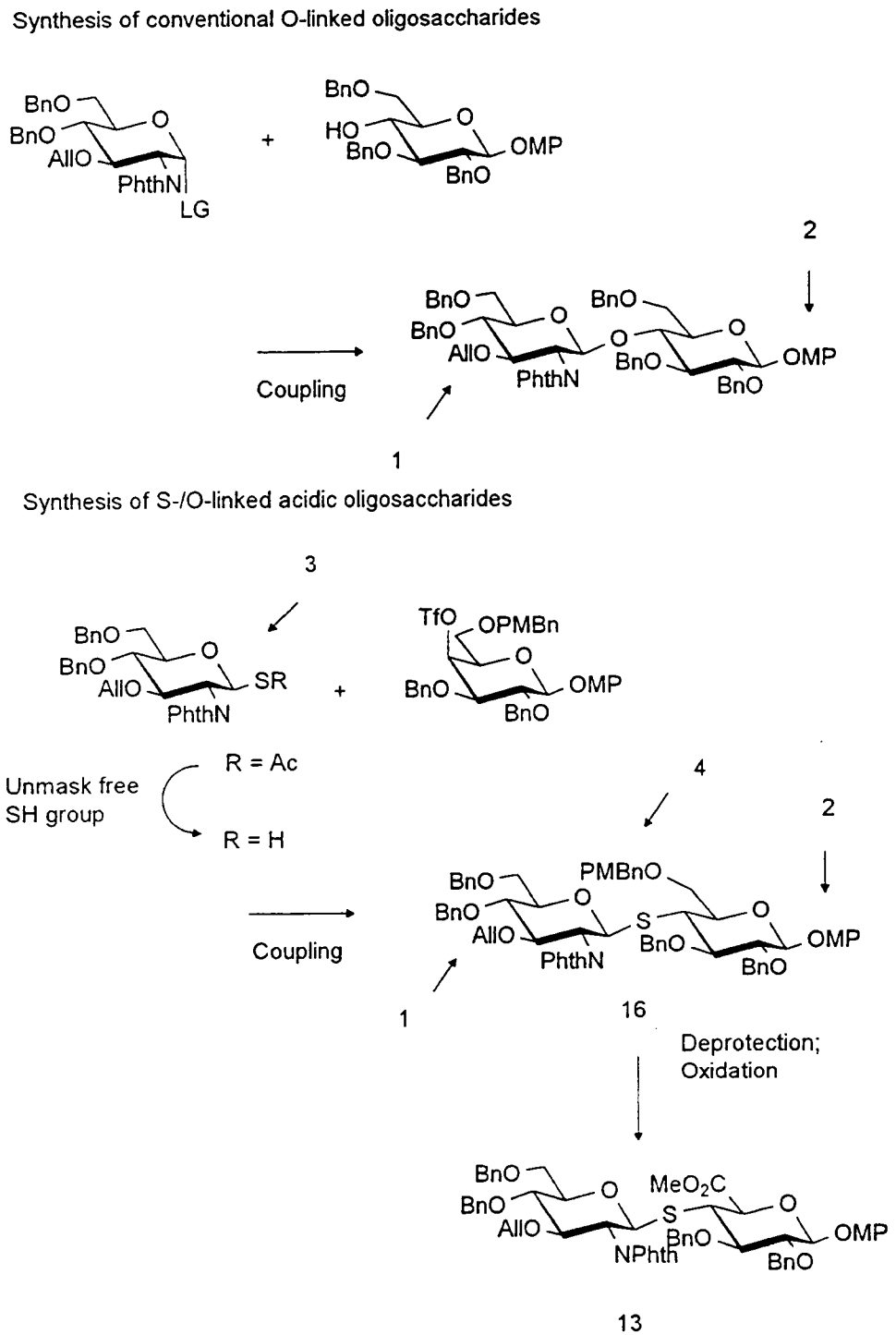
Scheme 5. Retrosynthetic analysis for *S*-disaccharide **13**

and **15** would be derived from known compounds **17** and **18**, as shown.

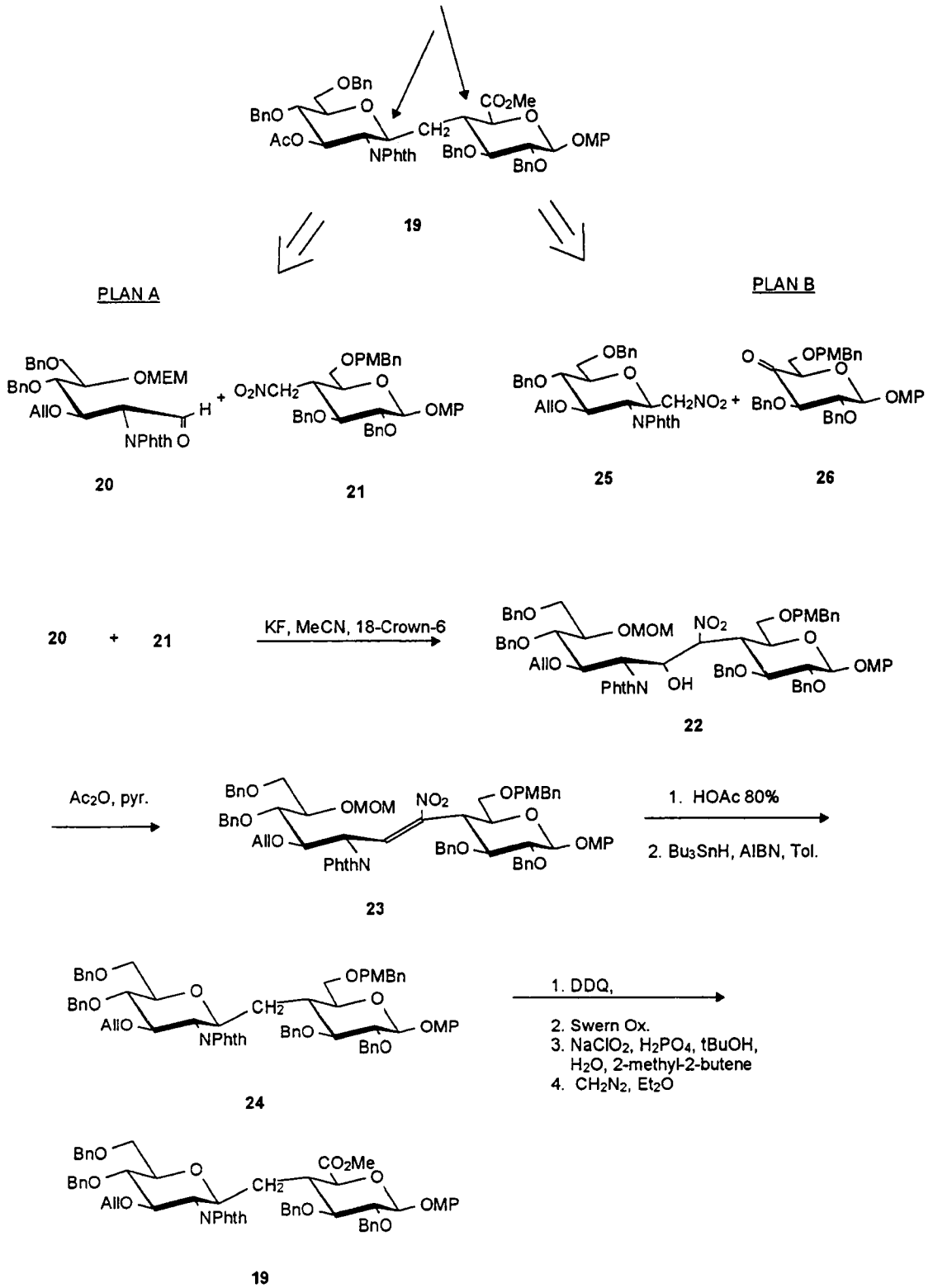
The second issue to be considered involves the differential protection present in **16**. As illustrated in Scheme 6, O-glycosylation requires three discrete levels of hydroxyl group protection. (1) All hydroxyl groups not participating in glycosylation reactions must be "persistently" protected until final (global) deprotection (not shown); benzyl groups fulfill this function here. (2) The "glycosyl acceptor" hydroxyl must be protected to allow selective unveiling [arrow 1, allyl group]. Finally, (3) the C-1 position must be protected to allow selective unveiling of the anomeric position and activation to a glycosyl donor [arrow 2, methoxyphenyl group]. However, the synthesis of S-linked disaccharide glucuronate **13** requires two *additional* levels of orthogonal protection for the following manipulations: (4) selective protection for sulfur-atom introduction and manipulation [arrow 3, acetyl group], and (5) selective protection at C-6 to allow oxidation [arrow 4, methoxybenzyl group]. The protecting group array present in **16** satisfies these requirements.

3. Synthesis of C-disaccharides

Compound **19**, the CH_2-linked case of **12**, is likely accessible through the method developed by Martin.[18] Its application in constructing **19** leads to the consideration of two distinct disconnections (Scheme 7). Martin's requisite step-by-step chemistry that would be involved in creating the CH_2 -linkage is also shown for one of these routes. Aldehydo sugar **20** and 4-*C*-nitromethyl compound **21** would be condensed using KF and 18-crown-6 in CH_3CN. The resultant *bis*-substituted nitromethyl compound **22** would then be converted to the α,β-unsaturated system **23**. 5'-OH deprotection



Scheme 6. Differential protection requirements for *O*- vs. *S*-oligosaccharide synthesis

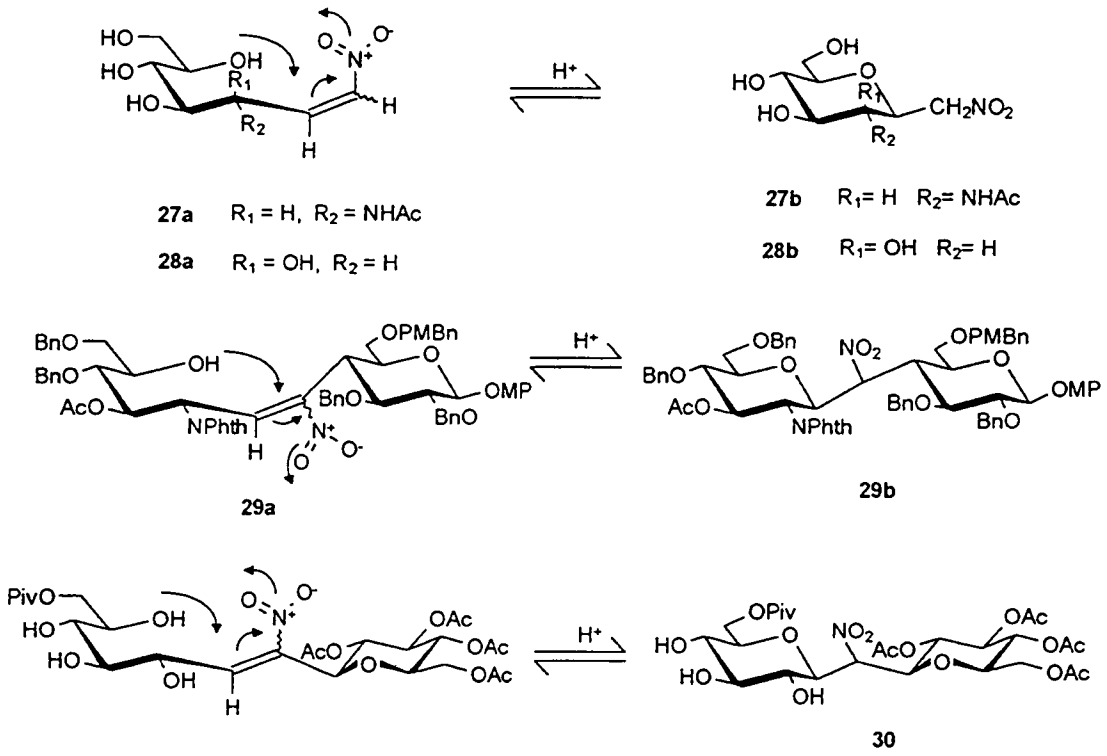


Scheme 7. Retrosynthetic analysis of *C*-disaccharide **19**

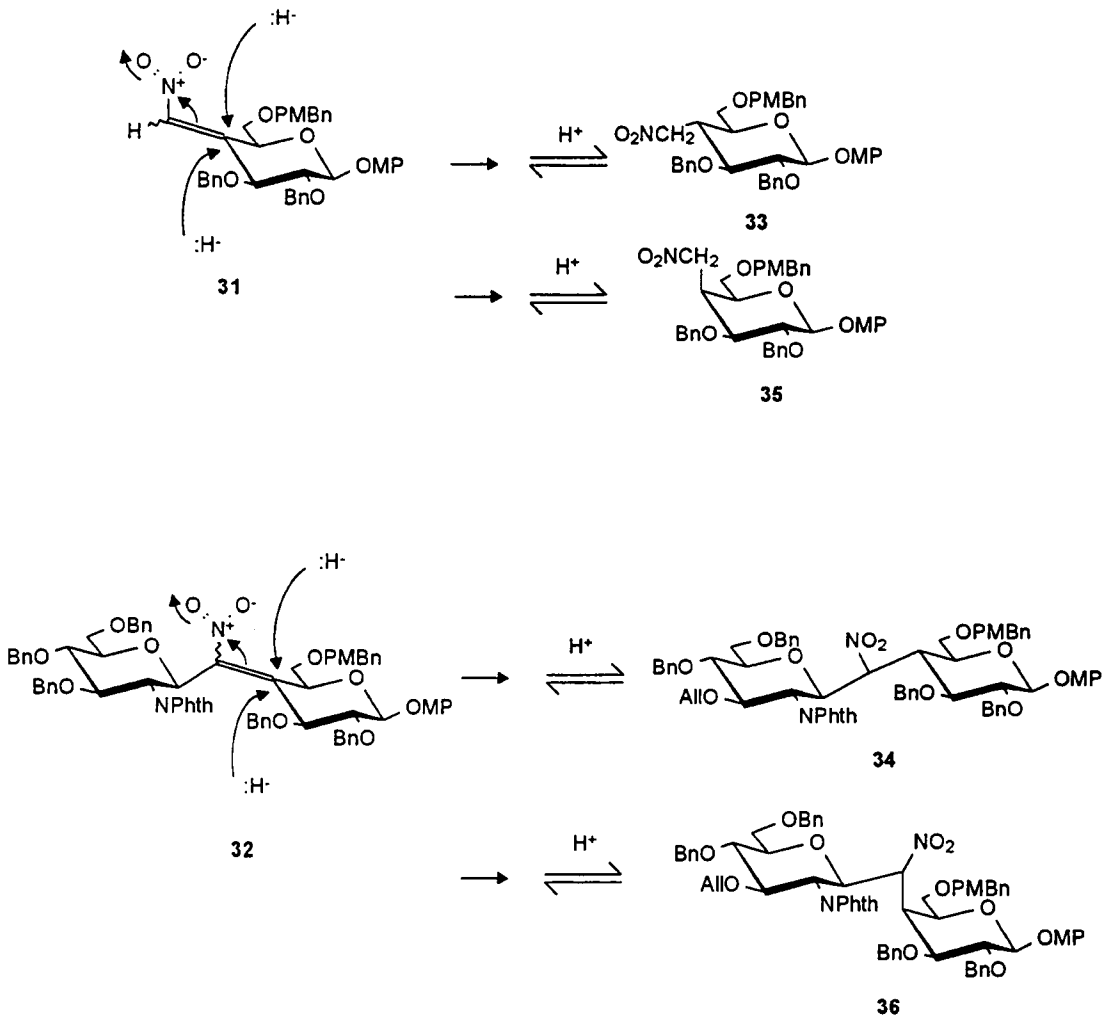
(accompanied by spontaneous ring closure) and subsequent free-radical denitration would then give the $-CH_2-$linked disaccharide **24**. Methyl ester **19** should then be furnished by routine protecting group and oxidation manipulations. Plan B would involve a similar set of manipulations involving synthons **25** and **26**.

The establishment of the proper stereochemistry of the C-glycosidic linkage requires careful consideration. The two carbon atoms whose configurations define this linkage in **19** are C-1 of the GlcNAc residue, and C-4 of the GlcUA residue (arrows point to these in **19**). The GlcNAc C-1 configuration would be established during a thermodynamically controlled intramolecular conjugate addition/cyclization of the GlcNAc 5-OH group to a nitroalkene intermediate (Scheme 8). As reported by Petrus[19] and Koll,[20] the equatorial position of the nitro-bearing carbon is preferred (*i.e.*, **27a** → **27b**). The desired "β" configuration of GlcNAc C-1 (*i.e.*, **28a** → **28b**, corresponding to Plan B, and and **29a** → **29b**, corresponding to Plan A) is thus predicted to be the major product of such a process. The viability of this phenomenon has already been demonstrated by Martin, who used it successfully to install a β-glucose residue in C-β,β-trehalose peracetate **30**.

The stereochemical configuration at C-4 of the GlcA residue would be established during a (kinetically controlled) conjugate addition of hydride to a nitroalkene intermediate. For example, axial (via the β face) conjugate addition of hydride to **31** or **32** would lead to the desired "glucuronate" disaccharides **33** and **34**, respectively, whereas equatorial (via the α face) conjugate addition of hydride would lead to undesired "galacturonate" disaccharides **35** and **36** (Scheme 9). Experimentation



Scheme 8. Stereochemical Control at C-1' of CH_2-linked disaccharide intermediates



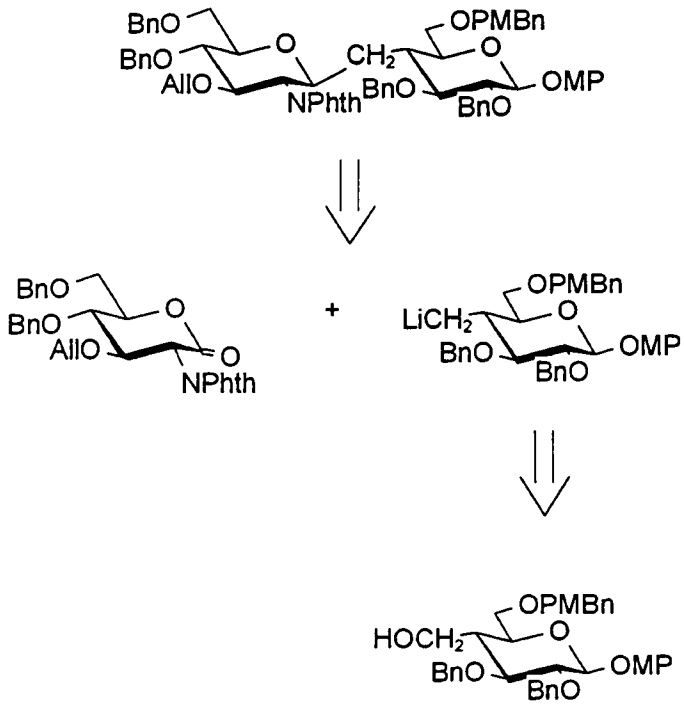
Scheme 9. Stereochemical control at C-4 of CH_2-linked disaccharide intermediates

with varied reducing agents and conditions should allow access to the desired isomer.

As several factors in the present case, such as the presence of a 2-amino-2-deoxy subsitution, are sufficiently different from Martin's substrates to arouse concern that his method may not be successful in producing the target compounds of this study, an alternative route using organolithium chemistry of Schmidt[21] for similar compounds was also devised (Scheme 10).

C. Significance

The studies described in this chapter represent novel and significant advances with respect to both chemistry and potential biological activity. There is a widespread interest in oligosaccharides with hydrolase stability.[22] The "block strategy" proposed here, *i.e.*, of linking of S- or CH_2- linked disaccharides by normal O-linkages, is a novel and practical approach to such oligosaccharide analogs. To date, nothing has been documented in the literature using the idea of block-wise "mixed" oligosaccharide synthesis. With respect to biological activity, the target compounds have the potential to shed light on several questions. First, although *C*- and *S*- oligosaccharides are generally known to confer hydrolytic stability to the glycosidic linkage, many questions remain about precisely how these proposed mimetics might function and whether they might adopt similar conformations to the natural oligosaccharides.[23] Second, no one has evaluated these types of compounds against hyaluronidases and related enzymes. Third, if the proposed mimetic oligosaccharides bind strongly to the CD44 receptor, these compounds are potential antimetastasis drugs (or drug leads). Finally, the



Scheme 10. Alternative retrosynthetic analysis of *C*-disaccharide **19**

oligosaccharides, modified with fluorescent tags, might make excellent, stable biochemical probes for the CD44 receptor that can shed light on fundamental questions concerning the CD44 receptor.

III. RESULTS AND DISCUSSION

A. Progress in the synthesis of S-linked oligosaccharides

1. Introduction

Although the S-linked arm of the project was embarked upon with assumption that it would quickly and unproblematically afford analogs, two unforeseen problems arose which forced us to re-assess the problem as quite challenging and interesting:

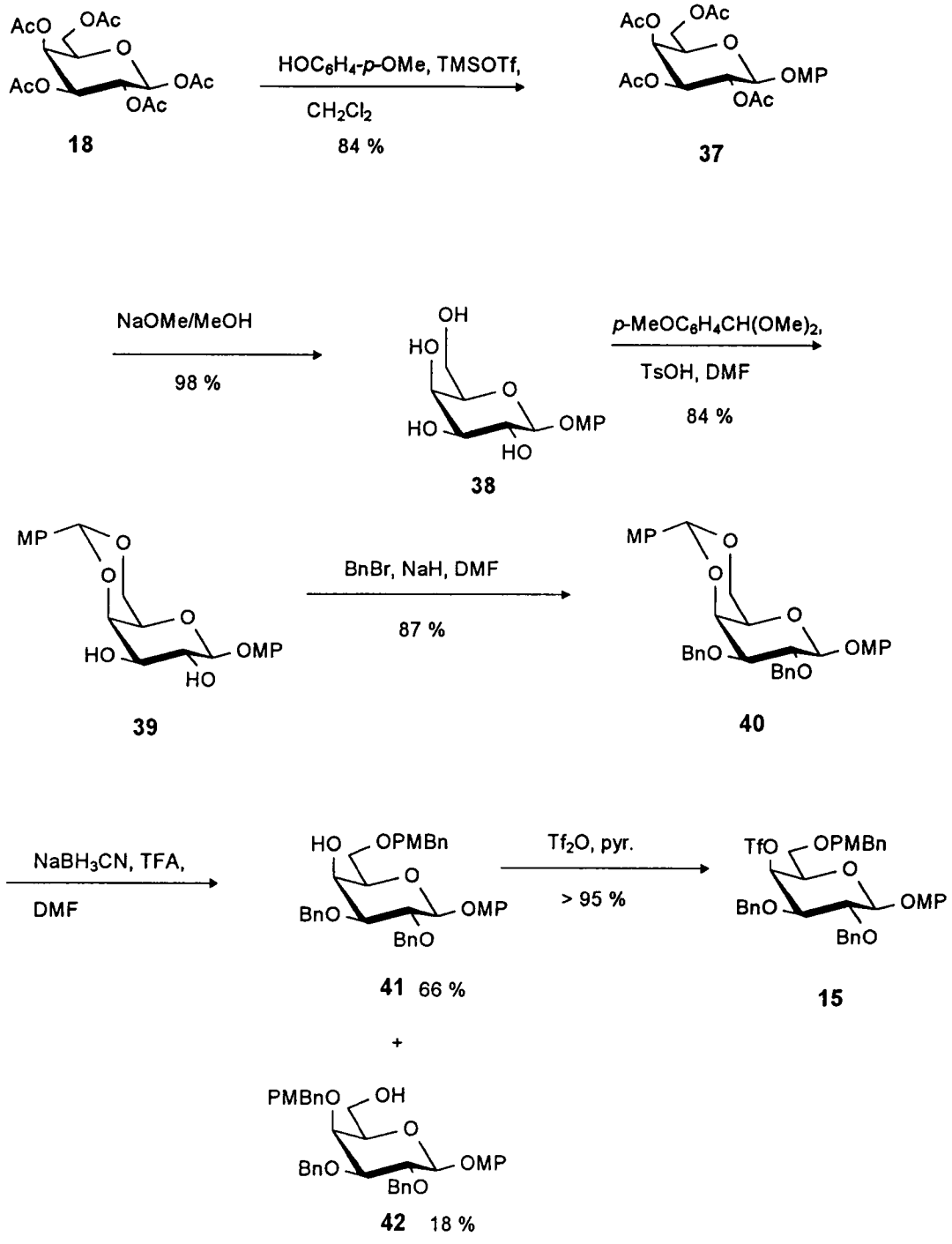
- The originally planned chemistry of Driguez and co-workers did not work; an alternative method had to be developed.
- Once synthesized, the interglycosidic –S– linkage proved to be an irritating and inconvenient restriction in the choice of protecting groups and other synthetic manipulations, due to its incompatibility with a wide array of reagents.

As detailed in the following sections, unforeseen snags scrapped several plans after they had already consumed significant time and effort, and the necessity of going back to the drawing board became a routine occurrence. The intricacies of oligosaccharide synthesis are well known. In particular, the way in which the steric and/or electronic effects of particular protecting groups affect the stability and/or reactivity of glycosyl donor or acceptors is often impossible to predict in advance, and trial and error is commonplace. The added restrictions here of coping with the introduction and presence of the sulfur group, as well as the necessity of installing the 6-carboxylate group (as mentioned

above), contributed to our being forced to investigate *several* combinations of protecting groups.

2. Synthesis of an S-disaccharide via modified Schmidt chemistry

Synthesis of the monosaccharide building blocks required for implementation of the retrosynthetic analysis (refer back to Scheme 5) was carried out as follows. Triflate **15** was prepared by a 6-step procedure beginning with commercially available D-galactose pentaacetate (**18**, Scheme 11). Glycosylation with 4-methoxyphenol under TMSOTf activation[24] afforded β-anomer **37** with only a small (<5 %) of the accompanying α-anomer. Zemplén deacetylation (NaOMe–MeOH) gave the corresponding tetraol **38**. Regioselective *bis*-protection of the 4- and 6- positions with the *p*-methoxybenzylidene group was accomplished via acetal exchange with anisaldehyde dimethyl acetal. The reaction was carried out at 50 °C to induce thermodynamic control; furthermore, it was necessary to conduct the reaction under reduced pressure in order to distil methanol by-product from the reaction mixture and drive the acetal exchange process to completion. As rationalized by Binkley,[25] the 4,6-substitution pattern present in product **39** is the preferred product among the possible regioisomers owing to its chair conformation 1,3-dioxane ring. Treatment of **39** with benzyl bromide and NaH in DMF then afforded **40**. Regioselective reductive cleavage of the benzylidene ring to result in partial deprotection to a free hydroxy group and a *p*-methoxybenzyl ether was achieved by treating **40** with sodium cyanoborohydride and trifluoroacetic acid in DMF.[26] The desired 4-hydroxy isomer **41** was, as predicted, the major product, and distinguished from the 6-hydroxy isomer (**42**, also isolated) by ^{1}H



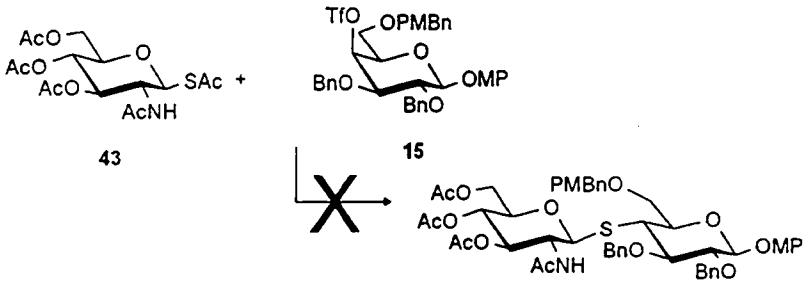
Scheme 11. Synthesis of potential *S*-disaccharide intermediate **15**

NMR spectroscopy. With the desired axial monohydroxy compound in hand, its conversion to target triflate **15** was simply a matter of treatment with trifluoromethane-sulfonic anhydride in pyridine, which proceeded in > 95% yield.

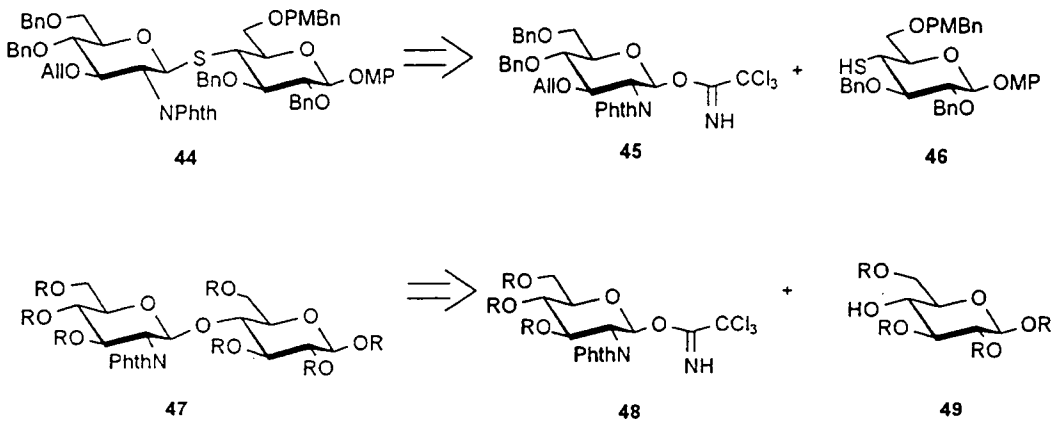
At this point, it was decided that known thioacetate **43**[27] (Scheme 12) would be used instead of the previously intended analog **14**, since it could rapidly be prepared according to the published procedure, and would thus afford an opportunity to assess the viability of the synthesis at an earlier stage, rather than having to develop the synthesis of differentially protected **14**.

According to Driguez' published methodology, the coupling reaction should occur as follows: the glycosylthioacetate component suffers *in situ* S-deacetylation via the action of cysteamine in DMF solvent and subsequently attacks the triflate component in an S_N2 reaction to afford disaccharide. Unfortunately, the application of this method here failed: all attempts to couple **43** with **15** were unsuccessful (Scheme 12). Although TLC showed 1-*S*-deacetylation to indeed be occurring under the reaction conditions, triflate **15** remained unaffected, even with the use of other solvents, higher temperatures, and extended reaction times. This result is puzzling, as triflate **15** is a successful S_N2 substrate toward other nucleophiles (*vide infra*).

Consideration was then given to a different strategy in which the electrophilic and nucleophilic roles of the sugars were reversed; *i.e.*, perhaps C-1 of the GlcNAc synthon could function as a glycosyl donor toward a 4-mercapto sugar (*i.e.*, **44** – **46**, Scheme13). This plan is analogous to "normal" oligosaccharide synthesis, in which C-1 of one of the sugar components functions as the electrophile rather than bearing a nucleophilic alcohol



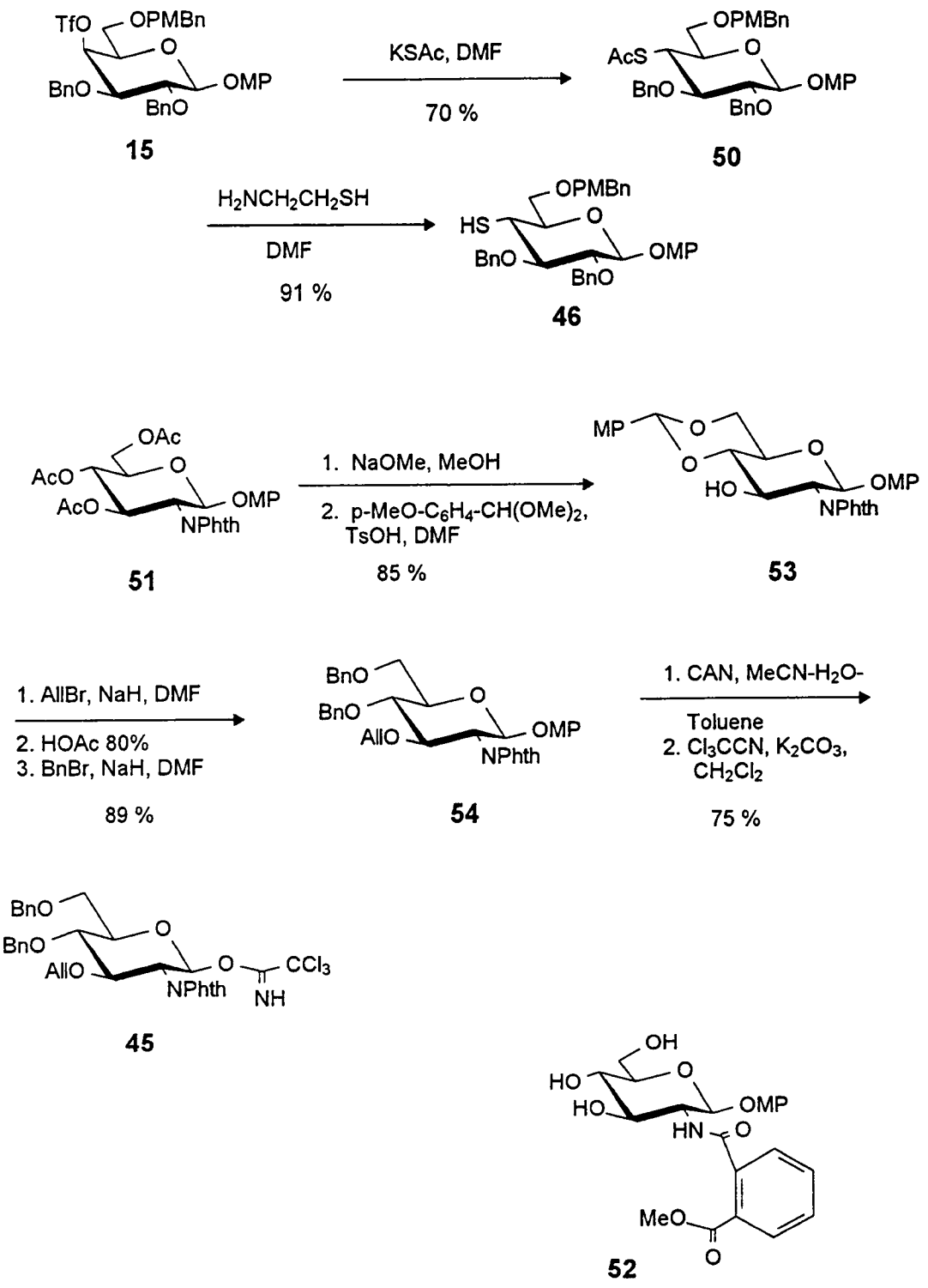
Scheme 12. Unsuccessful synthesis of *S*-disaccharide via the methodology of Driguez



Scheme 13. Revised retrosynthetic analysis for *S*-disaccharide

group (*i.e.*, **47** – **49**). Surprisingly, although 1-trichloroacetimidates are among the most often used glycosyl donors in the synthetic carbohydrate literature, there was (to our knowledge) no precedent for their use toward a thiol nucleophile.[28] As it nevertheless appeared to be a logical route to the desired *S*-disaccharide (perhaps even more logical than the Driguez's existing procedure), the requisite monosaccharides were synthesized, as described in Scheme 14.

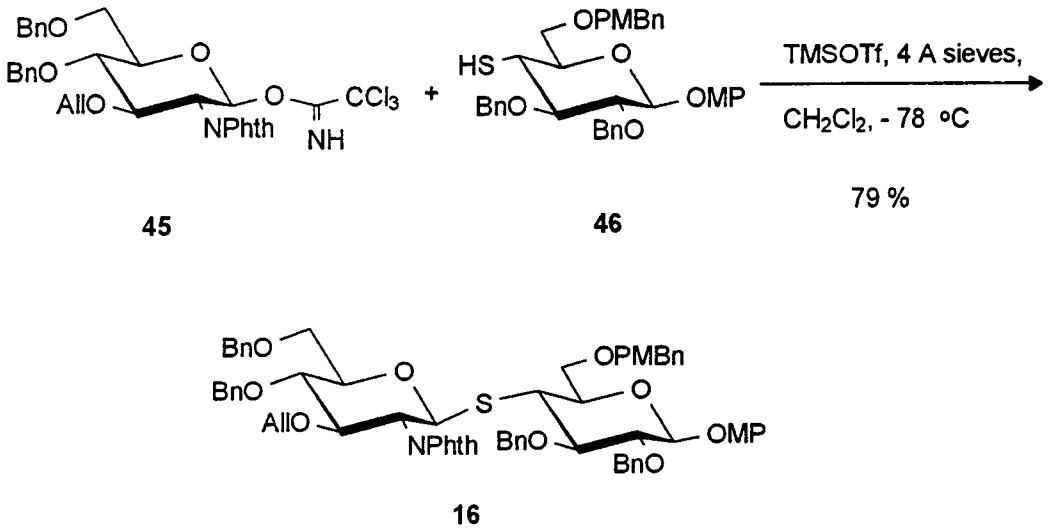
Triflate **15** was readily converted to thioacetate **50** via treatment with potassium thioacetate in DMF at 50 °C, and subsequently S-deacetylated to afford thiol **46**. Trichloroacetimidate **45** was synthesized in seven steps from known triacetate **51**[29] as follows. Zemplén deacetylation of **51** afforded a triol, which was immediately carried on through the next step. (In this and subsequent steps involving strong bases, careful monitoring of the reaction was necessary, as extended reaction times resulted in the formation of polar side products associated with opening of the phthalimido moiety. For example, methyl ester compounds of the type **52** were isolated and identified by ^{1}H NMR spectroscopy.) The triol was 4,6-protected as the methoxybenzylidene acetal via acetal exchange with anisaldehyde dimethyl acetal to afford **53**, and the remaining free hydroxy group was allylated with allyl bromide and NaH in DMF to afford an allyl derivative **53a** (not shown). The 4- and 6- positions were then converted to benzyl ethers by a two-step sequence of acetal hydrolysis followed by alkylation with benzyl bromide. Fully protected intermediate **54** thus obtained was then transformed into the desired glycosyl donor **45** via removal of the anomeric protecting group (with CAN) and treatment of the resulting free pyranoside with trichloroacetonitrile and K_2CO_3 in dichloromethane.



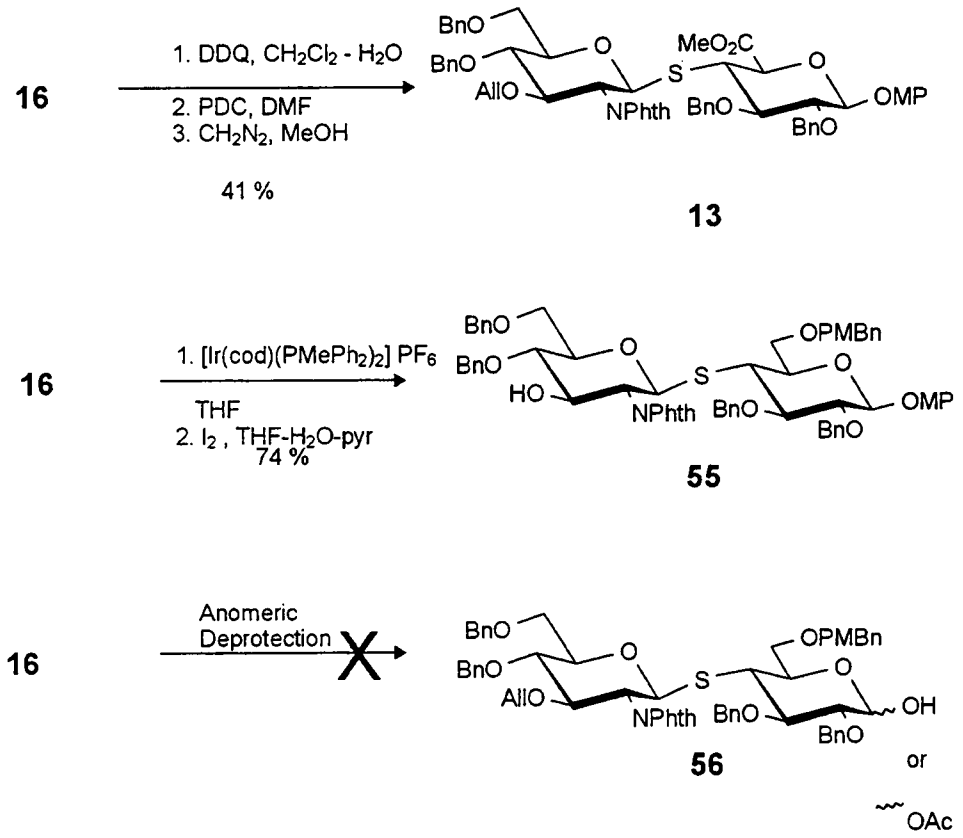
Scheme 14. Synthesis of modified *S*-disaccharide building blocks **45** and **46**.

Gratifyingly, coupling of **45** with thiol **46** proceeded in high yield under standard conditions (Scheme 15) to afford target disaccharide **16**. Apparently we were not the only ones to have noticed the potential utility of this type of approach: a few weeks after we conducted this work, Schmidt and co-workers utilized a similar strategy to synthesize an *S*-oligosaccharide.[30]

With disaccharide **16** in hand, proximity to the tetrasaccharide level seemed palpable. Prior to executing such couplings, it only remained for three further manipulations of **16** to be tested: (1) deprotection/oxidation/esterification of C-6 to the methyl ester, (2) deallylation of the 3'-position to the "disaccharide glycosyl acceptor," and (3) removal of the *p*-methoxyphenyl group and conversion to the trichloro-acetimidate "disaccharide glycosyl donor." (Scheme 16) Accordingly, treatment of **16** with DDQ, followed by oxidation with PDC in DMF and methylation of the resulting acid, afforded *S*-disaccharide methyl ester **13**, the target compound. Alternatively, conversion to the 3' alcohol **55** was also possible via a two-step process involving isomerization of the allyl group with cyclooctadieneyl-*bis*-(methyldiphenylphosphine) iridium hexafluorophosphate in THF, followed by cleavage of the resulting propenyl ether with iodine–water–pyridine. The acetate derivative of alcohol **55**, **55a**, was characterized extensively via 1- and 2-dimensional ^{1}H NMR spectroscopy. Figure 3 shows a TOCSY spectrum of **55a**. Table 1 lists chemical shift data for the ring protons of **55a**, in comparison with precursor species. Characterization of these disaccharides was also assisted by ESIMS. Although polar molecules such as proteins, nucleic acids, and unprotected carbohydrates have received the most attention in ESIMS methods, we

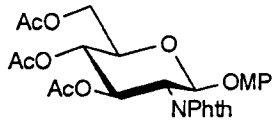


Scheme 15. Synthesis of *S*-disaccharide **16**.

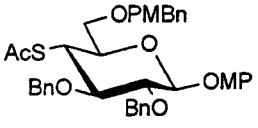


Scheme 16. Peripheral Manipulations on *S*-disaccharide **16**.

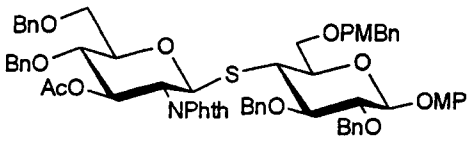
Table 1. Chemical shift (ppm) and coupling constants (Hz) for ring protons of **50, 51,** and **55a**.[a]



51



50



55a

Position	Glycosyl donor precursor 51	Glycosyl acceptor precursor 50	Disaccharide 55a
1	—	4.92 (8.3)	4.84 (7.9)
2	—	3.77	3.68 (8.3, 7.9)
3	—	~3.7	3.57 (83, 10.6)
4	—	~3.7	3.19 (10.6, 10.6)
5	—	~3.7	~3.8
6a, 6b	—	3.80, 3.60 (10.7, 10.6)	43.52 (10.0), ~3.8
1'	5.87 (8.5)	—	5.77 (9.8)
2'	4.58	—	4.32 (9.8, 10.3)
3'	5.85	—	5.79 (10.0, 10.3)
4'	5.23	—	3.80
5'	3.95	—	~3.6
6a', 6b'	4.35, 4.18	—	3.93 (11.0), ~3.8

[a] Chemical shifts and coupling constants were obtained at 400 MHz and assigned on the basis of decoupling and TOCSY experiments

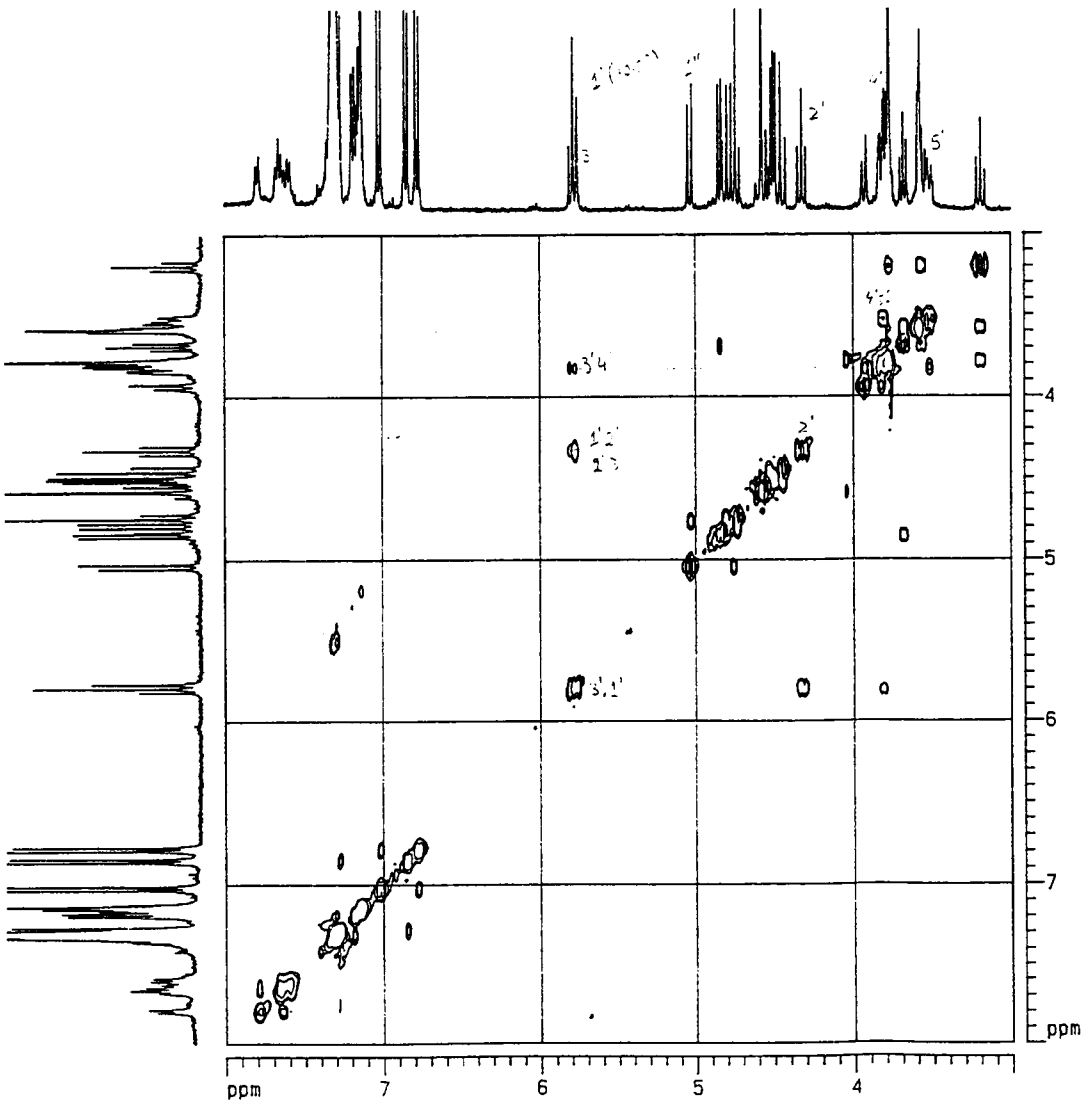


Figure 3. TOCSY ^{1}H NMR spectrum of **55a** (400 MHz)

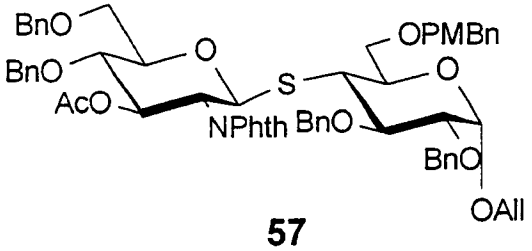
found that the positive-ion mode spectra of lipophilic compounds such as **16** and **55** provided precise MW confirmation, with the sodium and/or potassium adducts consitituting the predominant signals (Figure 3).

Unfortunately, all attempts to remove the *p*-methoxyphenyl group, either by oxidative, hydrolytic, or acetolytic means to generate **56**, resulted in no reaction or decomposition. Although the S-glycosidic linkages have been reported elsewhere to be stable to treatment with CAN,[31] we believe that the thioacetal sulfur suffers oxidation and subsequent decomposition by the reagent in a manner similar to that experienced by sulfido linkages when treated with CAN.[32]

Regrettably, changes of protecting groups in oligosaccharide synthesis, especially at the 1-position, usually require revisions back at the monosaccharide level.

3. Developing a viable protecting group array

Disaccharide **57** was targeted as a viable replacement for **16**. The *p*-methoxyphenyl group has been replaced by an allyl group, as allyl glycosides are readily



57

available. This, of course, also required that the 3'-position (previously protected by the allyl group) be changed, so the acetate group present in **57** was chosen. Intermediate **54** from above was modified as shown (Scheme 17) to afford donor **58**. Known allyl

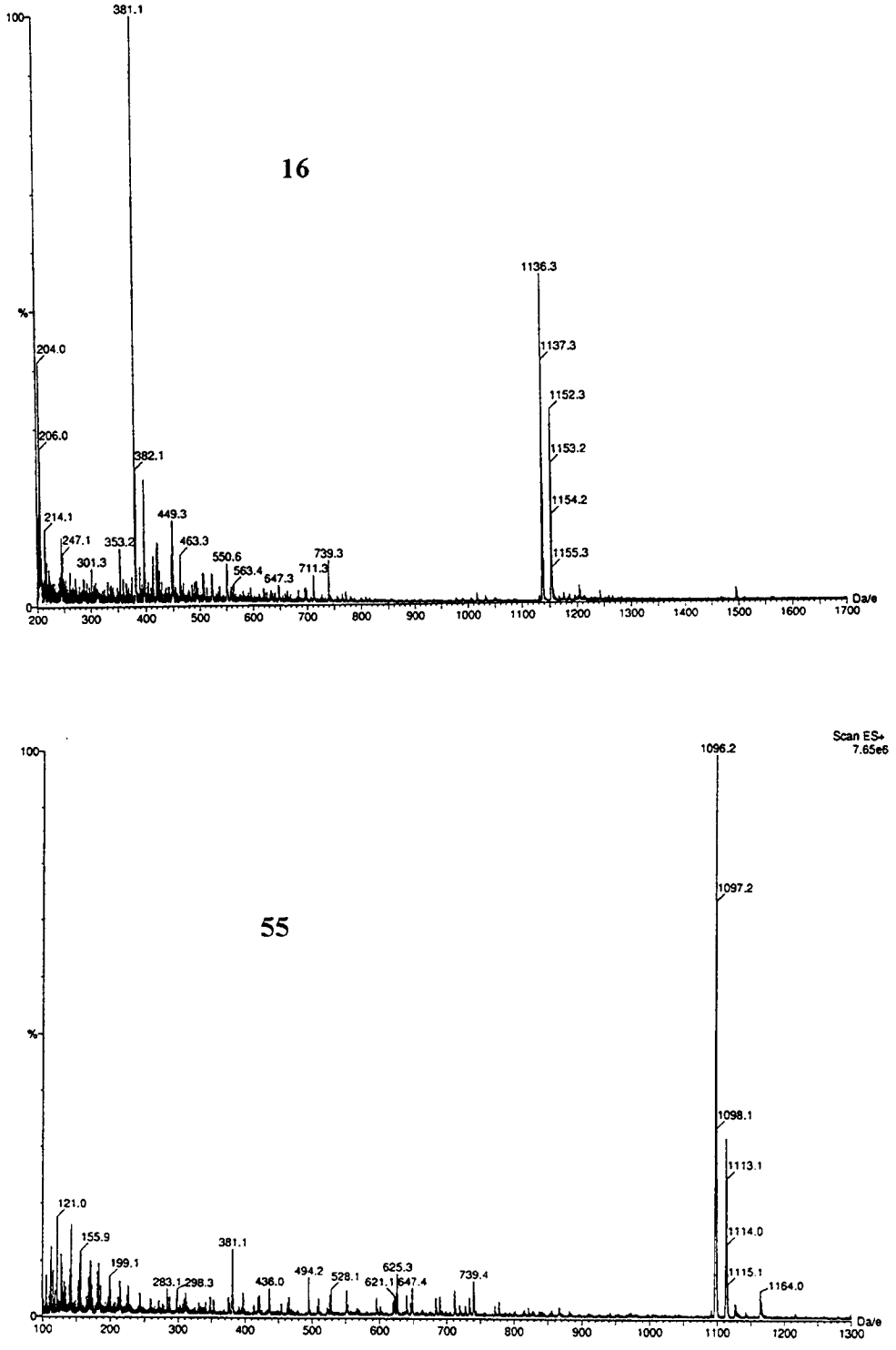
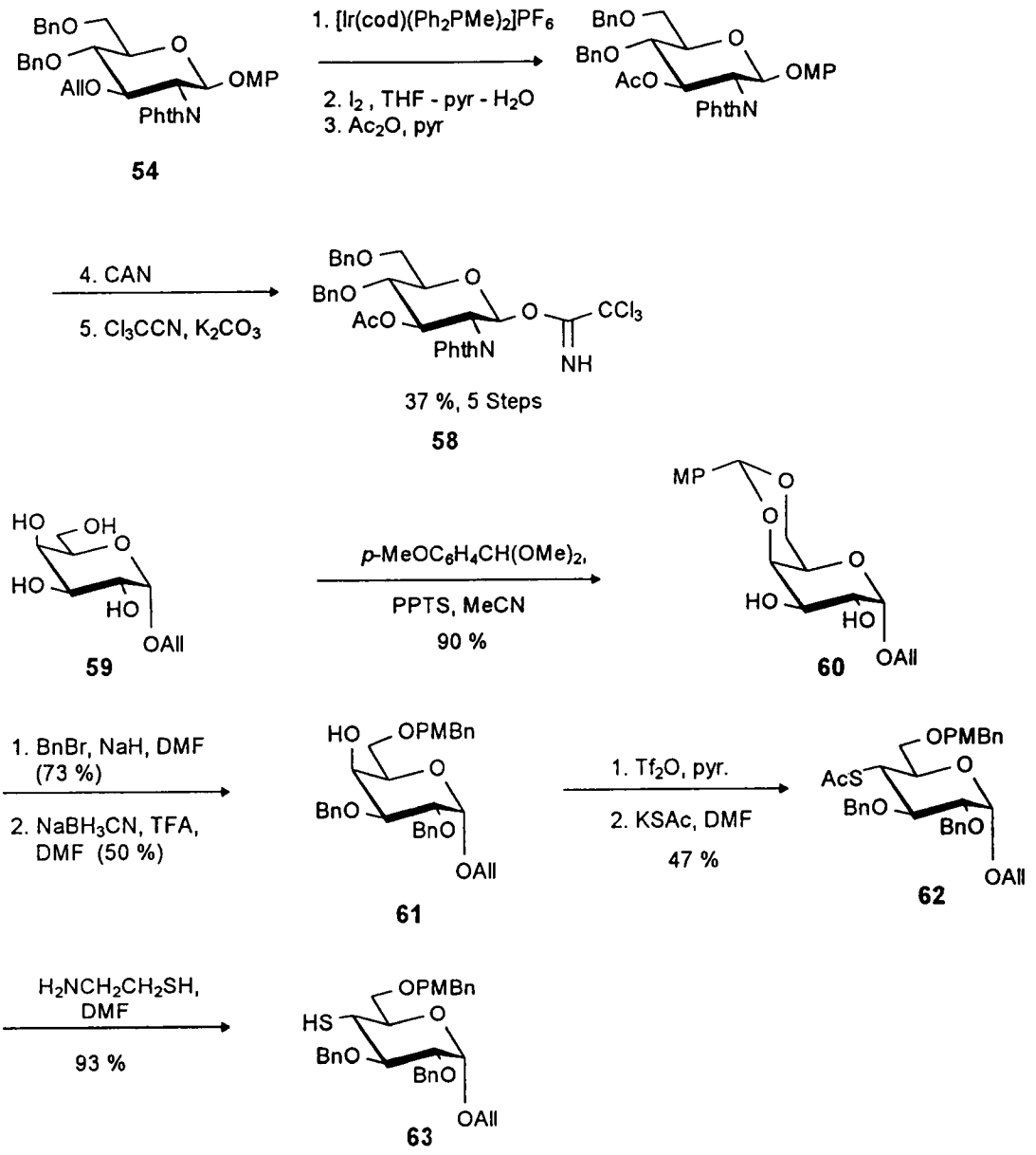


Figure 4. Positive-ion mode ESIMS spectra of **16** and **55**.

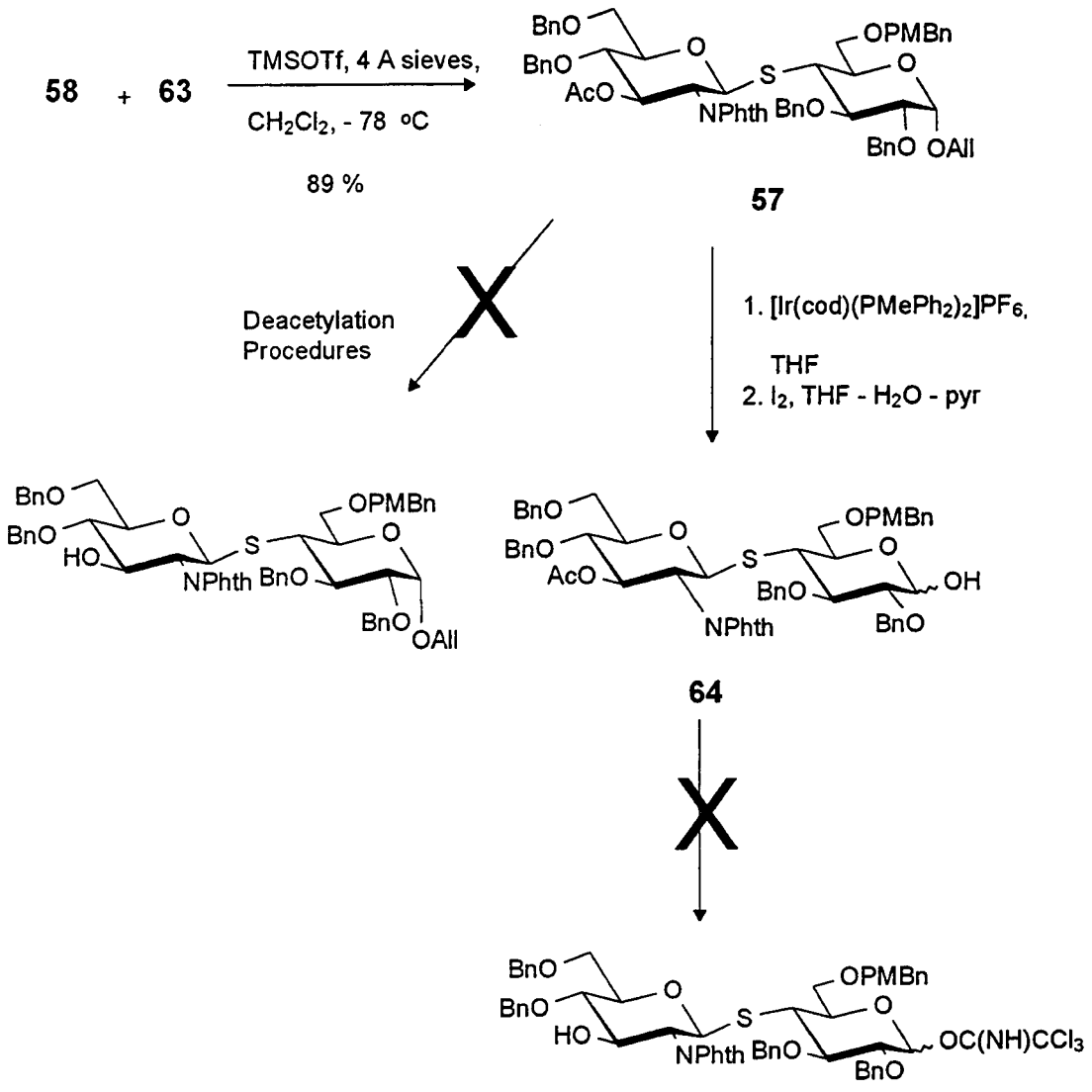


Scheme 17. Synthesis of monosaccharide synthons for modified *S*-disaccharide **57**.

glycoside **59**[33] was taken through a series of steps similar to those used to prepare **46**, with slight modifications. 4,6-*O*-protection of **59** using the same conditions as before (ADMA–TsOH–DMF) proceeded only in extremely poor yield. Experimentation with varied acid catalysts, solvents, and temperatures finally led to the use of ADMA–PPTS–MeCN at RT to give **60** in high yield. Benzylation of the remaining two hydroxyl groups (→**60a**, not shown), followed by regioselective reductive ring opening afforded axial alcohol **61**. Inversion to the desired equatorial thioacetyl compound **62**, followed by *S*-deacetylation, gave the requisite thiol acceptor **63**. In comparing the allyl series **59** → **63** with the methoxyphenyl analogs **18** → **46**, we noted that the allyl series suffered the disadvantages of being syrups (most of the *p*-methoxyphenyl compounds were crystalline) and of being produced in lower yields.

In any case, **58** and **63** were coupled uneventfully as before to give *S*-disaccharide **57** in good yield (Scheme 18). The resulting optimism was quickly squelched by the finding that the 3'-acetate group could not be cleanly removed. At least ten deacetylation procedures were tried but resulted in either no reaction or the appearance of multiple polar products. Additional problems prevailed at the other end of the molecule as well. Although **57**, unlike **16**, could be 1-*O*-deprotected, all attempts to convert the resulting free hemiacetal **64** to a trichloroacetimidate failed, with apparent decomposition. An attempt to trap the crude trichloroacetimidate (*i.e.*, without purification) with a glycosyl acceptor also failed. Disaccharide **57** was thus abandoned.

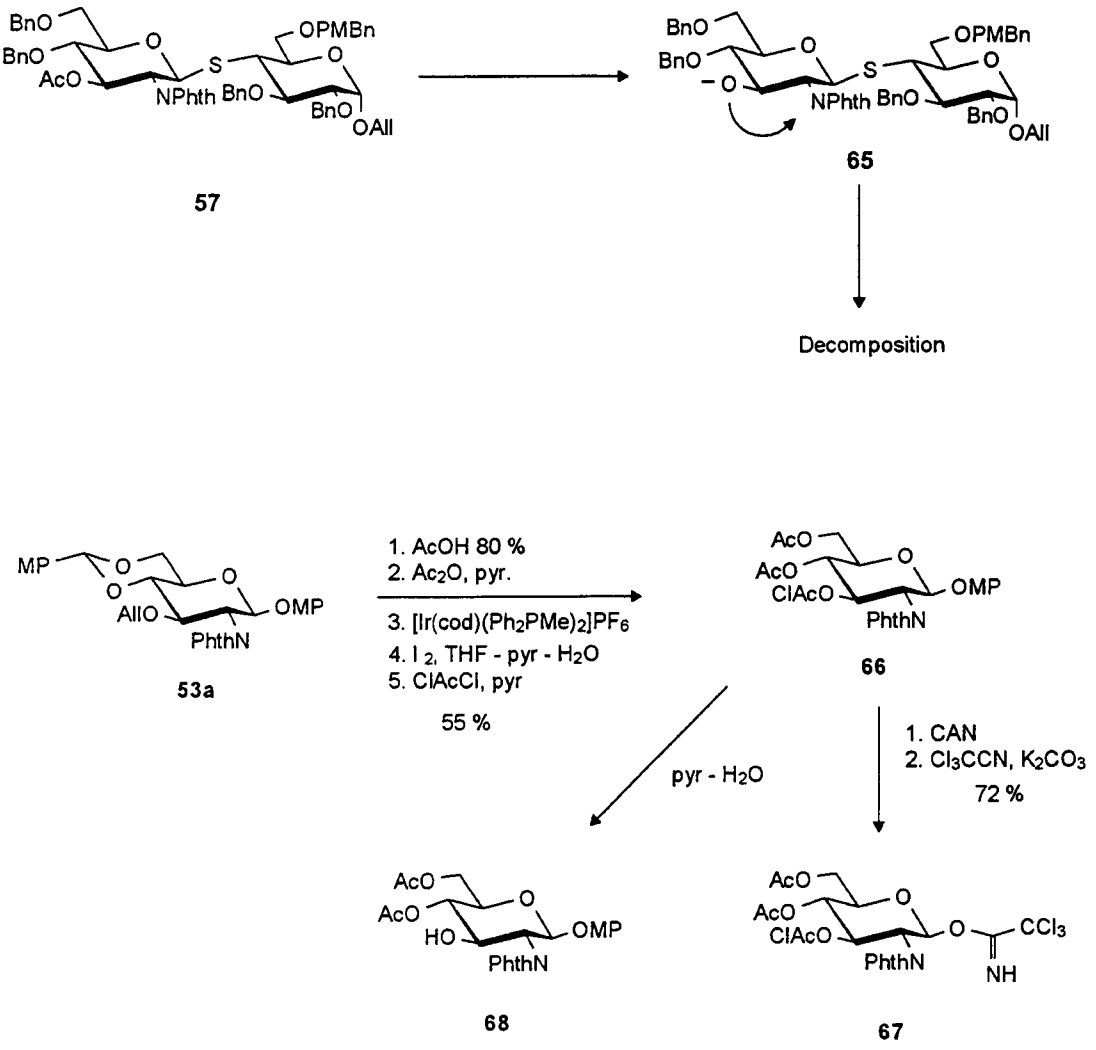
The selection of a new 3'-protecting group was analyzed as follows. The acetate-deprotection problems seemed reminiscent of the base-sensitivity alluded to above in the



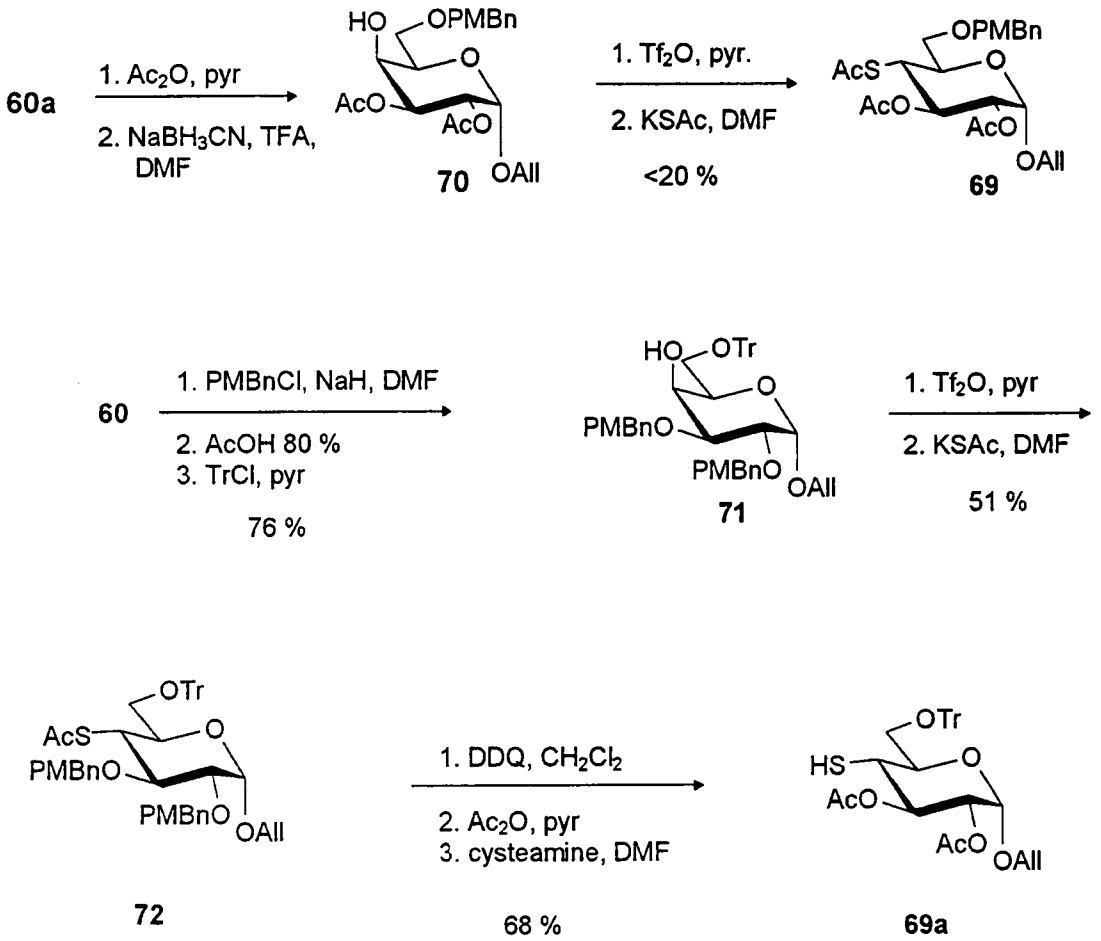
Scheme 18. Synthesis and further manipulations of *S*-disaccharide **57**.

synthesis of **45**. Apparently a transient oxide of the type **65** (immediately following deacetylation) can interact deleteriously with the adjacent phthalimido group (Scheme 19). Reasoning that less stringent base conditions might alleviate the problem, intermediate **53a** was converted to chloroacetate **66**, which was then transformed into trichloroacetimidate **67**. The future viability of the chloroacetyl group was confirmed by showing that its removal (i.e., **66** → **68**) was accomplished via extremely mild base hydrolysis (pyridine–water). No hydrolysis of the 4-*O*- or 6-*O*-acetates was observed.

The problem of 1-trichloroacetimidate decomposition was analyzed a follows. It is well known in oligosaccharide synthesis that ether protecting groups *increase* the reactivity of glycosyl donors, whereas ester groups *decrease* their reactivity. Accordingly, **69**, the 2,3-di-O-acetyl analog of **63** was targeted (Scheme 20). Although the *S*-acetate compound could indeed be prepared via diacetate alcohol **70** (prepared in two steps from **60a**) and treatment of the subsequent triflate with KSAc, the process was extremely low-yielding and afflicted by multiple side products. As might be expected on the basis of the greater electron-withdrawing effect of the acetate group compared to that of the benzyl ether group, a putative increased acidity of the 3-proton in **70** facilitates the E2 pathway to a much greater extent than is the case with **61**. Acyl groups thus cannot be present during the installation of the SAc group. The slightly more circuitous route of using *temporary* ether protection followed by replacement with the desired acetate groups at a later stage was therefore adopted. Thus, diol **60** prepared as above was alkyated via treatment with *p*-methoxybenzyl chloride and NaH in DMF, followed by hydrolysis of the *p*-methoxybenzylidene acetal, and protection of the



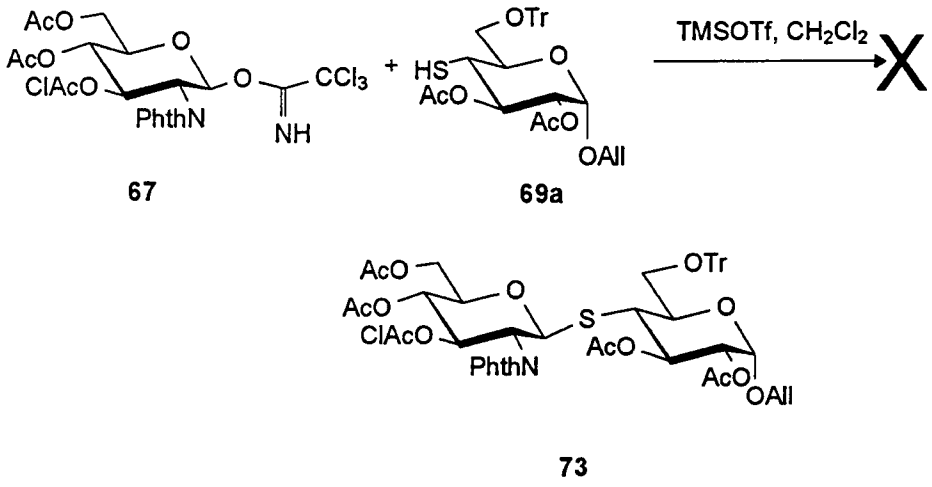
Scheme 19. Selection of a new 3-*O*-protecting group for 2-deoxy-2-phthalimido sugars.



Scheme 20. Synthesis of diacetate thiol **69a**.

6-position with trityl chloride afforded axial alcohol **71**. Conversion of this compound to thioacetate **72** was conducted routinely as above using Tf_2O in pyridine followed by KSAc in hot DMF. Finally, the desired diacetate thiol **69a** was prepared by adjusting the PMBn groups to acetates, and then selectively *S*-deacetylating using cysteamine.

Coupling of **69a** and **67** to afford disaccharide **73** was unsuccessful (Scheme 21). As previous experimentation had shown that donor **67** could be readily undergo glycosylation reactions with sterically unhindered alcohols (*e.g.*, ethanol), the problem in the present case is most likely due to steric hindrance of the 6-*O*-trityl group around the thiol nucleophile. The selection of this 6-*O*-protecting group has proven puzzling. Surprisingly, for example, the use of the smaller PMBn group that had been so successful before did not give any better results. An analog of **73** in which the protecting group array allows all the desired peripheral manipulations has therefore yet to be obtained. Due to time constraints resulting from the unforeseen difficulties in its synthesis, the synthesis of such a species, as well as its elaboration into mixed *O*-/*S*-oligosaccharides must be described elsewhere.

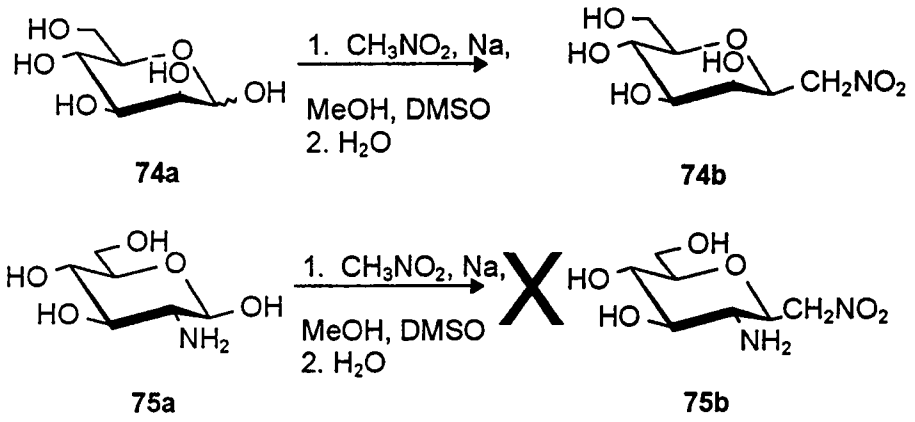


Scheme 21. Attempted synthesis of *S*-disaccharide **73** .

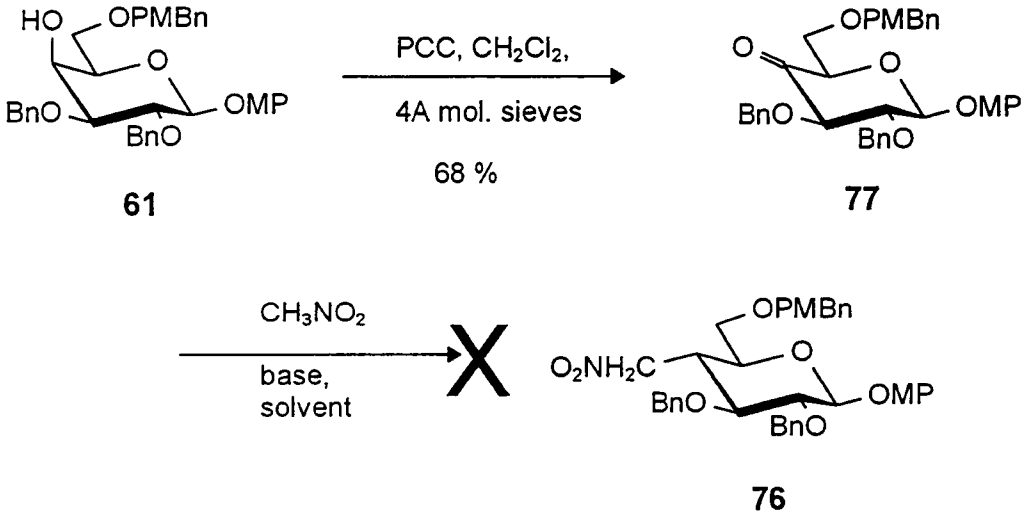
B. Progress in the synthesis of *C*-disaccharides

1. Attempted synthesis using 4-keto sugars

Implementation of Plan B (refer back to Scheme 7) required use of the same process developed by Petrus and co-workers[34] to convert a number of aldohexoses to their corresponding 2,6-anhydro-1-deoxy-1-nitroalditols (*i.e.*, treatment with $NaCH_2NO_2$ in MeOH–DMSO followed by aqueous reflux, Scheme 22). For example, their process converted D-mannose (**74a**) to **74b**. Unfortunately, this process is apparently not sufficiently general, as in our hands it did not convert D-glucosamine (**75a**) to the β-CH_2NO_2 isomer **75b**. Recourse to Plan A calls for a substituted nitromethane derivative such as **76**, which was envisioned as being derived from alcohol **61** (that had already been synthesized for the S-series) via keto sugar **77**, as outlined in Scheme 23. In the event, alcohol **61** proved difficult to oxidize. After at least ten oxidation procedures



Scheme 22. Attempted Synthesis of β-CH_2NO_2 compound **75b**



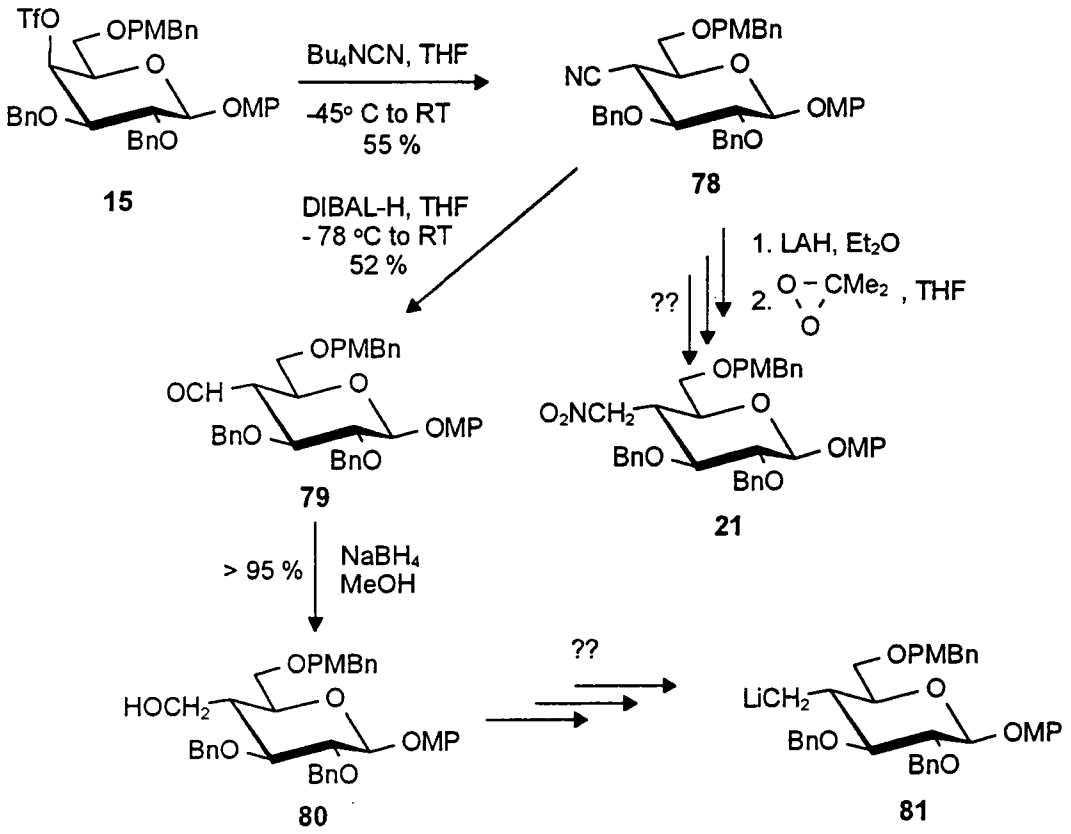
Scheme 23. Attempted synthesis of 4-branched nitro compound **76** via keto sugar **77**.

were tried, PCC in the presence of powdered 4Å molecular sieves, with dichloromethane as solvent, provided **77** in moderate yield. However, all attempts to condense this compound with nitromethane were unsuccessful.

2. Synthesis of a C-disaccharide acceptor using S_N2 chemistry

Since the equatorial configuration of the CH_2NO_2 group at position 4 in compound **76** was absolutely essential (refer back to the discussion in Section II.B.3. above), a modified route using a more definite stereochemical manipulation, the S_N2 reaction, was developed. Thus, the same axially substituted triflate derivative **15** prepared as before (see Section A.2) was subjected to ^-CN displacement under a variety of conditions until a satisfactory transformation (Bu_4NCN in THF at -45 °C) to the cyano compound **78** was found (Scheme 24). Insofar as preparations of branched carbohydrate compounds are generally reported to be low-yielding in the literature and are accessible by limited means, the conditions developed for **78** are of interest and are therefore summarized in Table 2. Nitrile **78** is a versatile intermediate in that it is a precursor for key synthons **21** *and* **81** (for the relevant retrosynthetic analysis, refer back to Schemes 7 and 10, respectively). As a precursor to branched organolithium compound **81**, nitrile **78** was converted in two steps to alcohol **80** via aldehyde **79**. On the other hand, it was anticipated that **78** could also be converted to **21** via reduction with $LiAlH_4$ followed by oxidation with dimethyldioxirane.[35] Compounds **78** and **80** have been entrusted to co-workers for such conversions.[36]

Two additional *C*-glycosyl donor building blocks, namely aldehydo sugar **20** and lactone **83** from (for the relevant retrosynthetic analysis, refer back to Schemes 7 and 10,



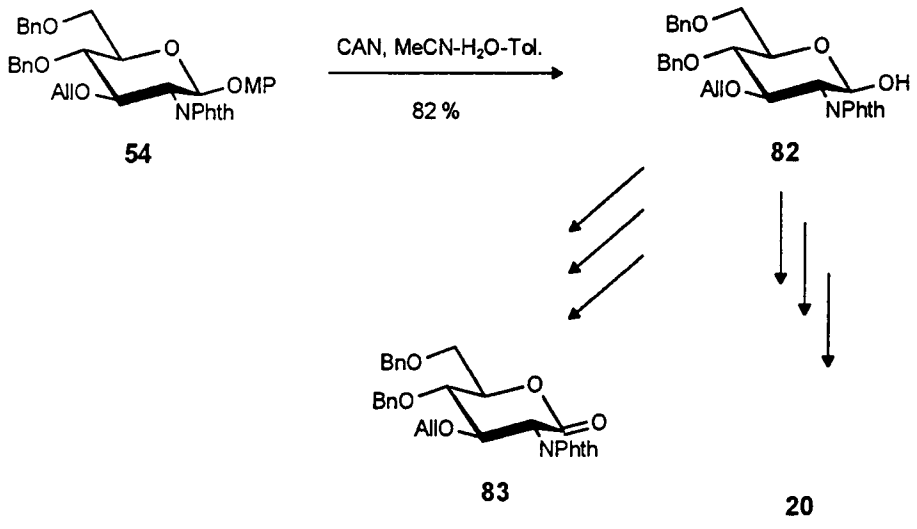
Scheme 24. Chemistry of nitrile **78**.

Table 2. Development of conditions for synthesis of equatorial nitrile **78**.

Reagents	Solvent	Temperature (°C)	Yield [a]
KCN	DMSO	RT	37 %
KCN	EtOH	RT	N.R.[b]
KCN, 18-Crown-6	THF	0 to 40	C.R.M.[c]
KCN, 18-Crown-6	DMF	0 to 40	C.R.M.
LiCN	DMF	0 to RT	C.R.M.
PMe_3, DEAD, TMSCN	THF	- 15 to RT	N.R.
Bu_4NCN	THF	RT	< 20 %
Bu_4NCN	THF	- 78	25 %
Bu_4NCN	THF	- 45 to RT	58 %

[a] Isolated yield.
[b] No reaction.
[c] Complicated reaction mixture; discarded without purification.

respectively) were both seen as being derived from differentially protected GlcNAc equivalent **82**, as shown in Scheme 25. Compound **82** was synthesized as shown from compound **54** (from Section A.2., Scheme 14) and has been handed over to co-workers for completion of the sequence.



Scheme 25. Synthesis of *C*-glycoside donors from compound **54**

IV. CONCLUSIONS

With respect to the objectives set forth in Section II.A., prototype *S*-disaccharides were synthesized, thus establishing the basis for blockwise synthesis of novel mixed *S/O*-disaccharides. The synthetic manipulations of *S*-disaccharides proved to be more difficult than anticipated, due to failure of the existing literature preparation to apply to the target molecules at hand and due to the sensitivity of the the S-linkage and its consequent restrictions on the selection of protecting groups and reagents. Consequently, Objective No. 2 (synthesis of mixed S-/O- higher oligomers) was not achieved during the time-frame of this study. In any case, novel compounds such as the *S*-disaccharide carboxylates prepared herein are intermediates for the synthesis of potentially useful probes of cancer metastasis with *in vivo* stability. In addition, such compounds might also find use as probes in conformational studies of oligosaccharide mimics, or as hyaluronidase inhibitors. With respect to Objective No. 3, key intermediates **78**, **80**, and **82** for the synthesis of *C*-disaccharides were prepared.

V. EXPERIMENTAL

A. General Methods.

All reactions were monitored by thin-layer chromatography (TLC). Adsorption chromatography was carried out using E. Merck silica gel products: (a) TLC on 0.2 mm aluminum-backed plates, (b) flash chromatography using 230-400 mesh silica gel. Visualization of the TLC plates was by 254 nm UV light and by spray–heat development using a *p*-anisaldehyde–sulfuric acid reagent.[37] Anhydrous solvents were prepared as follows: dichloromethane, pyridine, and toluene were distilled from calcium hydride; DMF was distilled at reduced pressure from calcium hydride; THF was refluxed with sodium–benzophenone ketyl and distilled. All reactions were carried out under a nitrogen atmosphere unless otherwise indicated. Solvents were evaporated at aspirator vacuum at about 25 °C unless otherwise indicated. Elemental analyses were furnished by Atlantic Microlab, Inc. of Atlanta, GA. ^{1}H and ^{13}C NMR spectra were determined at 250 MHz and 62.5 MHz, respectively, as ca. 0.1% solutions in chloroform-*d* or DMSO-d_6 using a Bruker AM 250 instrument, except for the data shown in Table 1 and Figure 3, which were obtained at 400 MHZ using a Bruker instrument. ^{1}H NMR shifts are reported as δ (ppm) downfield from an internal standard of tetramethylsilane (TMS); multiplicities are first-order values in Hz: s, singlet; bs, broad singlet; d, doublet; t, triplet; pt, pseudo triplet; bd, broad doublet; dd, doublet of doublets; ddd, doublet of (doublet of doublets); dm, doublet of multiplets; dt, doublet of triplets; dq, doublet of quartets; m, multiplet; bm, broad multiplet. The exchangeable protons of -OH, -SH, and -NH groups were determined by deuterium

exchange using D_2O. Assigned protons were determined by decoupling and/or D_2O exchange experiments. ^{13}C NMR chemical shifts are reported as δ (ppm) relative to $CDCl_3$ (77.00 ppm) as standard. Optical rotations were measured with a Perkin-Elmer Model 243 automatic polarimeter equipped with sodium and mercury lamps for solutions in a 0.1 dm cell at the indicated temperature. The mass spectral analyses were obtained on a Micromass VG Quattro II electrospray instrument at the University of Tennessee.

B. Preparation of compounds 37–82.

***p*-Methoxyphenyl 2,3,4,6-tetra-*O*-acetyl-β-D-galactopyranoside (37).** To a solution of β-D-galactose pentaacetate **18** (18.34 g) and *p*-methoxyphenol (8.8 g, 1.5 equiv) in dichloromethane (250 mL) at 0 °C was added dropwise trimethylsilyl trifluoromethanesulfonate (TMSOTf, 3 mL, 0.33 equiv). The reaction mixture was allowed to stir at 0 °C for 5 h at the end of which time the reaction was quenched with TEA (35 mL). After the addition of saturated $NaHCO_3$ and water, the reaction mixture was allowed to stir for 5 min. The suspension was extracted with dichloromethane, the combined organic layers were washed with brine, dried ($MgSO_4$), concentrated and submitted to flash chromatography (3:1 followed by 2:1 hexanes–ethyl acetate). Evaporation of the fractions at 20 °C afforded **37** as a white solid (17.97 g, 84%) containing a small amount of dichloromethane (as shown by ^1H NMR spectroscopy): mp 102–104 °C; $[\alpha]_D^{20}$ +3.6 (*c* 1.0, $CHCl_3$); R_f = 0. 61 (1: 1: 1 dichloromethane–ethyl acetate–hexanes); ^1H NMR ($CDCl_3$): δ 2.01 (s, 3H), 2.06 (s, 3H), 2.09 (s, 3H),

2.19 (s, 3H), 3.78 (s, 3H), 4.01 (t, 1H, J = 6.79 Hz), 4.20 (m, 2H), 4.92 (d, 1H, J = 7.93 Hz), 5.09 (dd, 1H, J = 3.40 Hz), 5.45 (m, 2H), 6.82 (d, 2H, J = 9.16 Hz), 6.95 (d, 2H, J = 9.07 Hz); ^{13}C NMR ($CDCl_3$): δ 20.53, 55.53, 61.23, 66.84, 68.68, 70.80, 100.74, 114.45, 118.52, 150.93, 155.66, 169.26, 170.00, 170.13; Anal. Calcd for $C_{21}H_{26}O_{11}\cdot 0.005\ CH_2Cl_2$: C, 55.47; H, 5.76. Found: C, 55.47; H, 5.74.

***p*-Methoxyphenyl β-D-galactopyranoside (38).** Compound **37** (15 g) was dissolved in dichloromethane (30 mL) and methanol (150 mL). The solution was allowed to stir for 20 min, after which time a solution of NaOMe in methanol (0.5 M, 2 mL, catalytic amount) was added. After 3 h TLC showed the reaction to be complete, and the reaction was neutralized with Dowex 50 × 2–100 (H^+ form). The suspension was then filtered and evaporated to afford **38** as a white solid (9.0 g, 98%): mp 158–160 °C; $[\alpha]_D^{20}$ –35.7 (*c* 1.1, H_2O); R_f = 0.90 (9:1 dichloromethane–methanol); ^{1}H NMR (DMSO-d_6): δ 3.37 (m, 1H), 3.54 (m, 4H), 3.69 (s, 4H), 4.46* (d, 1H, J = 4.57 Hz), 4.63** (m, 2H), 4.66 (d, 1H, J = 7.57 Hz), 4.81* (d, 1H, J =5.59 Hz), 5.11* (d, 1H, J = 4.98 Hz), 6.84 (d, 2H, J = 9.04 Hz), 6.97 (d, 2H, J = 9.03 Hz) *Exchanges with D_2O; **sharpens with addition of D_2O; ^{13}C NMR (DMSO-d_6): δ 55.34, 60.43, 68.16, 70.3 9, 73.32, 75.44, 102.16, 114.39, 117.65, 151.58, 154.24.

***p*-Methoxyphenyl 4,6-*O*-*p*-methoxybenzylidene-β-D-galactopyranoside (39).** To a solution of compound **38** (0.53 g) and *p*-toluenesulfonic acid (0.50 g, cat.) in DMF (8 mL) was added *p*-anisaldehyde dimethyl acetal (ADMA) (0.35 mL, 1.1 equiv). The flask was placed on the rotary evaporator at 50 °C and < 20 mm Hg. After 3 h, TLC showed the reaction to be complete. TEA (0.5 mL, excess) was added,

the reaction mixture was evaporated, the solid was redissolved in hot acetone, absorbed onto silica gel, and submitted to flash chromatography (dichloromethane with 2%, 5%, 7% and finally 10% acetone). Evaporation of the fractions at 20 °C afforded **39** as an off-white solid (0.63 g, 84%): mp 224-226 °C; $[\alpha]_D^{20}$ -74.9 (*c* 1.0, DMSO); R_f = 0.54 (9:1 dichloromethane-methanol); ^{1}H NMR (DMSO-d_6): δ 3.59 (m, 2H), 3.68 (s, 1H), 3.70 (s, 3H), 3.75 (s, 3H), 4.03 (s, 2H), 4.10 (s, 1H), 4.84 (d, 1H, *J* = 6.86 Hz), 5.04* (d, 1H, *J* = 5.17 Hz), 5.26* (d, 1H, *J* = 4.12 Hz), 5.52 (s, 1H), 6.92 (m, 6H), 7.38 (d, 2H, *J* = 8.60 Hz) *Exchanges with D_2O; ^{13}C NMR (DMSO-d_6): δ 55.06, 55.30, 65.96, 68.40, 69.70, 71.74, 75.77, 99.69, 101.51, 113.16, 114.37, 117.62, 127.53, 130.99, 151.25, 154.25, 159.38; Anal. Calcd for $C_{21}H_{24}O_8$; C, 62.37; H, 5.98. Found: C, 62.30; H, 5.99.

***p*-Methoxyphenyl 2,3-di-*O*-benzyl-4,6-*O*-*p*-methoxybenzylidene-β-D-galactopyranoside (40).** A suspension of NaH (0.23 g, 60 % in mineral oil, 5 equiv) in DMF (5 mL) was cooled to 0 °C. To this suspension was then added dropwise a solution of compound **39** (0.46 g) in DMF (2 mL). Upon completion of addition the reaction mixture was allowed to reach room temperature for 15 min and was then recooled to 0 °C. Benzyl bromide (1.1 mL, 8 equiv) was added dropwise, and the reaction was allowed to stir overtight at room temperature, after which time the reaction was quenched with satd NH_4Cl, diluted with water, extracted with CH_2Cl_2, dried ($MgSO_4$), concentrated, and submitted to flash chromatography (6: 1: 1 followed by 4: 1: 1 hexanes-ethyl acetate-dichloromethane). Evaporation of the fractions at 20 °C afforded **40** as a white solid (0.58 g, 87%) containing a small amount of hexanes:

mp 167–168 °C; $[\alpha]_D^{20}$ –6.3 (*c* 1.0, $CHCl_3$); R_f = 0.45 (1:1:1 hexanes–ethyl acetate–dichloromethane); ^1H NMR ($CDCl_3$): δ 3.39 (s, 1H), 3.61 (dd, 1H, *J* = 3.63 Hz), 3.79 (s, 3H), 3.81 (s, 3H), 4. 10 (m, 3H), 4.34 (d, 1H, *J* = 1.24 Hz), 4.78 (s, 2H), 4.87 (m, 2H), 4.99 (d, 1H, *J* = 10.78 Hz), 5.47 (s, 1H), 6.80 (d, 2H, *J* = 9.11 Hz), 6.89 (d, 2H, *J* = 8.72 Hz), 7.06 (d, 2H, *J* = 9.07 Hz), 7.34 (m, 10H), 7.50 (d, 2H, *J* = 8.67 Hz); ^{13}C NMR ($CDCl_3$): δ 55.20, 55.52, 66.42, 69.00, 71.84, 73.54, 75.31, 78.04, 79.18, 101.11, 103.05, 113.42, 114.36, 118.82, 127.49, 127.59, 127.64, 127.75, 127.98, 128.19, 128.25, 130.43, 138.32, 138.66, 151.57, 155.22, 160.01; Anal. Calcd for $C_{35}H_{36}O_8 \cdot 0.05\ C_6H_{14}$: C, 71.99; H, 6.28. Found: C, 71.84; H, 6.30.

***p*-Methoxyphenyl 2,3-di-*O*-benzyl-6-*O*-*p*-methoxybenzyl-β-D-galactopyranoside (41).** A suspension of compound **40** (7.6 g) and $NaBH_3CN$ (5.3 g, 7 equiv) in DMF (40 mL) was stirred for 10 min, followed by the addition of 3Å powdered molecular sieves (3.5 g). (CAUTION! $NaBH_3CN$ is highly toxic: all manipulations should be carried out with gloves and in a fume hood.) The suspension was cooled to 0 °C, and a solution of trifluoroacetic acid (14.2 mL, 14 equiv) in DMF (20 mL) was added dropwise over 1 h. The reaction was allowed to stir overnight at room temperature, after which time the reaction was filtered through Celite. The filtrate was combined with a solution of ice-cold satd $NaHCO_3$, which was stirred for 30 min and then extracted with CH_2Cl_2, dried ($MgSO_4$), concentrated, and submitted to flash chromatography (4:1:1 hexanes–ethyl acetate–dichloromethane). Evaporation of the fractions at 20 °C followed by recrystallization (dichloromethane–hexanes) afforded **41** as white needles (5.04 g, 66%) containing a small amount of hexanes: mp

93-95 °C; $[\alpha]_D^{20}$ –6.2 (*c* 1.0, $CHCl_3$); R_f = 0.33 (1:1 dichloromethane-toluene with 4% methanol); ^{1}H NMR ($CDCl_3$): δ 2.56* (d, 1H, *J* = 1.10 Hz), 3.60 (m, 3H), 3.74 (s, 1H), 3.76 (s, 3H), 3.80 (s, 3H), 3.90 (t, 1H, *J* = 8.57 Hz), 4.06** (bs, 1H), 4.50 (s, 2H), 4.74 (s, 2H), 4.83 (m, 2H), 5.00 (d, 1H, *J* = 10.89 Hz), 6.79 (d, 2H, *J* = 9. 10 Hz), 6.85 (d, 2H, *J* = 8.60 Hz), 7.03 (d, 2H, *J* = 9. 10 Hz), 7.30 (m, 12H) *Exchanges with D_2O; ** sharpens upon addition of D_2O; ^{13}C NMR ($CDCl_3$): δ 55.21, 55.56, 66.75, 68.90, 72.42, 73.36, 73.51, 75.30, 78.66, 80.60, 102.90, 113.79, 114.45, 118.54, 127.64, 127.80, 127.86, 128.13, 128.28, 128.43, 129.34, 130.07, 137.77, 138.41, 151.48, 155.24, 159.24; Anal. Calcd for $C_{35}H_{38}O_8 \cdot 0.035\ C_6H_{14}$; C, 71.72; H, 6.58 Found: C, 71.54; H, 6.60.

The 6-hydroxy regioisomer **42** (1.33 g, 18%) could be obtained by further elution of the column with 2:1:1 hexanes-ethyl acetate-dichloromethane: ^{1}H NMR ($CDCl_3$): δ 1.54* (bs, 1H), 3.46 (m, 2H), 3.59 (dd, 1H, *J* = 2.74 Hz), 3.72 (s, 2H), 3.76 (s, 3H), 3.80 (s, 3H), 4.08 (t, 1H, *J* = 8.68 Hz), 4.63 (d, 1H, *J* = 12.01 Hz), 4.84 (m, 5H), 5.00 (d, 1H, *J* = 10.82 Hz), 6.80 (d, 2H, *J* = 9.06 Hz), 6.87 (d, 2H, *J* = 8.53 Hz), 6.98 (d, 2H, *J* = 9.01 Hz), 7.31 (m, 12H). *Exchanges with D_2O.

***p*-Methoxyphenyl 2,3-di-*O*-benzyl-6-*O*-*p*-methoxybenzyl-4-*O*-trifluoromethanesulfonyl-β-D-galactopyranoside (15).** To a solution of compound **41** (2.6 g) in CH_2Cl_2 (5 mL) and pyridine (10 mL) at 0 °C was added triflic anhydride (3.0 mL, 4 equiv) dropwise over 1 h. The solution was allowed to stir overnight at 0 °C, after which time it was concentrated and passed through a short plug of silica gel (2:1 hexanes-ethyl acetate). Evaporation of the fractions yielded **15** (3.02 g, > 95%)

as an unstable pale yellow syrup, which was confirmed by NMR spectroscopy and used in subsequent steps without further characterization: ^{1}H NMR ($CDCl_3$): δ 3.62-3.90 (m, 6H), 3.77 (s, 3H), 3.80 (s, 3H), 4.34, 4.39, 4.57 (dd, 1H, J_1 = 14.9 Hz, J_2 = 11.8 Hz), 4.80-4.90 (m, 5H), 5.40 (d, 1H, J = 2.8 Hz), 6.80 (d, 2H, J = 9.1 Hz), 6.89 (d, 2H, J = 8.5 Hz), 6.98 (d, 2H, J = 9.1 Hz), 7.24-7.37 (m, 12H).

***p*-Methoxyphenyl 4-*S*-acetyl-2,3-di-*O*-benzyl-6-*O*-*p*-methoxybenzyl-4-thio-β-D-glucopyranoside (50).** A solution of triflate **15** (3.0 g) and KSAc (1.93 g, 4 equiv) in DMF (20 mL) was heated to 50 °C. After 2 h the reaction was complete as shown by TLC. The reaction was quenched with satd NH_4Cl, diluted with water, extracted with CH_2Cl_2, dried ($MgSO_4$), concentrated and submitted to flash chromatography (3:1 hexanes-ethyl acetate). Evaporation of the fractions at 20 °C followed by recrystallization (ether) afforded **50** as off-white crystals (1.88 g, 70%): mp 92-94 °C; $[\alpha]_D^{20}$ −13.0 (*c* 1.0, $CHCl_3$); R*f* = 0.33 (1:1:1 hexanes-dichloromethane-toluene with 4% methanol); ^{1}H NMR ($CDCl_3$): δ 2.27 (s, 3H), 3.65 (m, 6H), 3.77 (s, 3H), 3.79 (s, 3H), 4.46 (s, 2H), 4.68 (d, 1H, J = 11.02 Hz), 4.86 (m, 3H), 5.05 (d, 1H, J = 10.87 Hz), 6.78 (d, 2H, J = 7.02 Hz), 6.84 (d, 2H, J = 8.53 Hz), 7.05 (d, 2H, J = 9.00 Hz), 7.21 (d, 2H, J = 8.58 Hz), 7.30 (m, 10H); ^{13}C NMR ($CDCl_3$): δ 30.68, 46.19, 55.22, 55.59, 69.92, 73.19, 74.78, 75,03, 75.81, 80.71, 83.10, 102.45, 113.65, 114.53, 118.33, 127.54, 127.71, 128.17, 128.36, 129.25, 130.30, 138.20, 138.29, 151.48, 155.26, 159.12, 193.78; Anal. Calcd for $C_{37}H_{40}SO_8$: C, 68.92; H, 6.25 Found: C, 69.00; H, 6.27.

***p*-Methoxyphenyl 2,3-di-*O*-benzyl-6-*O*-*p*-methoxybenzyl-4-thio-β-D-**

glucopyranoside (46). Compound **50** (0.327 g) was dissolved in DMF (1 mL) and added via syringe to a solution containing cysteamine hydrochloride (0.18 g, 3 equiv) and DBU (0.1 mL, 1.3 equiv). After 45 min of stirring, TLC (1:1 toluene-dichloromethane with 4 % MeOH) showed the complete consumption of SM (R_f = 0.75) and the formation of a major product (R_f = 0.8). The reaction was poured into satd NH_4Cl, extracted with CH_2Cl_2, evaporated, and subjected to flash chromatography to afford **46** as a pale yellow syrup (0.358 g, 91 %), which was briefly characterized and used immediately in subsequent steps: R_f = 0.33 (1:1:1 hexanes-dichloromethane-toluene with 4% methanol); ^{1}H NMR ($CDCl_3$): δ 1.74* (d, 1H, J = 6.1 Hz, -SH), 3.07 (td, 1H, J_1 = 10.5 Hz, J_2 = 6.1 Hz, H-4), 3.42 (t, 1H, J = 10.1 Hz, H-3), 3.51 (dd, 1H, J_1 = 10.5 Hz, J_2 = 3.5 Hz), 3.64-3.90 (m, 3H), 3.77 (s, 3H), 3.78 (s, 3H), 4.44-4.57 (m, 2H), 4.77-5.08 (m, 5H), 6.73-7.00 (m, 5H), 7.02 (d, 2H, J = 9.0 Hz), 7.18-7.36 (m, 15H). * Exchanges slowly with D_2O; ** collapses slowly to pseudo-triplet upon addition of D_2O.

***p*-Methoxyphenyl 2-deoxy-4,6-*O*-*p*-methoxybenzylidene-2-phthalimido-β-D-glucopyranoside (53).** To a solution of known compound **51** (13.2 g) was added 1.5 mL of a 0.5 M solution of NaOMe. After 3 h, the reaction was neutralized with Dowex 50 × 8-400 (H^+ form), filtered, and concentrated to afford the triol as white powder, which was used as follows. The triol was dissolved in DMF (40 mL), treated with anisaldehyde dimethyl acetal (10.5 mL, 2.5 equiv) and TsOH (50 mg, cat. amt.), and placed on the rotary evaporator at 45 °C and < 10 torr for 2.5 h. After 3 h, TLC (1:1:1 hexanes-EtOAc-CH_2Cl_2) showed the complete conversion of starting material

(R_f = 0.1) to a major product (R_f = 0.5). The reaction was neutralized with triethylamine, concentrated, and subjected to flash chromatography (3:1:1, 2:1:1, then 1:1:1 hexanes-EtOAc-CH_2Cl_2) to afford **53** (10.66 g, 85 %) as a white powder: mp 147 °C; $[\alpha]_D^{20}$ +6.53 (*c* 0.92, $CHCl_3$); ^1H NMR ($CDCl_3$): δ 2.58* (d, 1H, *J* = 3.4 Hz, -OH), 3.68-3.86 (m, 3H), 4.40 (dd, 1H, J_1 = 8.8 Hz, J_2 = 4.0 Hz), 4.50 (dd, 1H, J_1 = 9.1 Hz, J_2 = 10.7 Hz), 4.70** (td, 1H, J_1 = 7.9 Hz, J_2 = 4.0 Hz, H-3), 5.55 (s, 1H), 5.80 (d, 1H, *J* = 8.7 Hz, H-1), 6.70-6.97 (m, 6H), 7.40 (d, 2H, *J* = 9.1 Hz), 7.70-7.79 (m, 2H), 7.82-7.92 (m, 2H); ^{13}C NMR ($CDCl_3$): δ 55.32, 55.60, 56.48, 66.30, 68.67, 77.95, 82.01, 98.11, 101.96, 113.79, 114.52, 118.61, 123.59, 127.65, 129.38, 131.62, 134.20, 150.60, 155.60, 160.37. *Exchanges with D_2O; ** collapses to pseudo-triplet upon addition of D_2O.

***p*-Methoxyphenyl 3-*O*-allyl-4,6-di-*O*-benzyl-2-deoxy-2-phthalimido-β-D-glucopyranoside (54).** Compound **53** (2.07 g) was dissolved in DMF (2 mL) and added to a suspension of NaH (0.24 g, 60 % in mineral oil, 1.5 equiv) in DMF (6 mL) at 0 °C. After 5 min, allyl bromide (2.2 mL, 6 equiv) was added all at once, and the reaction was allowed to warm to RT. After 4 h, the reaction was poured into satd NH_4Cl, extracted with CH_2Cl_2, dried ($MgSO_4$), and concentrated to afford the crude intermediate 3-*O*-allyl-4,6-*O*-benzylidene derivative **53a**. {Analytical samples of **53a** could be obtained as colorless needles by flash chromatography followed by recrystallization from EtOAc-hexanes: mp 151 °C; $[\alpha]_D^{20}$ +27.7 (*c* 1.0, $CHCl_3$); ^1H NMR ($CDCl_3$): δ 3.67-3.94 (m, 4H), 3.71 (s, 3H), 3.81 (s, 3H), 4.00 (dd, 1H, J_1 = 14.1 Hz, J_2 = 6.0 Hz), 4.32 (dd, 1H, J_1 = 13.0 Hz, J_2 = 4.9 Hz), 4.39 (dd, 1H, J_1 = 9.8

Hz, J_2 = 4.9 Hz), 4.48-4.57 (m, 2H), 4.88 (dd, 1H, J_1 = 10.8 Hz, J_2 = 1.6 Hz), 5.05 (dd, 1H, J_1 = 17.9 Hz, J_2 = 2.1 Hz), 5.48-5.67 (m, 2H), 5.76-5.80 (m, 1H), 6.70-6.97 (m, 6H), 7.43 (d, 2H, J = 9.8 Hz), 7.71-7.80 (m, 2H), 7.82-7.93 (m, 2H); ^{13}C NMR ($CDCl_3$): δ 55.16, 55.46, 55.76, 66.31, 6.53, 73.02, 75.02, 82.42, 98.13, 101.19, 113.53, 114.41, 116.93, 118.47, 123.39, 127.27, 129.63 131.48, 134.12, 134.42, 150.56, 155.50, 159.99; Anal. Calcd for $C_{32}H_{31}NO_9$: C, 67.01; H, 5.45; N, 2.44. Found: C, 66.94; H, 5.51; N, 2.39.}

Said crude allyl intermediate was dissolved in THF (4 mL) and treated with 80 % AcOH (20 mL). After stirring 7 h, the reaction was concentrated, and the resulting syrup was dissolved in in DMF (2 mL) and added to a suspension of NaH (0.5 g, 60 % in mineral oil, 3 equiv) in DMF (6 mL) at 0 °C. After 10 min, benzyl bromide (6 mL, 12 equiv) was added all at once, and the reaction was allowed to warm to RT. After 4 h, the reaction was poured into satd NH_4Cl, extracted with CH_2Cl_2, dried ($MgSO_4$), concentrated, and processed by flash chromatography followed by recrystallization from EtOAc-hexanes to afford **54** (2.21 g, 89 % from **53**) as colorless needles: mp 149 °C (dec); $[\alpha]_D^{20}$ + 19.6 (*c* 0.91, $CHCl_3$); ^{1}H NMR ($CDCl_3$): δ 3.70 (s, 3H), 3.72-3.81 (m, 3H), 3.95 (dd, 1H, J_1 = 12.8 Hz, J_2 = 3.3 Hz), 4.19-4.68 (m, 5H), 4.75-4.89 (m, 2H), 5.02 (dd, 1H, J_1 = 19.1 Hz, J_2 = 1.5 Hz), 5.47-5.65 (m, 1H, -OCH_2CH=CH_2), 5.68 (d, 1H, J = 8.3 Hz), 6.78 (dd, 4H, J_1 = 42.4, Hz, J_2 = 9.05 Hz), 7.22-7.34 (m, 11H), 7.68-7.77 (m, 2H), 7.85 (bs, 2H); ^{13}C NMR ($CDCl_3$): δ 54.81, 55.14, 55.42, 55.75, 56.30, 66.27, 68.52, 72.82, 73.00, 75.01, 75.92, 76.16, 82.37, 98.11, 101.18, 112.64, 113.49, 114.40, 116.89, 118.46, 123.37, 127.26, 129.62, 131.47, 134.11,

150.52, 155.46, 159.98.

3-*O*-Allyl-4,6-di-*O*-benzyl-2-deoxy-2-phthalimido-β-D-glucopyranosyl trichloroacetimidate (45). To a biphasic system of **54** (1.51 g) in 30 mL 1:1:1 MeCN-toluene-H_2O was added CAN (5.4 g, 4 equiv) all at once. After 3 h of stirring at RT, TLC (1:1:1 hexanes-EtOAc-dichloromethane) showed the complete consumption of SM (R_f = 0.67) and the formation of a major product (R_f = 0.35). The reaction was exhaustively extracted with EtOAc, and the combined organic phases were dried (Na_2SO_4), concentrated, and passed through a plug of silica gel to afford the crude free pyranose, which was immediately dissolved in dry CH_2Cl_2 and treated with Cl_3CCN (3.5 mL, excess) and K_2CO_3 (150 mg) and allowed to stir for 24 h, after which time TLC (1:1:1 hexanes-EtOAc-dichloromethane) showed the complete consumption of SM (R_f = 0.34) and the formation of a major product (R_f = 0.7). The reaction was filtered through a glass frit, concentrated, subjected to flash chromatography (2:1 hexanes-EtOAc), and recrystallized (CH_2Cl_2-hexanes) to afford **45** (1.19 g, 75 %) as colorless needles: ^{1}H NMR ($CDCl_3$): δ 3.75-3.83 (m, 4H), 3.94 (dd, 1H, J_1 = 12.7 Hz, J_2 = 6.3 Hz), 4.24 (dd, 1H, J_1 = 12.7 Hz, J_2 = 5.3 Hz), 4.36-4.70 (m, 5H), 4.81(d, 2H, J = 10.9 Hz), 5.02 (dd, 1H, J_1 = 17.3 Hz, J_2 = 1.6 Hz), 5.49-5.64 (m, 1H), 6.45 (d, 1H, J = 8.4 Hz, H-1), 7.20-7.38 (m, 12H), 7.70-7.75 (m, 2H), 7.81-7.86 (m, 2H), 8.57 (s, 1H, -NH).

***p*-Methoxyphenyl 4-*S*-(3-*O*-allyl-4,6-di-*O*-benzyl-2-deoxy-2-phthalimido-β-D-glucopyranosyl)-2,3-di-*O*-benzyl-6-*O*-*p*-methoxybenzyl-4-thio-β-D-glucopyranoside (16).** To a solution of **45** (0.107 g) and **46** (0.20 g, 2 equiv) in dry

CH_2Cl_2 and powdered 4Å molecular sieves at -78 °C were added two drops of TMSOTf. After stirring for 20 min, TLC (1:1:1 toluene–hexanes–dichloromethane with 3 % MeOH) showed the complete consumption of trichloroacetimidate donor (R_f = 0.65), remaining thiol acceptor (R_f = 0.8), and product (R_f = 0.7). The reaction was quenched by the addition of 4 drops of triethylamine, filtered through a glass frit, concentrated, and subjected to flash chromatography (4:1 hexanes–EtOAc) to afford first recovered thiol compound (0.09 g, corresponding to 90% of the unreacted 2nd equiv) and target disaccharide **16** (0.146 g, 79 %) as a pale-yellow glass: ^{1}H NMR ($CDCl_3$): δ 3.10 (pt, 1H, J = 10.5 Hz, H-4), 3.46–3.67 (m, 5H), 3.72 (s, 3H), 3.75 (s, 3H), 3.77–3.93 (m, 6H), 4.18 (dd, 1H, J_1 = 11.7 Hz, J_2 = 4.2 Hz), 4.26 (dd, 1H, J_1 = 6.46 Hz, J_2 = 3.4 Hz), 4.36–5.02 (m, 13H, CH_2Ar × 6, H-1'), 5.44–5.58 (m, 2H, H-1, -CH_2CH=CH_2), 6.72 (d, 2H, J = 9.0 Hz), 6.81 (d, 2H, J = 8.6 Hz), 6.98 (d, 2H, J = 9.0 Hz), 7.08–7.31 (m, 24H), 7.55–7.63 (m, 2H), 7.81-7.83 (m, 2H); ESIMS (positive-ion mode) calcd for $C_{66}H_{67}O_{13}SN$: $[M + Na^+]^{1+}$, 1136.4; $[M + K^+]^{1+}$, 1152.5. Found 1136.3, 1152.3.

Methyl [*p*-methoxyphenyl 4-*S*-(3-*O*-allyl-4,6-di-*O*-benzyl-2-deoxy-2-phthalimido-β-D-glucopyranosyl)-2,3-di-*O*-benzyl-4-thio-β-D-glucopyranosid]uronate (13). To a solution of **16** (16 mg) in 2 mL of 15:1 CH_2Cl_2–H_2O was added DDQ (13 mg, 4 equiv). After stirring at RT for 2 h, TLC (1:1 toluene-dichloromethane with 4 % MeOH) showed the complete consumption of SM (R_f = 0.8) and the formation of a major product (R_f = 0.55). The reaction was poured into ice water, extracted with CH_2Cl_2, dried ($MgSO_4$), concentrated, and subjected to

flash chromatography (2:1 hexanes-EtOAc) to afford an intermediate 6-*O*-deprotected alcohol {^{1}H NMR ($CDCl_3$): δ 2.43* (dd, 1H, J_1 = 7.7 Hz, J_2 = 5.4 Hz, -OH), 2.92 (pt, 1H, J = 10.3 Hz), 3.51-3.88 (m, 9H), 3.72 (s, 3H, ArOCH_3), 4.18 (dd, 1H, J_1 = 12.4 Hz. J_2 = 5.4 Hz), 4.25-4.29 (m, 1H), 4.50-4.55 (m, 2H) 4.66-5.02 (m, 3H), 6.75 (d, 2H, J = 9.0), 6.94-7.36 (m, 23H), 7.43-7.78 (m, 4H). *Exchanges with D_2O.}. Said alcohol was then dissolved in dry DMF (1 mL) with powdered 4Å molecular sieves and treated with PDC (54 mg, 10 equiv). After stirring for 2 days at 40 °C, TLC (9:1:1 dichloromethane-MeOH-AcOH) showed the consumption of SM (R_f = 0.8) and the formation of a major product (R_f = 0.3). The reaction was filtered through Celite, concentrated, passed through a short plug of silica gel (eluting with CH_2Cl_2 followed by 9:1 CH_2Cl_2-AcOH) to afford an intermediate carboxylic acid. {Analytical samples of this carboxylic acid could be obtained by additional chromatography (9:1 CH_2Cl_2-AcOH): ^{1}H NMR ($CDCl_3$): δ 3.37 (pt, 1H, J = 10.1), 3.48 (dd, 1H, J_1 = 10.6 Hz, J_2 = 7.9 Hz), 3.54-3.75 (m, 7H), 3.72 (s, 3H, ArOCH_3), 3.84 (dd, 1H, J_1 = 12.7 Hz, J_2 = 5.9 Hz), 4.08-4.27 (m, 2H), 4.37 (t, 1H, J = 10.5 Hz), 4.46-4.68 (m, 3H), 4.77 (dd, 1H, J_1 = 11.1 Hz, J_2 = 3.2 Hz), 4.85-5.01 (m, 2H), 5.40-5.63 (m, 1H, -CH_2C*H*=CH_2), 5.57 (d, 1H, J = 10.1 Hz), 6.84 (dd, 2H, J_1 = 48.5 Hz, J_2 = 9.0 Hz), 7.01-7.39 (m, 21H), 7.44-7.73 (m, 4H); ESIMS (negative-ion mode) calcd for $C_{58}H_{57}O_{13}NS$: $[M - H^+]^{1-}$, 1006.5; Found 1006.5}.

Said intermediate carboxylic acid was then immediately dissolved in ether and treated with diazomethane. After 1 h, TLC (4:1:9 hexanes-MeOH-dichloromethane) showed the complete consumption of SM (R_f = 0.15) and the formation of a major

product (R_f = 0.8). The solvent was evaporated, and the resulting syrup was purified by flash chromatography (3:1 hexanes-EtOAc) to afford **13** (6 mg, 41 % in three steps from **16**) as a pale-yellow glass: ^{1}H NMR ($CDCl_3$): δ 3.35 (t, 1H, J = 10.5 Hz), 3.56-3.68 (m, 4H), 3.69 (s, 3H, -OC*H*$_3$), 3.71 (s, 3H, -OC*H*$_3$), 3.85 (dd, 1H, J_1 = 12.8 Hz, J_2 = 6.4 Hz), 4.18 (dd, 1H, J_1 = 12.8 Hz, J_2 = 3.2 Hz), 4.23-4.58 (m, 4H), 4.68-4.98 (m, 7H), 5.41-5.55 (m, 1H, -CH_2C*H*=CH_2), 5.51 (d, 1H, J = 9.8 Hz), 6.81 (dd, 4H, J_1 = 49.2 Hz, J_2 = 9.0 Hz), 7.13-7.29 (m, 22H), 7.62-7.67 (m, 3H), 7.82-7.85 (m, 1H); ESIMS (positive-ion mode) calcd for $C_{59}H_{59}O_{13}NS$: $[M + Na^+]^{1+}$, 1044.5; $[M + K^+]^{1+}$, 1060.6. Found 1044.4, 1060.4.

***p*-Methoxyphenyl 4-*S*-(4,6-di-*O*-benzyl-2-deoxy-2-phthalimido-β-D-glucopyranosyl)-2,3-di-*O*-benzyl-6-*O*-*p*-methoxybenzyl-4-thio-β-D-glucopyranoside (55).** Cyclooctadieneyl-*bis*-(methyldiphenylphosphine) iridium hexafluorophosphate (25 mg) was suspended in dry THF (1 mL) and treated with hydrogen for 20 minutes until the solids had completely dissolved and the red color had changed to a pale tan. The solution was then purged for 15 min with dry nitrogen. To a solution of **16** (0.225 mg) in dry THF (2 mL) at 40 °C was then added said solution of activated catalyst, and the reaction was stirred for 24 h whereupon ^{1}H NMR analysis of aliquots clearly showed that the 3-*O*-allyl group (-OCH_2C*H*=CH_2 signal appears as a multiplet at δ 5.39-5.08) had completely isomerized to the 3-*O*-propenyl isomer (-OC*H*=CH_2CH_3 signal appears as a doublet of doublets at δ 5.94, J_1 = 12.1 Hz, J_2 = 1.4 Hz). The solvent was evaporated, and the resulting glass was redissolved in 4:1 THF-H_2O (5 mL) and treated with pyridine (0.5 mL) and I_2 (150 mg, 3 equiv). After stirring

for 45 minutes at RT, TLC (1:1:1 hexanes-EtOAc-dichloromethane) showed the complete consumption of propenyl ether (R_f = 0.82) and the formation of a major product (R_f = 0.6). The reaction was quenched with satd sodium thiosulfate, extracted with CH_2Cl_2, dried (Na_2SO_4), concentrated, and subjected to flash chromatography (3:1 then 2:1 hexanes-EtOAc) to afford **55** (164 mg, 74 %) as a colorless glass: ^{1}H NMR ($CDCl_3$): δ 2.08 * (d, 1H, J = 4.3 Hz, -OH), 3.12 (t, 1H, J = 10.3 Hz), 3.41-3.94 (m, 6H), 3.73 (s, 3H), 3.76 (s, 3H), 4.23 (t, 1H, J = 10.3 Hz, 1H), 4.39-5.02 (m, 10H), 5.57 (d,1H, J = 10.3 Hz), 6.59 (dd, 4H, J_1 = 62.4 Hz, J_2 = 9.0 Hz), 6.81 (d, 2H, J = 8.6 Hz), 7.01-7.33 (m, 22H), 7.45-7.62 (m, 3H), 7.79-7.80 (m, 1H). *Exchanges with D_2O; ESIMS (positive-ion mode) calcd for $C_{63}H_{63}O_{13}NS$: $[M + Na^+]^{1+}$, 1096.3; $[M + K^+]^{1+}$, 1112.4. Found 1096.2, 1112.0.

3-*O*-Acetyl-4,6-di-*O*-benzyl-2-deoxy-2-phthalimido-β-D-glucopyranosyl trichloroacetimidate (58). Compound **54** was deallylated by the same procedure used in the preceding paragraph. Thus **54** (0.718 g) was processed to afford a crude intermediate 3-hydroxy compound (**54a**). The deallylation was checked by verifying the presence of the hydroxyl proton: ^{1}H NMR ($CDCl_3$): δ 2.53 (d, 1H, J = 4.7 Hz, exchanges with D_2O; see also the spectrum in Appendix D). Said intermediate alcohol was then subjected to the following three-step procedure. First, the alcohol was acetylated by stirring with pyridine (4 mL) and acetic anhydride (1 mL) for 3 h, after which time the reaction was poured onto ice, extracted with ether, dried ($MgSO_4$), and concentrated. Second, the resulting syrup was dissolved in 1:1:1 toluene-MeCN-H_2O (15 mL) and treated with CAN (4 g, 10 equiv) for 3 h, after which time TLC (1:1:1

hexanes-EtOAc-dichloromethane) showed the complete consumption of intermediate 3-*O*-acetyl-methoxyphenyl glycoside (R_f = 0.7) and the formation of a major product (R_f = 0.35). The reaction was extracted with EtOAc, dried (Na_2SO_4), and concentrated. The resulting pale yellow syrup containing the crude free hemiacetal was then redissolved in dry CH_2Cl_2 and treated with K_2CO_3 (200 mg) and Cl_3CCN (0.75 mL, excess). After stirring overnight, the reaction appeared complete, as TLC (1:1:1 hexanes-EtOAc-dichloromethane) showed no remaining free OH compound (R_f = 0.35) and the formation of a single major product (R_f = 0.6). The reaction was filtered through a glass frit, concentrated, subjected to flash chromatography (2:1 hexanes-EtOAc) and recrystallized from ether-hexanes to afford **58** (0.283 g, 37 % for five steps from **54**) as a white solid: ^{1}H NMR ($CDCl_3$): δ 1.77 (s, 3H, COC*H*$_3$), 3.86-4.02 (m, 5H), 4.49-4.73 (m, 4H), 5.87 (dd, 1H, J_1 = 10.6 Hz, J_2 = 8.5 Hz), 6.64 (d, J = 8.8 Hz, H-1), 7.15-7.40 (m, 10H), 7.68-7.73 (m, 2H), 7.80-7.83 (m, 2H), 8.62 (s, 1H, -NH, exchanges with D_2O).

Allyl 4,6-*O*-(*p*-methoxybenzylidene)-α-D-galactopyranoside (60). To a solution of known allyl α-D-galactopyranoside (2.8 g) in dry MeCN was added anisaldehyde dimethyl acetal (ADMA, 4.5 mL, 2 equiv) and TsOH monohydrate (400 mg, cat. amt.). After stirring for 4 h at RT, the reaction was neutralized by the addition of NaOMe, concentrated, and subjected to flash chromatography (CH_2Cl_2 with 2, 5, 8, and 12% acetone) to afford **60** (3.9 g, 90%) as a white powder: mp 117-118 °C; $[\alpha]_D^{20}$ +78.2 (*c* 1.0, $CHCl_3$); ^{1}H NMR ($CDCl_3$): δ 2.05* (d, 1H, J = 8.7 Hz), 2.35* (d, 1H, J = 9.1 Hz), 3.73 (s, 1H), 3.80 (s, 3H), 3.90-3.93** (m, 2H), 4.04-4.35** (m, 7H),

5.10 (d, 1H, J = 2.6 Hz), 5.20-5.35 (m, 2H), 5.51 (s, 1H), 6.88 (d, 2H, J = 8.7 Hz), 7.42 (d, 2H, J = 8.7 Hz). *Exchanges with D_2O; ** sharpens upon addition of D_2O; ^{13}C NMR ($CDCl_3$): δ 55.31, 62.99, 68.84, 69.30, 69.64, 70.04, 75.85, 98.25, 101.27, 113.63, 118.00, 127.60, 133.50; Anal. Calcd for $C_{17}H_{22}O_7 \cdot 0.1\ C_4H_8O_2$: C, 60.20; H, 6.62. Found: C, 60.20; H, 6.62.

Allyl 2,3-di-*O*-benzyl-6-*O*-*p*-methoxybenzyl-α-D-galactopyranoside (61). To a suspension of NaH (6.5 g, 60 % in mineral oil, 4 equiv) in dry DMF (80 mL) at 0 °C was added a solution of **60** (13.8 g) in DMF (40 mL). After 15 minutes of stirring and warming to RT, the mixture was recooled to 0 °C and benzyl bromide (39 mL, 8 equiv) was added all at once. The reaction was allowed to warm to RT and stir overnight, after which time TLC (1:1:1 hexanes-EtOAc-dichloromethane) showed the complete consumption of SM (R_f = 0.15) and the formation of a major product (R_f = 0.75). The reaction was thereupon poured into satd NH_4Cl-ice, extracted with CH_2Cl_2, dried ($MgSO_4$), concentrated, and subjected to flash chromatography (8:1 then 5:1 hexanes-EtOAc) to afford the intermediate dibenzyl *p*-methoxybenzylidene compound (15.46 g, 73 %) as an amorphous pale yellow solid: mp 83-84 °C; $[\alpha]_D^{20}$ +81.5 (*c* 1.0, $CHCl_3$); ^1H NMR ($CDCl_3$): δ 3.61 (s, 1H), 3.78 (s, 3H), 3.93-4.19 (m, 6H), 4.62-4.87 (m, 5H), 4.95 (d, 1H, J = 3.1 Hz), 5.16-5.33 (m, 2H), 5.41 (s, 1H); 5.82-5.98 (m, 1H), 6.86 (d, 2H, J = 8.7 Hz), 7.23-7.43 (m, 12H) ; ^{13}C NMR ($CDCl_3$): δ 55.28, 62.70, 68.47, 69.35, 72.18, 73.57, 74.79, 75.53, 76.09, 96.99, 101.04, 113.45, 117.99, 127.48, 127.59, 127.93, 128.26, 130.49, 133.86, 138.89, 160.00; Anal. Calcd for $C_{31}H_{34}O_7$: C, 71.80; H, 6.61. Found: C, 71.80; H, 6.62.

Said intermediate (15 g) was then dissolved in DMF (65 mL), followed by the addition of $NaBH_3CN$ (12.6 g, 7 equiv) and powdered 3Å molecular sieves (20 g). (CAUTION! $NaBH_3CN$ is highly toxic: all manipulations should be carried out with gloves and in a fume hood.) The suspension was cooled to 0 °C and treated dropwise with a solution of trifluoroacetic acid (42 mL, 19 equiv) in DMF (50 mL). The reaction was allowed to warm to RT and was then stirred at 35 °C overnight, whereupon TLC (1:1 toluene-dichloromethane with 4 % MeOH) showed the consumption of SM (R_f = 0.6) and the formation of two major products (desired 4-hydroxy compound, R_f = 0.45, and the unwnated 6-hydroxy regioisomer, R_f = 0.3). The reaction was carefully poured into satd $NaHCO_3$-ice over 10 min and then stirred for an additional 30 min. The resulting mixture was then extracted with CH_2Cl_2, dried ($MgSO_4$), concentrated, and subjected to flash chromatography (4:1 hexanes-EtOAc) to afford **61** (7.45 g, 50 %) as a syrup: $[\alpha]_D^{20}$ +48.6 (*c* 1.0, $CHCl_3$); ^1H NMR ($CDCl_3$): δ 3.51-3.73 (m, 4H), 3.80 (s, 3H), 3.87-4.22 (m, 9H), 4.50 (s, 3H), 4.62-4.92 (m, 8H)5.17-5.63 (m, 2H), 5.85-6.07 (m, 1H), 6.86 (d, 2H, *J* = 8.5 Hz), 7.23-7.77 (m, 20H); ^{13}C NMR ($CDCl_3$): δ 55.28, 66.11, 66.29, 69.23, 72.75, 73.28, 75.79, 77.69, 96.22, 113.81 117.99, 127.79, 127.95, 128.35, 128.48, 129.31, 133.91; Anal. Calcd for $C_{31}H_{36}O_7 \cdot 0.04\ CH_2Cl_2$: C, 71.15; H, 6.94. Found: C, 71.37; H, 6.92.

Allyl 4-*S*-acetyl-*2,3*-di-*O*-benzyl-6-*O*-*p*-methoxybenzyl-4-thio-α-D-galactopyranoside (62). To a solution of **61** (7.4 g) in CH_2Cl_2 (15 mL) and pyridine (50 mL) at 0 °C was added triflic anhydride (8 mL, 3.3 equiv) dropwise over 1 h. The solution was allowed to stir overnight at 0 °C after which time it was concentrated

(bath temp < 20 °C) and passed through a short plug of silica gel (2:1 hexanes-ethyl acetate). Evaporation of the fractions yielded the crude triflate as an unstable pale yellow syrup, which was immediately dissolved in dry DMF (30 mL) and treated with KSAc (9.7 g, 6 equiv). The reaction was stirred at 55 °C for 3 h whereupon it was poured into water-ice, extracted with EtOAc, dried (Na_2SO_4), concentrated, and subjected to flash chromatography to provide **62** (3.9 g, 47 %) as a light brown syrup: $[\alpha]_D^{20}$ +43.7 (*c* 1.0, $CHCl_3$); ^{1}H NMR ($CDCl_3$): 2.24 (s, 3H), 3.57 (d, 1H, J = 3.8 Hz), 3.60-3.72 (m, 3H), 3.76 (s, 3H), 3.79-4.05 (m, 8H), 4.17 (dd, 1H, J_1 = 7.5 Hz, J_2 = 5.0 Hz), 4.42 (dd, 1H, dd, 1H, J_1 = 15. Hz, J_2 = 12.5 Hz), 4.59-4.94 (m, 6H), 5.19-5.36 (m, 2H), 5.66-5.95 (m, 1H), 6.84 (d, 2H, J = 8.5 Hz), 7.21-7.31 (m, 14H) ; Anal. Calcd for $C_{33}H_{38}O_7S \cdot 0.12\ H_2O$: C, 68.23; H, 6.64. Found: C, 68.46; H, 6.66.

Allyl 2,3-di-*O*-benzyl-6-*O*-*p*-methoxybenzyl-4-thio-α-D-galactopyranoside (63). A solution of compound **62** (0.16 g) in DMF (2 mL) was added via syringe to a solution of cysteamine hydrochloride (0.125 g, 4 equiv) and DBU (80 μL, 2 equiv) in DMF (2 mL). After 30 min TLC (1:1:1 hexanes-toluene-dichloromethane with 4 % MeOH) showed the complete conversion of SM (R_f = 0.8) into product (R_f = 0.85), whereupon the reaction was poured into satd NH_4Cl, extracted with EtOAc, dried (Na_2SO_4), concentrated, and chromatographed (3:1 hexanes-EtOAc) to afford **63** (0.138 g, 93 %) as an unstable light brown syrup, which was characterized by ^{1}H NMR spectroscopy and used immediately in the next step. ^{1}H NMR ($CDCl_3$): δ 1.64* (d, 1H, J = 6.5 Hz, -SH), 3.05-3.13** (m, 1H, H-4), 3.53 (dd, 1H, J_1 = 9.4 Hz, J_2 = 3.6 Hz, H-2), 3.63-3.77 (m, 4H, H-3, H-5, H-6a, H-6b), 3.79 (s, 3H), 4.01 (dd, 1H, J_1 =

13.0 Hz, J_2 = 6.6 Hz), 4.17 (dd, 1H, J_1 = 13.0 Hz, J_2 = 5.2 Hz), 4.39-5.00 (m, 6H), 4.87 (d, J = 3.5 Hz, H-1), 5.21-5.35 (m, 2H), 5.85-5.99 (m, 1H), 6.86 (d, 2H, J = 8.6 Hz), 7.23-7.43 (m, 15H); * Exchanges slowly with D_2O; ** sharpens slowly to a pseudo-triplet upon addition of D_2O.

Allyl 4-*S*-(3-*O*-acetyl-4,6-di-*O*-benzyl-2-deoxy-2-phthalimido-β-D-glucopyranosyl)-2,3-di-*O*-benzyl-6-*O*-*p*-methoxybenzyl-4-thio-α-D-glucopyranoside (57). To a solution of **58** (0.184 g), **63** (0.30 g, 2 equiv), and powdered 4Å molecular sieves in dry CH_2Cl_2 at -78 °C were added three drops of TMSOTf. After 30 min, TLC (1:1:1 hexanes-toluene-dichloromethane with 4 % MeOH) showed the complete consumption of trichloroacetimidate donor (R_f = 0.4) and the formation of a major product (R_f = 0.55), along with remaining thiol compound (R_f = 0.7). The reaction was quenched by the addition of 8 drops of triethylamine, filtered through a glass frit, concentrated, and subjected to flash chromatography (4:1 hexanes-EtOAc) to afford first the recovered thiol compound (0.114 g, 76% recovery of 2nd equivalent) and then target disaccharide **57** (0.258 g, 89%) as a colorless oil: ^{1}H NMR ($CDCl_3$): δ 3.14 (t, 1H, J = 11.0 Hz, H-4), 3.42-3.49 (m, 2H), 3.53-4.06 (m, 7H), 3.72 (s, 3H, ArOCH_3), 4.28 (t, 1H, J = 10.3 Hz), 4.35-4.73 (m, 9H), 4.78 (d, 1H, J = 3.5 Hz, H-1), 5.17 (dd, 1H, J_1 = 10.1 Hz, J_2 = 1.0 Hz, -OCH_2CH=C$\boldsymbol{H}_{cis}H_{trans}$), 5.27 (dd, 1H, J_1 = 17.3 Hz, J_2 = 1.4 Hz, -OCH_2CH=$CH_{cis}\boldsymbol{H}_{trans}$), 5.70 (d, 1H, J = 10.6 Hz, H-1'), 5.77 (t, 1H, J = 9.5 Hz), 5.74-5.93 (m, 1H, -$OCH_2C\boldsymbol{H}$=CH_2), 6.82 (d, 2H, J = 8.6 Hz), 7.06-7.36 (m, 23H), 7.42-7.61 (m, 3H), 7.67-7.75 (m, 1H).

To test the viability of 1-*O*-deprotection, an analytical sample of **57** was

manipulated as follows. For the isomerization to the propenyl glycoside, cyclooctadieneyl-*bis*-(methyldiphenylphosphine) iridium hexafluorophosphate (13 mg) was suspended in dry THF and treated with hydrogen for 20 min until the solids had completely dissolved and the red color had completely changed to a pale tan color. The solution was then purged for 15 min with dry nitrogen. A solution of **57** (0.083 g) in dry THF at 35 °C was then added to said solution of activated catalyst, and the reaction was stirred for 12 h, whereupon ^{1}H NMR analysis of aliquots clearly showed that the allyl glycoside (the -OCH_2CH=CH_2 signal appears as a multiplet at δ 5.74-5.93) had completely isomerized to the 1-propenyl glycoside isomer (the -OCH=CH_2CH_3 signal appears as a doublet of doublets at δ 6.11, J_1 = 12.3 Hz, J_2 = 1.4 Hz, and the -OCH=CH_2CH_3 signal appears as a doublet at δ 1.49, J = 5.9 Hz). The solvent was evaporated, and the resulting oil was redissolved in 4:1 THF-H_2O (3 mL) and treated with pyridine (0.4 mL) and I_2 (0.10 g). After stirring for 15 minutes at RT, TLC (1:1:1 hexanes-EtOAc-CH_2Cl_2) showed the conversion of propenyl derivative (R_f = 0.65) to a mixture of free pyranoside anomers (R_f = 0.35, 0.40) to be complete. The reaction was quenched with satd sodium thiosulfate, extracted with CH_2Cl_2, dried (Na_2SO_4), concentrated, and subjected to silica gel column chromatography (3:1, 2:1, then 1:1 hexanes-EtOAc) to afford an analytical sample of **55** (0.075 g, 95%) as a clear film: ^{1}H NMR ($CDCl_3$, of a ca. 1:1 mixture of anomers): δ 1.70 (s, 3H, -$COCH_3$), 2.71* (d, 0.5H, J = 1.4 Hz, α-O*H*), 3.11 (t, 1H, J = 11.0 Hz, H-4), 3.40-3.9 (m, 8H), 3.72 (s, 3H, ArOCH_3), 4.20-4.35 (m, 2H), 4.45-4.71 (m, 13H), 5.10** (pt, 0.5H, J = 1.3 Hz, H-1_{eq}, *i.e.*, α-anomer), 5.56 ** (dd, ½H, J_1 = 5.3 Hz, J_2 = 1.5 Hz, H-

1_{ax}, *i.e.*, β-anomer), 5.72 (d, 1H, J = 10.6 Hz, H-1′), 5.78 (t, 1H, J = 9.5 Hz), 6.79 (d, 2H, J = 9.5 Hz), 7.05-7.3 (m, 22H), 7.45-7.6 (m, 3H), 7.72-7.77 (m, 1H), 8.63 * (d, ½H, J = 5.5 Hz, β-O*H*). * Exchanges with D_2O. ** Sharpens upon addition of D_2O.

***p*-Methoxyphenyl 4,6-di-*O*-acetyl-3-*O*-chloroacetyl-2-deoxy-2-phthalimido-β-D-glucopyranoside (66).** The conversion of **53a** to **66** was carried out by the following five-step sequence of standard procedures; each step afforded only a single product, and only one chromatographic separation was required (during the last step). Compound **53a** (2.55 g) was dissolved in CH_2Cl_2 (10 mL) and treated with 80 % AcOH (50 mL). After stirring for 3.5 h at RT, TLC (9:3:3:1 dichloromethane-hexanes-EtOAc-acetone) showed the conversion of the *p*-methoxybenzylidene derivative (R_f = 0.75) to the diol (R_f = 0.2). Three volumes of toluene were added, and the reaction was concentrated to a syrup, treated with pyridine (15 mL) and acetic anhydride (7.5 mL), and stirred at RT overnight, whereupon TLC showed the complete conversion of the diol (R_f = 0.2) to a diacetate derivative (R_f = 0.65). After concentration of the solution to a syrup and passage through a short plug of silica gel, said crude diacetate derivative was subsequently deallylated using the same two-step isomerization-hydrolysis procedure as above. Thus, the crude product was stirred with 30 mg of activated iridium catalyst at 40 °C for 2 days to isomerize the allyl group. Water (4 mL), pyridine (2.5 mL) and I_2 (2.4 g, 2 equiv) were then added, and the reaction was allowed to stir for 30 min, whereupon TLC (1:1:1 toluene-EtOAc-dichloromethane) showed the consumption of SM (R_f = 0.55) and the

formation of a major product (R_f = 0.35). The reaction was quenched with satd sodium thiosulfate, extracted with dichloromethane, dried (Na_2SO_4), and concentrated to afford a 3-hydroxy compound intermediate. Finally, the 3-hydroxy compound thus obtained was treated with chloroacetyl chloride (0.7 mL, 2 equiv) in pyridine at 0 °C and stirred for 45 min, whereupon TLC (1:1:1 toluene–EtOAc–dichloromethane) showed its conversion to the chloroacetyl derivative (R_f = 0.35 to R_f = 0.45). The reaction was poured into satd $NaHCO_3$, extracted with CH_2Cl_2, dried ($MgSO_4$), concentrated, and subjected to flash chromatography (2:1:1 hexanes–EtOAc–dichloromethane) to afford **66** (1.41 g, 55% for 5 steps from **53a**) as a pale-yellow solid: ^{1}H NMR ($CDCl_3$): δ 1.89 (s, 3H, -COC*H*$_3$), 2.05 (s, 3H, -COC*H*$_3$), 3.72 (ArOC*H*$_3$), 3.96–4.02 (m, 1H, H-5), 4.07–4.16 (m, 2H, -COC*H*$_2$Cl), 4.30 (dd, 1H, J_1 = 12.0 Hz, J_2 = 1.8 Hz, H-6a), 4.45 (dd, 1H, J_1 = 12.2 Hz, J_2 = 5.3 Hz, H-6b), 4.57 (dd, 1H, J_1 = 10.6 Hz, J_2 = 8.5 Hz, H-2), 5.22 (t, 1H, J = 9.7 Hz), 5.86 (t, 1H, J = 10.3 Hz, H-3), 5.87 (d, 1H, J = 8.5 Hz, H-1), 6.79 (dd, 4H, J_1 = 27.6 Hz, J_2 = 9.0 Hz), 7.73–7.78 (m, 2H), 7.85-7.88 (m, 2H).

To test the selective removal of the chloroacetyl group, a small sample of **66** was dissolved in 1:1 pyridine–water. After 12 h, TLC showed the complete deprotection of **66** to **68**, as authenticated by comparison of its TLC and ^{1}H NMR data to the compound already in hand (said 3-hydroxy compound synthesized in the preceding paragraph).

4,6-Di-*O*-acetyl-3-*O*-chloroacetyl-2-deoxy-2-phthalimido-β-D-

glucopyranosyl trichloroacetimidate (67). Compound **66** (1.4 g) was dissolved in 1:1:1 toluene-MeCN-H_2O (60 mL), and treated with CAN (7 g, 5 equiv). After stirring for 45 min at RT, TLC (1:1:1 toluene-dichloromethane-EtOAc) showed the complete consumption of starting material (R_f = 0.6) and the presumed formation of the free pyranoside (R_f = 0.25) as a single anomer. The reaction was diluted with an equal volume of water, extracted with EtOAc, dried ($MgSO_4$), and concentrated {The ^{1}H NMR spectrum ($CDCl_3$) of the crude product confirmed the disappearance of the methoxyphenyl group, as well as the presence of signals associated with the free anomeric hydroxyl moiety: δ 3.4 (exchanged with D_2O, -O*H*), 5.55 (broad doublet, *J* = 8.3 Hz, sharpens with addition of D_2O, H-1)}. The resulting bright-yellow syrup was immediately taken up in dry CH_2Cl_2 and treated with Cl_3CCN (3 mL, excess) and K_2CO_3 (600 mg). After stirring for 18 h at RT, TLC showed the complete conversion of presumed free pyranoside to a single product (R_f = 0.4). The reaction was filtered through a glass frit, concentrated, subjected to flash chromatography (2:1:1 hexanes-EtOAc-CH_2Cl_2), and recrystallized from CH_2Cl_2-hexanes to afford **67** (1.06 g, 72% from **66**) as unstable white granules. Extensive ^{1}H NMR decoupling experimentation (see Appendix) on the beautifully resolved ring protons was found to conclusively confirm the assigned structure, and show that the sample consisted entirely of the β-isomer: ^{1}H NMR ($CDCl_3$) δ 1.98 (s, 3H, -COC*H*$_3$), 2.05 (s, 3H, -COC*H*$_3$), 3.81 (s, 2H, -COC*H*$_2$Cl), 4.00-4.06 (m, 1H, H-5), 4.14 (dd, 1H, J_1 = 12.5 Hz, J_2 = 1.8 Hz, H-6a), 4.32 (dd, 1H, J_1 = 12.5 Hz, J_2 = 4.1 Hz, H-6b), 4.61 (dd, J_1 = 10.6 Hz, J_2 =

9.0 Hz, H-2), 5.23 (t, 1H, J = 9.8 Hz, H-4), 5.92 (dd, 1H, J_1 = 10.5 Hz, J_2 = 9.2 Hz, H-3), 6.55 (d, 1H, J = 8.8 Hz, H-1), 7.64-7.69 (m, 2H), 7.73-7.79 (m, 2H), 8.61 (s, 1H, -NH). * Exchanges with D_2O; ** sharpens upon treatment with D_2O.

Allyl 2,3-di-*O*-*p*-methoxybenzyl-6-*O*-trityl-α-D-glucopyranoside (71). A solution of diol **60** (3.0 g) in DMF (10 mL) was added to a suspension of NaH (1.4 g, 60% in mineral oil, 4 equiv) in DMF (20 mL), and stirred vigorously for 20 minutes, whereupon *p*-methoxybenzyl chloride (7.2 mL, 6 equiv) was added. The reaction was allowed to stir for 2 h, after which time TLC (1:1:1 hexanes-EtOAc-dichloromethane) showed the conversion of the 2,3-diol (R_f = 0.1) to a single product (R_f = 0.85). The reaction mixture containing the presumed 2,3-di-*O*-methoxybenzyl-4,6-*O*-*p*-methoxybenzylidene derivative was poured into satd NH_4Cl-ice, extracted with EtOAc, dried ($MgSO_4$), and concentrated to a syrup. As previous experimentation had shown that the *p*-methoxybenzylidene group could be completely hydrolyzed on dry silica gel to the desired 4,6-diol, said syrupy intermediate was adsorbed onto silica gel and allowed to dry overnight. The silica gel was then suspended in 8:1 dichloromethane-MeOH, and filtered, with TLC analysis of the filtrate showing no remaining 2,3-di-*O*-methoxybenzyl-4,6-methoxybenzylidene derivative, and a new product (R_f = 0.2), corresponding to the 4,6-diol. After evaporation of the solvents, the crude 4,6-diol thus obtained was redissolved in pyridine and treated with TrCl (7 g, 3 equiv). The reaction was stirred overnight at 40 °C, whereupon TLC (1:1:1:1 toluene-dichloromethane-EtOAc-hexanes) showed the complete conversion of the

4,6-diol (black char, R_f = 0.1) to the 6-*O*-trityl derivative (yellow char turning to black char, R_f = 0.85). Then 15 mL of MeOH was added to the reaction, and after 1 h, the solution was evaporated and the residue subjected to flash chromatography, eluting first with hexanes, then with 9:1, 6:1, and 4:1 hexanes-EtOAc. {NOTE: in this and all other chromatographic operations with trityl derivatives, it was necessary to pre-treat the column with 1% TEA, and to maintain a 1-2 % concentration of TEA during the entire elution sequence}. Compound **71** (4.72 g, 76% for three steps from **60**) was obtained as a pale yellow glass: ^{1}H NMR ($CDCl_3$): δ 2.30 * (bs, 1H, -OH), 3.17 (dd, 1H, J_1 = 9.7 Hz, J_2 = 5.2 Hz), 3.31 (dd, 1H, J_1 = 9.7 Hz, J_2 = 6.6 Hz), 3.68-3.82 (m, 3H), 3.72 (s, 3H, ArOCH_3), 3.73 (s, 3H, ArOCH_3), 3.87 ** (bs, 1H, H-4), 3.99 (dd, 1H, J_1 = 12.8 Hz, J_2 = 6.5 Hz), 4.15 (dd, 1H, J_1 = 13.0 Hz, J_2 = 5.2 Hz), 4.47-4.67 (m, 4H, 2 × ArCH_2-), 4.75 (d, 1H, J = 2.84, H-1), 5.14 (dd, 1H, J_1 = 10.3 Hz, J_2 < 1.5 Hz, -OCH_2CH=C$H_{cis}H_{trans}$), 5.25 (dd, 1H, J_1 = 16.0 Hz, J_2 < 1.5 Hz, -OCH_2CH=$CH_{cis}H_{trans}$), 5.8-5.98 (m, 1H, -OCH_2CH=CH_2), 6.78 (dd, 4H, J_1 = 8.5 Hz, J_2 = 6.2 Hz), 7.11-7.38 (m, 19H).

Allyl 4-*S*-acetyl-2,3-di-*O*-*p*-methoxybenzyl-4-thio-6-*O*-trityl-α-D-glucopyranoside (72). To compound **71** (0.95 g) in 1:1 CH_2Cl_2-pyridine (10 mL) at 0 °C was added Tf_2O (0.67 mL, 3 equiv) dropwise over 30 min. After stirring for 12 h at 5 °C, TLC (2:2:2:1 toluene-hexanes-dichloromethane-EtOAc) showed the complete conversion of the alcohol (R_f = 0.75) to triflyl compound (R_f = 0.80). The reaction was carefully evaporated at < 20 °C, and the resulting paste was dissolved in

the minimum volume acetone and passed through a plug of silica gel. After removal of solvents, the resulting syrup was dissolved in DMF (8 mL), treated with KSAc (0.92 g, 6 equiv), and heated to 55 °C. After stirring for 45 min, TLC (12:4:4:2:1 hexanes-toluene-dichloromethane-EtOAc-MeCN) showed the complete conversion of the triflate intermediate (yellow char turning to blue, $R_f = 0.75$) to presumed thioacetate compound (yellow char turning to black, $R_f = 0.70$). The reaction was poured into ice water, extracted with ether, dried ($MgSO_4$), concentrated, and purified by silica gel column chromatography (6:1, 5:1, then 4:1 hexanes-EtOAc) to afford **72** (0.524 g, 51%) as a light brown oil: ^{1}H NMR ($CDCl_3$): δ 1.99 (s, 3H, SCOC*H*$_3$), 3.05-3.17 (m, 2H, H-3, H-5), 3.43 (t, 1H, $J = 11.1$ Hz, H-4), 3.52 (dd, 1H, $J_1 = 9.2$ Hz, $J_2 = 3.5$ Hz, H-2), 3.65-3.85 (m, 2H, -OC***H***$_2$CH=CH$_2$), 3.71 (s, 3H, ArOC*H*$_3$), 3.74 (s, 3H, ArOC*H*$_3$), 4.06 (dd, 1H, $J_1 = 13.0$ Hz, $J_2 = 6.8$ Hz, H-6a), 4.22 (dd, 1H, $J_1 = 12.9$ Hz, $J_2 = 5.2$ Hz, H-6b), 4.47-4.74 (m, 4H, 2 X -OC*H*$_2$Ar), 4.83 (d, 1H, $J = 3.6$ Hz, H-1), 5.18 (dd, 1H, $J_1 = 10.3$ Hz, $J_2 = 1.1$ Hz, -OCH$_2$CH=C***H***$_{cis}$H$_{trans}$), 5.30 (dd, 1H, $J_1 = 17.2$ Hz, $J_2 = 1.4$ Hz, -OCH$_2$CH=CH$_{cis}$***H***$_{trans}$), 5.86-5.99 (m, 1H, -OCH$_2$C***H***=CH$_2$), 6.77 (dd, 4H, $J_1 = 11.4$ Hz, $J_2 = 8.6$ Hz), 7.09-7.37 (m, 18H).

Allyl 2,3-di-*O*-acetyl-4-deoxy-4-thio-6-*O*-trityl-α-D-glucopyranoside (69a). To a solution of compound **72** (2.16 g) in 15:1 CH_2Cl_2-H_2O (32 mL) was added DDQ (2.0 g, 3 equiv). After stirring for 1 h, TLC (1:1:1 hexanes-EtOAc-dichloromethane) showed the complete consumption of starting material ($R_f = 0.8$) and formation of a major product (long smear centered at $R_f = 0.4$). The reaction was diluted with an

equal volume of water, extracted with CH_2Cl_2, dried (Na_2SO_4), concentrated, redissolved in pyridine (30 mL), and treated with Ac_2O (10 mL) and DMAP (25 mg, cat amt.). After 4 h, TLC no longer showed the abovementioned long smear, and also showed the formation of a new major product (concise spot, $R_f = 0.65$). Three volumes of toluene were added and the solvents were evaporated. All attempts to purify the presumed triacetate were fruitless, as black tarry material could not be removed. However, carrying the intermediate through the next step resulted in clean material. Said crude triacetate was thus dissolved in DMF (5 mL) and added to a pre-prepared solution of cysteamine hydrochloride (1.32 g, 4 equiv) and DBU (0.9 mL, 2 equiv) in DMF (15 mL). After stirring for 15 min, TLC showed the complete consumption of presumed triacetate ($R_f = 0.65$) and the formation of a major product ($R_f = 0.7$). The reaction was thereupon diluted with an equal volme of water and extracted with EtOAc. The combined organics were dried (Na_2SO_4), concentrated, and subjected to silica gel chromatography (6:1, then 5:1 hexanes–EtOAc) to afford **69a** (0.98 g, 68% for three steps from **72**) as a pale-yellow syrup. Extensive ^{1}H NMR decoupling experiments ($CDCl_3$) of the beautifully resolved ring protons conclusively confirmed the assigned structure: δ 1.07 * (d, 1H, $J = 9.0$ Hz, -SH), 2.00 (s, 3H, -COCH_3), 2.02 (s, 3H, -COCH_3), 3.04 ** (dt, 1H, $J_1 = 10.6$ Hz, $J_2 = 9.1$ Hz, overlapping so as to appear as a pseudo quartet, H-4), 3.24 (dd, 1H, $J_1 = 10.3$ Hz, $J_2 = 4.2$ Hz, H-5), 3.49 (dd, 1H, $J_1 = 8.9$ Hz, $J_2 = 1.1$ Hz, -OCH_aH$_b$CH=CH$_2$), 3.69 (dd, 1H, $J_1 = 12.1$ Hz, $J_2 =$ 3.9 Hz, -OCH$_a$$H_b$CH=CH$_2$), 3.97 (dd, 1H, $J_1 = 13.1$ Hz, $J_2 = 6.2$ Hz, H-6a), 4.14 (dd,

1H, J_1 = 13.1 Hz, J_2 = 5.2 Hz, H-6b), 4.83 (dd, 1H, J_1 = 10.0 Hz, J_2 = 3.6 Hz, H-2), 5.11-5.26 (m, 4H, H-1, H-3, -$OCH_2CH{=}CH_2$), 5.73-5.86 (m, 1H, -$OCH_2CH{=}CH_2$), 7.13-7.42 (m, 17H). * Exchanges with D_2O; ** collapses to pseudo triplet upon treatment with D_2O.

***p*-Methoxyphenyl 2,3-di-*O*-benzyl-6-*O*-*p*-methoxybenzyl-β-D-*xylo*-hexopyranosid-4-ulose (77).** To a solution of alcohol **41** (0.189 g) in dry CH_2Cl_2 (4 mL) and powdered 4Å molecular sieves at RT was added PCC (0.70g, 10 equiv) all at once. The reaction was stirred for 7 h at RT, whereupon TLC (1:1:1 hexanes-EtOAc-dichloromethane) showed consumption of starting material (black char, R_f = 0.55) and the formation of a major product (brown char, R_f = 0.75). The reaction was diluted with ether, filtered through a bed of Celite, and concentrated. The resulting brown syrup was subjected to flash chromatography (3:1:1, 2:1:1, then 1:1:1 hexanes-EtOAc-CH_2Cl_2), followed by recrystallization (ether) to afford **77** (0.129 g, 68%) as colorless needles: ^{1}H NMR ($CDCl_3$): δ 3.65 (dd, 1H, J_1 = 10.8 Hz, J_2 = 7.2 Hz), 3.76 (s, 3H), 3.77 (s, 3H), 3.92 (dd, 1H, J_1 = 10.8 Hz, J_2 = 3.6 Hz), 4.01 (dd, 1H, J_1 = 9.1 Hz, J_2 = 6.3 Hz), 4.22-4.26 (m, 1H), 4,41 (bs, 1H), 4.61-4.97 (m, 3H), 5.30 (d, J = 6.3 Hz), 6.79-6.84 (m, 4H), 7.03 (d, 2H, J = 9.0 Hz), 7.18 (d, 2H, J = 8.6 Hz), 7.29-7.84 (m, 12H). ^{13}C NMR ($CDCl_3$): 55.24, 55.62, 68.23, 73.3, 73.85, 74.63, 77.66, 82.97, 83.13, 101.95, 113.75, 114.62, 118.24, 127.86, 127.96, 128.09, 128.40, 129.37, 129.91, 137.37, 150.99, 162.61, 201.82.

***p*-Methoxyphenyl 2,3-di-*O*-benzyl-4-*C*-cyano-4-deoxy-6-*O*-*p*-**

methoxybenzyl-β-D-glucopyranoside (78). To a solution of **41** (0.78 g) in dry CH_2Cl_2 (5 mL) and dry pyridine (5 mL) at 0 °C was added dropwise Tf_2O (0.67 mL, 3 equiv). The resulting orange solution was stirred at 0 °C overnight whereupon TLC (1:1 toluene-CH_2Cl_2 with 3 % MeOH) showed complete consumption of starting material. The solution was evaporated at < 20 °C. The resulting orange paste was dissolved in 1:1 CH_2Cl_2-acetone and passed through a plug of silica gel (2:1:1 hexanes-ethyl acetate-CH_2Cl_2) to yield the crude triflate as a pale yellow syrup which was used as follows without further purification. To the triflate in dry THF (6 mL) at -45 °C was added tetrabutylammonium cyanide (4 mL, 0.5 M soln in THF, 1.5 equiv). (CAUTION! Bu_4CN is highly toxic: all manipulations should be carried out with gloves and in a fume hood.) The solution was allowed to stir and warm to room temperature, whereupon TLC (12:4:4:2:1 hexanes-toluene-CH_2Cl_2-EtOAc-MeCN) showed complete consumption of the triflate, formation of product (light brown char, R_f = 0.42), as well as formation of a second slightly less polar byproduct (black char, R_f = 0.48) The reaction was concentrated, and subjected to flash chromatography (20:5:1 then 20:6:1 hexanes-CH_2Cl_2-MeCN) followed by recrystallization from ether-hexanes to afford the desired nitrile as colorless needles (0.435 g, 55%). mp 80 °C; $[\alpha]_D^{20}$ = -19.1 (*c* 1.0, $CHCl_3$); ^{1}H NMR ($CDCl_3$): δ 7.22-7.30 (m,10 H), 7.18 (pd, *J* = 8.6 Hz, 2 H), 6.92 (pd, *J* = 9.1 Hz, 2 H), 6.79 (pd, *J* = 8.6 Hz, 2 H), 6.74 (pd, *J* = 9.0 Hz, 2 H), 4.71-4.98 (m, 5H, 2 × ArCH_2OR + H-1), 4.46 (dd, J_1 = 16.2 Hz, J_2 = 11.5 Hz, 2H, ArCH_2OR), 3.63-3.81 (m, 10H, 2 × ArOCH_3 + H-3, H-5, H-6a, H-6b), 3.51 (t, *J*

= 8.3 Hz, 1 H, H-2), 2.96 (t, J = 10.2 Hz, 1H, H-4); ^{13}C NMR ($CDCl_3$): δ 35.90, 55.16, 55.53, 69.11, 72.30, 73.33, 75.14, 75.81, 79.27, 81.40, 102.80, 113.75, 114.54, 117.42, 118.51, 127.88, 128.00, 128.13, 128.25, 128.38, 129.28, 129.56, 137.20, 137.74, 151.02, 155.51, 159.24. Anal. Calcd for $C_{36}H_{37}NO_7$: C, 72.59; H, 6.26. Found: C, 72.43; H, 6.26.

***p*-Methoxyphenyl 2,3-di-*O*-benzyl-4-deoxy-4-*C*-formyl-6-*O*-*p*-methoxybenzyl-β-D-glucopyranoside (79).** To a solution of nitrile **78** (0.164 g) in dry THF (8 mL) at -78 °C was added DIBAL-H (1.1 mL, 1.5 M soln in toluene, 6 equiv), and the reaction was allowed to warm to room temperature overnight. TLC (3:3:1 toluene-CH_2Cl_2-MeCN) then showed complete consumption of SM (light brown char, R_f = 0.75) and formation of the presumed imine (black char, smear centered at R_f = 0.65). After quenching with EtOAc, the reaction was stirred with 1.0 M H_3PO_4 (10 mL) for 30 min whereupon TLC (1:1:1 hexanes-CH_2Cl_2-EtOAc) showed a concise spot (R_f = 0.72) corresponding to the aldehyde. The reaction was treated with Rochelle's salts, filtered through Celite, and extracted with CH_2Cl_2. After drying ($MgSO_4$) and evaporation, the crude syrup was passed through a short plug of silica gel to yield the desired aldehyde as an unstable white solid (0.085 g, 52%), which was characterized by ^{1}H and ^{13}C NMR spectroscopy and used in the next step without further purification. ^{1}H NMR ($CDCl_3$): δ 9.67 (d, J = 2.7 Hz, 1 H, RC*H*O), 7.17-7.35 (m, 12 H), 7.00 (pd, J = 9.0 Hz, 2 H), 6.85 (pd, J = 8.8 Hz, 2 H), 6.81 (pd, J = 9.2 Hz, 2 H), 4.54-5.08 (m, 5H, 2 × ArCH_2OR + H-1), 4.42 (dd, J_1 = 16.3 Hz, J_2 = 11.5 Hz, 2

H, ArCH_2OR), 4.01 (dd, J_1 = 8.9 Hz, J_2 = 10.7 Hz, 1 H, H-2), 3.56-3.87 (m, 10 H, 2 × ArOCH_3 + H-3, H-5, H-6a, H-6b), 3.02 (td, J_1 = 2.6 Hz, J_2 = 10.5 Hz, 1 H, H-4); ^{13}C NMR ($CDCl_3$): δ 29.68, 55.24, 55.62, 57.16, 70.20, 72.05, 73.15, 74.97, 75.15, 78.76, 82.48, 102.71, 113.81, 114.58, 118.39, 127.83, 128.01, 128.16, 128.38, 128.42, 129.40, 129.61, 138.83, 138.08, 151.27, 155.42, 159.31, 200.03.

4-Methoxyphenyl 2,3-di-*O*-benzyl-4-deoxy-4-*C*-hydroxymethyl-6-*O*-*p*-methoxybenzyl-β-D-glucopyranoside (80). To a solution of aldehyde **79** (0.097 g) in CH_2Cl_2 (2 mL) and MeOH (6 mL) at RT was added $NaBH_4$ (0.020 g) all at once. TLC (1:1:1 CH_2Cl_2-EtOAc-hexanes) showed complete consumption of SM and formation of product (R_f = 0.55). After the reaction was quenched with acetone (2 mL), the solvents were evaporated and the compound was subjected to flash chromatography (2:1 hexanes-EtOAc) followed by recrystallization from ether to yield the desired alcohol as colorless needles (0.092 g, 95%). mp 83 °C; $[\alpha]_D^{20}$ = -42.5; ^{1}H NMR ($CDCl_3$): δ 7.20-7.38 (m, 12 H), 7.01 (pd, J = 9.0 Hz, 2 H), 6.84 (pd, J = 9.7 Hz, 2 H), 6.81 (pd, J = 9.3 Hz, 2 H), 4.65-5.09 (m, 5 H, 2 × ArCH_2OR + H-1), 4.48 (dd, J_1 = 19.2 Hz, J_2 = 11.4 Hz, 2 H, ArCH_2OR), 3.62-3.79 (m, 12 H, 2 × ArOCH_3 + H-2, H-3, H-5, H-6a, H-6b, RCH_2OH), 1.75-1.90 (m, 1 H, H-4). Anal. Calcd for $C_{36}H_{40}O_8$: C, 71.98; H, 6.71. Found: C, 71.99; H, 6.76.

3-*O*-Allyl-4,6-di-*O*-benzyl-2-deoxy-2-phthalimido-D-glucopyranose (82). To a biphasic system of **54** (3.5 g) in 30 mL 1:1:1 MeCN-toluene-H_2O was added CAN (12.6 g, 4 equiv) all at once. After 3 h of stirring at RT, the reaction was

exhaustively extracted with CH_2Cl_2, and the combined organic phases were dried (Na_2SO_4), concentrated, and subjected to flash column chromatography (4:1, 3:1, then 2:1 hexanes-EtOAc) to afford the crude free pyranose (2.88 g, 82%) as a pale-orange solid, which appeared by TLC and ^1H NMR spectroscopy to consist entirely of the β anomer: 2.98* (d, 1H, J = 8.1 Hz, -OH), 3.61-3.82 (m, 4H), 3.93 (dd, 1H, J_1 = 12.8 Hz, J_2 = 3.3 Hz), 4.05-4.22 (m, 2H), 4.30-4.43 (m, 1H), 4.48-4.65 (m, 5H), 4.7-4.85 (m, 2H), 5.00 (dd, 1H, J_1 = 17.9 Hz, J_2 = 2.1 Hz), 5.25-5.41** (m, 2H), 5.45-5.67 (m, 1H, -OCH_2CH=CH_2), 7.11-7.35 (m, 11H), 7.68-7.74 (m, 2H), 7.80-7.93 (m, 2H). *Exchanges with D_2O; ** sharpens upon addition of D_2O.

REFERENCES

A Concise, Enantioselective Synthesis of (−)- and (+)-Hongconin

1. M. Bols. *Carbohydrate Building Blocks*, Wiley: New York, 1996.
2. Hainan-Renmin Hospital Guanxinbin-Keyan-Xiaozu, *Hainan-Weisheng* **1977**, *2*, 43.
3. (a) Chen, Z.; Huang, H.; Wang, Y.; Li, Y.; Ding, J. *Zhongcaoyao* **1981**, *12*, 484; *Chem. Abstr.* 97: 20699. (b) Chen, Z.; Huang, H.; Wang, C.; Li, Y.; Ding, J.; Sankawa, U.; Noguchi, H.; Iitaka, Y. *Heterocycles* **1984**, *22*, 691. (c) Chen, Z.; Huang, H.; Wang, C.; Li, Y.; Ding, J.; Sankawa, U.; Noguchi, H.; Iitaka, Y. *Chem. Pharm. Bull.* **1986**, *14*, 2743.
4. (a) Schmid, H.; Meijer, T. M.; Eböthner, A. *Helv. Chim. Acta* **1950**, *33*, 595. (b) Schmid, H.; Eböthner, A.; Burger, M. *ibid.* **1950**, *33*, 609. (c) Schmid, H.; Eböthner, A.; Meijer, T. M. *ibid.* **1950**, *33*, 1751. (d) Schmid, H.; Eböthner, A. *ibid.* **1951**, *34*, 1041. (e) Schmid, H.; Eisenhuth, W. *ibid.* **1958**, *41*, 2021.
5. Ding, J.; Huang, H. *Zhongcaoyao* **1982**, *13*, 499; *Chem. Abstr.* 98: 113584.
6. (a) Winters, M. P.; Stranberg, M.; Moore, H. W. *J. Org. Chem.* **1994**, *59*, 7572. (b) Moore, H. W. *Science* **1977**, *197*, 527.
7. (a) Kraus, G. A.; Li, J.; Gordon, M.; Jensen, J. H. *J. Org. Chem.* **1994**, *59*, 2219. (b) Green, I. R.; Hugo, V. I.; Oosthuizen, F.; Giles, R. G. F. *Synth. Commun.* **1996**, *26*, 867.
8. (a) Freskos, J. N.; Morrow, G. W.; Swenton, J. S. *J. Org. Chem.* **1985**, *50*, 805. (b) Kraus and co-workers had previously developed the use of **6** in phthalide annulation chemistry to synthesize racemic kalafungin, pachybasin, and

chrysophanol: Kraus, G. A.; Cho, H.; Crowley, S.; Roth, B.; Sugimoto, H.; Prugh, S. *J. Org. Chem.* **1983**, *48*, 3439.

9. (a) Swenton, J. S.; Freskos, J. N. *J. Chem. Soc., Chem. Commun.* **1985**, 658. (b) Swenton, J. S.; Freskos, J. N.; Dalidowicz, P.; Kerns, M. L. *J. Org. Chem.* **1996**, *61*, 459.

10. Tatsuta, K.; Akimoto, K.; Annaka, M.; Ohno, Y.; Kinoshita, M. *Bull. Chem. Soc. Jpn.* **1985**, *58*, 1699.

11. Deshpande, P. P.; Price, K. N.; Baker, D. C. *J. Org. Chem.* **1996**, *61*, 455.

12. Deshpande, P. P.; Price, K. N.; Baker, D. C. *Bioorg. Med. Chem. Lett.* **1995**, *5*, 1059.

13. Nicolaou, K. C.; Hwang, C.-K.; Duggan, M. E. *J. Chem. Soc., Chem. Commun.* **1986**, 925.

14. 115:1 Toluene–MeOH (**1a**: $R_f = 0.38$; **1b**: $R_f = 0.45$).

15. Berkowitz, D. B.; Danishefsky, S. J.; Schulte, G. K. *J. Am. Chem. Soc.* **1992**, *114*, 4158. 3,4-Di-*O*-acetyl-D-fucal was prepared from D-fucose using a standard literature preparation for 6-deoxyglycals: Pigman, W.; Roth, W. *Methods Carbohydr. Chem.* **1963**, *2*, 405.

16. Khanapure, S. P.; Reddy, R. T.; Biehl, E. R. *J. Org. Chem.* **1987**, *52*, 5685.

17. Schaumberg, J. P.; Hokanson, G. C.; French, J. C.; Smal, E.; Baker, D. C. *J. Org. Chem.* **1985**, *50*, 1651, footnote 33 therein.

18. Garegg, P. J.; Samuelsson B. *Carbohydr. Res.* **1978**, *67*, 267.

Molecular Probes of Cancer Metastasis—Background, Rationale, Overall Project Design, and Preliminary Biological Evaluations

1. *Glycobiology;* Fukuda, M; Hindsgaul, O. Eds.; Wiley: New York, 1994.
2. (a) Cysyk, R. L., The National Cancer Institute, unpublished results. (b) Randolph, J. T. *Design, Synthesis, and Study of Compounds of Interest as Antiinflammatory, Antiviral, and Antitumor Agents* (Doctoral Dissertation); The University of Alabama: Tuscaloosa, AL, 1992.
3. *Cancer Chemotherapeutic Agents;* Foye, W. O., Ed.; American Chemical Society: Washington, DC, 1995.
4. Buick, R. N., in *Antineoplastic Agents;* Remers, W. A., Ed.; Wiley: New York, 1984; p 3.
5. (a) Fidler, I.; Hart, I. *Science*, **1982**, *217*, 998. (b) Frixen, U. et al. *J. Cell Biol.* **1991**, *113*, 173. (c) Stetler-Stevenson, W.; Aznavoorian, S.; Liotta, L. *Annu. Rev. Cell Biol.* **1993**, *9*, 541. (d) Takeichi, M. *Curr. Opin. Cell Biol.* **1993**, *5*, 806.
6. Zetter, B. *Sem. Canc. Biol.* **1993**, *4*, 219.
7. Dejana, E.; Martin-Padura, I.; Lauri, D.; Bernasconi, S.; Bani, M.; Garofolo, A.; Giavazzi, R.; Magnani, J.; Mantovani, A.; Menard, S. *Lab. Invest.* **1992**, *66*, 324.
8. Castronovo, V.; Taraboletti, G.; Sobol, M. *J. Biol. Chem.* **1991**, *266*, 20440.
9. Stryer, L. *Biochemistry,* 4th ed., W. H. Freeman: New York, 1995; p 474.
10. (a) Laurent, T. C.; Fraser, J. R. E. in *Functions of the Proteoglycans (CIBA Foundation Symposium 124);* Evered, D., Whelan, J., Eds.; Wiley: Chichester

1986; pp 9-29. (b) Toole, B. P.; Biswas, C.; Gross, J. *Proc. Natl. Acad. Sci. USA* **1979**, *76*, 6299.

11. (a) Knudson, W.; Biswas, C.; Toole, B. P. *Proc. Natl. Acad. Sci. USA* **1984**, *81*, 6767. (b) Knudson, W.; Biswas, C.; Toole, B. P. *J. Cell. Biochem.* **1989**, *25*, 183. (c) Knudson, C. B.; Knudson, W. *Cancer Lett.* **1990**, *52*, 113.
12. (a) Nemec, R. E.; Toole, B. P.; Knudson, W. *Biochem. Biophys. Res. Commun.* **1987**, *149*, 249. (b) Hofmann, M.; Rudy, R.; Zöller, M.; Tölg, C.; Ponta, H.; Herrlich, P.; Günthert, U. *Cancer Res.* **1991**, *51*, 5292.
13. Birch, M.; Mitchell, S.; Hart, I. *Cancer Res.* **1991**, *51*, 6660.
14. (a) Thomas, L.; Byers, H.; Vink, J.; Stamenkovitch, I. *J. Cell. Biol.* **1992**, *118*, 971. (b) Bartozolli, A.; Peach, R.; Aruffo, A.; Stamenkovic, I. *J. Exp. Med.* **1994**, *180*, 53.
15. Turley, E.; Austen, L.; Vandeligt, K.; Clary, C. *J. Cell. Biol.* **1991**, *112*, 1041.
16. Underhill, C. *J. Cell Sci.* **1992**, *103*, 293.
17. Günthert, U.; Hofmann, M.; Rudy, W.; Reber, S.; Zöller, M.; Haußmann, I.; Matzku, S.; Wenzel, A.; Ponta, H.; Herrlich, P. *Cell* **1991**, *65*, 13.
18. Seiter, S.; Arch. R.; Reben, S.; Komitowski, D.; Hofmann, M.; Ponta, H.; Herrlich, P.; Matzku, S.; Zöller, M. *J. Exp. Med.* **1993**, *177*, 443.
19. Guo, Y.; Wang, J.; Ma, J.; Che, X.; Narula, J.; Bigby, M.; Wu, M.; Sy, M. *Cancer Res.* **1994**, *54*, 1561.
20. Knudsen, W. in *The Biology of Hyaluronan;* Evered, D.; Whelan, J. Eds.; Wiley: Chichester (Ciba Foundation Symposium, 143), 1989; pp 159-186.

21. (a) Underhill, C. in *The Biology of Hyaluronan;* Evered, D.; Whelan, J. Eds.; Wiley: Chichester (Ciba Foundation Symposium, 143), 1989; pp 87-106. (b) Underhill, C. *J. Cell Sci.* **1992**, *103*, 293.

22. Toole, B. in *The Biology of Hyaluronan;* Evered, D.; Whelan, J. Eds.; Wiley: Chichester (Ciba Foundation Symposium, 143), 1989; pp 138-149.

23. (a) Cysyk, R.; August, M.; Duncan, K.; Malinowski, N. *Oncol. Res.* **1994**, *5*, 1. (b) Cysyk, R., The National Cancer Institute, unpublished results.

24. (a) Humphries, M. J.; Olden, K.; Yamada, K.A. *Science* **1986**, *233*, 467. (b) Gehlsen, K. R.; Argraves, W. S.; Pierschbacher, M. D.; Ruoslahti, E. *J. Cell Biol.* **1988**, *106*, 925.

25. Kumagai, H.; Tajima, M.; Ueno, Y.; Giga-Hama, Y.; Ohba, M. *Biochem. Biophys. Res. Commun.* **1991**, *177*, 74.

26. Knudsen, W.; Nemec, R.; Toole, B. *Biochem. Biophys. Res. Commun.* **1987**, *149*, 249.

27. (a) Pauli, B.; Lee, C. *Lab. Invest.* **1988**, *58*, 379. (b) Zhu, D.; Cheng, C.; Pauli, B. *Proc. Natl. Acad. Sci. USA* **1991**, *88*, 9568. (c) Zhu, D.; Cheng, C.; Pauli, B. *J. Clin. Invest.* **1992**, *89*, 1718.

28. (a) Pauli, B.; Lee, C. *Lab. Invest.* **1988**, *58*, 379. (b) Zhu, D.; Cheng, C.; Pauli, B. *Proc. Natl. Acad. Sci. USA* **1991**, *88*, 9568. (c) Zhu, D.; Cheng, C.; Pauli, B. *J. Clin. Invest.* **1992**, *89*, 1718.

29. These reviews do not contradict the remark in Section II.A. which mentioned the lack of a review of HA–CD44 metastasis, since they concern *general* issues of

HA–CD44 binding, not metastasis: (a) Sy, M. S.; Liu, D.; Schiavone, R.; Ma, J.; Mori, H.; Guo, Y. *Curr. Top. Microbiol. Immunol.* **1996**, *213*, 129. (b) Knudson, W. *Am. J. Pathol.* **1996**, *148*, 1721. (c) Entwistle, J.; Hall, C. L.; Turley, E. A. *J. Cell. Biochem.* **1996**, *61*, 569.

30. a) Heldin, P.; De La Torre, M.; Ytterberg, D.; Bergh, J. *Oncol. Rep.* **1996**, *3*, 1011. b) Kogerman, P.; Sy, M.-S.; Culp, L. A. *Clin. Exp. Metastasis* **1996**, *14*, 73. c) Goebeler, M.; Kaufmann, D.; Broecker, E.-B.; Klein, C. E. *J. Cell Sci.* **1996**, *109*, 1957. d) Goshen, R.; Ariel, I.; Shuster, S.; Hochberg, A.; Vlodavsky, I.; De Groot, N.; Ben-Rafael, Z.; Stern, R. *Mol. Hum. Reprod.* **1996**, *2*, 685.

31. Assmann, V.; Kern, H. F.; Elsaesser, H.-P. *Clin. Cancer Res.* **1996**, *2*, 1607.

32. a) Gardner, M. J.; Catterall, J. B.; Jones, L. M. H.; Turner, G. A. *Clin. Exp. Metastasis* **1996**, *14*, 325. b) Yeo, T.-K.; Nagy, J. A.; Yeo, K.-T.; Dvorak, H. F.; Toole, B. P. *Am. J. Pathol.* **1996**, *148*, 1733.

33. Wang, C.; Zhang, S.; Turley, E. A. *Round Table Ser. - R. Soc. Med. Press* **1996**, *45*, 37.

34. Mitchell, B. S.; Whitehouse, A.; Prehm, P.; Delpech, B.; Schumacher, U. *Clin. Exp. Metastasis* **1996**, *14*, 107.

35. Lokeshwar, V. B.; Lokeshwar, B. L.; Pham, H. T.; Block, N. L. *Cancer Res.* **1996**, *56*, 651.

36. a) Laurent, U. B. G.; Laurent, T. C.; Hellsing, L. K.; Persson, L.; Hartman, M.; Lilja, K. *Acta Neurol. Scand.* **1996**, *94*, 194. b) Jaworski, D. M.; Kelly, G. M.;

Piepmeier, J. M.; Hockfield, S. *Cancer Res.* **1996**, *56*, 2293.

37. (a) Akima, K.; Ito, H.; Iwata, Y.; Matsuo, K.; Watari, N.; Yanagi, M.; Hagi, H.; Oshima, K.; Yagita, A. *J. Drug Targeting* **1996**, *4*, 1. b) Spruss, T.; Bernhardt, G. *Contrib. Oncol.* **1996**, *51*, 145.

38. a) Civalleri, D.; Esposito, M.; DeCian, F.; Balletto, N.; Mondini, G.; Gogioso, L.; Viale, M.; Vannozzi, O. *Clin. Drug Invest.* **1996**, *12*, 94. b) Croix, B. S.; Rak, J. W.; Kapitain, S.; Sheehan, C.; Graham, C. H.; Kerbel, R. S. *J. Natl. Cancer Inst.* **1996**, *88*, 1285.

39. Zhao, J. Y.; Dovichi, N. J.; Hindsgaul, O.; Gosselin, S.; Palcic, M. M. *Glycobiology* **1994**, *4*, 239.

40. Grootenhuis, P. D. J.; Westerdulin, P.; Müleman, D.; Petitou, M.; van Boeckel, C. A. A. *Nat. Struct. Biol.* **1995**, *2*, 736.

41. Herbert, J. M.; Herault, J. P.; Bernat, A.; van Amsterdam, R. G. M.; Vogel, G. M. T.; Lormeau, J. C.; Petitou, M.; Müleman, D. *Circ. Res.* **1996**, *79*, 590.

42. Couchman, J.; Woods, A. in *Cell Surface and Extracellular Glycoconjugates*; Roberts, D.; Mecham, R. Eds.; Academic: San Diego, 1993; p 42.

43. Underhill, C. *J. Cell Sci.* **1992**, *103*, 293.

44. West, D.; Kumar, S. in *The Biology of Hyaluronan;* Evered, D.; Whelan, J. Eds.; Wiley: Chichester (Ciba Foundation Symposium, 143), 1989; pp 187-207.

45. Underhill, C.; Culty, M.; Nguyen, H. *J. Cell. Biol.* **1992**, *116*, 1055.

46. Orkin, R.; McGuire, P.; Castellot, J. *J. Cell. Phys.* **1987**, *133*, 267.

47. Kresse, H.; Truppe, W.; Basner, R.; Figura, K. *Biochem. Biophys. Res. Comm.*

1977, *78*, 713.

48. (a) Lesley, J.; Hyman, R. *Eur. J. Immunol.* **1992**, *22*, 2719. (b) Liao, H.; Levesque, M. C.; Patton, K; Jones, D.; Moody, M. A.; Telen, J. J.; Haynes, B. F.; *J. Immunol.* **1993**, *151*, 6490.

49. Günthert, A. R.; Straeter, J.; von Reyher, U.; Henne, C.; Joos, S.; Koretz, K.; Moldenhauer, G.; Krammer, P. H.; Möller, P. *J. Cell Biol.* **1996**, *134*, 1089.

50. Routine procedures exist for the preparation of oligosaccharide fragments with known length and known initial and terminal residues. See Chapter 2.

51. Underhill and Toole's studies on SV-3T3 cells stood for many years as the basis for this claim (Underhill, C.; Toole, B.; Chi-Rosso, G. *J. Biol. Chem.* **1983**, *258*, 8086, and references cited therein). Knudsen's more recent finding that highly invasive human bladder carcinoma cells also show a hexasaccharide binding requirement (Knudsen, W.; Nemec, R.; Toole, B. *Biochem. Biophys. Res. Comm.* **1987**, *149*, 249) are roughly consistent with the results obtained by the present studies showing activity beginning with the octamer.

52. Cysyk, R., The National Cancer Institute, personal communication.

53. (a) Underhill, C.; Toole, B.; Chi-Rosso, G. *J. Biol. Chem.* **1983**, *258*, 8086, and references cited therein. (b) Knudsen, W.; Nemec, R.; Toole, B. *Biochem. Biophys. Res. Comm.* **1987**, *149*, 249.

1. Kresse, H.; Glössl, J. *Adv. Enzymol.* **1987**, *60*, 217.

2. Chun, L. E.; Koob, T. J.; Eyre, D. R. *Anal. Biochem.* **1988**, *171*, 197. (b) Christner, J. E.; Brown, M. L.; Dziewiakowski, D. D. *J. Biol. Chem.* **1979**, *254*, 4624.

3. Pritchard, D. G.; Lin, B.; Willingham, T. R.; Baker, J. R. *Archiv. Biochem. Biophys.* **1994**, *315*, 431.

4. Abramson, C. *Archiv. Biochem. Biophys.* **1967**, *121*, 103.

5. (a) Christner, J. E.; Brown, M. L.; Dziewiakowski, D. D. *J. Biol. Chem.* **1979**, *254*, 4624. (b) Chun, L. E.; Koob, T. J.; Eyre, D. R. *Anal. Biochem.* **1988**, *171*, 197.

6. (a) Linker, A.; Meyer, K.; Hoffman, P. *J. Biol. Chem.* **1956**, *219*, 13. (b) Linker, A.; Meyer, K.; Hoffman, P. *J. Biol. Chem.* **1960**, *235*, 924.

7. Shimada, E.; Matsumura, G. *J. Biochem.* **1980**, *88*, 1015.

8. Yamada, S.; Yoshida, K.; Sugiura, M.; Sugahara, K. *J. Biochem.* **1992**, *112*, 440.

9. Meyer, K.; Hoffman, P.; Linker, A. *The Enzymes*, 2nd Ed., 1960, Vol. 4, p 447.

10. Roden, L.; Baker, J. R.; Cifonelli, J. A.; Matthews, M. B. *Methods Enzymol.* **1972**, *28*, 73.

11. Livant, P.; Rodén, L.; Krishna, N. R. *Carbohydr. Res.* **1992**, *237*, 271.

12. (a) Black, G. E.; Fox, A. *ACS Symp. Ser.* **1996**, *619*, 81. (b) Peter-Katalinic, J. *Croat. Chem. Acta* **1996**, *69*, 731. (c) Garone, L.; Edmunds, T.; Hanson, E.; Bernasconi, R.; Huntington, J. A.; Meagher, J. L.; Fan, B.; Gettin, P. G. W. *Biochemistry*, **1996**, *35*, 8881. (d) Reinhold, V. N.; Reinhold, B. B.; Chan, S. *Methods Enzymol.* **1996**, *271*, 377.

13. J. Watson, *Introduction to Mass Spectrometry.* Unpublished textbook, Ch. 11.

14. (a) Ravandi, A.; Kuksis, A.; Marai, L.; Myher, J. J.; Steiner, G.; Lewisa, G.; Kamido, H. *FEBS Lett.* **1996**, *381*, 77. (b) Rohde, M. F.; Katta, V.; Derby, P.; Rush, R. S. *ACS Symp. Ser.* **1996**, *619*, 408. (c) Vollmer, G.; Schneider, M. R. *J. Steroid Biochem. Mol. Biol.* **1996**, *58*, 103. (d) Entwistle, J.; Hall, C. L.; Turley, E. A. *J. Cell. Biochem.* **1996**, *61*, 569.

15. Petitou, M. in *Heparin and Related Polysaccharides*; D. A. Lane, Ed.; Plenum: New York, 1992; pp 21-30.

16. (a) Niessen, W. M. A.; Van der Hoeven, R. A. M.; Van der Greef, J. *Org. Mass Spectrom.*, **1992**, *27*, 341. (b) An, J.; O'Neill, M. A.; Albersheim, P.; Darvill, A. G. *Carbohydr. Res.* **1994**, *252*, 235. (c) Bhat, U. R.; Forsberg, L.S.; Carlson, R. W. *J. Biol. Chem.* **1994**, *269*, 14402. (d) Sugahara, K.; Ohkita, Y.; Shibata, Y.; Yoshida, K.; Ikegami, A. *J. Biol. Chem.* **1995**, *270*, 7204.

17. M. Zhao, et al., *J. Biol. Chem.* **1995**, *270*, 26657.

18. Xie, M. G.; Denis, B.; Bertheau, Y.; Casetta, B.; Arpino, P. *Rapid Commun. Mass Spectrom.* **1995**, *9*, 1572-1575.

19. Cowman, M. K.; Balazs, E. A.; Bergmann, C. W.; Meyer, K. *Biochemistry* **1981**, *20*, 1379.

20. Kery, V.; Orvisky, E.; Stancikova, M. *Carbohydr. Polym.* **1992**, *17*, 227.

21. (a) Corradini, C. *Ann. Chim.* **1994**, *84*, 385. (b) Mou, S.; Li, Z. *Sepu* **1995**, *13*, 320, *Chem. Abstr.*, 123 (1995) 358061.

22. (a) Hotchkiss, A. T. Jr.; Hicks, K. B. *Anal. Biochem.* **1990**, *184*, 200. (b) Lieker, H. P.; Thielecke, K.; Buchholz, K.; Reilly, P. J. *Carbohydr. Res.* **1993**, *238*, 307. (c) Balmer, D. M.; McLellan, D. *Fruit Process.* **1995**, *5*, 86. (d) Kawasaki, N.; Morimoto, K.; Hayakawa, T. *Eisei Shikensho Hokoku* **1995**, *113*, 69, *Chem. Abstr.*, 124 (1996) 76674. (e) Thurl, S.; Mueller-Werner, B.; Sawatzki, G. *Anal. Biochem.* **1996**, *235*, 202. (f) Wallis, A. F. A.; Wearne, R. H.; Wright, P. J. *Appita J.* **1996**, *49*, 258.

23. Johnson, D. C.; LaCourse, W. R. *J. Chrom. Libr.* **1995**, *58*, 391.

24. For examples, see: (a) Hernandez, L. M.; Ballou, L.; Ballou, C. E. *Carbohydr. Res.* **1990**, *203*, 1. (b) An, J.; O'Neill, M. A.; Albersheim, P.; Darvill, A. G. *Carbohydr. Res.* **1994**, *252*, 235.

25. *ibid.*

26. LaCourse, W. R.; Johnson, D. C. *Anal. Chem.* **1993**, *65*, 50.

27. Hicks, K. B. *J. Chrom. Libr.* **1995**, *58*, 370.

28. Hotchkiss, A. T.; Hicks, K. B. *Anal. Biochem.* **1990**, *184*, 200.

29. (a) Akima, K.; Ito, H.; Iwata, Y.; Matsuo, K.; Watari, N.; Yanagi, M.; Hagi, H.;

Oshima, K.; Yagita, A. *J. Drug Targeting* **1996**, *4*, 1. (b) Spruss, T.; Bernhardt, G. *Contrib. Oncol.* **1996**, *51*, 145. (c) Pouyani, T.; Harbison, G. S.; Prestwich, G. D. *J. Am. Chem. Soc.* **1994**, *116*, 7515, and references cited therein.

30. (a) Ammeral, R. N.; Delgado, G. A.; Tenbarge, F. L.; Friedman, R. B. *Carbohydr. Res.* **1991**, *215*, 179. (b) Dunkel, M. P. H.; Amado, R. *Carbohydr. Res.* **1995**, *268*, 151. (c) Hardy, M. R.; Townsend, R. R. *Proc. Natl. Acad. Sci. USA* **1988**, *85*, 3289. (d) Hotchkiss, A. T.; Hicks, K. B. *Anal. Biochem.* **1990**, *184*, 200. (e) LaCourse, W. R.; Johnson, D. C. *Anal. Chem.* **1993**, *65*, 50. (f) Lieker, H.P.; Thielecke, K.; Buchholz, K.; Reilly, P. J. *Carbohydr. Res.* **1993**, *238*, 307. (g) McGuire, J. M.; Douglas, M.; Smith, K. D. *Carbohydr. Res.* **1996**, *292*, 1. (h) Spiro et al.; *Carbohydr. Res.*, 1996

31. LaCourse, W. R.; Johnson, D. C. *Anal. Chem.* **1993**, *65*, 50.

32. The possibility of sequential depolymerization of reducing-end GlcNAc residues during the electrospray process itself was excluded on the basis of the aforementioned HPAEC data, which clearly showed the existence of the intervening oligomers, as well as by the fact that no such depolymerization phenomena were observed in the course of our previous ESIMS analysis of HAL-derived oligomers, which were analyzed by and large as pure samples.

33. (a) Cramer, J. A.; Bailey, L. C.; Baily, C. A.; Miller, R. T. *Biochim. Biophys. Acta* **1994**, *1200*, 315. (b) Harrison, R. *Biochem. J.* **1988**, *252*, 875. (c) Yang,

C.-H.; Srivastava, P. N. *J. Biol. Chem.* **1975**, *250*, 79.

34. Kery, V.; Orvisky, E.; Stancikova, M. *Carbohydr. Polym.* **1992**, *17*, 227.

1. Fraser, J.; Laurent, T. in *The Biology of Hyaluronan*, Evered, D.; Whelan, J. Eds. Wiley: Chichester, 1989; pp 41-59.

2. (a) Rodén, L.; Campbell, P.; Fraser, J.; Laurent, T.; Pertoft, H.; Thompson, J. Enzymic Pathways of Hyaluronan Catabolism. In *The Biology of Hyaluronan (Ciba Foundation Symposium, 143)*; Evered, D.; Whelan, J. Eds.; Wiley: Chichester, 1989; pp 60–86. (b) Fraser, J.; Laurent, T. Turnover and metabolism of hyaluronan. In *The Biology of Hyaluronan (Ciba Foundation Symposium, 143)*; Evered, D.; Whelan, J. Eds.; Wiley: Chichester, 1989; pp 41–59.

3. (a) McGuire, P.; Castellot, J.; Orkin, R. *J. Cell Physiol.* **1987**, *133*, 267. (b) Truppe, W.; Basner, R.; Figura, K.; Kresse, H. *Biochem. Biophys. Res. Commun.* **1977**, *78*, 713.

4. Bernfield, M.; Banerjee, S. D.; Koda, J. E.; Rapraeger, A. C. In *The Role of Extracellular Matrix in Development;* Trelstad, R., Ed; Alan R. Liss: New York, 1984; p 545.

5. (a) Rodén, L.; Campbell, P.; Fraser, J.; Laurent, T.; Pertoft, H.; Thompson, J. Enzymic Pathways of Hyaluronan Catabolism. In *The Biology of Hyaluronan (Ciba Foundation Symposium, 143)*; Evered, D.; Whelan, J. Eds.; Wiley: Chichester, 1989; pp 60–86. (b) Kresse, H.; Glössl, J. *Adv. Enzymol.* **1987**, *60*, 217.

6. Kanie, O.; Crawley, S. C.; Palcic, M. M.; Hindsgaul, O. *Carbohydr. Res.* **1993**, *243*, 139.

7. Basten, J.; Jaurand, G.; Olde-Hanter, B.; Petitou, M.; van Boeckel, C. A. A. *Bioorg. Med Chem. Lett.* **1992**, *2*, 901.

8. (a) Postema, M. H. D. *Tetrahedron* **1992**, *48*, 8545. (b) Herscovici, J.; Antonakis, K. *Stud. Nat. Prod. Chem.* **1992**, *10*, 337. (c) Kishi, Y. *Pure Appl. Chem.* **1993**, *65*, 771, and references cited therein.

9. Sinnot, M. *Chem. Rev.* **1990**, *90*, 1171.

10. Kishi, Y. *Pure Appl. Chem.* **1993**, *65*, 771.

11. (a) Fügedi, P.; Garegg, P. J. Loen, H.; Norberg, T. *Glycoconjugate J.* **1987**, *4*, 97. (b) Hasegawa, A. *ACS Symp. Ser.* **1994**, *560*, 184.

12. Kishi, Y. *Pure Appl. Chem.* **1993**, *65*, 771.

13. Eisele, T.; Toepfer,A.; Kretzschmer, G.; Schmidt, R. R. *Tetrahedron Lett.* **1996**, *37*, 1389.

14. Schmidt, R. R.; Kinzy, W. *Adv. Carbohydr. Chem. Biochem.* **1994**, *50*, 21, and references cited therein.

15. Toshima, K.; Tatsuta, K. *Chem. Rev.* **1993**, *93*, 1503.

16. Ogawa's group has recently synthesized a native (O-linked) HA tetrasaccharide, as well as analogous di- and trisaccharides with varying residues (either GlcUA or GlcNAc) at the reducing and non-reducing ends: (a) Ogawa, T.; Slaghek, T.; Nakahara, Y. *Tetrahedron Lett.* **1992**, *33*, 4971. (b) Ogawa, T.; Slaghek, T.; Nakahara, Y.; Kamerling, J.; Vliegenthart, J. *Carbohydr. Res.* **1994**, *255*, 61.

17. (a) Blanc-Muesser, M.; Driguez, H. *J. Chem. Soc., Perkin Trans. 1* **1988**, 3345. (b) Schou, C.; Rasmussen, G.; Schulein, M.; Henrissat, B.; Driguez, H. *J.*

Carbohydr. Chem. **1993**, *12*, 743. (c) Wang, L.-X.; Lee, Y. C. *Carbohydr. Lett.* **1995**, *1*, 185.

18. (a) Martin, O.; Lai, W. *J. Org. Chem.* **1990**, *55*, 5188. (b) Martin, O.; Lai, W. *J. Org. Chem.* **1993**, *58*, 176.

19. Petrus, L.; Bystricky, S.; Sticzak, T.; Bilik, V. *Chim. Zvesti* **1982**, *36*, 103.

20. Koll, P.; Fortsch, A.; Kogelberg, H. *Carbohydr. Res.* **1987**, *164*, 391.

21. Preuss, R.; Schmidt, R. R. *J. Carbohydr. Chem.* **1991**, *10*, 887.

22. *The Chemistry of C-Glycosides,* Levy, D. E.; Tang, C. Eds.; Pergamon: Oxford, UK, 1995.

23. Such issues, for example, were discussed for *C*- vs. *O*-glycosylic compounds by Prof. Y. Kishi in a recent symposium address [*Abstr. Papers 212th ACS National Meeting,* ORGN-028].

24. Slaghek, T.; Nakahara, Y.; Ogawa, T.; Kamerling, J. P.; Vliegenthart, J. F. G. *Carbohydr. Res.* **1994**, *225*, 61.

25. Binkley, R. W. *Modern Carbohydrate Chemistry,* Dekker: New York, 1988; pp 125-129.

26. Johansson, R.; Samuelsson, B. *J. Chem Soc., Perkin Trans. 1* **1984**, 2371.

27. Horton, D.; Wolfram, M. L. *J. Org. Chem.* **1962**, *27*, 1794.

28. Although a mercapto glycosyl acceptor had not been reported to be coupled with a trichloacetimdate glycosyl donor, Magnusson and co-workers used a mecapto acceptor with a glycosyl halide acceptor: Nilsson, P. ; Magnusson, G. *Carbohydr. Res.* **1981**, *94*, 91.

29. Nakano, T.; Ito, Y.; Ogawa, T. *Tetrahedron Lett.* **1990**, *31*, 1597.

30. The compound in question is the same one as shown in Fig. 2: Schmidt, R. R.; Kinzy, W. *Adv. Carbohydr. Chem. Biochem.* **1994**, *50*, 21.

31. Eisele, T.; Toepfer,A.; Kretzschmer, G.; Schmidt, R. R. *Tetrahedron Lett.* **1996**, *37*, 1389.

32. Ho, T.-L. *Synth. Commun.* **1979**, *9*, 237.

33. El Shenawy, H. A.; Scheurch, C. *Carbohydr. Res.* **1984**, *131*, 227.

34. (a) Petrus, L.; Bystricky, S.; Sticzak, T.; Bilik, V. *Chim. Zvesti* **1982**, *36*, 103.
(b) Koll, P.; Fortsch, A.; Kogelberg, H. *Carb. Res.* **1987**, *164*, 391.

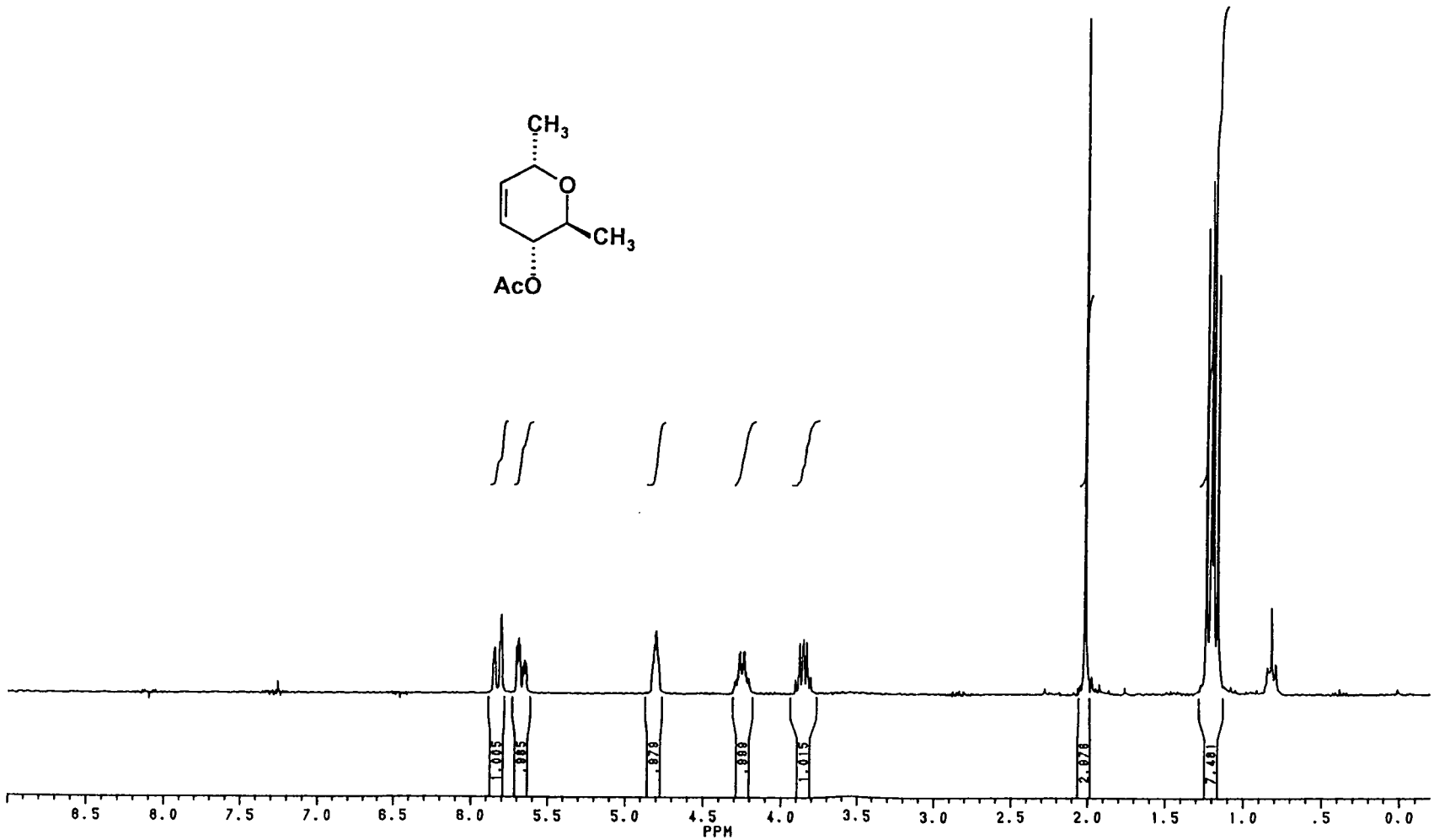
35. Murray, R.; Rajadyaksha, S.; Mohan, L. *J. Org. Chem.* **1989**, *54*, 5783.

36. In fact, a co-worker has recently demonstrated the viability of this Scheme by converting **78** to **21** as shown.

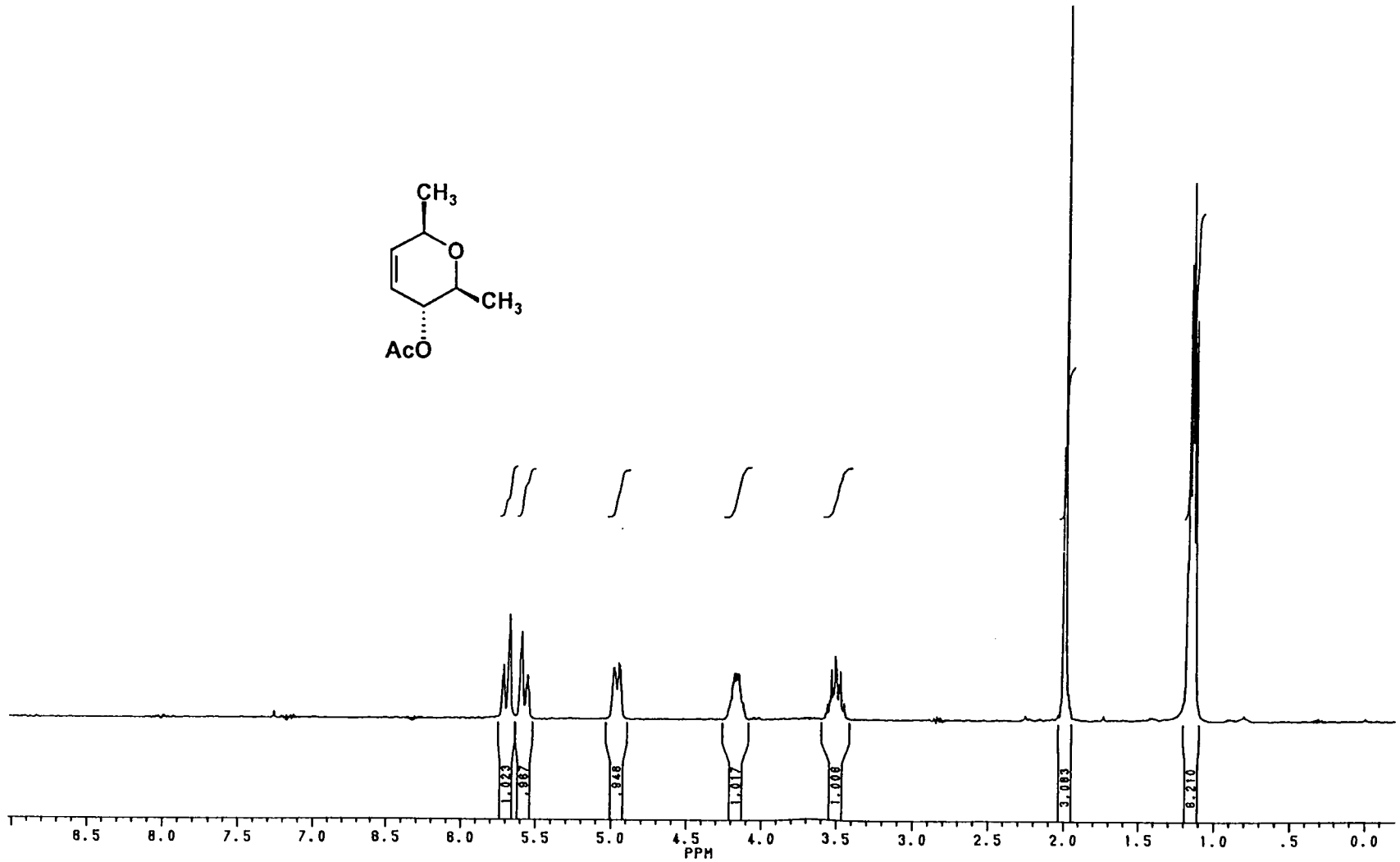
37. Schaumberg, J. P.; Hokanson, G. C.; French, J. C.; Smal, E.; Baker, D. C. *J. Org. Chem.* **1985**, *50*, 1651, footnote 33 therein.

APPENDICES

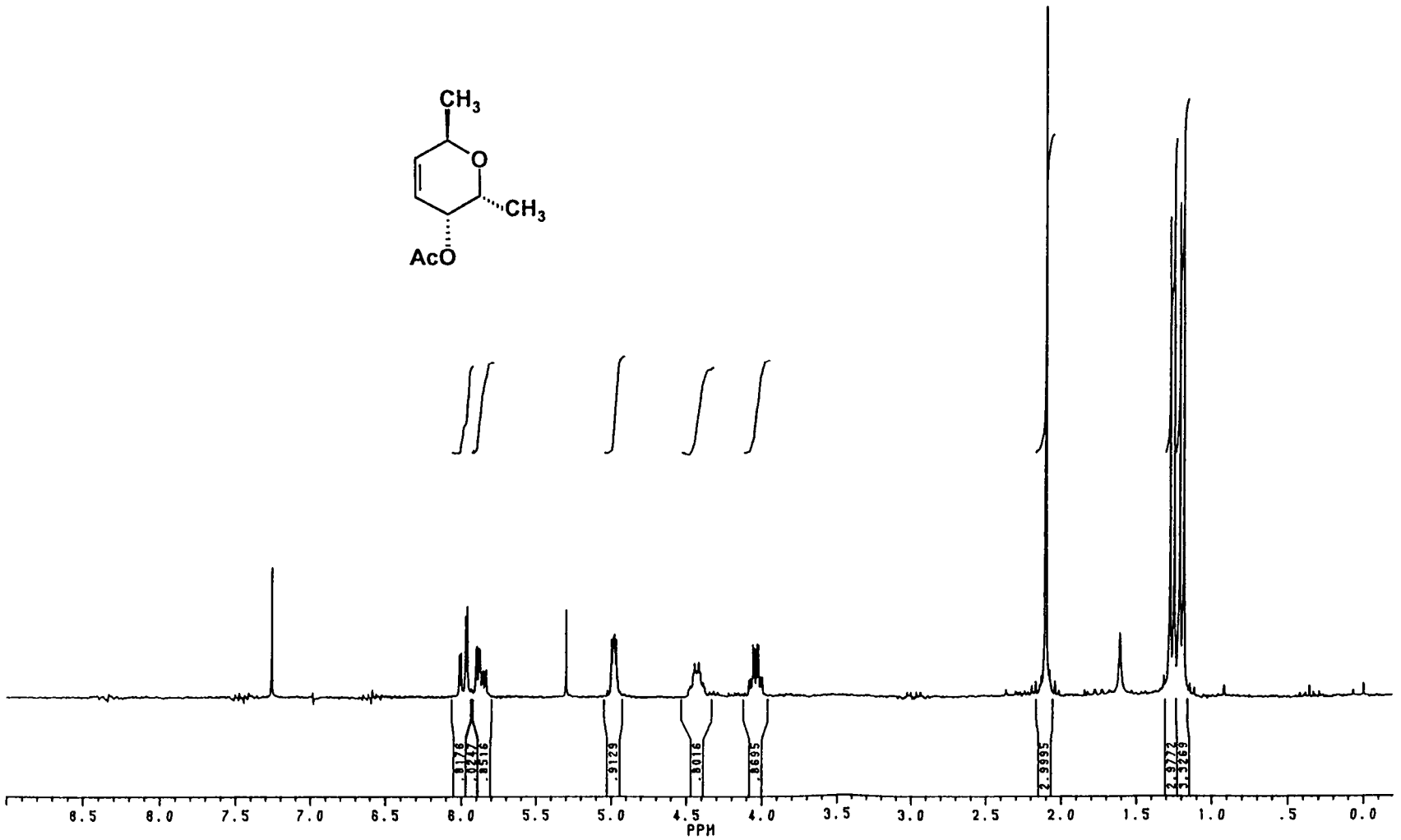
APPENDIX A. ^{1}H and ^{13}C NMR Spectra of Compounds Involved in the Synthesis of Hongconin and Analogs



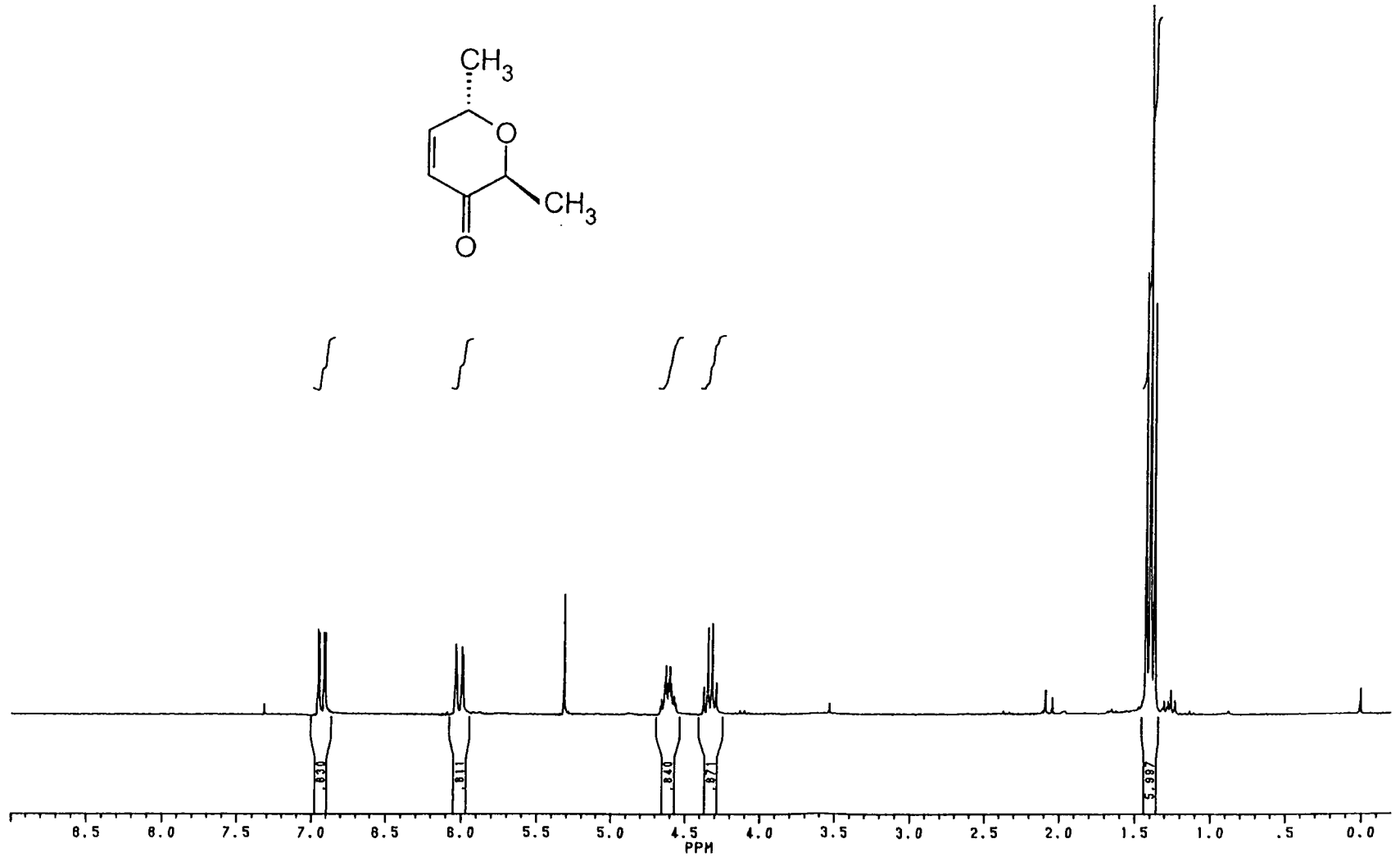
^{1}H NMR Spectrum (250 MHz, $CDCl_3$) of 5-*O*-Acetyl-2,6-anhydro-1,3,4,7-tetradeoxy-L-*arabino*-hept-3-enitol (**8a**).



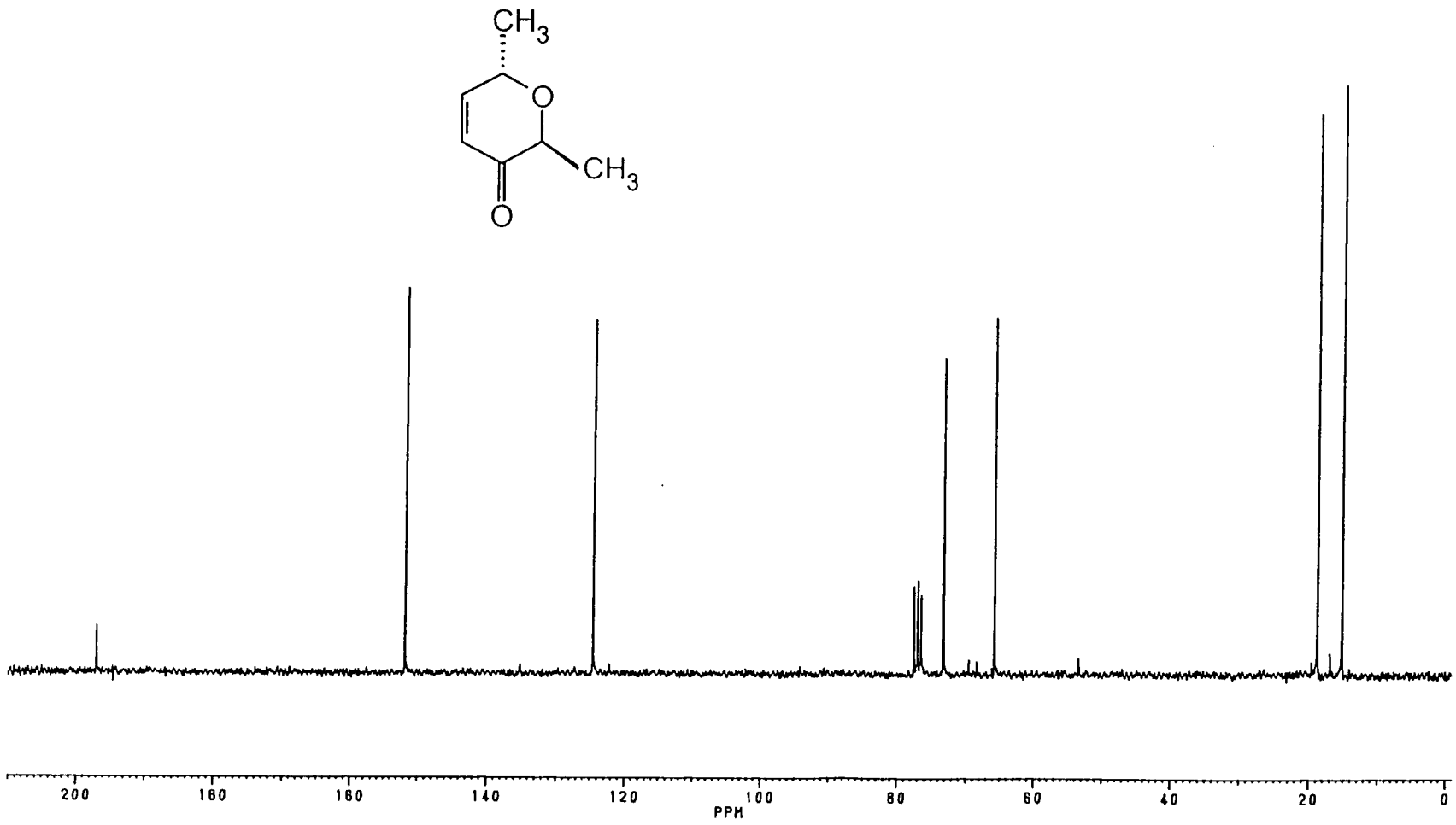
^{1}H NMR Spectrum of (250 MHz, $CDCl_3$) 3-*O*-Acetyl-2,6-anhydro-1,4,5,7-tetradeoxy-D-*ribo*-hept-4-enitol (**8b**).



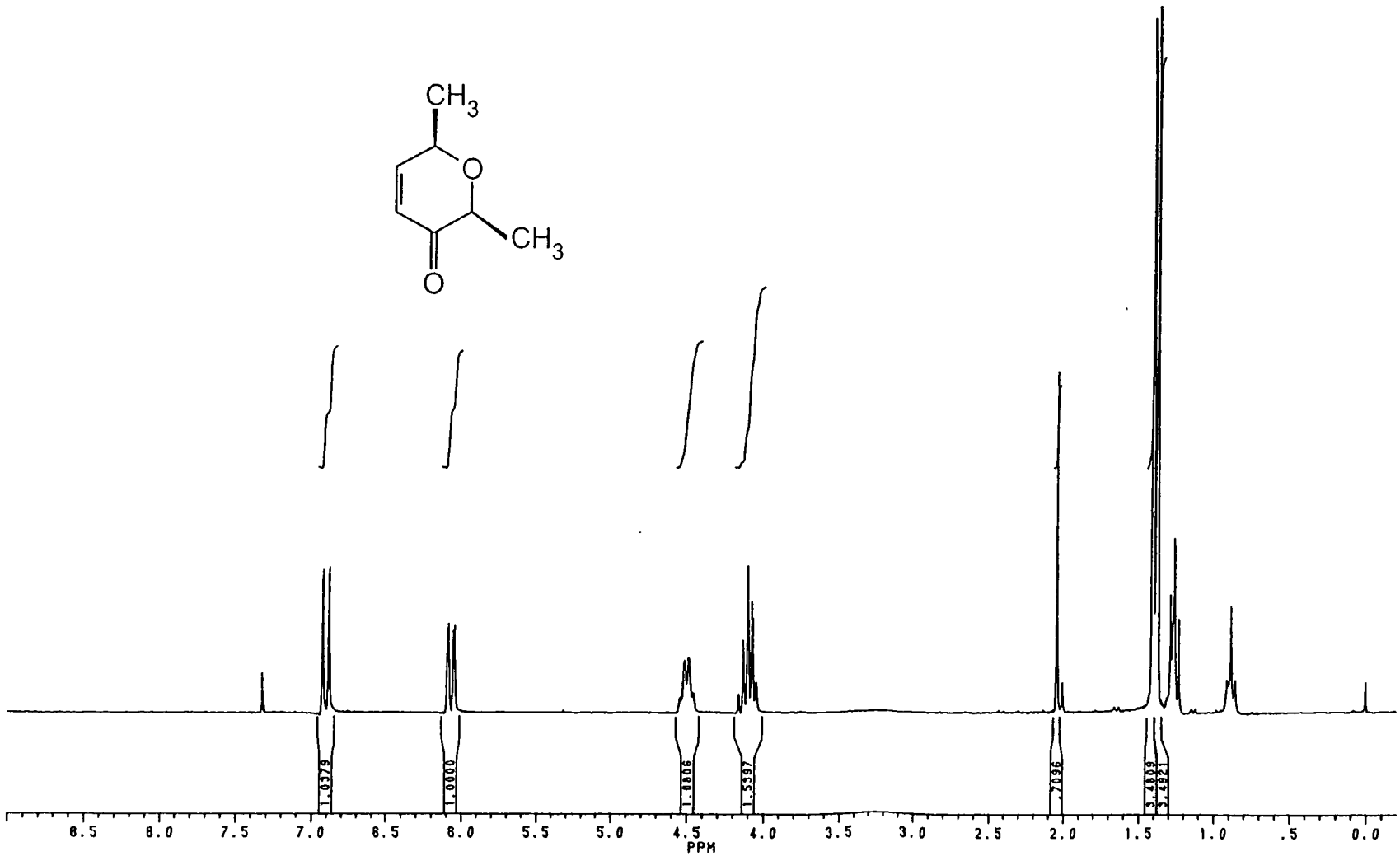
^{1}H NMR Spectrum (250 MHz, $CDCl_3$) of 3-*O*-Acetyl-2,6-anhydro-1,4,5,7-tetradeoxy-D-*arabino*-hept-4-enitol (**8c**).



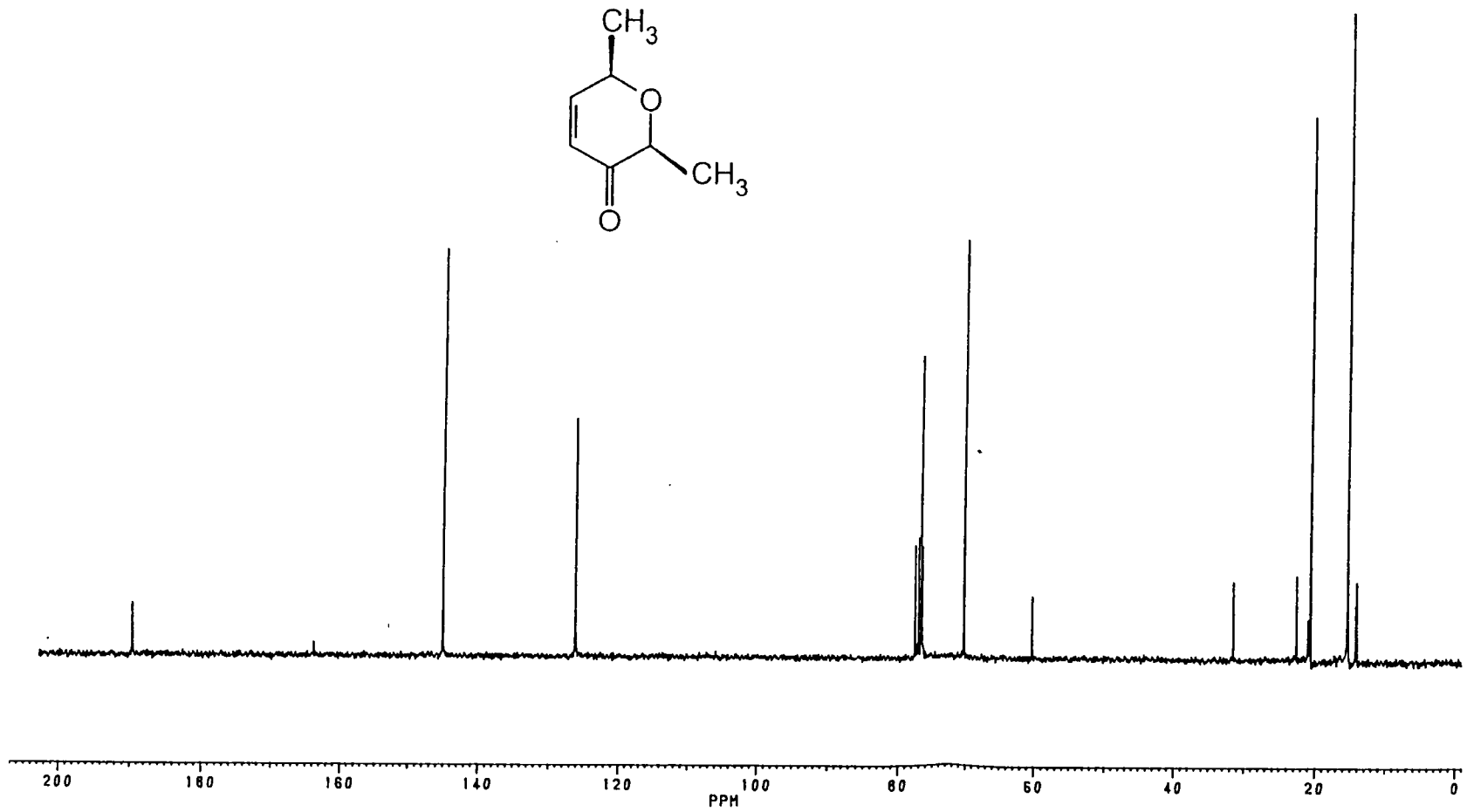
^{1}H NMR Spectrum (250 MHz, $CDCl_3$) of 2,6-anhydro-1,4,5,7-tetradeoxy-L-*threo*-hept-4-en-3-ulose (**9a**).



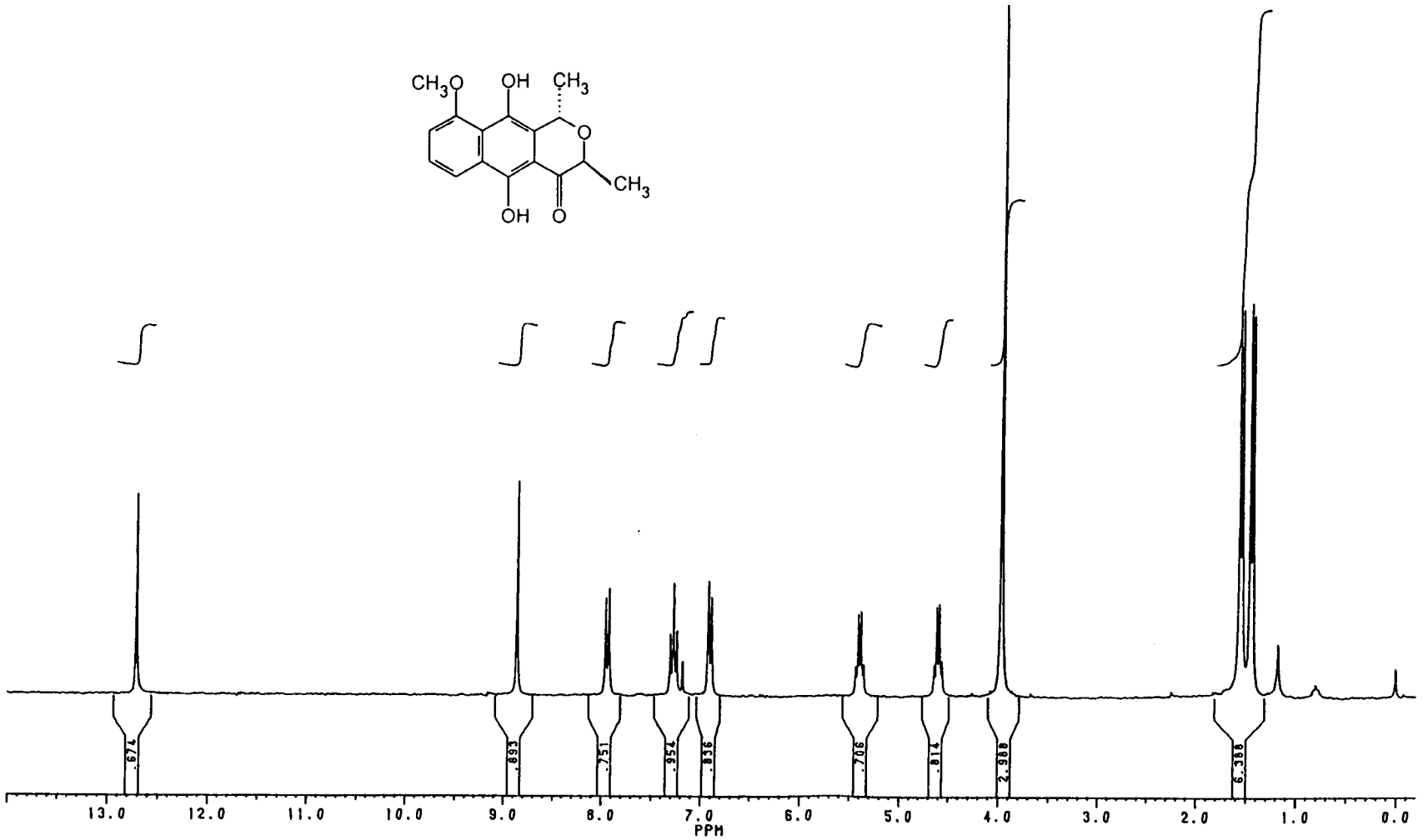
^{13}C NMR Spectrum (62.5 MHz, $CDCl_3$) of 2,6-anhydro-1,4,5,7-tetradeoxy-L-*threo*-hept-4-en-3-ulose (**9a**).



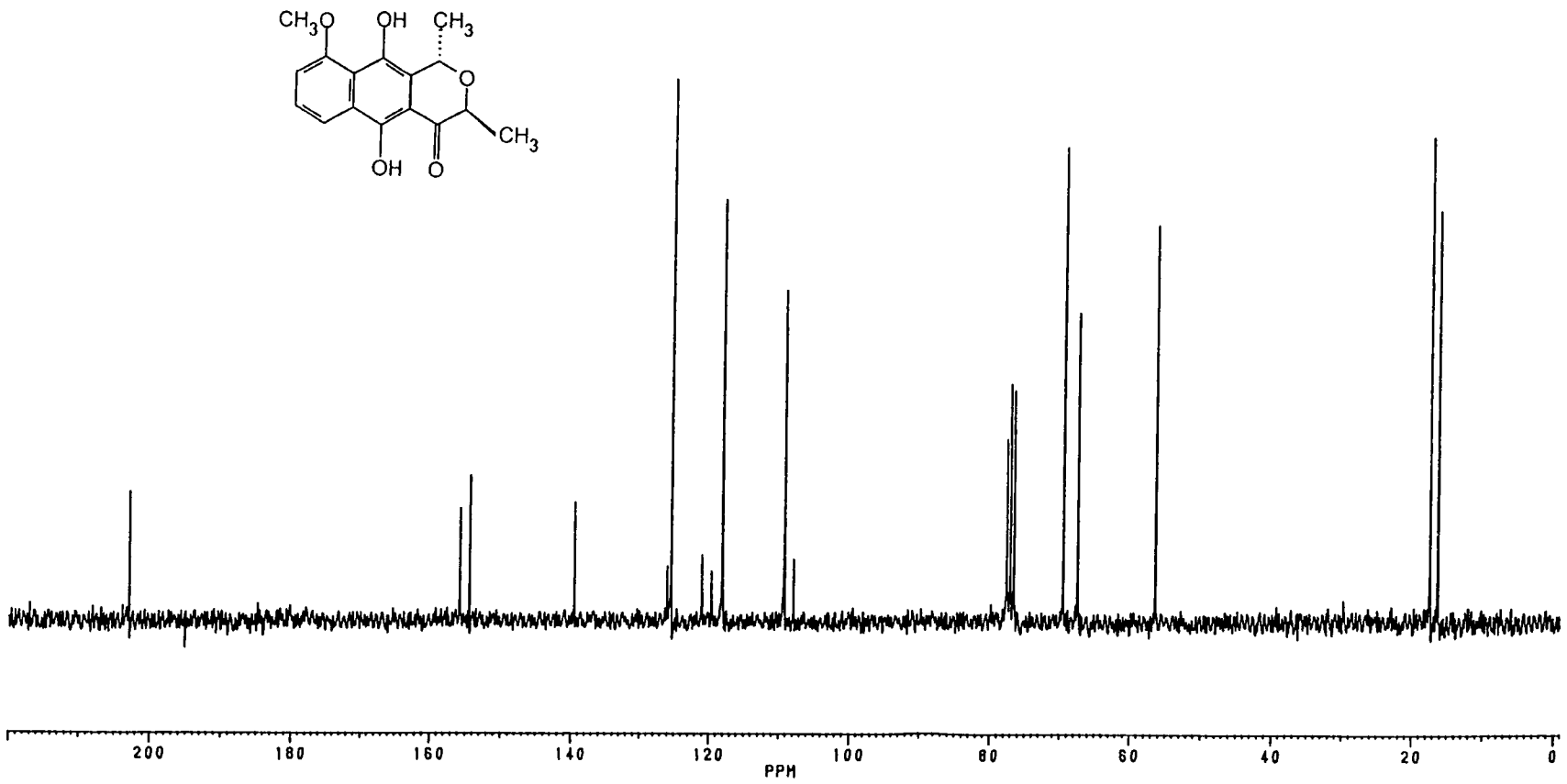
^{1}H NMR Spectrum (250 MHz, $CDCl_3$) of 2,6-anhydro-1,4,5,7-tetradeoxy-D-*erythro*-hept-4-en-3-ulose (**9b**).



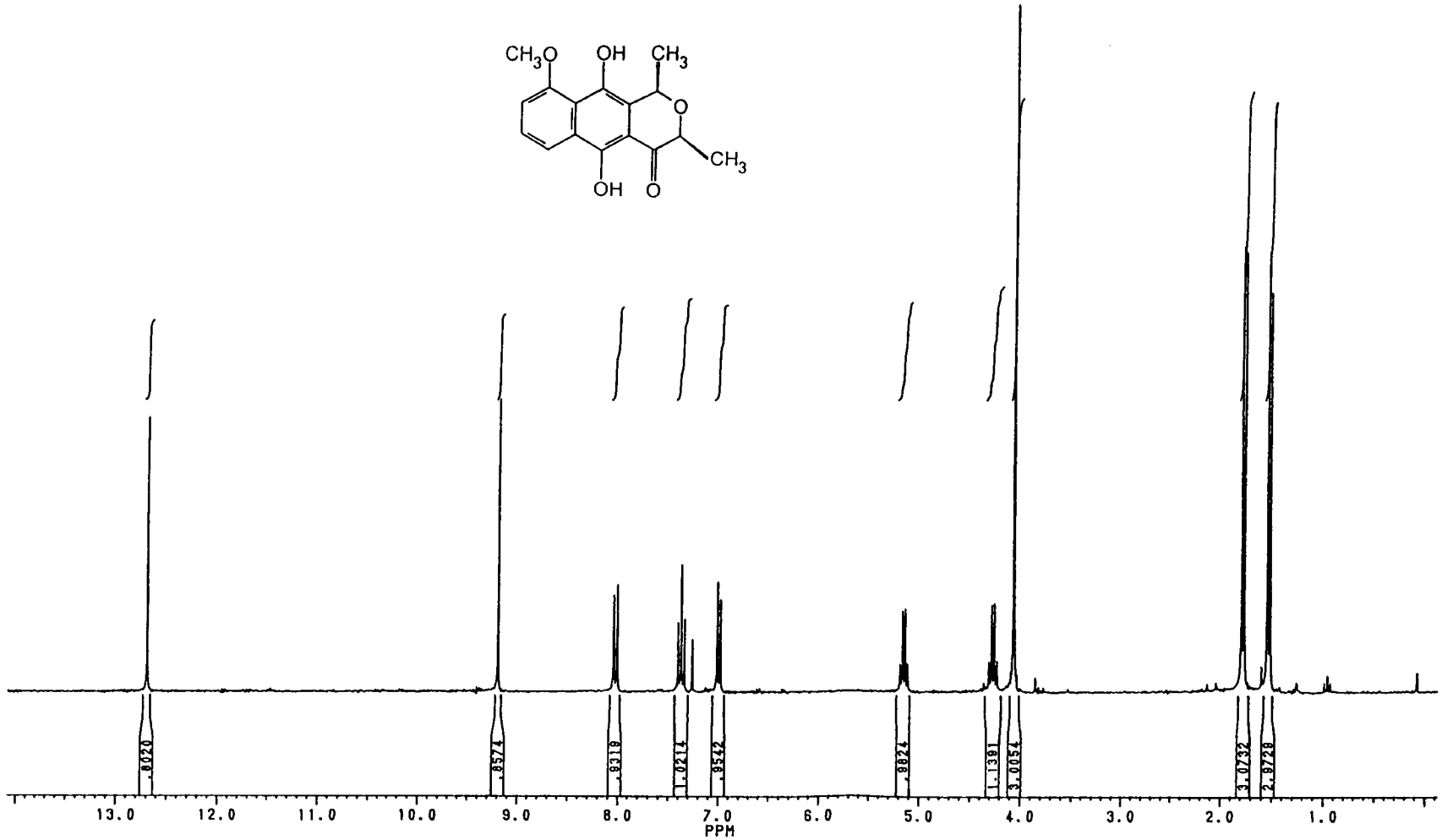
^{13}C NMR Spectrum (62.5 MHz, $CDCl_3$) of 2,6-anhydro-1,4,5,7-tetradeoxy-D-*erythro*-hept-4-en-3-ulose (**9b**).



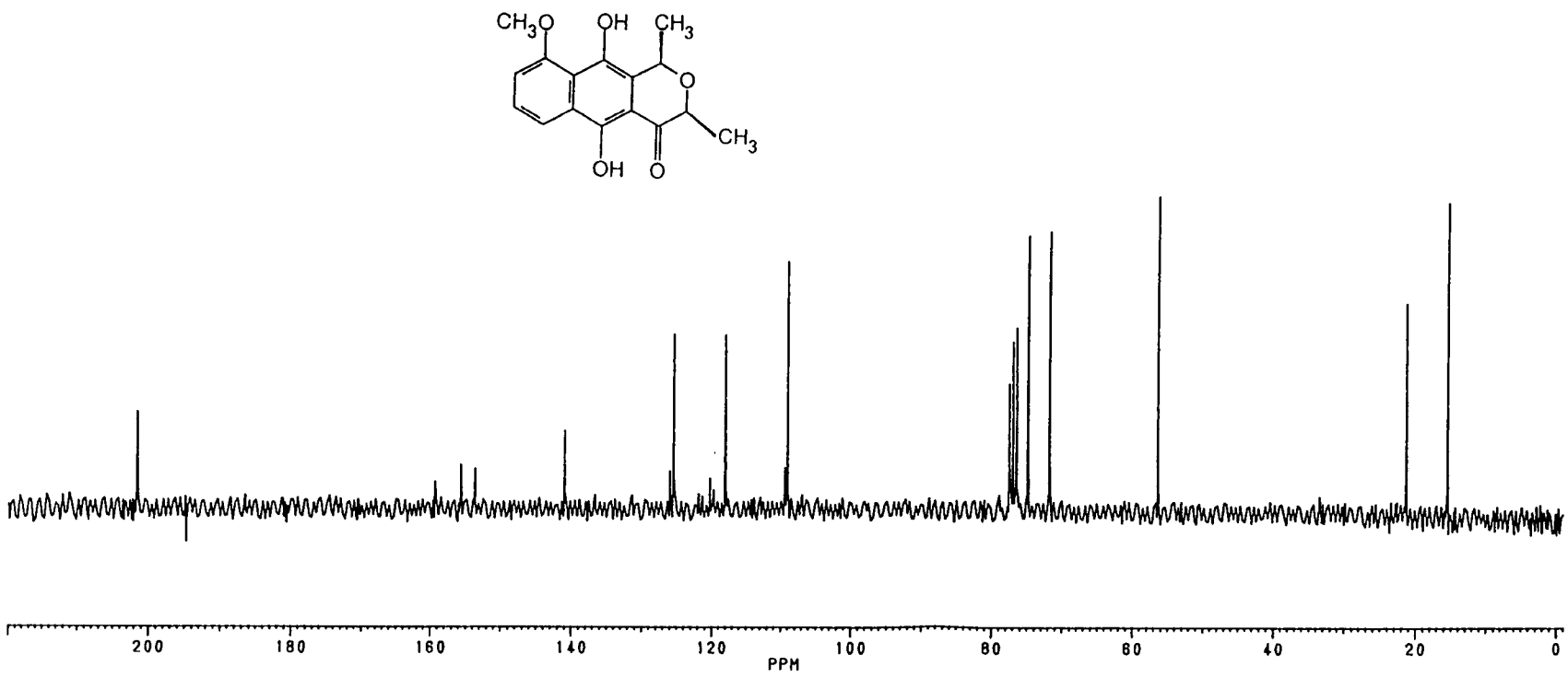
^{1}H NMR Spectrum (250 MHz, $CDCl_3$) of (1*S*,3*S*)-(+)-3,4-Dihydro-5,10-dihydroxy-9-methoxy-1,3-dimethyl-1*H*-naphtho[2,3-*c*]pyran-4-one (*ent*-Hongconin, **1a**).



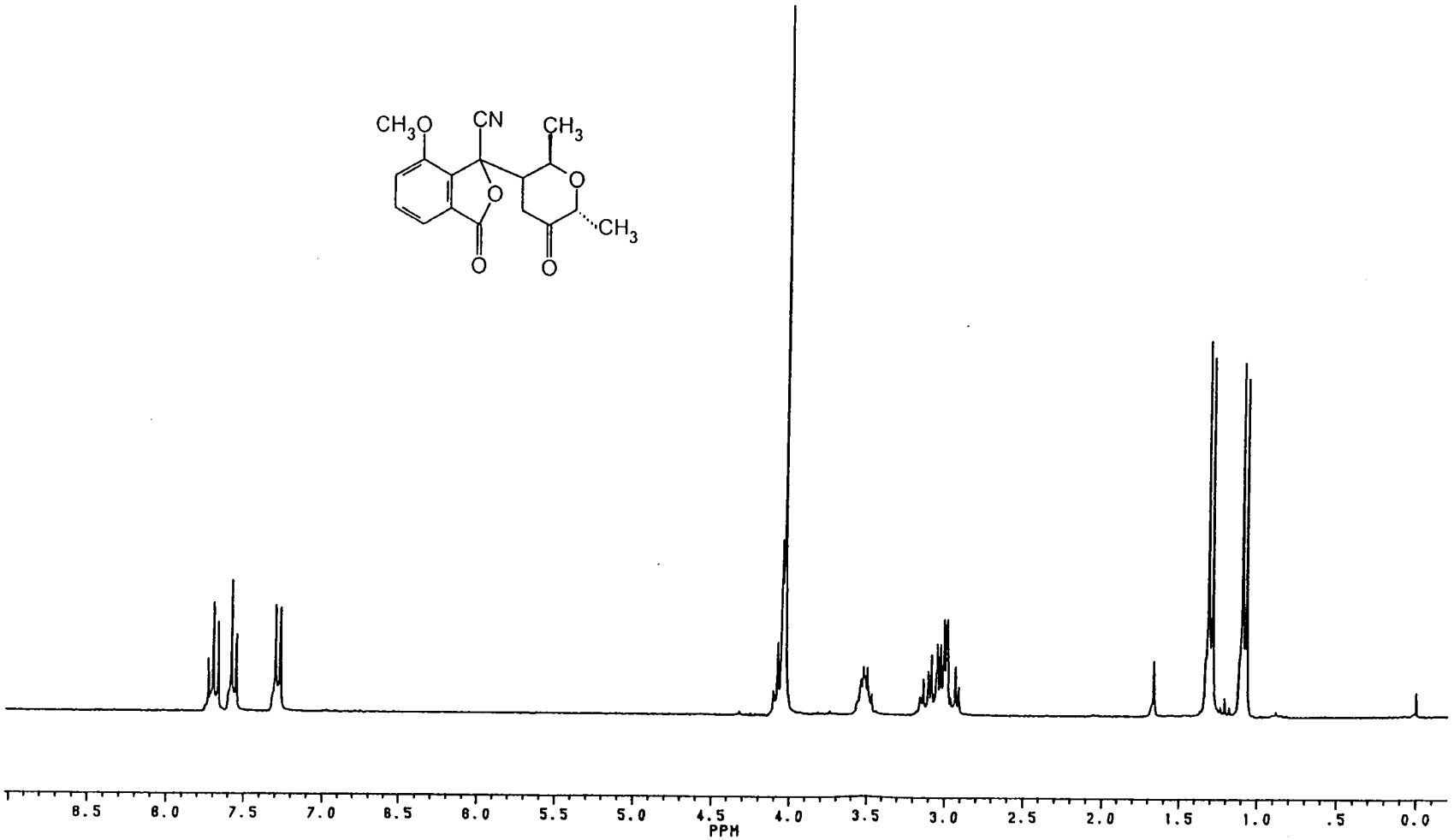
^{13}C NMR Spectrum (62.5 MHz, $CDCl_3$) of (1*S*,3*S*)-(+)-3,4-Dihydro-5,10-dihydroxy-9-methoxy-1,3-dimethyl-1*H*-naphtho[2,3-*c*]pyran-4-one (*ent*-Hongconin, **1a**).



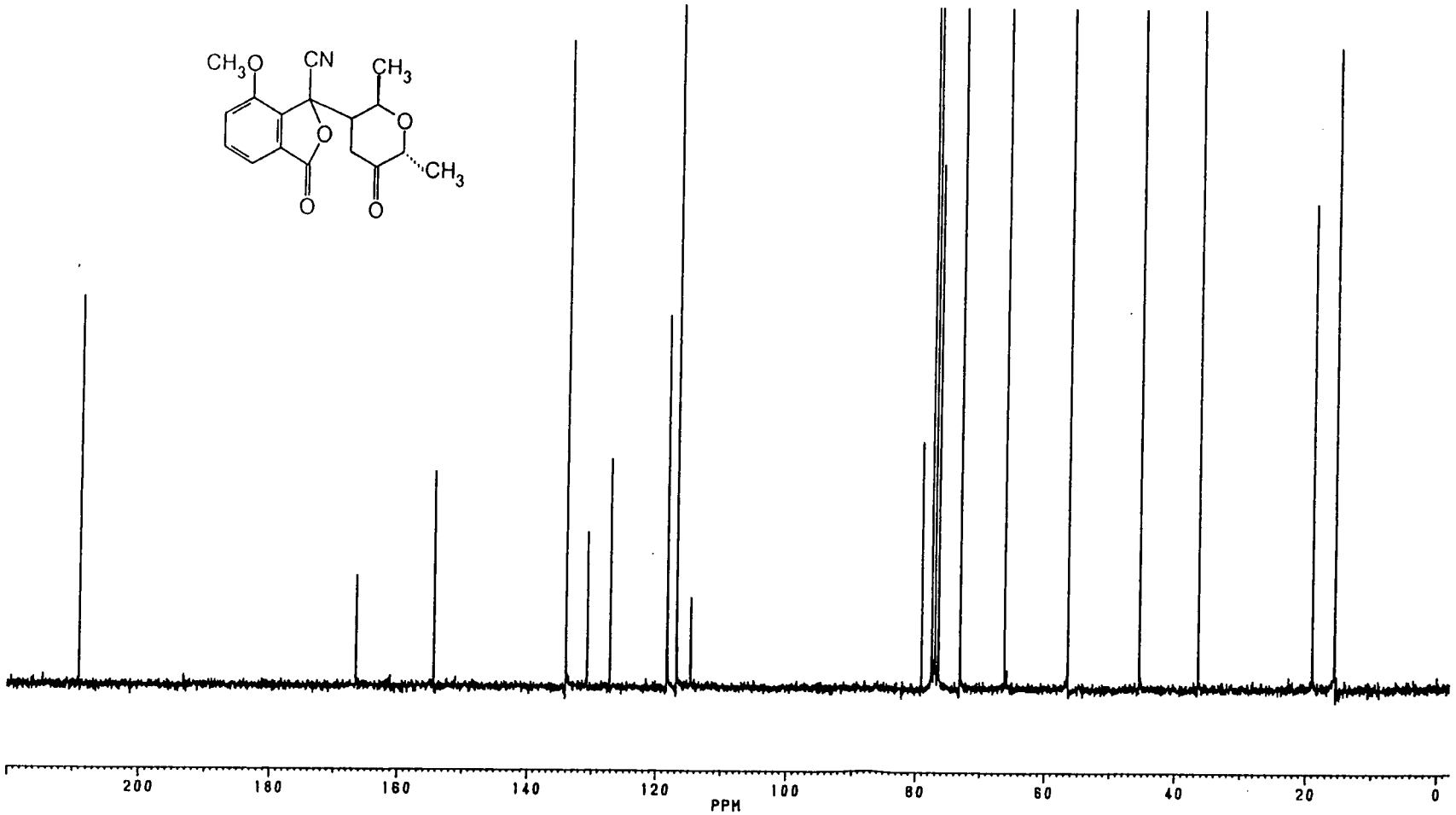
^{1}H NMR Spectrum (250 MHz, $CDCl_3$) of (1*R*,3*S*)-(+)-3,4-Dihydro-5,10-dihydroxy-9-methoxy-1,3-dimethyl-1*H*-naphtho[2,3-*c*]pyran-4-one (*iso*-Hongconin, **1b**).



^{13}C NMR Spectrum (62.5 MHz, $CDCl_3$) of (1*R*,3*S*)-(+)-3,4-Dihydro-5,10-dihydroxy-9-methoxy-1,3-dimethyl-1*H*-naphtho[2,3-*c*]pyran-4-one (*iso*-Hongconin, **1b**).

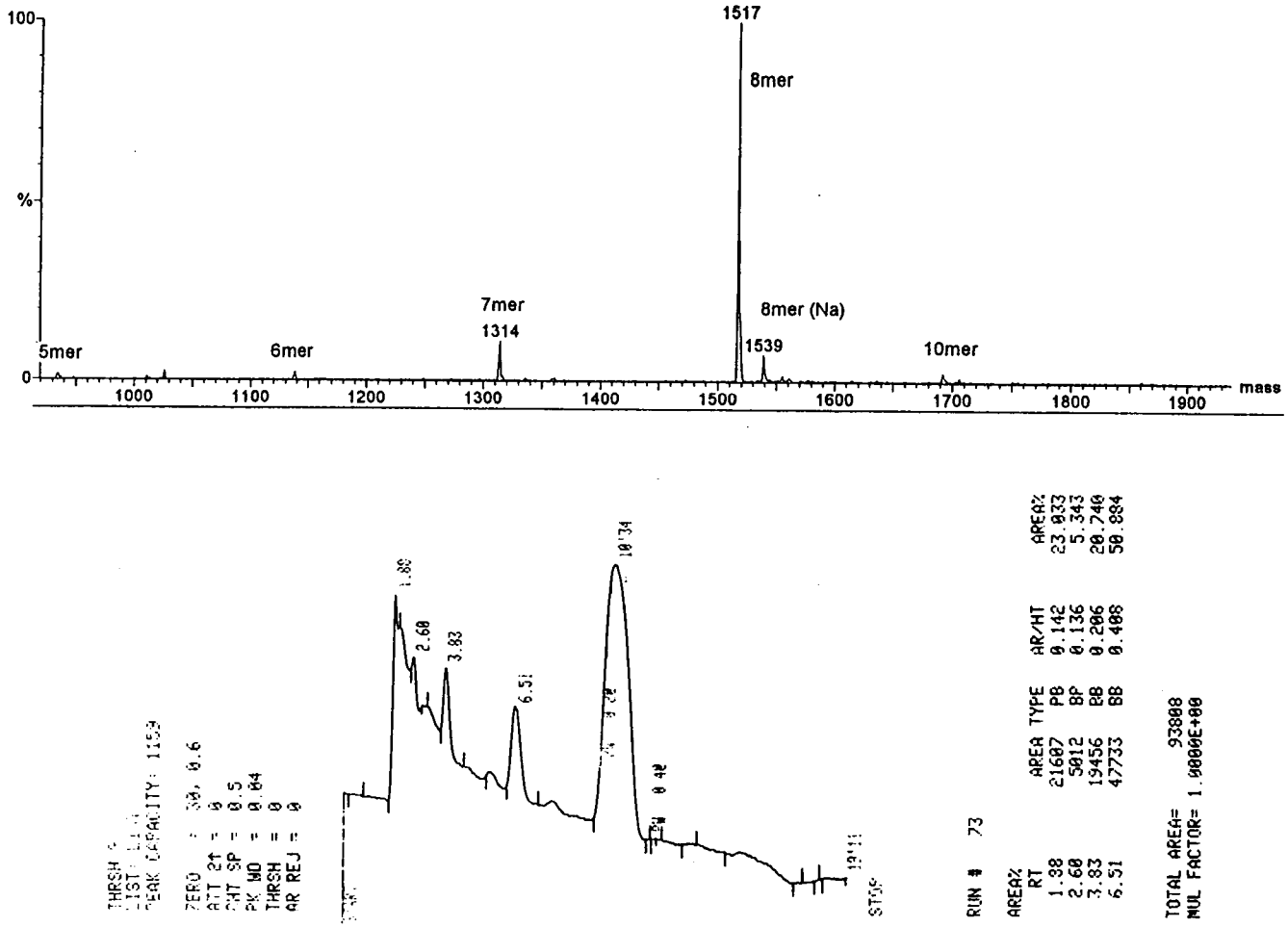


^{1}H NMR Spectrum (250 MHz, $CDCl_3$) of (1*R*,3*R*)-(−)-3,4-Dihydro-5,10-dihydroxy-9-methoxy-1,3-dimethyl-1*H*-naphtho[2,3-*c*]pyran-4-one (Hongconin, 1) and 1-(2,6-dimethyl-5-oxo-tetrahydropyran-3-yl)-7-methoxy-3-oxo-1,3-dihydroisobenzofuran-1-carbonitrile (**11**).

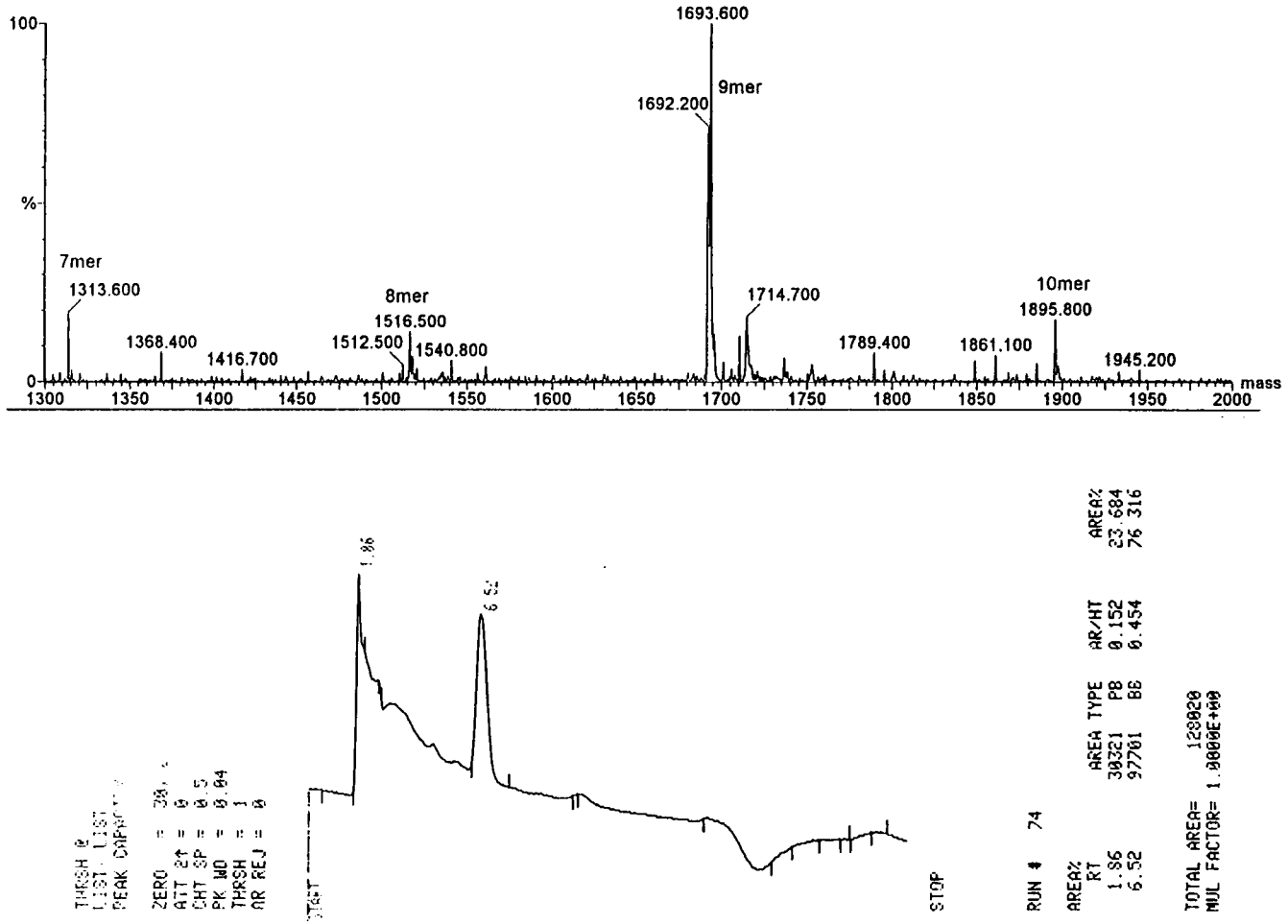


^{13}C NMR Spectrum (62.5 MHz, $CDCl_3$) of (1*R*,3*R*)-(−)-3,4-Dihydro-5,10-dihydroxy-9-methoxy-1,3-dimethyl-1*H*-naphtho[2,3-*c*]pyran-4-one (Hongconin, 1) and 1-(2,6-dimethyl-5-oxo-tetrahydropyran-3-yl)-7-methoxy-3-oxo-1,3-dihydroisobenzofuran-1-carbonitrile (**11**).

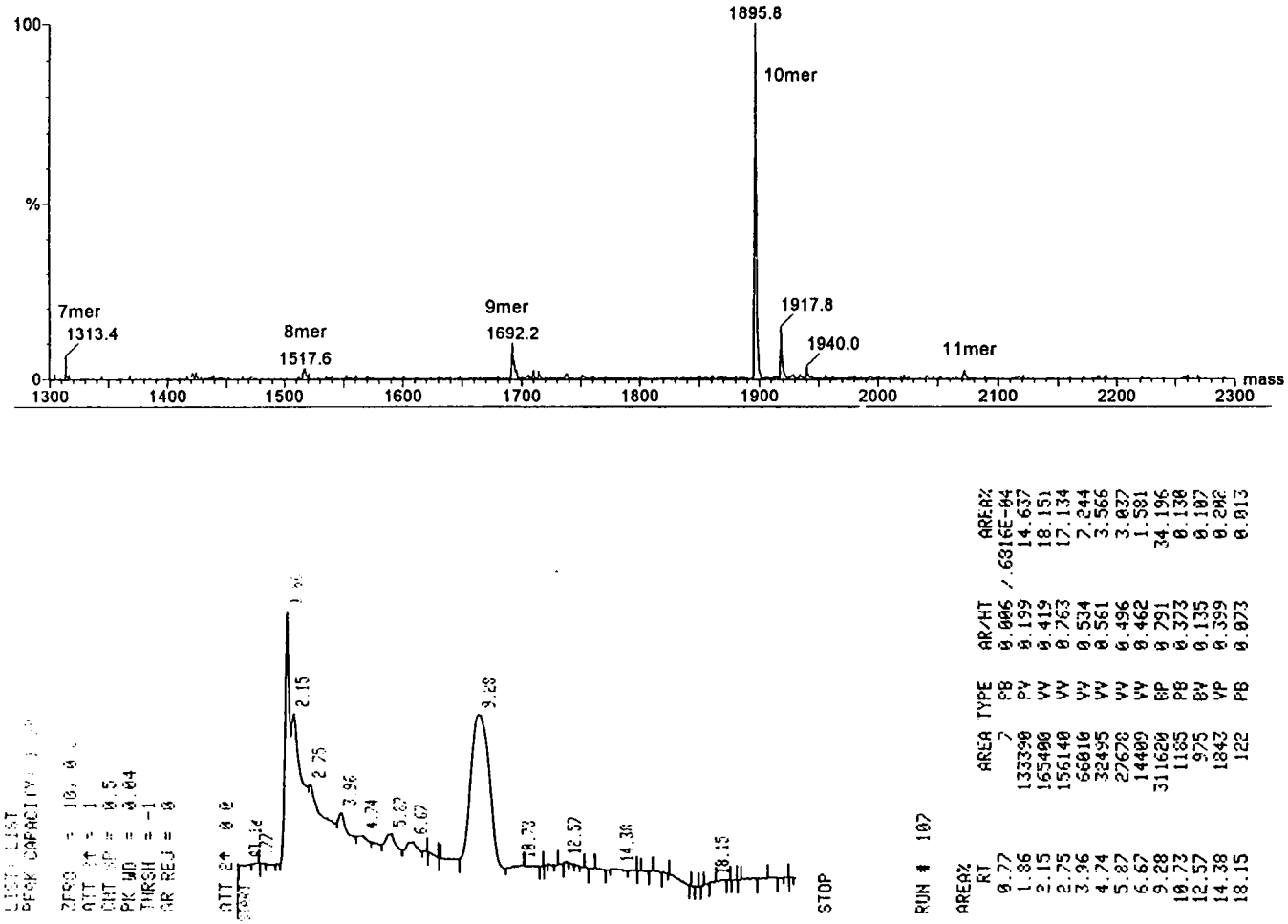
APPENDIX B. Negative-ion mode ESIMS Spectra and
Dionex HPAEC Chromatograms for selected
HA Lyase-Derived Oligosaccharides



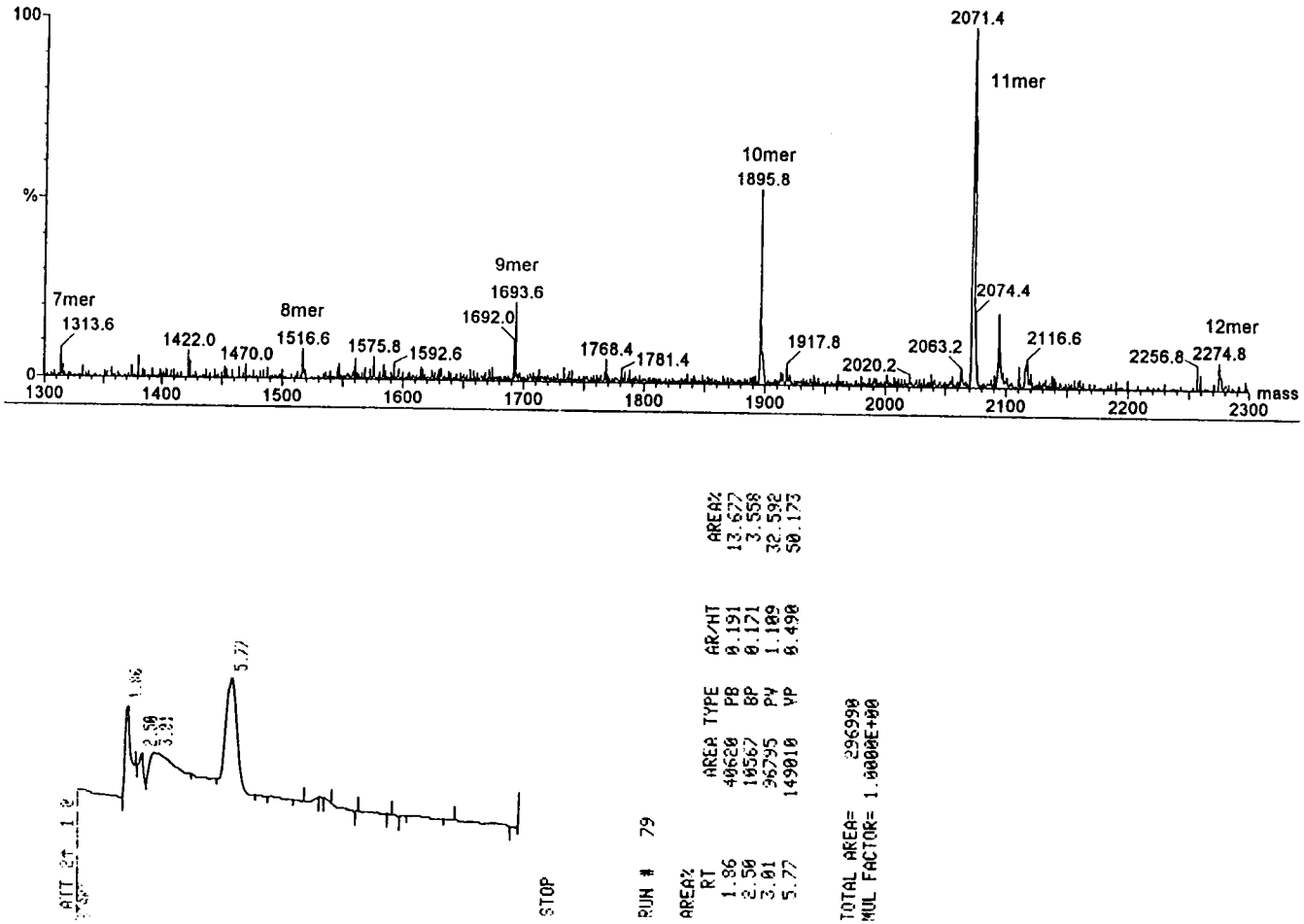
MAX ENT-generated MW distribution and Dionex HPAEC trace (280 mM acetate) for 8mer-containing fraction.



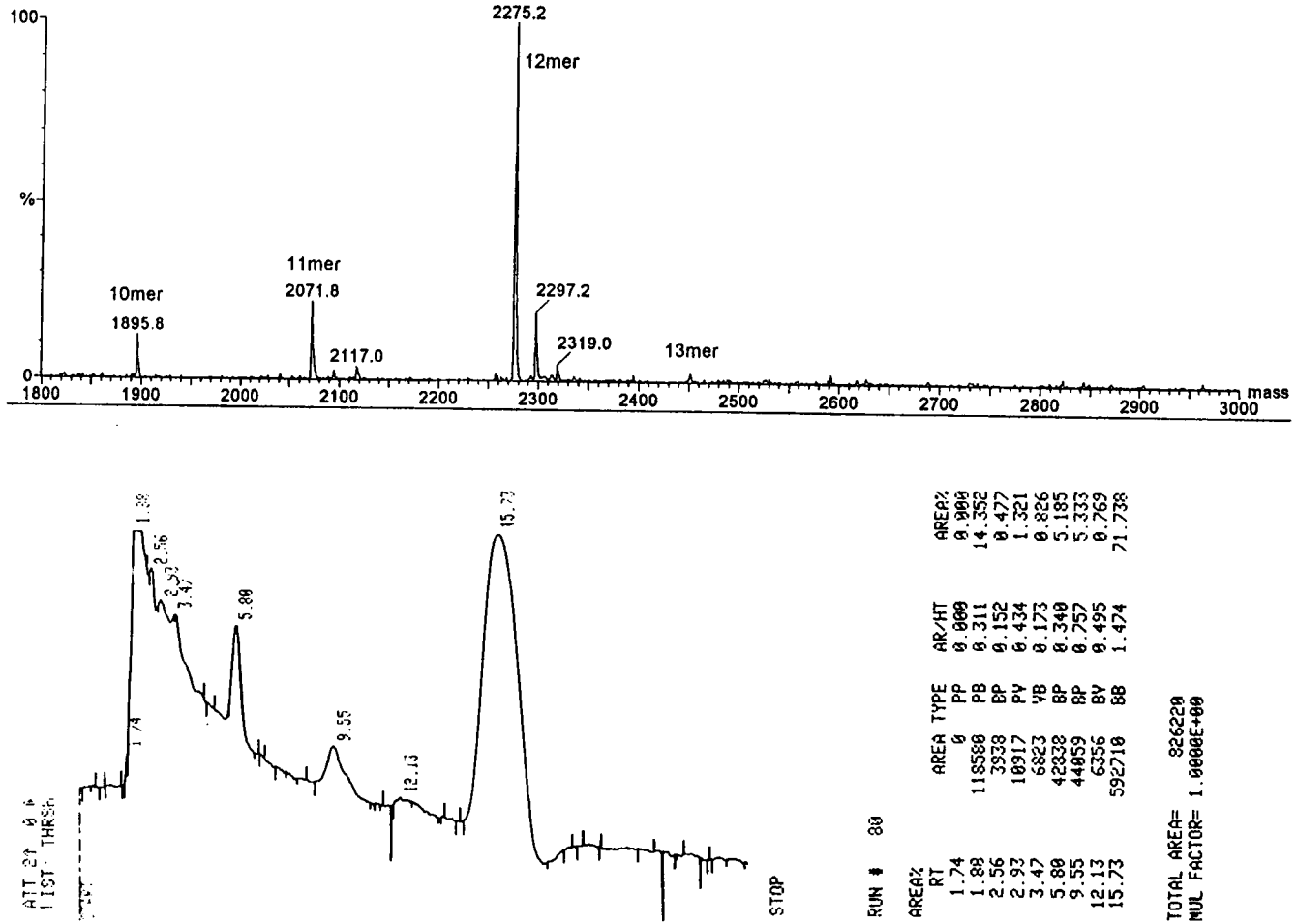
MAX ENT-generated MW distribution and Dionex HPAEC trace (280 mM acetate) for 9mer-containing fraction.



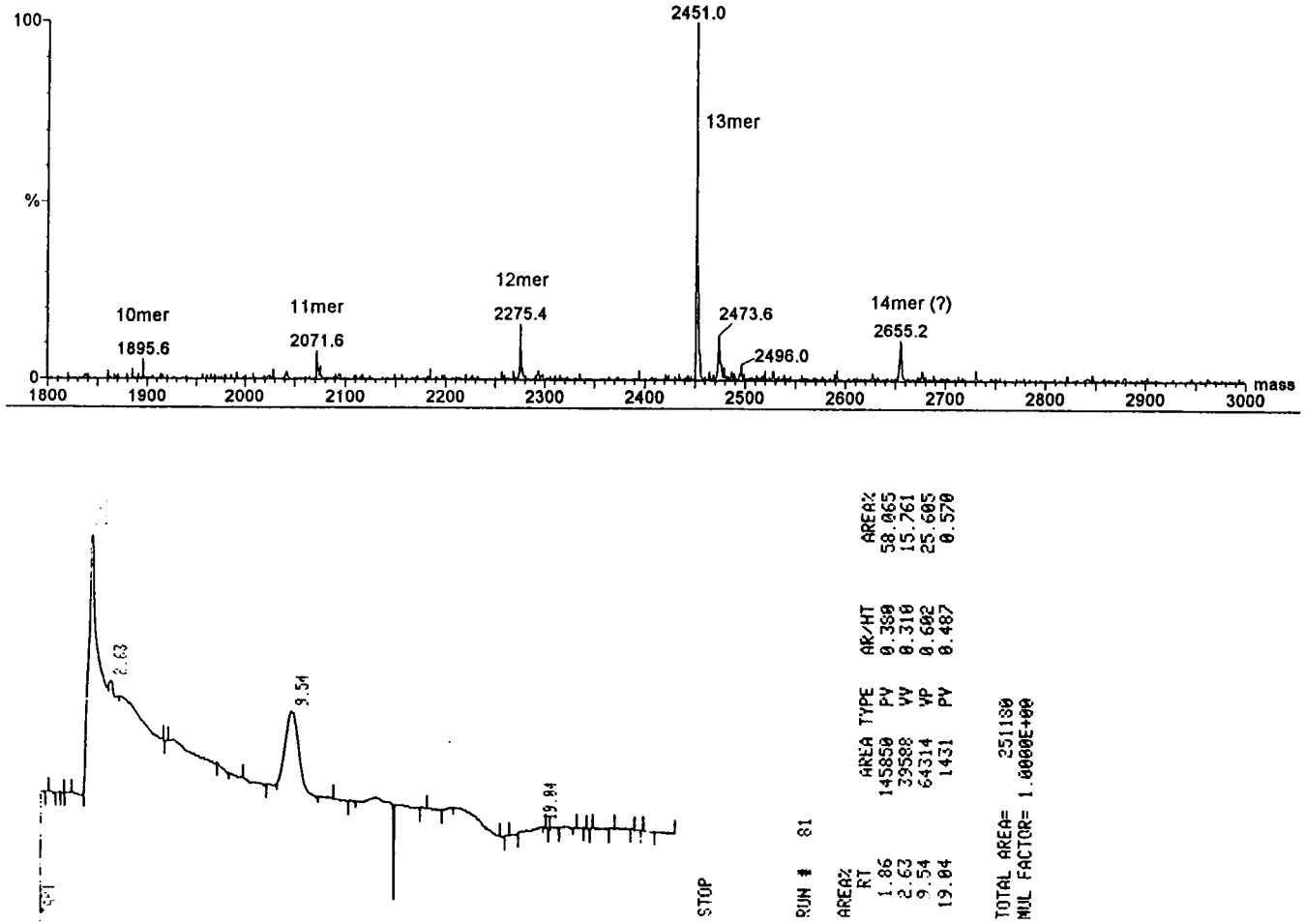
MAX ENT-generated MW distribution and Dionex HPAEC trace (350 mM acetate) for 10mer-containing fraction.



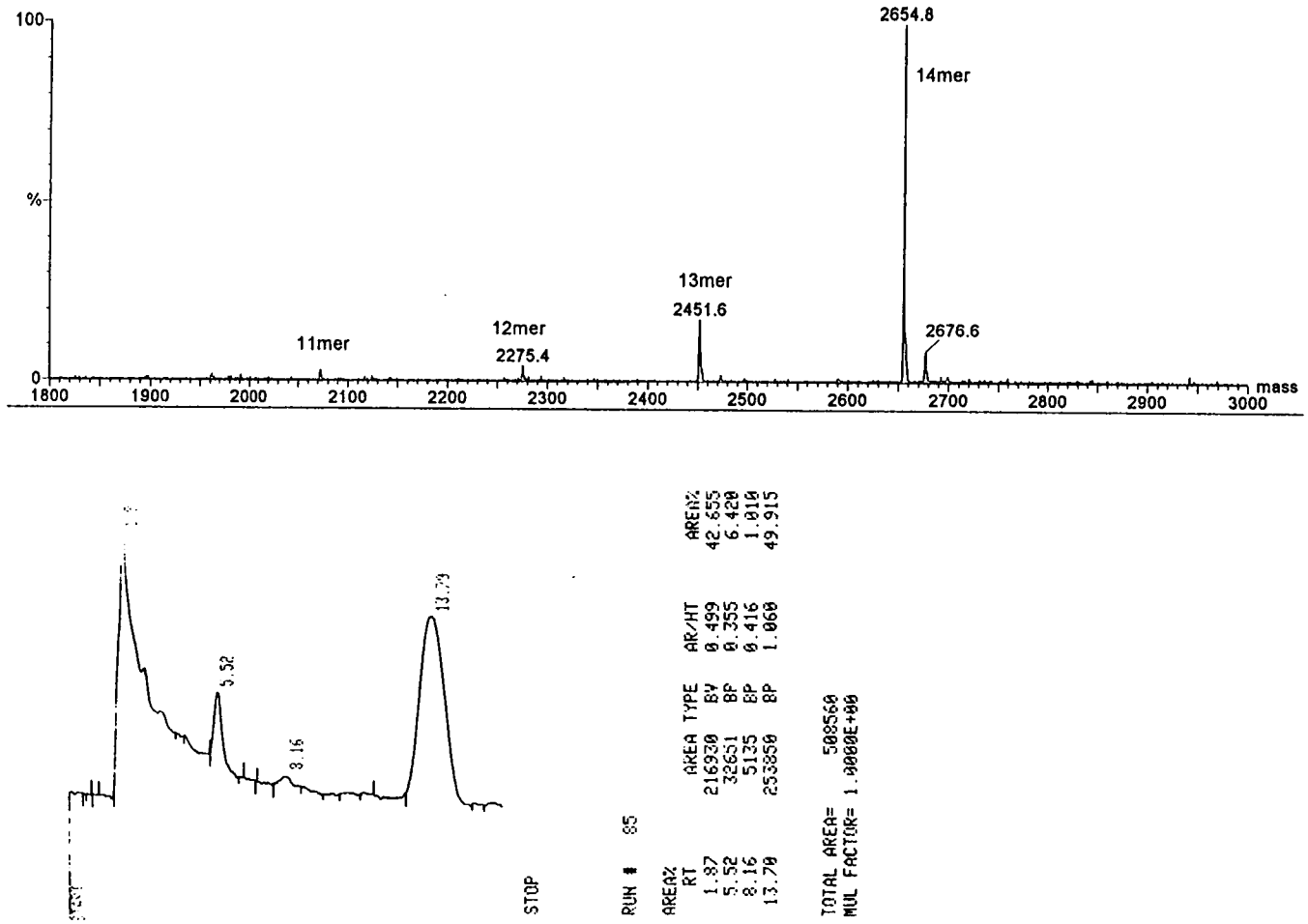
MAX ENT-generated MW distribution and Dionex HPAEC trace (350 mM acetate) for 11mer-containing fraction.



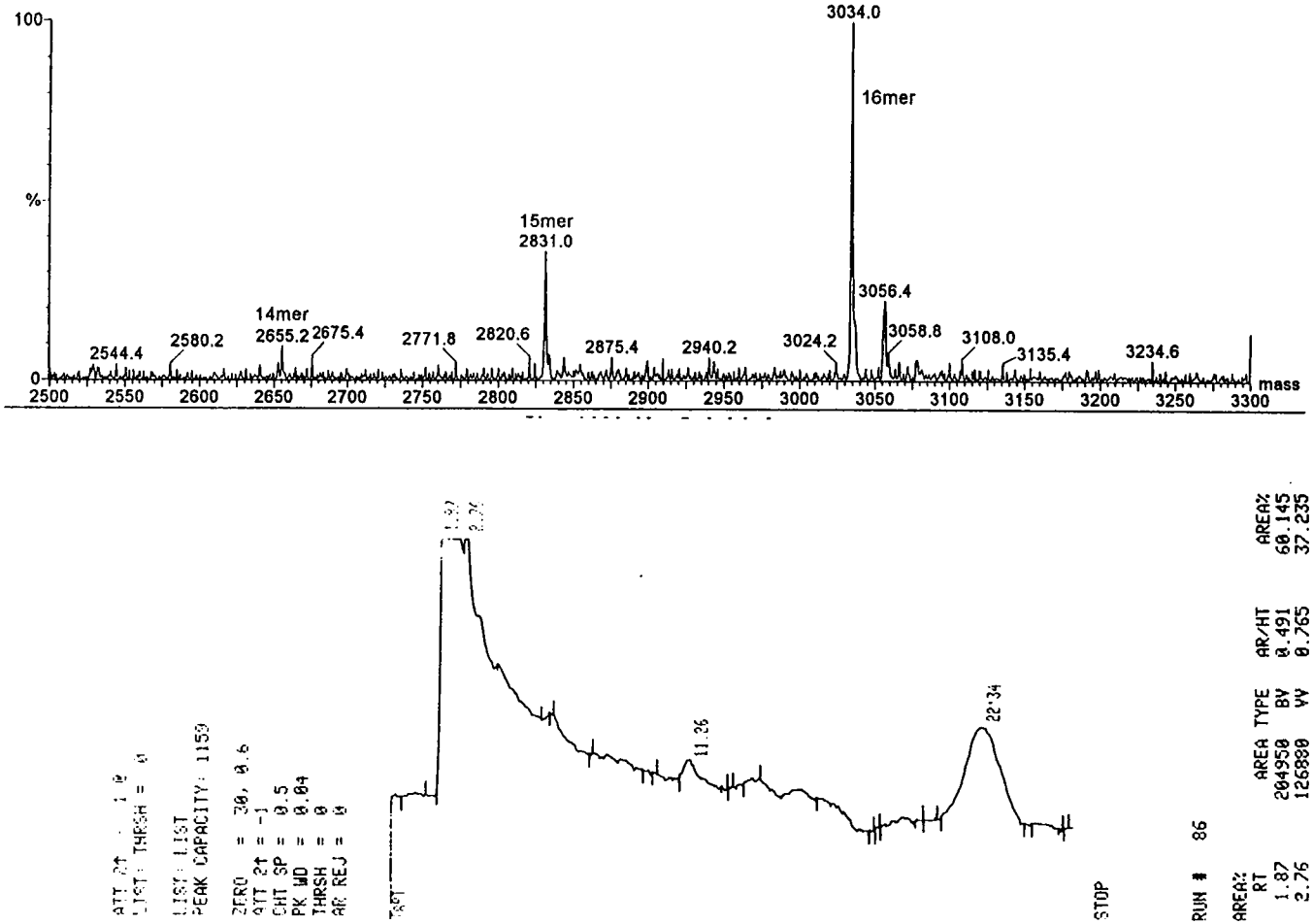
MAX ENT-generated MW distribution and Dionex HPAEC trace (350 mM acetate) for 12mer-containing fraction.



MAX ENT-generated MW distribution and Dionex HPAEC trace (350 mM acetate) for 13mer-containing fraction.



MAX ENT-generated MW distribution and Dionex HPAEC trace (400 mM acetate) for 14mer-containing fraction.



MAX ENT-generated MW distribution and Dionex HPAEC trace (400 mM acetate) for 16mer-containing fraction.

APPENDIX C. Negative-ion Mode ESIMS Data for BTH-Derived Oligosaccharides dp 4-28

Observed vs. Predicted ESIMS *m/z* Values for
Bovine Testes Hyaluronidase Oligomers, dp 4-28[a]

Oligomer ($No.CO_2^-$ groups)	Observed signals at CV = 25 V *m/z*	rel. int.	at CV = 55-65 V *m/z*	rel. int.	Assignment [species]	Pred. *m/z*
4-mer (2)	[000.0]*[b]				[M = 776.7]	
	—[c]	—	N.C.[d]		$[M - H^+]^{1-}$	775.7
	387.3	100			$[M - 2H^+]^{2-}$	387.3
5-mer (3)	[000.0]*				[M = 952.8]	
	—	—	N.C.		$[M - H^+]^{1-}$	951.8
	475.2	100			$[M - 2H^+]^{2-}$	475.4
	486.2	17			$[M - 3H^+ + Na^+]^{2-}$	486.4
	316.6	61			$[M - 3H^+]^{3-}$	316.6
6-mer (3)	[1155.3]*				[M = 1156.0]	
	—[d]	—	1155.2	16	$[M - H^+]^{1-}$	1155.0
	576.9	100	576.9	51	$[M - 2H^+]^{2-}$	577.0
	587.8	57	587.9	100	$[M - 3H^+ + Na^+]^{2-}$	588.0
	384.4	11	—	—	$[M - 3H^+]^{3-}$	384.3

[a] This table combines the data of 2 acquired spectra per sample. Each sample provided data for the predominant even-numbered oligomer present, and for the next-lower odd-numbered oligomer. Observed signals derive from acquisitions at CV = 25 V (*m/z* values and relative intensities shown in columns 3 and 4, respectively) or at CV = 55-65 V (columns 5 and 6). Relative intensities are assigned separately to each individual oligomer, with the predominant peak for that oligomer set as 100 %.

[b] Values marked with an asterisk correspond to the neutral MW extrapolated from the raw data (CV = 25 V series) by the MAX ENT program, and correspond in all cases to within ± 0.06 % of the calculated MW. Distributions extrapolated from the CV = 55-65 V series were found to contain greater error, and are not included.

[c] Indicates signal not observed.

[d] Experiment not conducted.

BTH Oligosaccharide ESIMS data, continued

Oligomer ($No.CO_2^-$ groups)	Observed signals at CV = 25 V *m/z*	rel. int.	at CV = 55-65 V *m/z*	rel. int.	Assignment [species]	Pred. *m/z*
7-mer	[1332.1]*				[M = 1332.1]	
(4)	—	—	—	—	$[M - H^+]^{1-}$	1331.1
	—	—	664.9	100	$[M - 2H^+]^{2-}$	665.0
	—	—	676.0	76	$[M - 3H^+ + Na^+]^{2-}$	676.0
	—	—	686.9	50	$[M - 4H^+ + 2Na^+]^{2-}$	687.0
	443.0	100	443.0	36	$[M - 3H^+]^{3-}$	443.0
	450.3	3	450.3	13	$[M - 4H^+ + Na^+]^{3-}$	450.4
	332.0	17	332.1	4	$[M - 4H^+]^{4-}$	332.0
8-mer (4)	[1534.6]*				[M = 1535.3]	
	—	—	—	—	$[M - H^+]^{1-}$	1534.3
	766.5	11	766.5	87	$[M - 2H^+]^{2-}$	766.6
	777.5	9	777.4	100	$[M - 3H^+ + Na^+]^{2-}$	777.6
	788.5	5	788.5	65	$[M - 4H^+ + 2Na^+]^{2-}$	788.6
	510.7	100	—	—	$[M - 3H^+]^{3-}$	510.8
	518.0	29	—	—	$[M - 4H^+ + Na^+]^{3-}$	518.1
	382.8	56	—	—	$[M - 4H^+]^{4-}$	382.8
9-mer	[1711.0]*				[M = 1711.4]	
(5)	—	—	—	—	$[M - H^+]^{1-}$	1710.4
	—	—	854.7	5	$[M - 2H^+]^{2-}$	854.7
	569.5	5	569.5	100	$[M - 3H^+]^{3-}$	569.5
	577.0	6	576.9	64	$[M - 4H^+ + Na^+]^{3-}$	576.8
	—	—	584.1	12	$[M - 5H^+ + 2Na^+]^{3-}$	584.1
	427.0	100	—	—	$[M - 4H^+]^{4-}$	426.9
	341.3	10	—	—	$[M - 5H^+]^{5-}$	341.3

BTH Oligosaccharide ESIMS data, continued

Oligomer (No.CO_2^- groups)	Observed signals at CV = 25 V *m/z*	rel. int.	at CV = 55-65 V *m/z*	rel. int.	Assignment [species]	Pred. *m/z*
10-mer	[1914.8]*				[M = 1914.6]	
(5)	—	—	—	—	$[M - H^+]^{1-}$	1913.6
	—	—	956.2	66	$[M - 2H^+]^{2-}$	956.3
	—	—	967.2	63	$[M - 3H^+ + Na^+]^{2-}$	967.3
	—	—	978.3	43	$[M - 4H^+ + 2Na^+]^{2-}$	978.3
	956.3	4	989.2	28	$[M - 5H^+ + 3Na^+]^{2-}$	989.3
	637.3	28	637.2	100	$[M - 3H^+]^{3-}$	637.2
	644.6	11	644.5	40	$[M - 4H^+ + Na^+]^{3-}$	644.5
	651.9	3	651.8	10	$[M - 5H^+ + 2Na^+]^{3-}$	651.9
	477.8	100	—	—	$[M - 4H^+]^{4-}$	477.7
	483.3	11	—	—	$[M - 5H^+ + Na^+]^{4-}$	483.1
	382.1	47	—	—	$[M - 5H^+]^{5-}$	381.9
11-mer	[2091.2]*				[M = 2090.8]	
(6)	—	—	—	—	$[M - H^+]^{1-}$	2089.7
	—	—	—	—	$[M - 2H^+]^{2-}$	1044.4
	—	—	695.9	100	$[M - 3H^+]^{3-}$	695.9
	—	—	703.2	64	$[M - 4H^+ + Na^+]^{3-}$	703.2
	—	—	710.6	28	$[M - 5H^+ + 2Na^+]^{3-}$	710.6
	—	—	717.8	12	$[M - 6H^+ + 3Na^+]^{3-}$	717.9
	521.8	33	521.8	43	$[M - 4H^+]^{4-}$	521.7
	527.0	4	527.2	17	$[M - 5H^+ + Na^+]^{4-}$	527.2
	417.3	100	—	—	$[M - 5H^+]^{5-}$	417.3
	347.5	4	—	—	$[M - 6H^+]^{6-}$	347.5

BTH Oligosaccharide ESIMS data, continued

Oligomer ($No.CO_2^-$ groups)	Observed signals at CV = 25 V *m/z*	rel. int.	at CV = 55-65 V *m/z*	rel. int.	Assignment [species]	Pred. *m/z*
12-mer	[2293.7]*				[M = 2293.9]	
(6)	—	—	—	—	$[M - H^+]^{1-}$	2292.9
	—	—	1145.9	38	$[M - 2H^+]^{2-}$	1146.0
	—	—	1156.9	43	$[M - 3H^+ + Na^+]^{2-}$	1157.0
	—	—	1167.9	24	$[M - 4H^+ + 2Na^+]^{2-}$	1168.0
	—	—	1178.8	17	$[M - 5H^+ + 3Na^+]^{2-}$	1179.0
	—	—	1189.8	15	$[M - 6H^+ + 4Na^+]^{2-}$	1189.0
	763.7	12	763.7	100	$[M - 3H^+]^{3-}$	763.6
	771.0	8	771.0	81	$[M - 4H^+ + Na^+]^{3-}$	771.0
	778.3	4	778.1	42	$[M - 5H^+ + 2Na^+]^{3-}$	778.3
	—	—	785.6	18	$[M - 6H^+ + 3Na^+]^{3-}$	785.6
	572.6	49	—	—	$[M - 4H^+]^{4-}$	572.5
	578.1	15	—	—	$[M - 5H^+ + Na^+]^{4-}$	578.0
	583.6	2	—	—	$[M - 6H^+ + 2Na^+]^{4-}$	583.5
	457.9	100	—	—	$[M - 5H^+]^{5-}$	457.8
	381.5	18	—	—	$[M - 6H^+]^{6-}$	381.3
13-mer	[2469.9]*				[M = 2469.4]	
(7)	—	—	—	—	$[M - H^+]^{1-}$	2468.4
	—	—	—	—	$[M - 2H^+]^{2-}$	1233.7
	—	—	822.3	23	$[M - 3H^+]^{3-}$	822.1
	—	—	829.7	21	$[M - 4H^+ + Na^+]^{3-}$	829.5
	—	—	837.0	17	$[M - 5H^+ + 2Na^+]^{3-}$	836.8
	—	—	844.3	9	$[M - 6H^+ + 3Na^+]^{3-}$	844.1
	616.6	4	616.5	100	$[M - 4H^+]^{4-}$	616.3
	—	—	622.0	57	$[M - 5H^+ + Na^+]^{4-}$	621.8
	—	—	627.5	16	$[M - 6H^+ + 2Na^+]^{4-}$	627.3
	493.1	88	—	—	$[M - 5H^+]^{5-}$	492.9
	497.5	11	—	—	$[M - 6H^+ + Na^+]^{5-}$	497.3
	410.8	100	—	—	$[M - 6H^+]^{6-}$	410.6
	351.9	3	—	—	$[M - 7H^+]^{7-}$	351.8

BTH Oligosaccharide ESIMS data, continued

Oligomer (No.CO_2^- groups)	Observed signals at CV = 25 V *m/z*	rel. int.	at CV = 55-65 V *m/z*	rel. int.	Assignment [species]	Pred. *m/z*
14-mer	[2673.7]*				[M = 2673.3]	
(7)	—	—	—	—	$[M - H^+]^{1-}$	2672.3
	—	—	1335.5	13	$[M - 2H^+]^{2-}$	1335.6
	—	—	1346.7	16	$[M - 3H^+ + Na^+]^{2-}$	1346.6
	—	—	1357.5	14	$[M - 4H^+ + 2Na^+]^{2-}$	1357.6
	—	—	1368.5	14	$[M - 5H^+ + 3Na^+]^{2-}$	1368.6
	890.2	11	890.1	100	$[M - 3H^+]^{3-}$	890.1
	897.5	9	897.4	92	$[M - 4H^+ + Na^+]^{3-}$	897.4
	904.8	6	904.7	65	$[M - 5H^+ + 2Na^+]^{3-}$	904.7
	912.2	3	911.9	40	$[M - 6H^+ + 3Na^+]^{3-}$	912.1
	—	—	919.4	23	$[M - 7H^+ + 4Na^+]^{3-}$	919.4
	667.4	39	667.3	55	$[M - 4H^+]^{4-}$	667.3
	672.9	18	672.9	27	$[M - 5H^+ + Na^+]^{4-}$	672.8
	678.4	4	678.3	11	$[M - 6H^+ + 2Na^+]^{4-}$	678.3
	533.8	100	—	—	$[M - 5H^+]^{5-}$	533.6
	538.2	23	—	—	$[M - 6H^+ + Na^+]^{5-}$	538.0
	444.7	99	—	—	$[M - 6H^+]^{6-}$	444.5
	—	—	—	—	$[M - 7H^+]^{7-}$	380.9
15-mer	[2849.2]*		N. C.		[M = 2849.4]	
(8)	—	—			$[M - H^+]^{1-}$	2848.4
	—	—			$[M - 2H^+]^{2-}$	1423.7
	—	—			$[M - 3H^+]^{3-}$	948.8
	956.0	1			$[M - 4H^+ + Na^+]^{3-}$	956.1
	711.5	2			$[M - 4H^+]^{4-}$	711.3
	716.9	1			$[M - 5H^+ + Na^+]^{4-}$	716.8
	569.1	12			$[M - 5H^+]^{5-}$	568.9
	474.1	100			$[M - 6H^+]^{6-}$	473.9
	477.8	27			$[M - 7H^+ + Na^+]^{6-}$	477.6
	406.2	66			$[M - 7H^+]^{7-}$	406.0
	355.3	3			$[M - 8H^+]^{8-}$	355.2

BTH Oligosaccharide ESIMS data, continued

Oligomer ($No.CO_2^-$ groups)	Observed signals at CV = 25 V *m/z*	rel. int.	at CV = 55-65 V *m/z*	rel. int.	Assignment [species]	Pred. *m/z*
16-mer	[3053.2]*		N. C.		[M = 3052.6]	
(8)	—	—			$[M - H^+]^{1-}$	3051.6
	—	—			$[M - 2H^+]^{2-}$	1525.3
	1016.7	3			$[M - 3H^+]^{3-}$	1016.5
	1024.0	4			$[M - 4H^+ + Na^+]^{3-}$	1023.9
	1031.3	3			$[M - 5H^+ + 2Na^+]^{3-}$	1031.2
	1038.6	2			$[M - 6H^+ + 3Na^+]^{3-}$	1038.5
	1045.9	—			$[M - 7H^+ + 4Na^+]^{3-}$	1045.8
	1053.3	—			$[M - 8H^+ + 5Na^+]^{3-}$	1053.2
	762.3	13			$[M - 4H^+]^{4-}$	762.1
	767.7	9			$[M - 5H^+ + Na^+]^{4-}$	767.6
	773.3	3			$[M - 6H^+ + 2Na^+]^{4-}$	773.1
	609.6	43			$[M - 5H^+]^{5-}$	609.5
	614.1	18			$[M - 6H^+ + Na^+]^{5-}$	613.9
	507.9	100			$[M - 6H^+]^{6-}$	507.8
	511.4	23			$[M - 7H^+ + Na^+]^{6-}$	511.4
	435.2	56			$[M - 7H^+]^{7-}$	435.1
	—	—			$[M - 8H^+]^{8-}$	380.6

BTH Oligosaccharide ESIMS data, continued

Oligomer (No.CO_2^- groups)	Observed signals at CV = 25 V *m/z*	rel. int.	at CV = 55-65 V *m/z*	rel. int.	Assignment [species]	Pred. *m/z*
17-mer	[3229.2]*				[M = 3228.7]	
(9)	—	—	—	—	$[M - H^+]^{1-}$	3227.7
	—	—	—	—	$[M - 2H^+]^{2-}$	1613.3
	—	—	1075.2	7	$[M - 3H^+]^{3-}$	1075.2
	—	—	1082.6	10	$[M - 4H^+ + Na^+]^{3-}$	1082.6
	—	—	1089.9	9	$[M - 5H^+ + 2Na^+]^{3-}$	1089.9
	—	—	1097.3	9	$[M - 6H^+ + 3Na^+]^{3-}$	1097.2
	—	—	1104.5	7	$[M - 7H^+ + 4Na^+]^{3-}$	1104.5
	806.2	1	806.3	52	$[M - 4H^+]^{4-}$	806.2
	—	—	811.8	67	$[M - 5H^+ + Na^+]^{4-}$	811.7
	—	—	817.2	43	$[M - 6H^+ + 2Na^+]^{4-}$	817.2
	—	—	822.8	29	$[M - 7H^+ + 3Na^+]^{4-}$	822.7
	644.8	2	644.9	100	$[M - 5H^+]^{5-}$	644.7
	649.3	1	649.3	71	$[M - 6H^+ + Na^+]^{5-}$	649.1
	—	—	653.7	27	$[M - 7H^+ + 2Na^+]^{5-}$	653.5
	537.2	6	537.0	8	$[M - 6H^+]^{6-}$	537.1
	540.9	2	—	—	$[M - 7H^+ + Na^+]^{6-}$	540.8
	460.4	47	46	3	$[M - 7H^+]^{7-}$	460.2
	463.5	8	—	—	$[M - 8H^+ + Na^+]^{7-}$	463.4
	402.8	100	—	—	$[M - 8H^+]^{8-}$	402.6
	357.9	7	—	—	$[M - 9H^+]^{9-}$	357.7

BTH Oligosaccharide ESIMS data, continued

Oligomer ($No.CO_2^-$ groups)	Observed signals at CV = 25 V *m/z*	rel. int.	at CV = 55-65 V *m/z*	rel. int.	Assignment [species]	Pred. *m/z*
18-mer	[3432.8]*				[M = 3431.9]	
(9)	—	—	—	—	$[M - H^+]^{1-}$	3430.9
	—	—	1714.5	4	$[M - 2H^+]^{2-}$	1714.9
	1143.0	1	1143.0	41	$[M - 3H^+]^{3-}$	1143.0
	1150.5	2	1150.5	71	$[M - 4H^+ + Na^+]^{3-}$	1150.3
	1157.7	2	1157.7	70	$[M - 5H^+ + 2Na^+]^{3-}$	1157.6
	1165.1	1	1165.0	54	$[M - 6H^+ + 3Na^+]^{3-}$	1164.9
	—	—	1172.3	46	$[M - 7H^+ + 4Na^+]^{3-}$	1172.3
	—	—	1179.6	34	$[M - 8H^+ + 5Na^+]^{3-}$	1179.6
	—	—	1187.0	25	$[M - 9H^+ + 6Na^+]^{3-}$	1186.9
	857.1	5	857.1	100	$[M - 4H^+]^{4-}$	857.0
	862.6	6	862.6	93	$[M - 5H^+ + Na^+]^{4-}$	862.5
	868.1	3	868.0	50	$[M - 6H^+ + 2Na^+]^{4-}$	868.0
	873.6	1	873.5	21	$[M - 7H^+ + 3Na^+]^{4-}$	873.5
	685.5	16	685.5	40	$[M - 5H^+]^{5-}$	685.4
	689.9	11	689.9	35	$[M - 6H^+ + Na^+]^{5-}$	689.8
	694.3	3	694.3	8	$[M - 7H^+ + 2Na^+]^{5-}$	694.2
	698.7	1	698.6	6	$[M - 8H^+ + 3Na^+]^{5-}$	698.6
	571.2	37	570.9	8	$[M - 6H^+]^{6-}$	571.0
	574.8	17	—	—	$[M - 7H^+ + Na^+]^{6-}$	574.6
	489.4	83	—	—	$[M - 7H^+]^{7-}$	489.3
	—	—	492.3	4	$[M - 8H^+ + Na^+]^{7-}$	492.4
	428.2	100	—	—	$[M - 8H^+]^{8-}$	428.0
	—	—	—	—	$[M - 9H^+]^{9-}$	380.3

BTH Oligosaccharide ESIMS data, continued

Oligomer ($No.CO_2^-$ groups)	Observed signals at CV = 25 V *m/z*	rel. int.	at CV = 55-65 V *m/z*	rel. int.	Assignment [species]	Pred. *m/z*
19-mer	[3608.8]*				[M = 3608.0]	
(10)	—	—	—	—	$[M - H^+]^{1-}$	3607.0
	—	—	—	—	$[M - 2H^+]^{2-}$	1803.0
	—	—	—	—	$[M - 3H^+]^{3-}$	1201.7
	—	—	1208.9	4	$[M - 4H^+ + Na^+]^{3-}$	1209.0
	—	—	1216.4	5	$[M - 5H^+ + 2Na^+]^{3-}$	1216.3
	—	—	901.1	18	$[M - 4H^+]^{4-}$	901.0
	—	—	906.6	28	$[M - 5H^+ + Na^+]^{4-}$	906.5
	—	—	912.1	28	$[M - 6H^+ + 2Na^+]^{4-}$	912.0
	—	—	720.7	80	$[M - 5H^+]^{5-}$	720.6
	—	—	725.2	100	$[M - 6H^+ + Na^+]^{5-}$	725.0
	—	—	729.6	60	$[M - 7H^+ + 2Na^+]^{5-}$	729.4
	—	—	733.9	12	$[M - 8H^+ + 3Na^+]^{5-}$	733.8
	—	—	600.4	28	$[M - 6H^+]^{6-}$	600.3
	514.6	9	—	—	$[M - 7H^+]^{7-}$	514.4
	450.2	73	—	—	$[M - 8H^+]^{8-}$	450.0
	400.1	100	—	—	$[M - 9H^+]^{9-}$	399.9

BTH Oligosaccharide ESIMS data, continued

Oligomer (No.CO_2^- groups)	Observed signals at CV = 25 V *m/z*	rel. int.	at CV = 55-65 V *m/z*	rel. int.	Assignment [species]	Pred. *m/z*
20-mer	[3812.8]*	N/A			[M = 3811.2]	
(10)	—	—	—	—	$[M - H^+]^{1-}$	3810.2
	—	—	—	—	$[M - 2H^+]^{2-}$	1904.6
	—	—	1269.4	23	$[M - 3H^+]^{3-}$	1269.4
	—	—	1276.8	36	$[M - 4H^+ + Na^+]^{3-}$	1276.7
	—	—	1284.2	44	$[M - 5H^+ + 2Na^+]^{3-}$	1284.1
	—	—	1291.5	37	$[M - 6H^+ + 3Na^+]^{3-}$	1291.4
	—	—	1298.8	35	$[M - 7H^+ + 4Na^+]^{3-}$	1298.7
	—	—	1306.1	27	$[M - 8H^+ + 5Na^+]^{3-}$	1306.0
	—	—	1313.4	22	$[M - 9H^+ + 6Na^+]^{3-}$	1313.4
	951.9	2	951.9	61	$[M - 4H^+]^{4-}$	951.8
	957.4	4	957.4	92	$[M - 5H^+ + Na^+]^{4-}$	957.3
	962.9	3	962.9	74	$[M - 6H^+ + 2Na^+]^{4-}$	962.8
	761.4	7	761.5	82	$[M - 5H^+]^{5-}$	761.2
	765.8	9	765.9	100	$[M - 6H^+ + Na^+]^{5-}$	765.6
	770.2	5	770.4	38	$[M - 7H^+ + 2Na^+]^{5-}$	770.0
	634.3	20	634.1	22	$[M - 6H^+]^{6-}$	634.2
	638.0	17	637.9	14	$[M - 7H^+ + Na^+]^{6-}$	637.9
	641.7	6	641.3	16	$[M - 8H^+ + 2Na^+]^{6-}$	641.5
	543.6	47	543.2	19	$[M - 7H^+]^{7-}$	543.5
	546.7	28	—	—	$[M - 8H^+ + Na^+]^{7-}$	546.6
	549.8	7	—	—	$[M - 9H^+ + 2Na^+]^{7-}$	549.7
	475.6	100	—	—	$[M - 8H^+]^{8-}$	475.4
	478.3	40	—	—	$[M - 9H^+ + Na^+]^{8-}$	478.1
	422.7	83	—	—	$[M - 9H^+]^{9-}$	422.5
	—	—	—	—	$[M - 10H^+]^{10-}$	380.1

BTH Oligosaccharide ESIMS data, continued

Oligomer (No.CO_2^- groups)	Observed signals at CV = 25 V *m/z*	rel. int.	at CV = 55-65 V *m/z*	rel. int.	Assignment [species]	Pred. *m/z*
21-mer	[3989.0]*				[M = 3987.4]	
(11)	—	—	—	—	$[M - H^+]^{1-}$	3986.3
	—	—	—	—	$[M - 2H^+]^{2-}$	1992.7
	—	—	1328.1	9	$[M - 3H^+]^{3-}$	1328.1
	—	—	1335.3	14	$[M - 4H^+ + Na^+]^{3-}$	1335.4
	—	—	1342.8	11	$[M - 5H^+ + 2Na^+]^{3-}$	1342.8
	—	—	995.8	21	$[M - 4H^+]^{4-}$	995.8
	—	—	1001.4	23	$[M - 5H^+ + Na^+]^{4-}$	1001.3
	—	—	1006.9	14	$[M - 6H^+ + 2Na^+]^{4-}$	1006.8
	—	—	1012.3	9	$[M - 7H^+ + 3Na^+]^{4-}$	1012.3
	—	—	1017.7	11	$[M - 8H^+ + 4Na^+]^{4-}$	1017.8
	—	—	796.6	97	$[M - 5H^+]^{5-}$	796.5
	—	—	801.0	68	$[M - 6H^+ + Na^+]^{5-}$	800.9
	663.6	3	663.6	100	$[M - 6H^+]^{6-}$	663.6
	—	—	667.4	76	$[M - 7H^+ + Na^+]^{6-}$	667.2
	568.7	6	—	—	$[M - 7H^+]^{7-}$	568.6
	571.5	5	—	—	$[M - 8H^+ + Na^+]^{7-}$	571.8
	497.5	14	—	—	$[M - 8H^+]^{8-}$	497.4
	500.3	4	—	—	$[M - 9H^+ + Na^+]^{8-}$	500.2
	442.2	56	—	—	$[M - 9H^+]^{9-}$	442.0
	444.7	16	444.5	35	$[M - 10H^+ + Na^+]^{9-}$	444.5
	397.9	100	—	—	$[M - 10H^+]^{10-}$	397.7
	361.6	15	—	—	$[M - 11H^+]^{11-}$	361.5

BTH Oligosaccharide ESIMS data, continued

Oligomer ($No.CO_2^-$ groups)	Observed signals at CV = 25 V *m/z*	rel. int.	at CV = 55-65 V *m/z*	rel. int.	Assignment [species]	Pred. *m/z*
22-mer	[4191.6]*	N/A			[M = 4190.6]	
(11)	—	—	—	—	$[M - H^+]^{1-}$	4189.5
	—	—	—	—	$[M - 2H^+]^{2-}$	2094.3
	—	—	1395.9	24	$[M - 3H^+]^{3-}$	1395.8
	—	—	1403.3	32	$[M - 4H^+ + Na^+]^{3-}$	1403.2
	—	—	1410.7	31	$[M - 5H^+ + 2Na^+]^{3-}$	1410.5
	—	—	1417.9	25	$[M - 6H^+ + 3Na^+]^{3-}$	1417.8
	—	—	1425.2	19	$[M - 7H^+ + 4Na^+]^{3-}$	1425.2
	—	—	1432.6	12	$[M - 8H^+ + 5Na^+]^{3-}$	1432.5
	—	—	1046.7	61	$[M - 4H^+]^{4-}$	1046.6
	1052.2	3	1052.2	76	$[M - 5H^+ + Na^+]^{4-}$	1052.1
	—	—	1057.7	48	$[M - 6H^+ + 2Na^+]^{4-}$	1057.6
	—	—	1063.2	24	$[M - 7H^+ + 3Na^+]^{4-}$	1063.1
	—	—	1068.7	15	$[M - 8H^+ + 4Na^+]^{4-}$	1068.6
	—	—	1074.4	8	$[M - 9H^+ + 5Na^+]^{4-}$	1074.1
	837.2	5	837.2	100	$[M - 5H^+]^{5-}$	837.1
	841.7	4	841.6	80	$[M - 6H^+ + Na^+]^{5-}$	841.5
	—	—	845.9	31	$[M - 7H^+ + 2Na^+]^{5-}$	845.9
	697.6	12	697.5	25	$[M - 6H^+]^{6-}$	697.4
	701.2	7	701.2	15	$[M - 7H^+ + Na^+]^{6-}$	701.1
	597.8	29	—	—	$[M - 7H^+]^{7-}$	597.6
	600.9	13	—	—	$[M - 8H^+ + Na^+]^{7-}$	600.8
	523.0	58	—	—	$[M - 8H^+]^{8-}$	522.8
	525.7	19	—	—	$[M - 9H^+ + Na^+]^{8-}$	525.6
	464.8	100	—	—	$[M - 9H^+]^{9-}$	464.6
	467.2	24	—	—	$[M - 10H^+ + Na^+]^{9-}$	467.1
	418.2	96	—	—	$[M - 10H^+]^{10-}$	418.1
	—	—	—	—	$[M - 11H^+]^{11-}$	380.0

BTH Oligosaccharide ESIMS data, continued

Oligomer (No.CO_2^- groups)	Observed signals at CV = 25 V *m/z*	rel. int.	at CV = 55-65 V *m/z*	rel. int.	Assignment [species]	Pred. *m/z*
23-mer	[4368.0]*				[M = 4366.7]	
(12)	—	—	—	—	$[M - H^+]^{1-}$	4365.7
	—	—	—	—	$[M - 2H^+]^{2-}$	2182.3
	—	—	—	—	$[M - 3H^+]^{3-}$	1454.6
	—	—	1090.5	12	$[M - 4H^+]^{4-}$	1090.7
	—	—	1096.1	11	$[M - 5H^+ + Na^+]^{4-}$	1096.1
	—	—	1101.6	8	$[M - 6H^+ + 2Na^+]^{4-}$	1101.7
	—	—	872.3	46	$[M - 5H^+]^{5-}$	872.3
	—	—	876.7	40	$[M - 6H^+ + Na^+]^{5-}$	876.7
	—	—	881.2	16	$[M - 7H^+ + 2Na^+]^{5-}$	881.1
	—	—	885.5	7	$[M - 8H^+ + 3Na^+]^{5-}$	885.5
	726.8	12	726.8	100	$[M - 6H^+]^{6-}$	726.8
	—	—	730.5	62	$[M - 7H^+ + Na^+]^{6-}$	730.5
	—	—	734.1	24	$[M - 8H^+ + 2Na^+]^{6-}$	734.1
	623.0	20	622.8	28	$[M - 7H^+]^{7-}$	622.8
	—	—	626.0	19	$[M - 8H^+ + Na^+]^{7-}$	625.9
	545.0	37	544.9	6	$[M - 8H^+]^{8-}$	544.8
	484.2	58	—	—	$[M - 9H^+]^{9-}$	484.2
	435.7	96	—	—	$[M - 10H^+]^{10-}$	435.7
	396.1	100	—	—	$[M - 11H^+]^{11-}$	396.0
	—	—	—	—	$[M - 12H^+]^{12-}$	362.9

BTH Oligosaccharide ESIMS data, continued

Oligomer ($No.CO_2^-$ groups)	Observed signals at CV = 25 V *m/z*	rel. int.	at CV = 55-65 V *m/z*	rel. int.	Assignment [species]	Pred. *m/z*
24-mer	4570.2*				[M = 4569.9]	
(12)	—	—	—	—	$[M - H^+]^{1-}$	4568.9
	—	—	—	—	$[M - 2H^+]^{2-}$	2283.9
	—	—	1522.2	14	$[M - 3H^+]^{3-}$	1522.3
	—	—	1529.6	20	$[M - 4H^+ + Na^+]^{3-}$	1529.6
	—	—	1536.8	22	$[M - 5H^+ + 2Na^+]^{3-}$	1536.9
	—	—	1544.2	20	$[M - 6H^+ + 3Na^+]^{3-}$	1544.3
	—	—	1141.6	49	$[M - 4H^+]^{4-}$	1141.5
	—	—	1146.9	66	$[M - 5H^+ + Na^+]^{4-}$	1147.0
	—	—	1152.4	49	$[M - 6H^+ + 2Na^+]^{4-}$	1152.5
	—	—	1158.2	29	$[M - 7H^+ + 3Na^+]^{4-}$	1158.0
	913.0	9	913.0	92	$[M - 5H^+]^{5-}$	913.0
	917.5	6	917.4	65	$[M - 6H^+ + Na^+]^{5-}$	917.4
	—	—	921.7	23	$[M - 7H^+ + 2Na^+]^{5-}$	921.8
	760.9	14	761.1	100	$[M - 6H^+]^{6-}$	760.6
	652.0	28	651.9	7	$[M - 7H^+]^{7-}$	651.8
	—	—	654.7	6	$[M - 8H^+ + Na^+]^{7-}$	655.0
	570.4	51	—	—	$[M - 8H^+]^{8-}$	570.2
	573.1	14	—	—	$[M - 9H^+ + Na^+]^{8-}$	573.0
	506.9	96	—	—	$[M - 9H^+]^{9-}$	506.8
	509.3	19	—	—	$[M - 10H^+ + Na^+]^{9-}$	509.2
	456.1	100	—	—	$[M - 10H^+]^{10-}$	456.0
	414.5	56	—	—	$[M - 11H^+]^{11-}$	414.4
	—	—	—	—	$[M - 12H^+]^{12-}$	379.8

BTH Oligosaccharide ESIMS data, continued

Oligomer (No.CO_2^- groups)	Observed signals at CV = 25 V *m/z*	rel. int.	at CV = 55-65 V *m/z*	rel. int.	Assignment [species]	Pred. *m/z*
25-mer	4747.8*				[M = 4746.0]	
(13)	—	—	—	—	$[M - H^+]^{1-}$	4745.0
	—	—	—	—	$[M - 2H^+]^{2-}$	2372.0
	—	—	—	—	$[M - 3H^+]^{3-}$	1581.0
	—	—	—	—	$[M - 4H^+]^{4-}$	1185.5
	—	—	1190.9	20	$[M - 5H^+ + Na^+]^{4-}$	1191.0
	—	—	948.1	42	$[M - 5H^+]^{5-}$	948.2
	—	—	952.5	44	$[M - 6H^+ + Na^+]^{5-}$	952.6
	—	—	956.8	32	$[M - 7H^+ + 2Na^+]^{5-}$	957.0
	—	—	790.1	100	$[M - 6H^+]^{6-}$	790.0
	—	—	793.7	78	$[M - 7H^+ + Na^+]^{6-}$	793.7
	—	—	797.1	63	$[M - 8H^+ + 2Na^+]^{6-}$	797.3
	—	—	—	—	$[M - 7H^+]^{7-}$	677.0
	592.3	6	—	—	$[M - 8H^+]^{8-}$	592.2
	526.3	13	—	—	$[M - 9H^+]^{9-}$	526.3
	528.8	5	—	—	$[M - 10H^+ + Na^+]^{9-}$	528.8
	473.7	33	—	—	$[M - 10H^+]^{10-}$	473.6
	475.6	17	—	—	$[M - 11H^+ + Na^+]^{10-}$	475.8
	430.6	86	—	—	$[M - 11H^+]^{11-}$	430.4
	394.6	100	—	—	$[M - 12H^+]^{12-}$	394.5
	—	—	—	—	$[M - 13H^+]^{13-}$	364.1

BTH Oligosaccharide ESIMS data, continued

Oligomer ($No.CO_2^-$ groups)	Observed signals at CV = 25 V *m/z*	rel. int.	at CV = 55-65 V *m/z*	rel. int.	Assignment [species]	Pred. *m/z*
26-mer	[4950.4]*				[M = 4949.2]	
(13)	—	—	—	—	$[M - H^+]^{1-}$	4948.2
	—	—	—	—	$[M - 2H^+]^{2-}$	2473.6
	—	—	1648.6	10	$[M - 3H^+]^{3-}$	1648.7
	—	—	1656.0	17	$[M - 4H^+ + Na^+]^{3-}$	1656.1
	—	—	1663.1	20	$[M - 5H^+ + 2Na^+]^{3-}$	1663.4
	—	—	1670.6	17	$[M - 6H^+ + 3Na^+]^{3-}$	1670.7
	—	—	1677.8	14	$[M - 7H^+ + 4Na^+]^{3-}$	1678.1
	—	—	1685.1	9	$[M - 8H^+ + 5Na^+]^{3-}$	1685.4
	—	—	1236.2	42	$[M - 4H^+]^{4-}$	1236.3
	—	—	1241.8	71	$[M - 5H^+ + Na^+]^{4-}$	1241.8
	—	—	1247.2	66	$[M - 6H^+ + 2Na^+]^{4-}$	1247.3
	—	—	1252.6	49	$[M - 7H^+ + 3Na^+]^{4-}$	1252.8
	—	—	1258.2	27	$[M - 8H^+ + 4Na^+]^{4-}$	1258.3
	—	—	988.8	60	$[M - 5H^+]^{5-}$	988.8
	—	—	993.1	65	$[M - 6H^+ + Na^+]^{5-}$	993.2
	—	—	997.5	30	$[M - 7H^+ + 2Na^+]^{5-}$	997.6
	—	—	823.9	100	$[M - 6H^+]^{6-}$	823.9
	—	—	827.6	76	$[M - 7H^+ + Na^+]^{6-}$	827.5
	—	—	831.2	28	$[M - 8H^+ + 2Na^+]^{6-}$	831.2
	706.1	9	706.0	19	$[M - 7H^+]^{7-}$	706.0
	617.8	17	617.8	—	$[M - 8H^+]^{8-}$	617.6
	620.5	7	620.5	—	$[M - 9H^+ + Na^+]^{8-}$	620.4
	623.1	2	622.9	20	$[M - 10H^+ + 2Na^+]^{8-}$	623.1
	549.0	33	548.9	14	$[M - 9H^+]^{9-}$	548.9
	551.5	12	—	—	$[M - 10H^+ + Na^+]^{9-}$	551.3
	494.0	69	—	—	$[M - 10H^+]^{10-}$	493.9
	496.3	19	—	—	$[M - 11H^+ + Na^+]^{10-}$	496.1
	449.0	100	—	—	$[M - 11H^+]^{11-}$	448.9
	451.0	17	—	—	$[M - 12H^+ + Na^+]^{11-}$	450.9
	411.5	61	—	—	$[M - 12H^+]^{12-}$	411.4
	—	—	—	—	$[M - 13H^+]^{13-}$	379.7

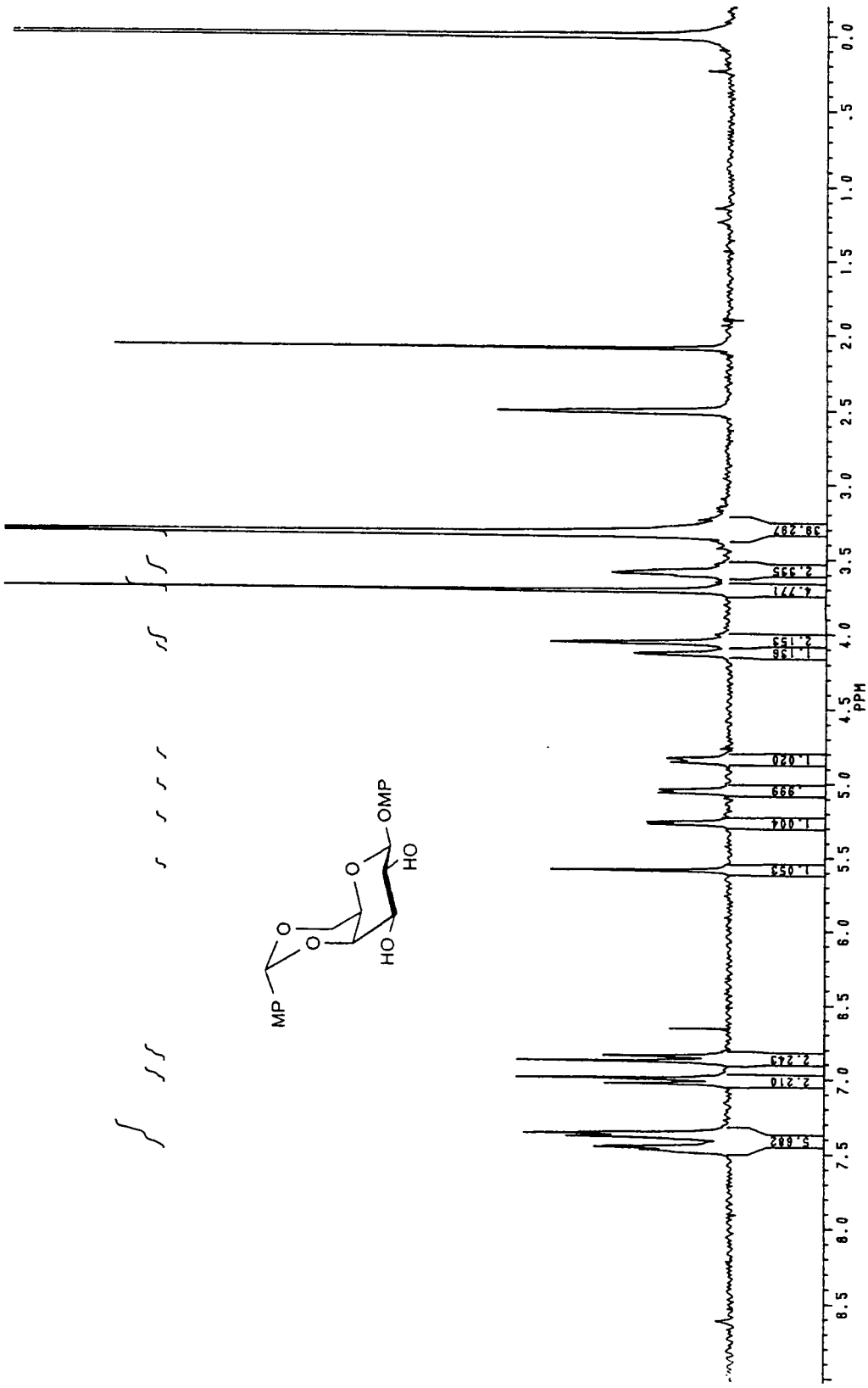
BTH Oligosaccharide ESIMS data, continued

Oligomer ($No.CO_2^-$ groups)	Observed signals at CV = 25 V *m/z*	rel. int.	at CV = 55-65 V *m/z*	rel. int.	Assignment [species]	Pred. *m/z*
27-mer	[5126.8]*				[M = 5125.3]	
(14)	—	—	—	—	$[M - H^+]^{1-}$	5124.3
	—	—	—	—	$[M - 2H^+]^{2-}$	2561.7
	—	—	—	—	$[M - 3H^+]^{3-}$	1707.4
	—	—	1280.2	8	$[M - 4H^+]^{4-}$	1280.3
	—	—	1285.6	13	$[M - 5H^+ + Na^+]^{4-}$	1285.8
	—	—	1024.0	20	$[M - 5H^+]^{5-}$	1024.1
	—	—	1028.4	16	$[M - 6H^+ + Na^+]^{5-}$	1028.5
	—	—	1032.8	12	$[M - 7H^+ + 2Na^+]^{5-}$	1032.8
	—	—	853.2	37	$[M - 6H^+]^{6-}$	853.2
	—	—	857.0	68	$[M - 7H^+ + Na^+]^{6-}$	856.9
	—	—	860.5	28	$[M - 8H^+ + 2Na^+]^{6-}$	860.5
	—	—	864.2	13	$[M - 9H^+ + 3Na^+]^{6-}$	864.2
	—	—	731.1	100	$[M - 7H^+]^{7-}$	731.2
	—	—	734.4	90	$[M - 8H^+ + Na^+]^{7-}$	734.3
	—	—	—	—	$[M - 8H^+]^{8-}$	639.7
	568.4	5	—	—	$[M - 9H^+]^{9-}$	568.5
	511.6	14	—	—	$[M - 10H^+]^{10-}$	511.5
	464.9	45	—	—	$[M - 11H^+]^{11-}$	464.9
	426.2	84	—	—	$[M - 12H^+]^{12-}$	426.0
	428.1	21	—	—	$[M - 13H^+ + Na^+]^{12-}$	427.9
	393.4	100	—	—	$[M - 13H^+]^{13-}$	393.2
	365.2	10	—	—	$[M - 14H^+]^{14-}$	365.1

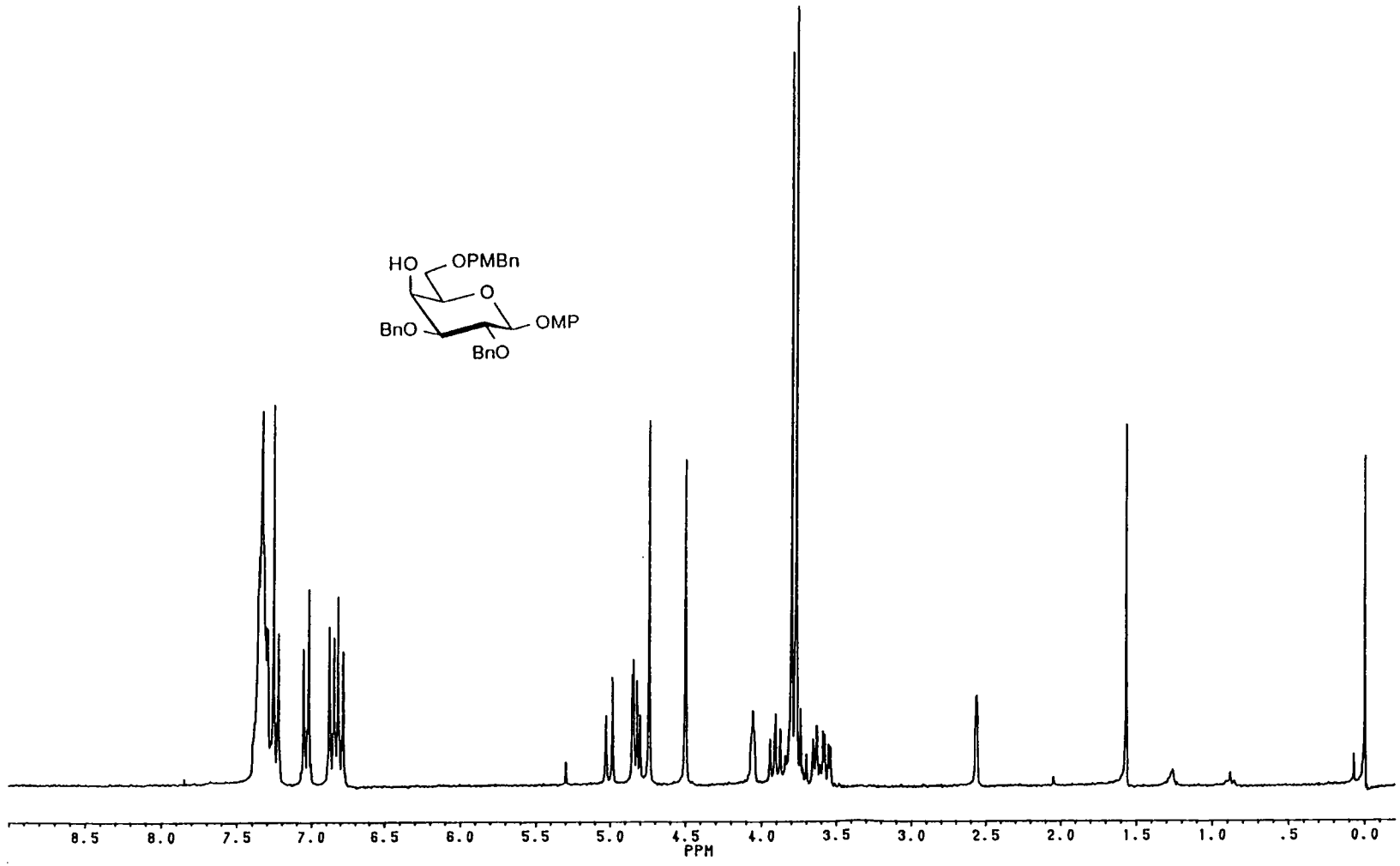
BTH Oligosaccharide ESIMS data, continued

Oligomer (No.CO_2^- groups)	Observed signals at CV = 25 V *m/z*	rel. int.	at CV = 55-65 V *m/z*	rel. int.	Assignment [species]	Pred. *m/z*
28-mer	[5330.2]*				[M = 5328.5]	
(14)	—	—	—	—	$[M - H^+]^{1-}$	5327.5
	—	—	—	—	$[M - 2H^+]^{2-}$	2663.3
	—	—	—	—	$[M - 3H^+]^{3-}$	1775.2
	—	—	1331.1	33	$[M - 4H^+]^{4-}$	1331.1
	—	—	1336.6	53	$[M - 5H^+ + Na^+]^{4-}$	1336.6
	—	—	1342.0	70	$[M - 6H^+ + 2Na^+]^{4-}$	1342.1
	—	—	1347.5	55	$[M - 7H^+ + 3Na^+]^{4-}$	1347.6
	—	—	1352.9	37	$[M - 8H^+ + 4Na^+]^{4-}$	1353.1
	—	—	1358.4	30	$[M - 9H^+ + 5Na^+]^{4-}$	1358.6
	—	—	1064.7	41	$[M - 5H^+]^{5-}$	1064.7
	—	—	1069.1	56	$[M - 6H^+ + Na^+]^{5-}$	1069.1
	—	—	1073.5	41	$[M - 7H^+ + 2Na^+]^{5-}$	1073.5
	—	—	1077.7	22	$[M - 8H^+ + 3Na^+]^{5-}$	1077.9
	—	—	887.1	91	$[M - 6H^+]^{6-}$	887.1
	—	—	890.7	97	$[M - 7H^+ + Na^+]^{6-}$	890.7
	—	—	894.4	42	$[M - 8H^+ + 2Na^+]^{6-}$	894.4
	760.4	5	760.6	100	$[M - 7H^+]^{7-}$	760.2
	763.4	4	763.5	78	$[M - 8H^+ + Na^+]^{7-}$	763.4
	665.1	10	664.9	50	$[M - 8H^+]^{8-}$	665.1
	667.8	7	—	—	$[M - 9H^+ + Na^+]^{8-}$	667.8
	670.6	3	—	—	$[M - 10H^+ + 2Na^+]^{8-}$	670.6
	591.1	22	—	—	$[M - 9H^+]^{9-}$	591.1
	593.6	11	—	—	$[M - 10H^+ + Na^+]^{9-}$	593.4
	531.9	46	—	—	$[M - 10H^+]^{10-}$	531.8
	534.0	19	—	—	$[M - 11H^+ + Na^+]^{10-}$	534.0
	483.5	80	—	—	$[M - 11H^+]^{11-}$	483.4
	485.5	24	—	—	$[M - 12H^+ + Na^+]^{11-}$	485.4
	443.2	100	—	—	$[M - 12H^+]^{12-}$	443.0
	444.9	23	—	—	$[M - 13H^+ + Na^+]^{12-}$	444.9
	409.0	64	—	—	$[M - 13H^+]^{13-}$	408.9
	—	—	—	—	$[M - 14H^+]^{14-}$	379.6

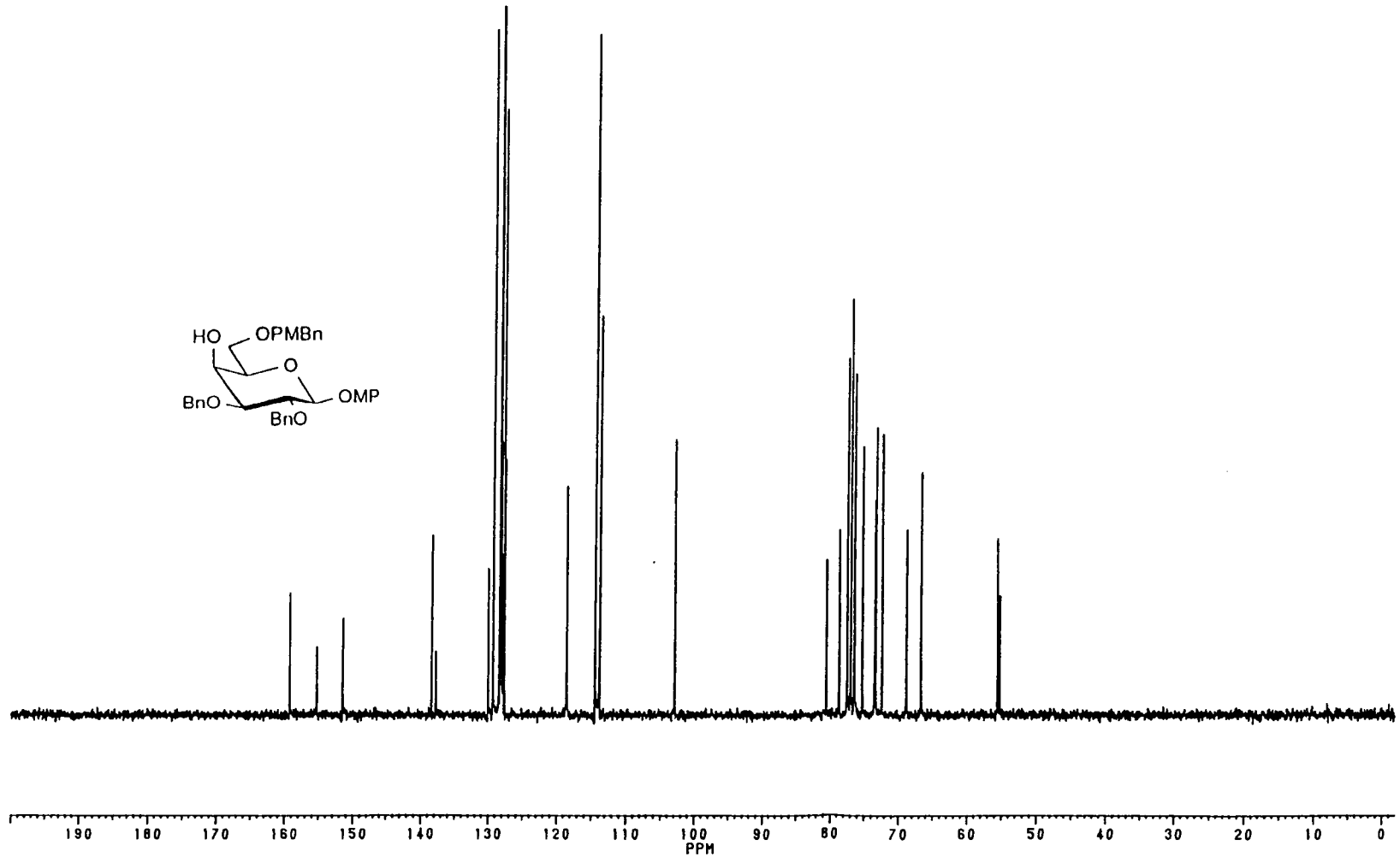
APPENDIX D. ^{1}H and ^{13}C NMR Spectra of Intermediates Involved in the Synthesis of *S*- and *C*-Oligosaccharides



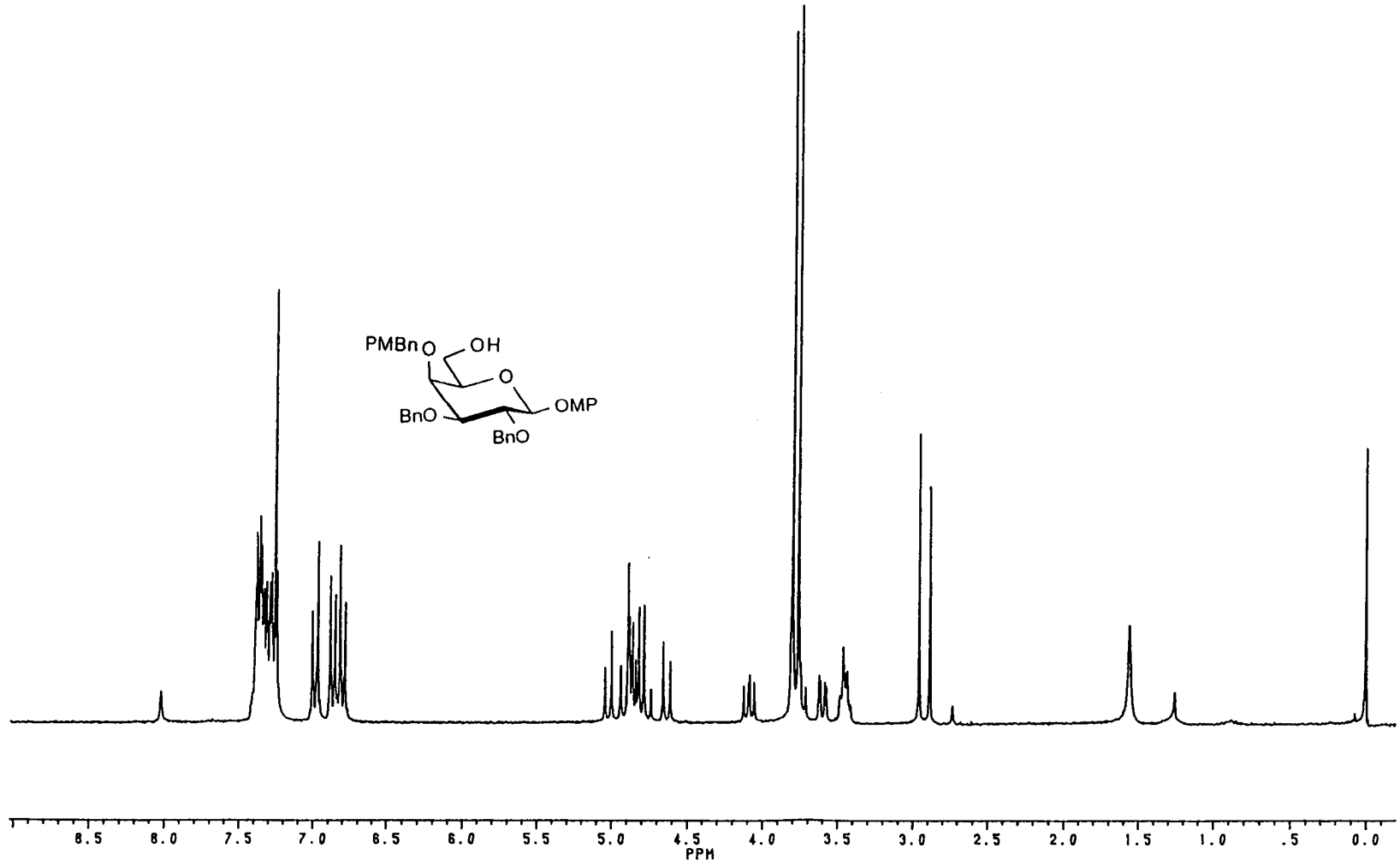
^{1}H NMR spectrum (250 MHz, DMSO-*d6*) of *p*-methoxyphenyl 4,6-*O*-*p*-methoxybenzylidene-β-D-galactopyranoside (**39**).



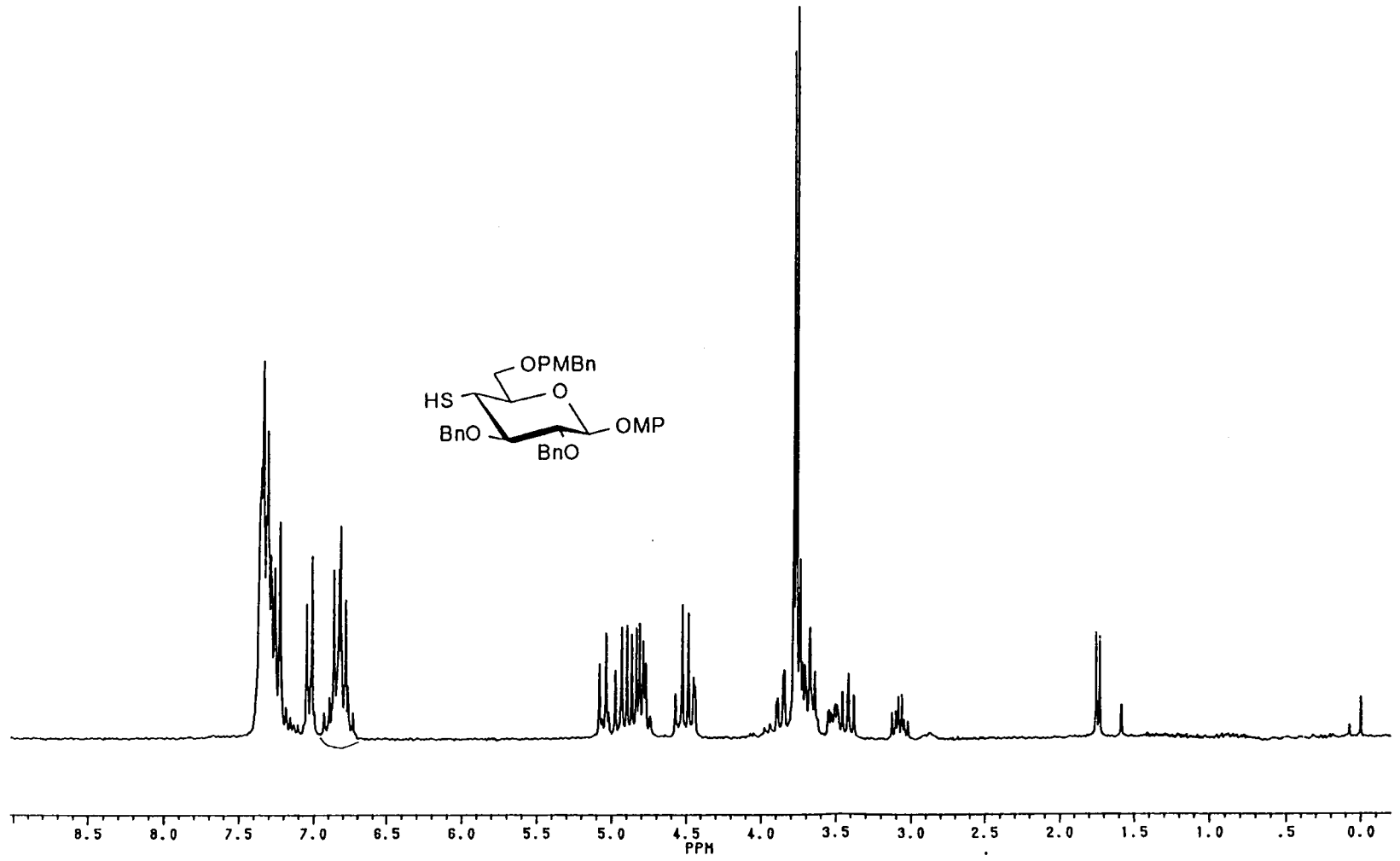
^{1}H NMR spectrum (250 MHz, $CDCl_3$) of *p*-methoxyphenyl 2,3-di-*O*-benzyl-6-*O*-*p*-methoxybenzyl-β-D-galactopyranoside (**41**).



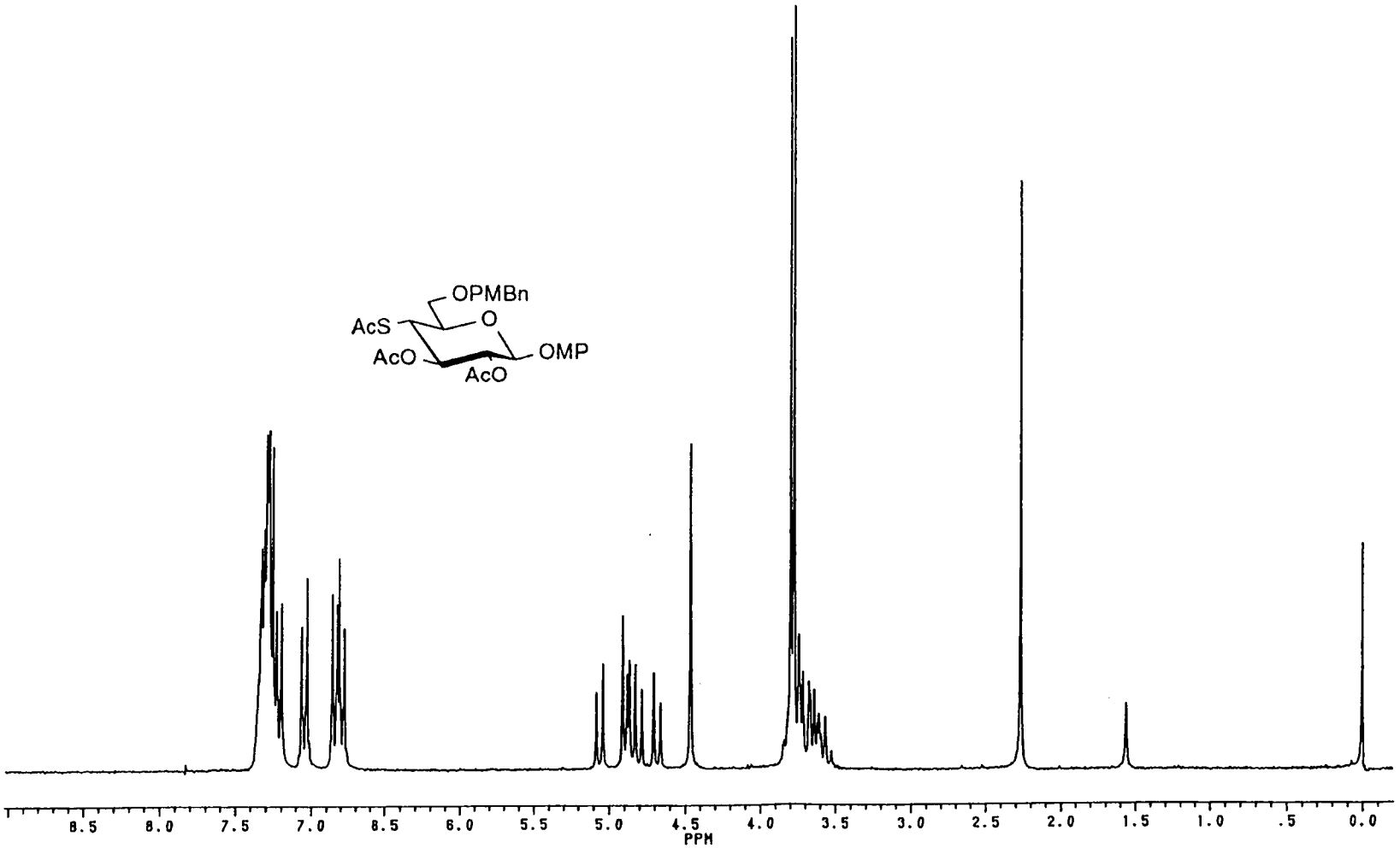
^{13}C NMR spectrum (250 MHz, $CDCl_3$) of *p*-methoxyphenyl 2,3-di-*O*-benzyl-6-*O*-*p*-methoxybenzyl-β-D-galactopyranoside (**41**).



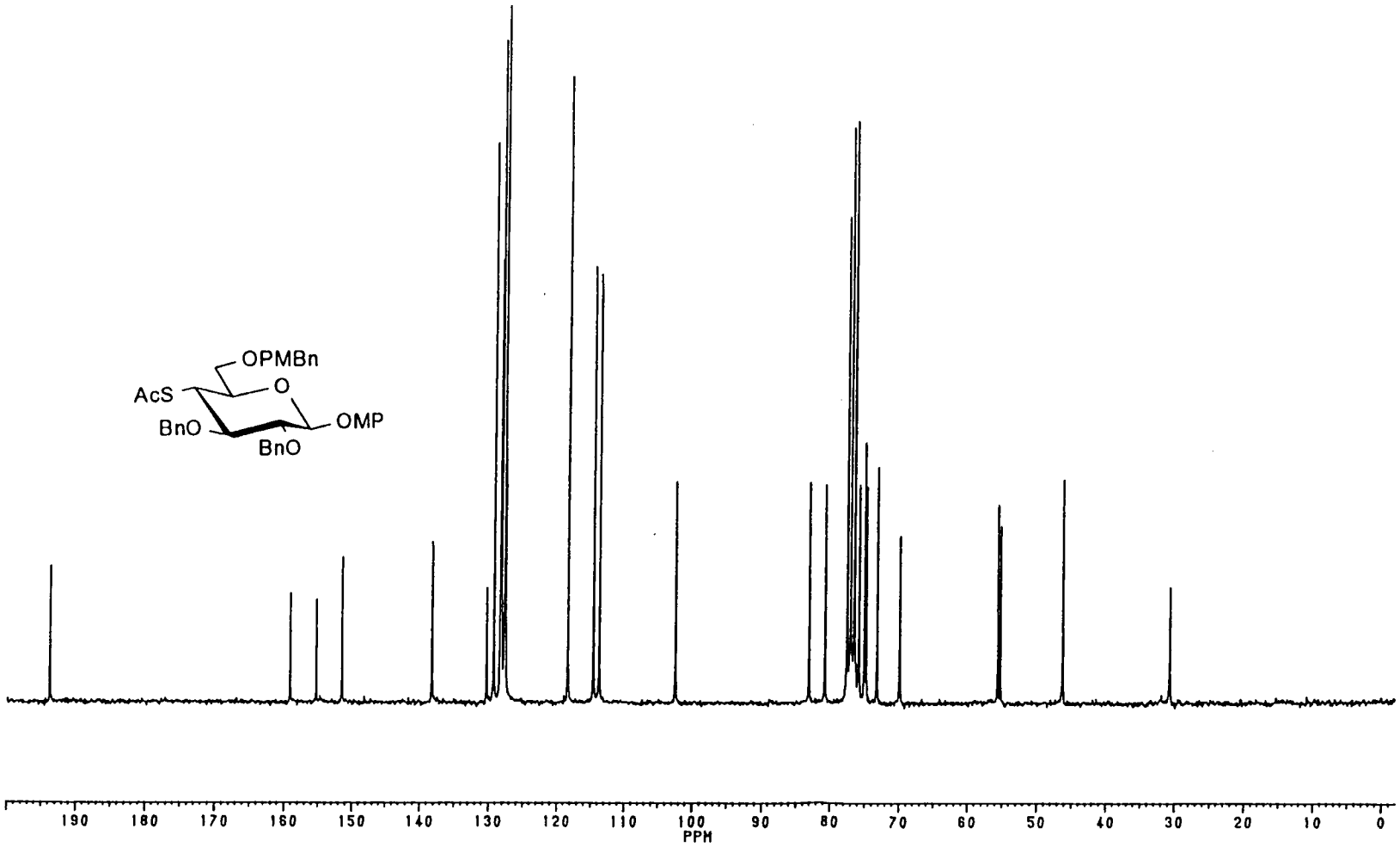
^{1}H NMR spectrum (250 MHz, $CDCl_3$) of *p*-methoxyphenyl 2,3-di-*O*-benzyl-4-*O*-*p*-methoxybenzyl-β-D-galactopyranoside (**42**).



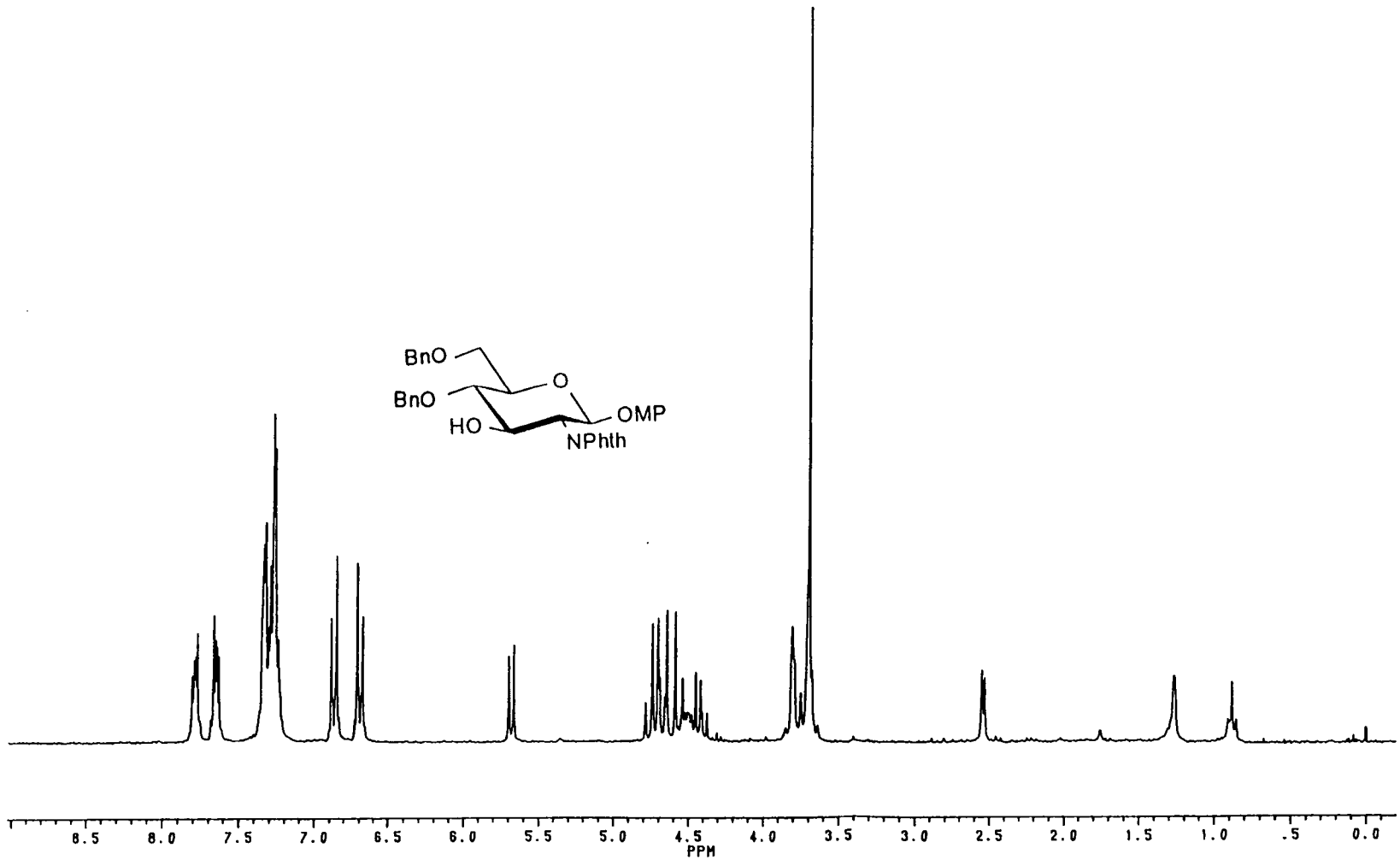
^{1}H NMR spectrum (250 MHz, $CDCl_3$) of *p*-methoxyphenyl 2,3-di-*O*-benzyl-6-*O*-*p*-methoxybenzyl-4-thio-β-D-glucopyranoside (**46**).



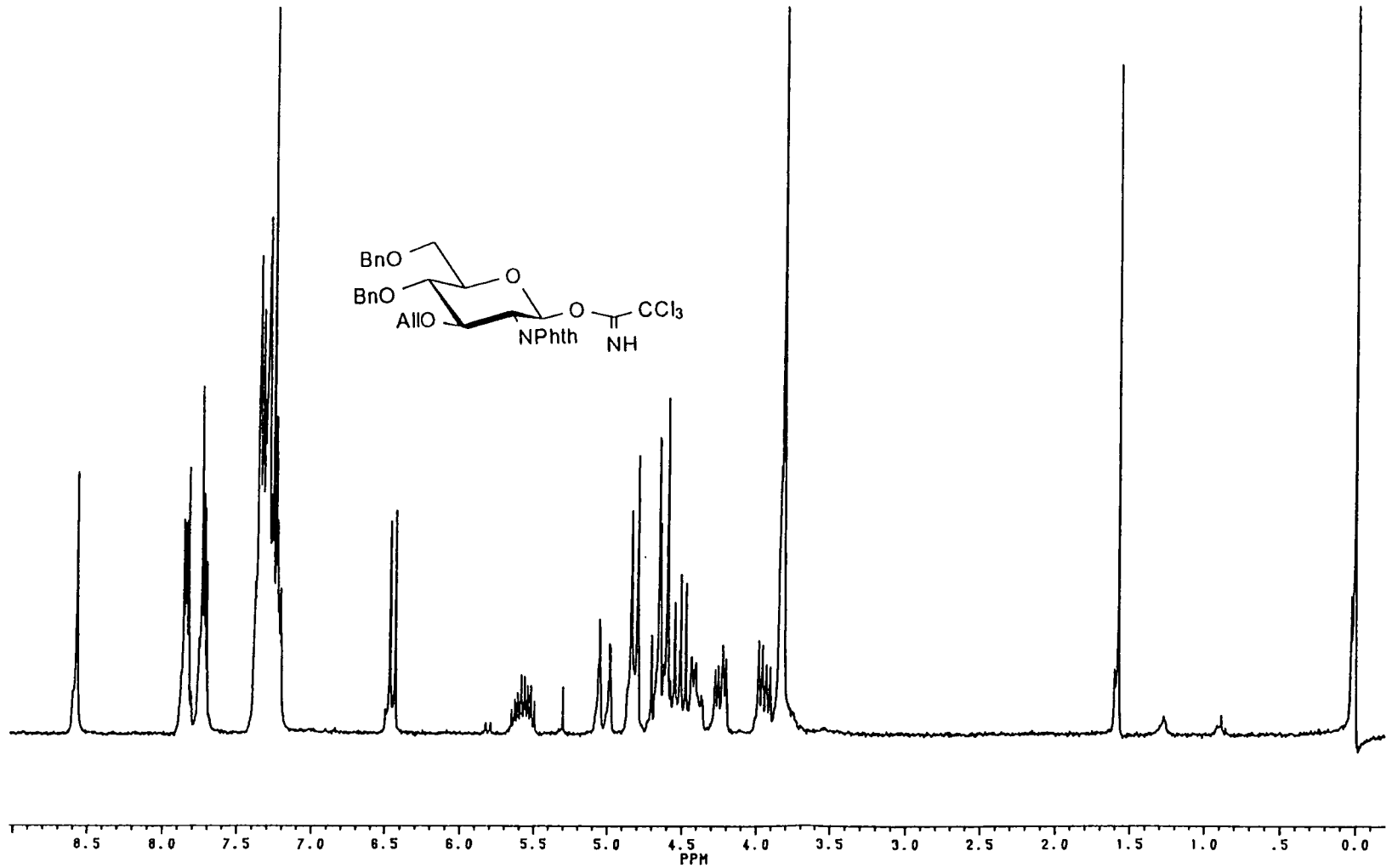
^{1}H NMR spectrum (250 MHz, $CDCl_3$) of *p*-methoxyphenyl 4-*S*-acetyl-2,3-di-*O*-benzyl-6-*O*-*p*-methoxybenzyl-4-thio-β-D-glucopyranoside (**50**).



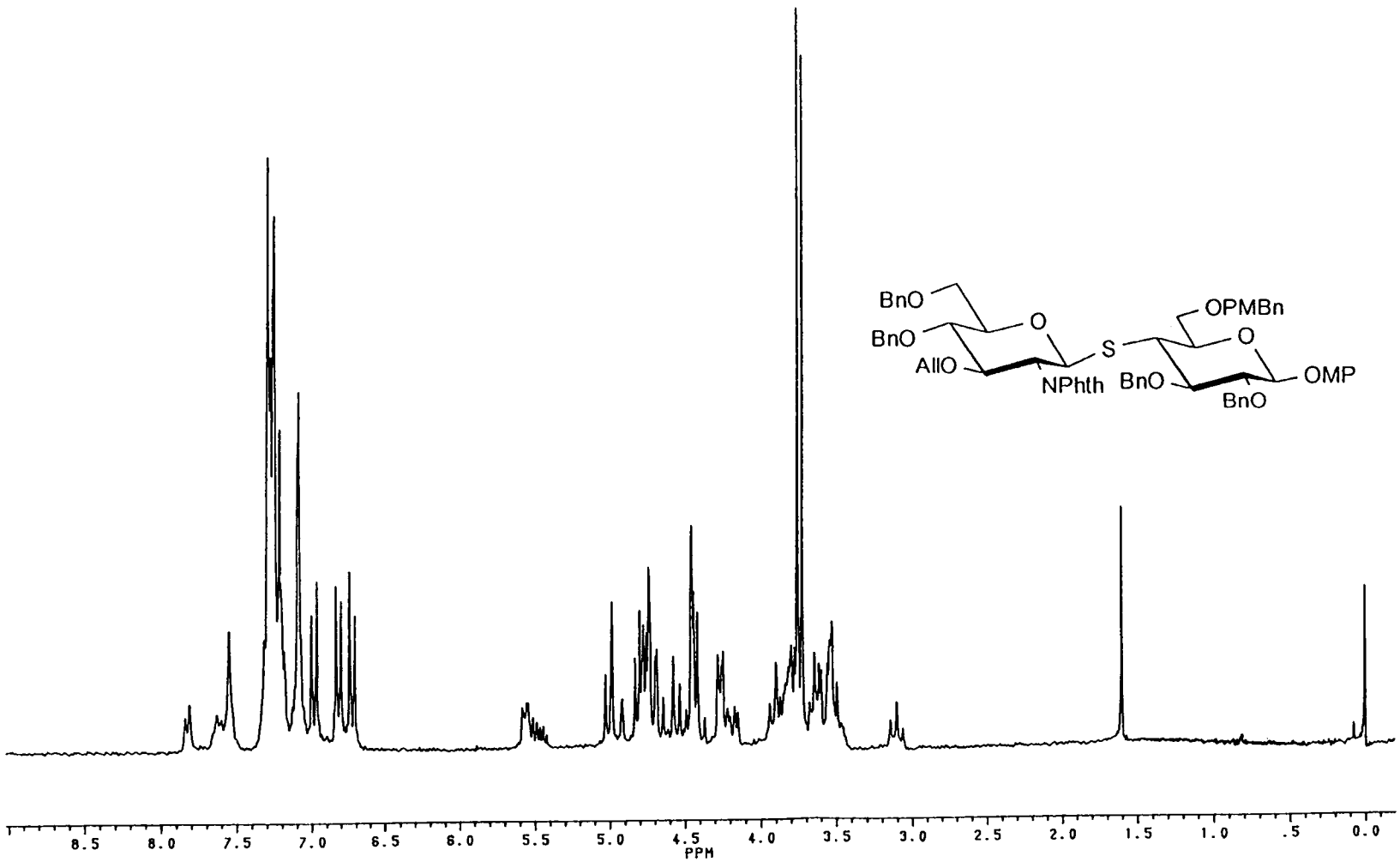
^{13}C NMR spectrum (62.5 MHz, $CDCl_3$) of *p*-methoxyphenyl 4-*S*-acetyl-2,3-di-*O*-benzyl-6-*O*-*p*-methoxybenzyl-4-thio-β-D-glucopyranoside (**50**).



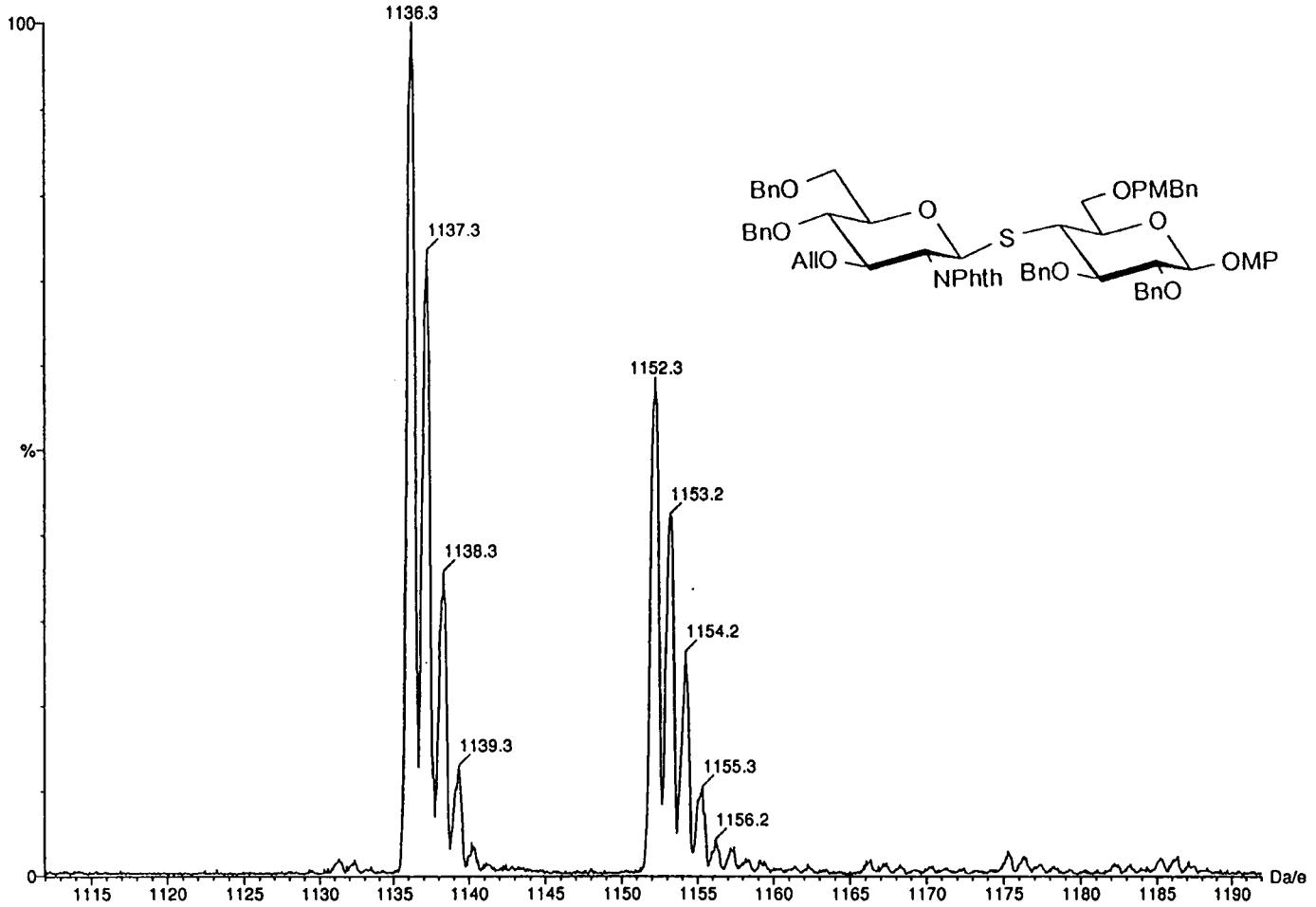
^{1}H NMR spectrum (250 MHz, $CDCl_3$) of *p*-methoxyphenyl 4,6-di-*O*-benzyl-2-deoxy-2-phthalimido-β-D-glucopyranoside (**54a**).



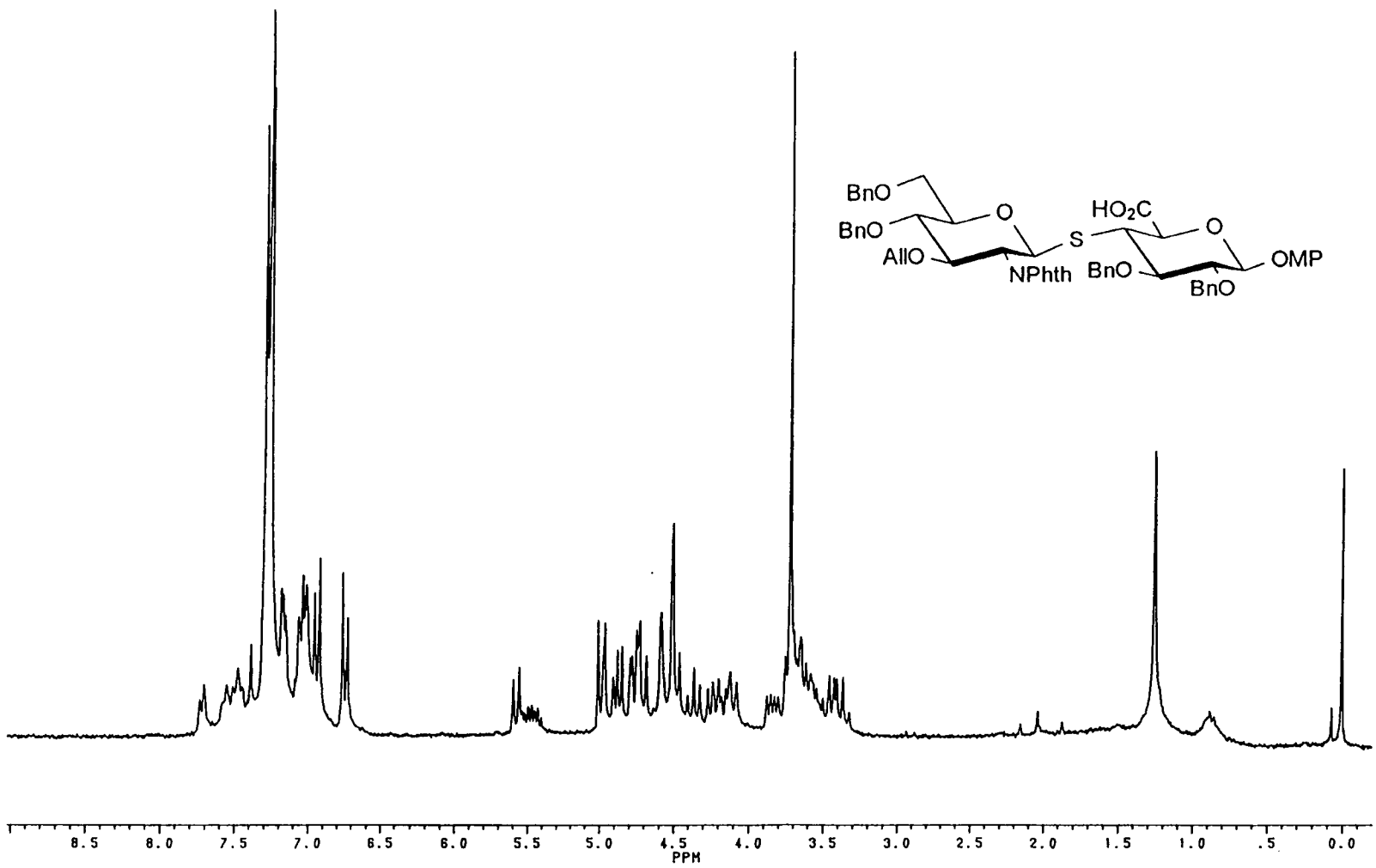
^{1}H NMR spectrum (250 MHz, $CDCl_3$) of 3-*O*-allyl-4,6-di-*O*-benzyl-2-deoxy-2-phthalimido-β-D-glucopyranosyl trichloroacetimidate (**45**).



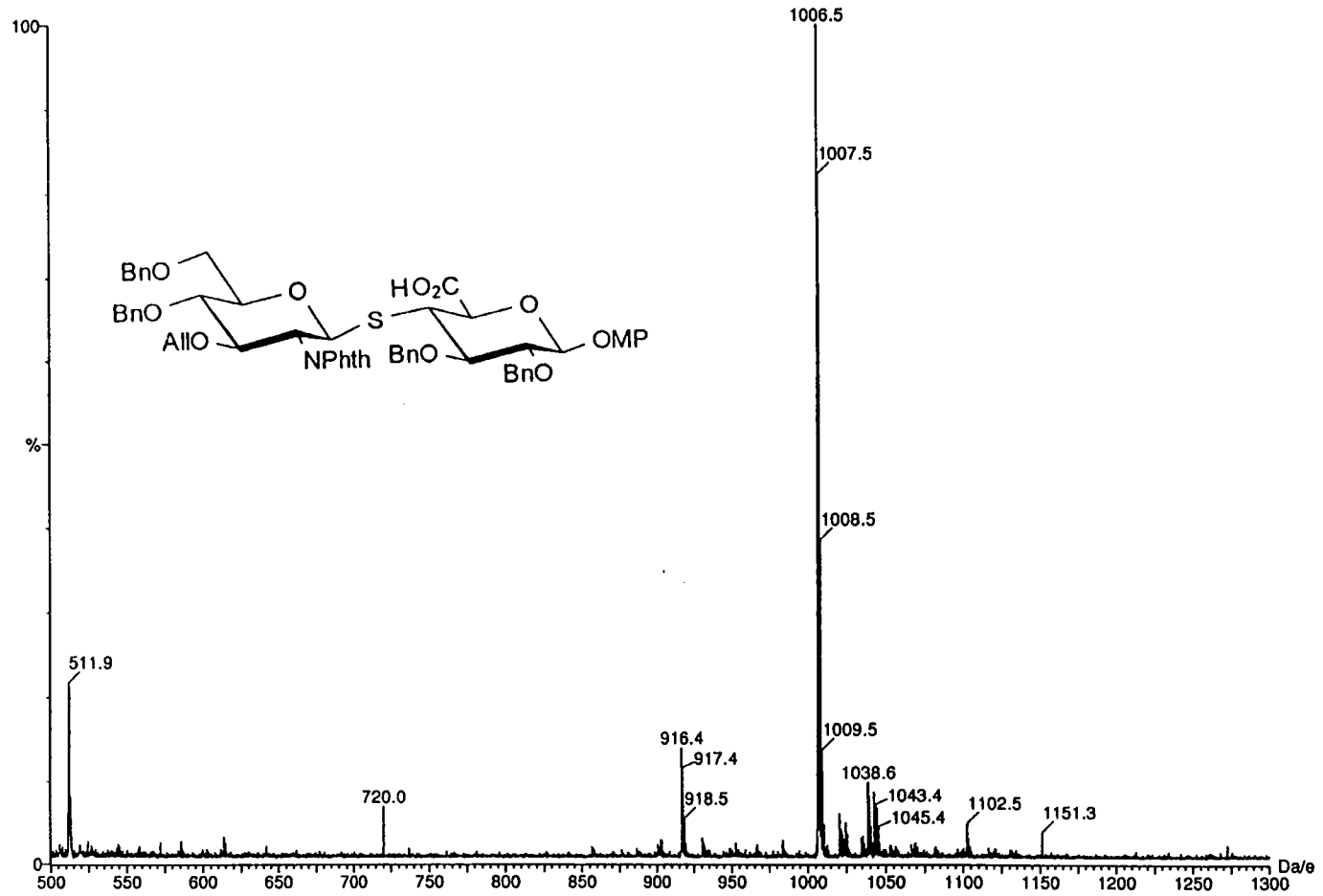
^{1}H NMR spectrum (250 MHz, $CDCl_3$) of *p*-methoxyphenyl 4-*S*-(3-*O*-allyl-4,6-di-*O*-benzyl-2-deoxy-2-phthalimido-β-D-glucopyranosyl)-2,3-di-*O*-benzyl-6-*O*-*p*-methoxybenzyl-4-thio-β-D-glucopyranoside (**16**).



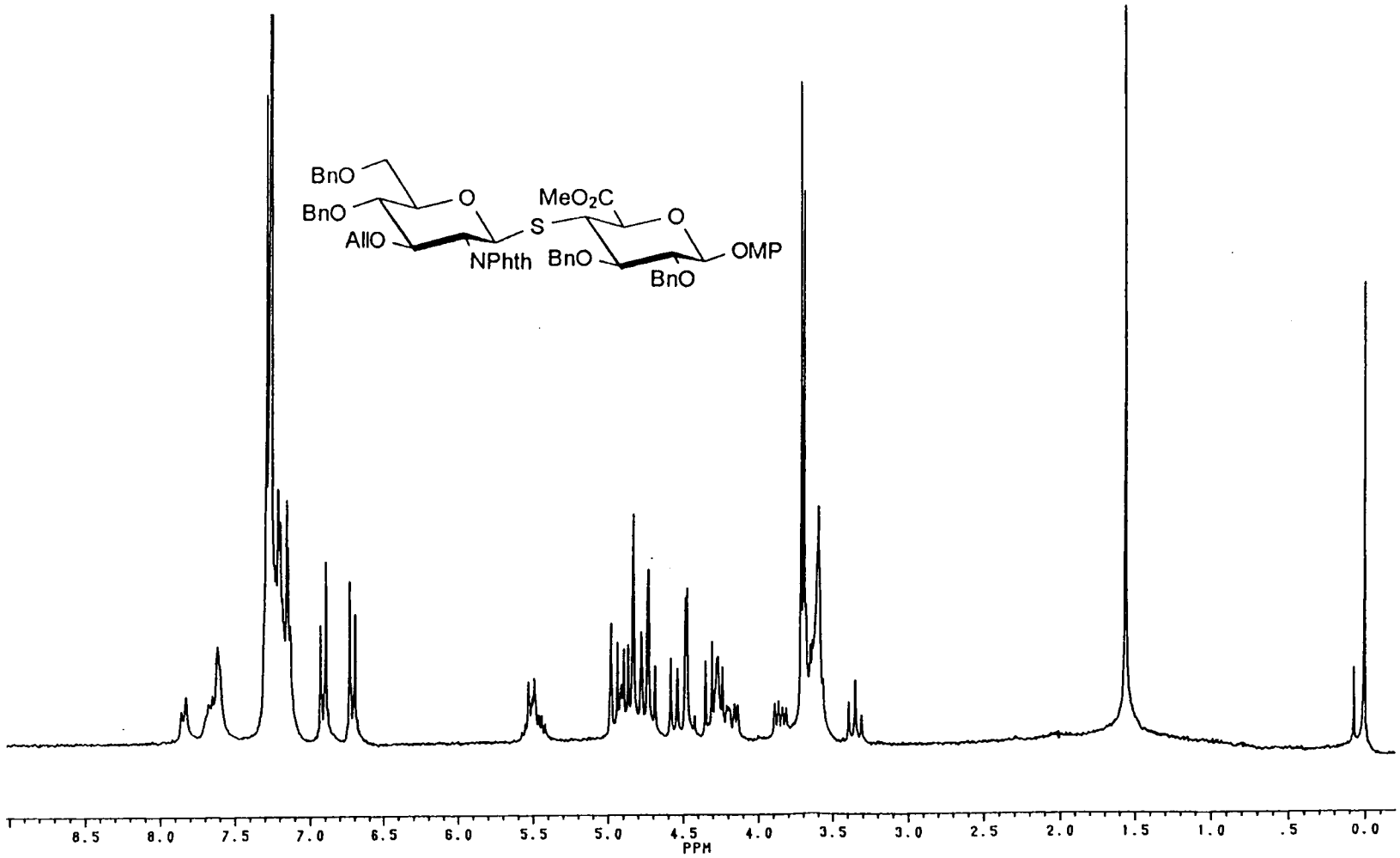
Positive-ion mode ESIMS spectrum of *p*-methoxyphenyl 4-*S*-(3-*O*-allyl-4,6-di-*O*-benzyl-2-deoxy-2-phthalimido-β-D-glucopyranosyl)-2,3-di-*O*-benzyl-6-*O*-*p*-methoxybenzyl-4-thio-β-D-glucopyranoside (**16**).



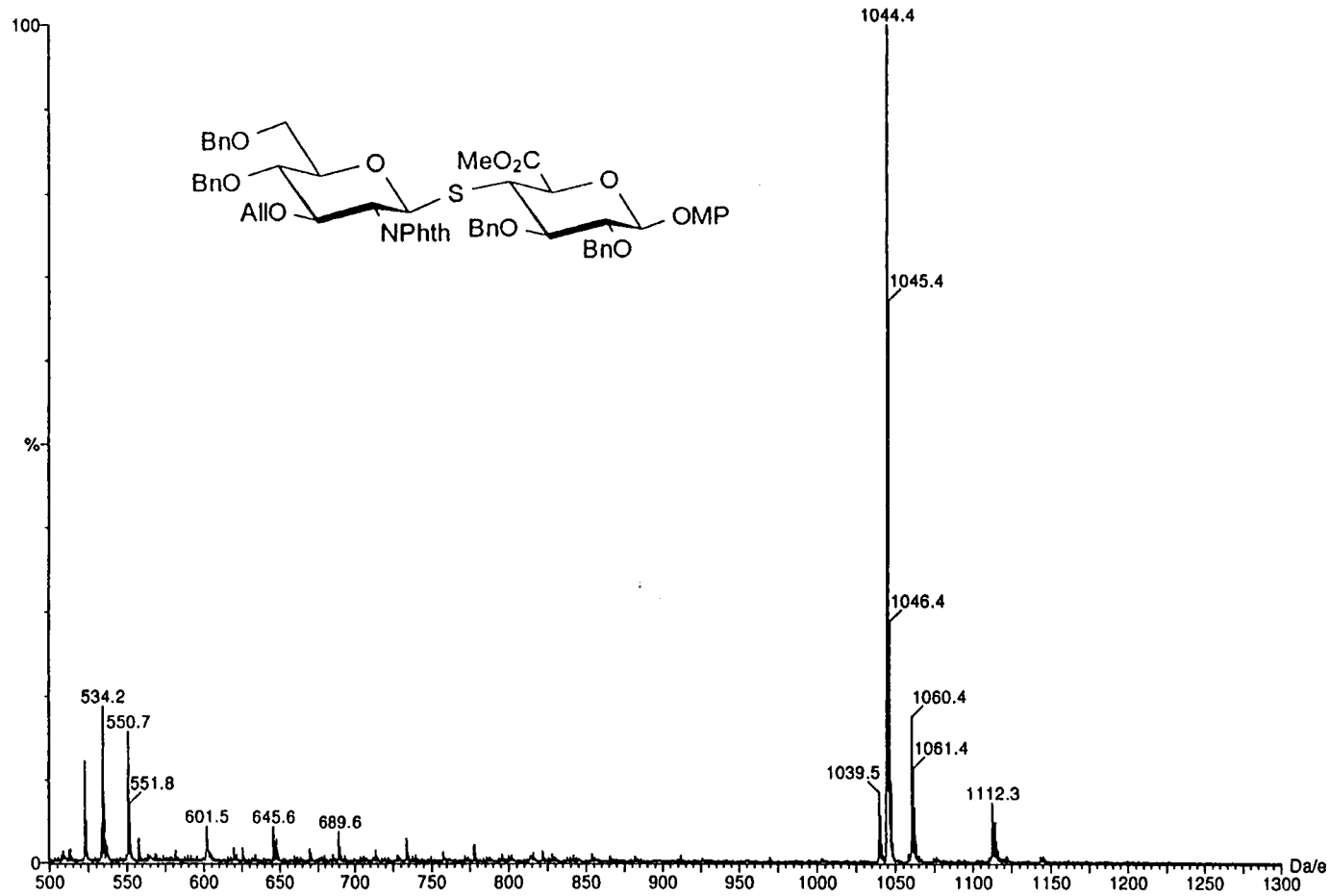
^{1}H NMR spectrum (250 MHz, $CDCl_3$) of *p*-methoxyphenyl 4-*S*-(3-*O*-allyl-4,6-di-*O*-benzyl-2-deoxy-2-phthalimido-β-D-glucopyranosyl)-2,3-di-*O*-benzyl-4-thio-β-D-glucopyranosiduronic acid (**16a**).



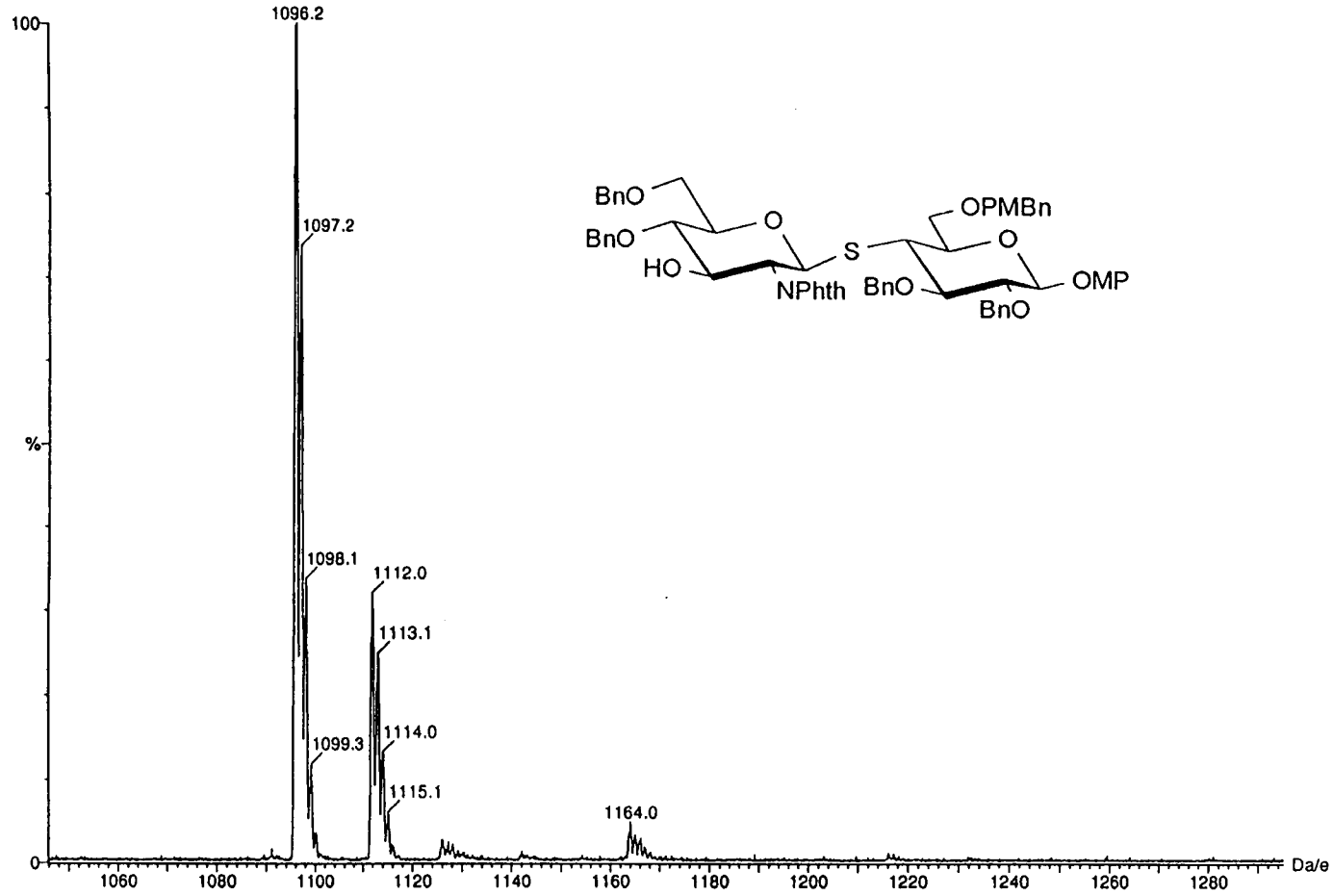
Negative-ion mode ESIMS spectrum of *p*-methoxyphenyl 4-*S*-(3-*O*-allyl-4,6-di-*O*-benzyl-2-deoxy-2-phthalimido-β-D-glucopyranosyl)-2,3-di-*O*-benzyl-4-thio-β-D-glucopyranosiduronic acid (**16a**).



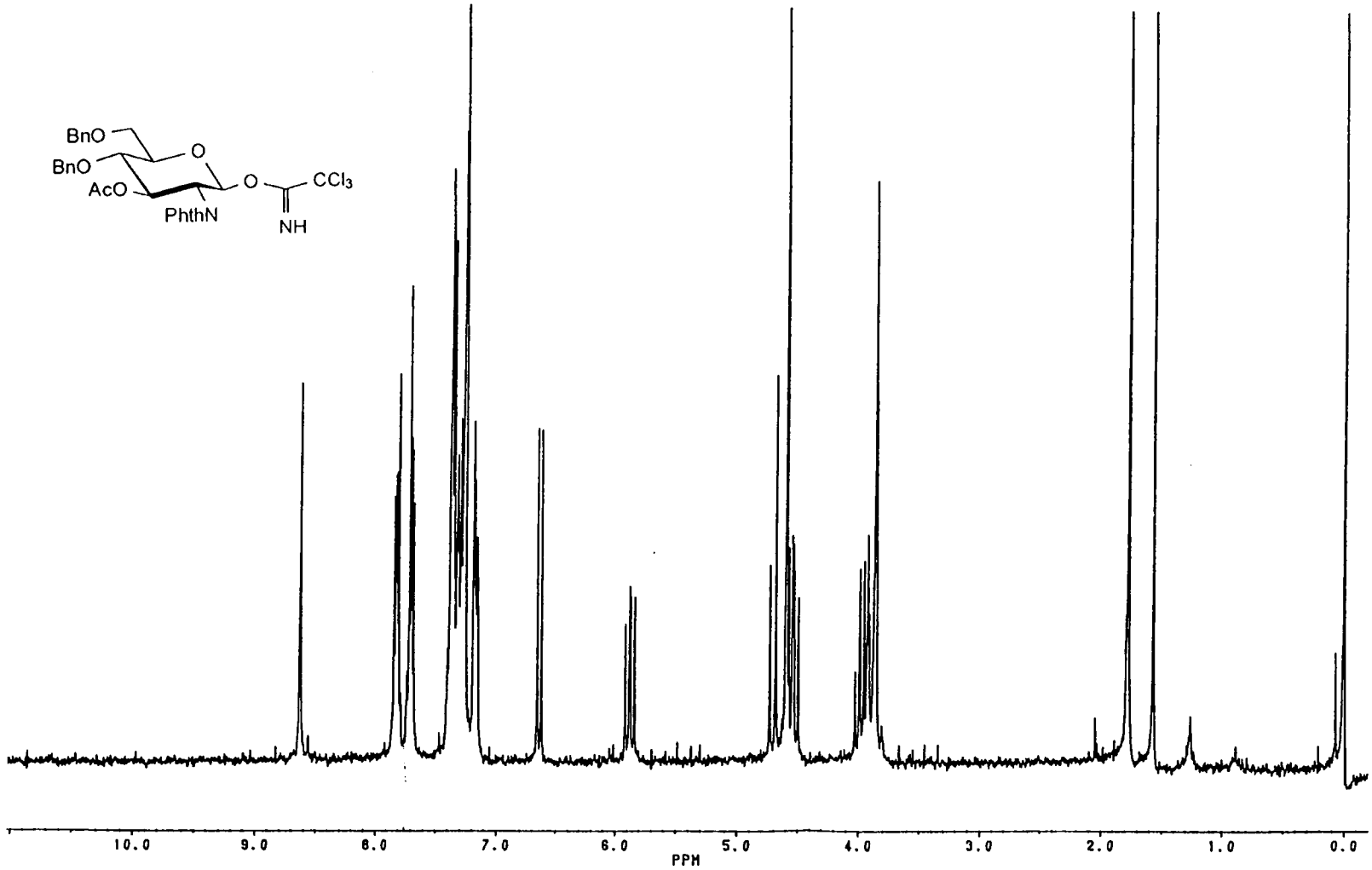
^{1}H NMR spectrum (250 MHz, $CDCl_3$) of methyl [*p*-methoxyphenyl 4-*S*-(3-*O*-allyl-4,6-di-*O*-benzyl-2-deoxy-2-phthalimido-β-D-glucopyranosyl)-2,3-di-*O*-benzyl-4-thio-β-D-glucopyranosid]uronate (**13**).



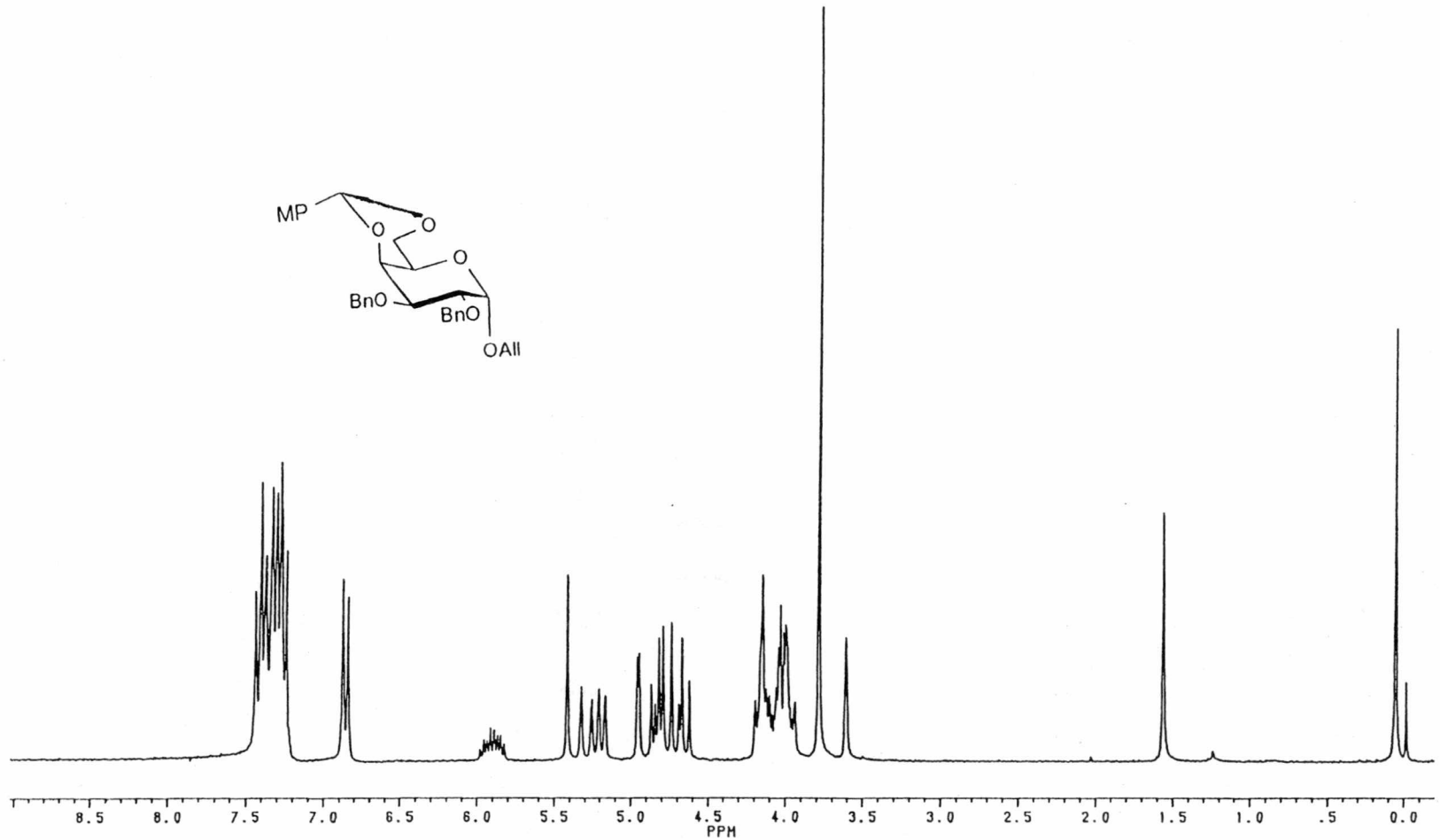
Positive-ion mode ESIMS spectrum of methyl [*p*-methoxyphenyl 4-*S*-(3-*O*-allyl-4,6-di-*O*-benzyl-2-deoxy-2-phthalimido-β-D-glucopyranosyl)-2,3-di-*O*-benzyl-4-thio-β-D-glucopyranosid]uronate (**13**).



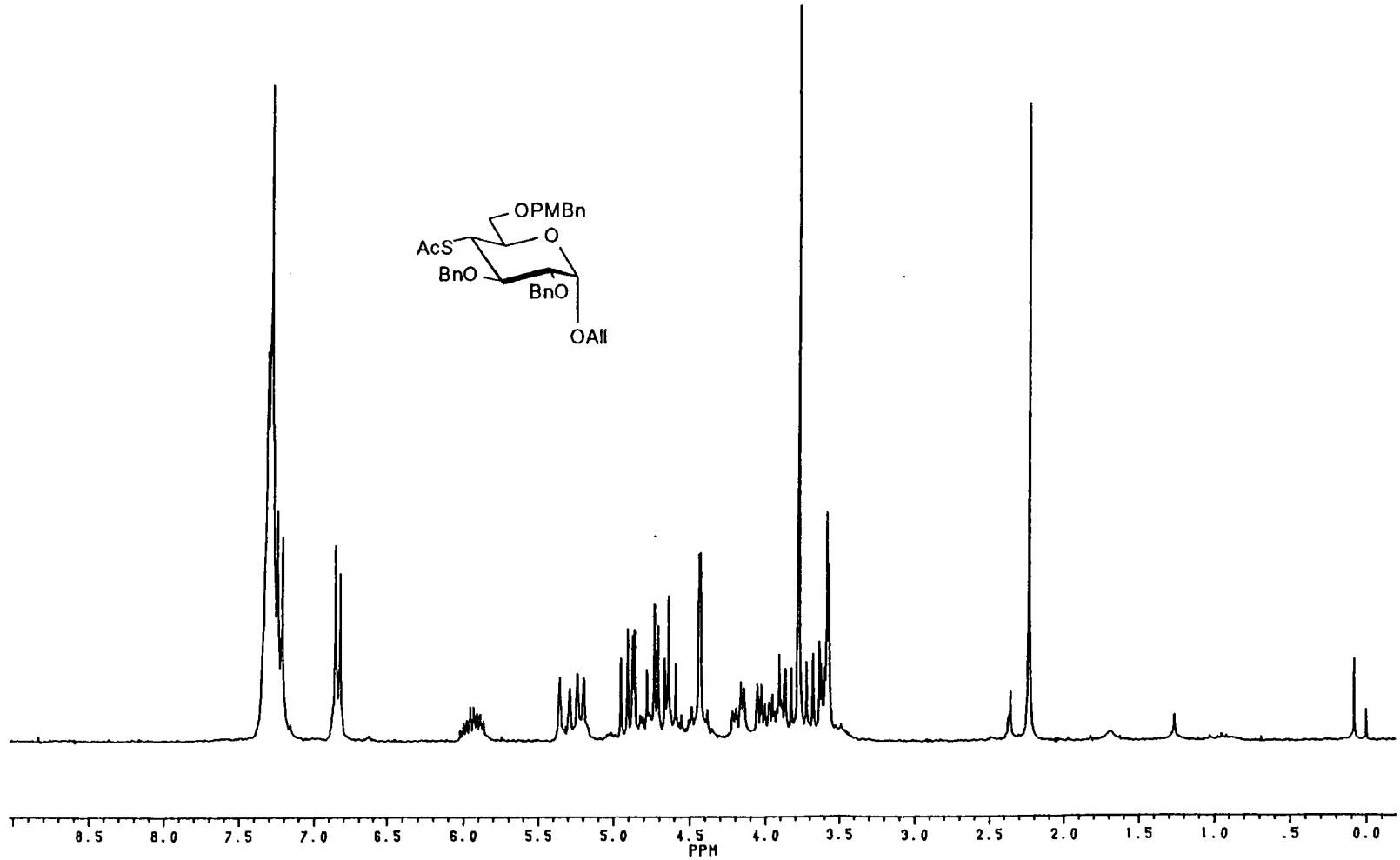
Positive-ion mode ESIMS spectrum of *p*-methoxyphenyl 4-*S*-(4,6-di-*O*-benzyl-2-deoxy-2-phthalimido-β-D-glucopyranosyl)-2,3-di-*O*-benzyl-6-*O*-*p*-methoxybenzyl-4-thio-β-D-glucopyranoside (**55**).



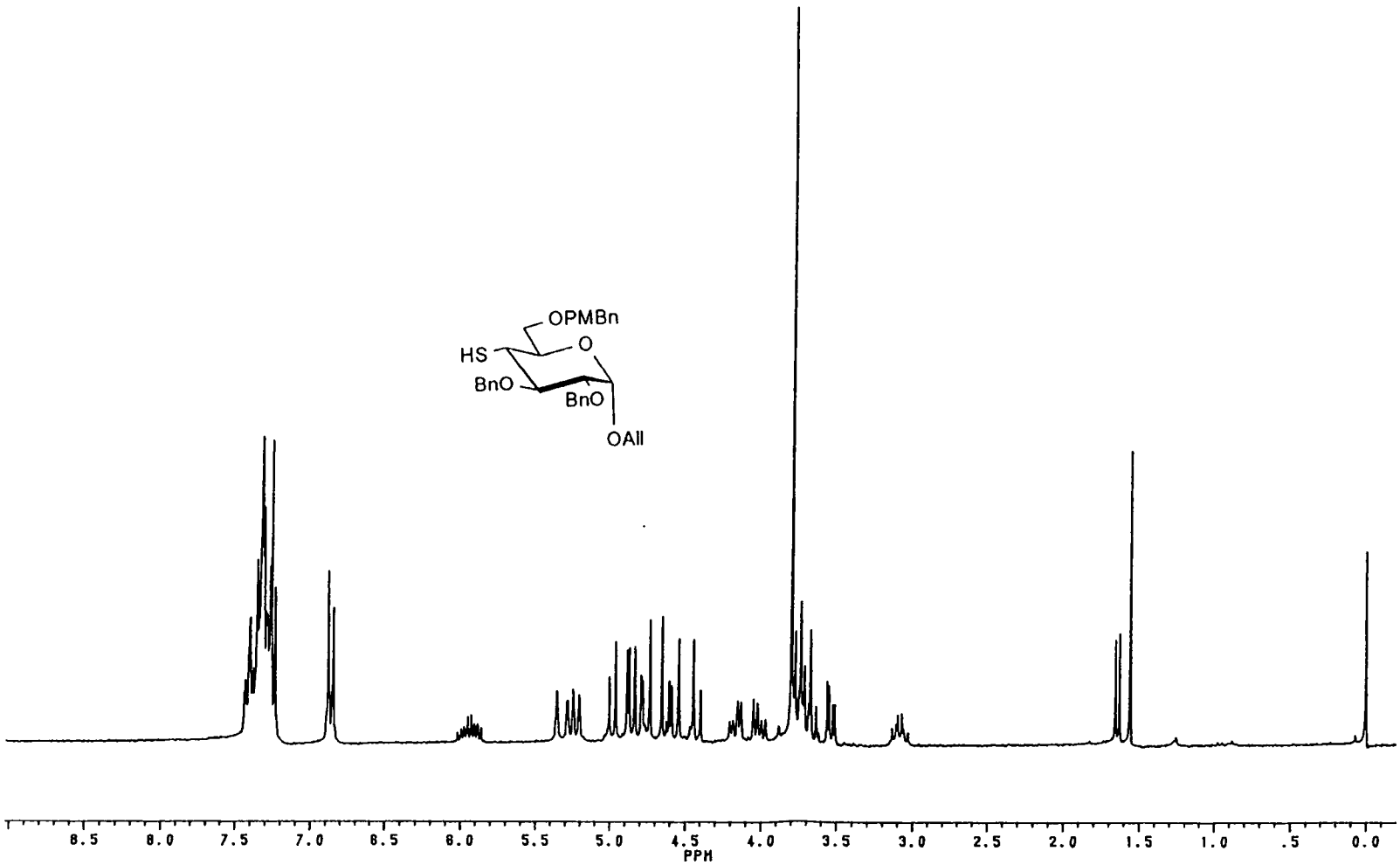
^{1}H NMR spectrum (250 MHz, $CDCl_3$) of 3-*O*-acetyl-4,6-di-*O*-benzyl-2-deoxy-2-phthalimido-β-D-glucopyranosyl trichloroacetimidate (**58**).



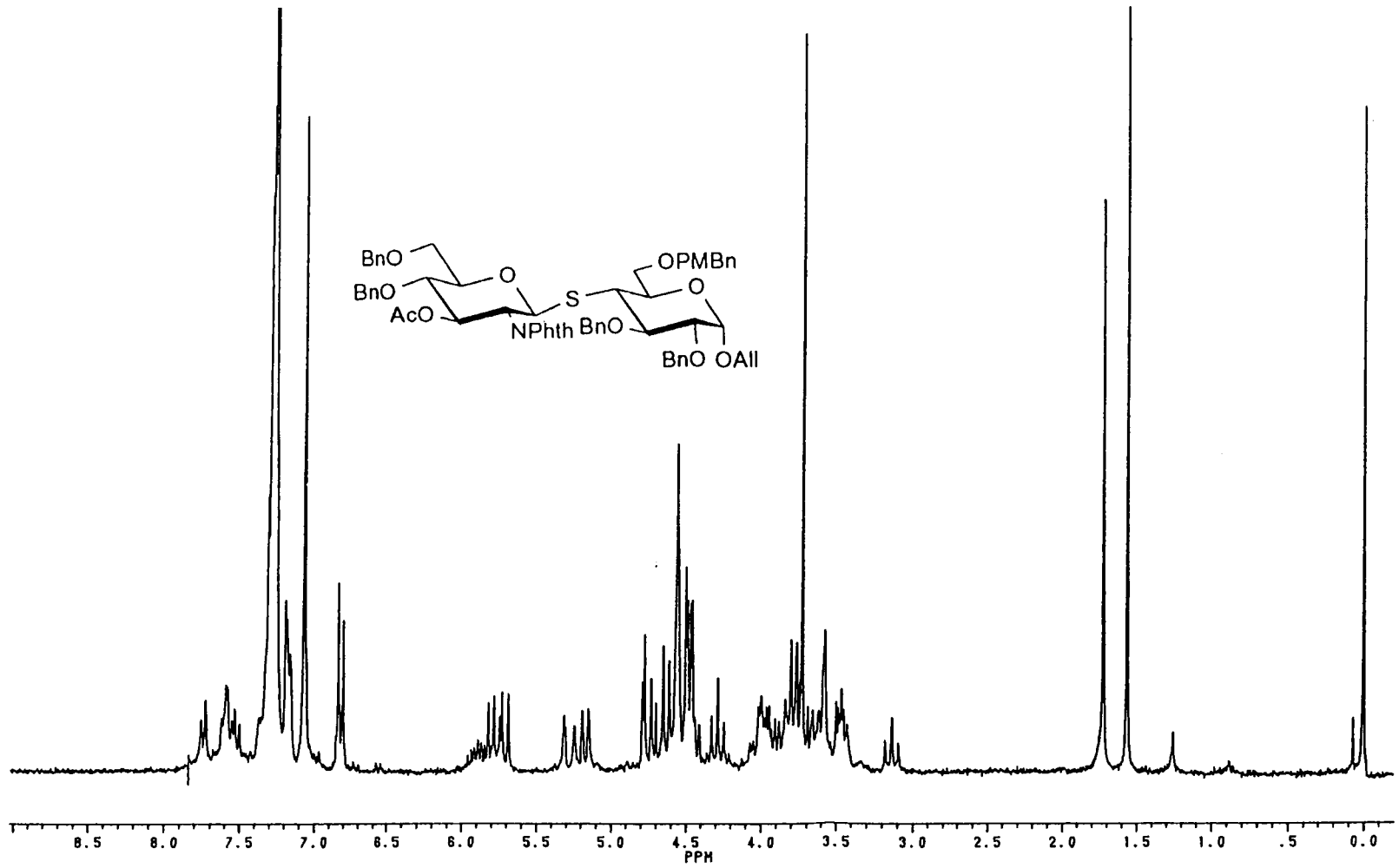
^{1}H NMR spectrum (250 MHz, $CDCl_3$) of allyl 2,3-di-*O*-benzyl-4,6-*O*-(*p*-methoxybenzylidene)-α-D-galactopyranoside (**60a**).



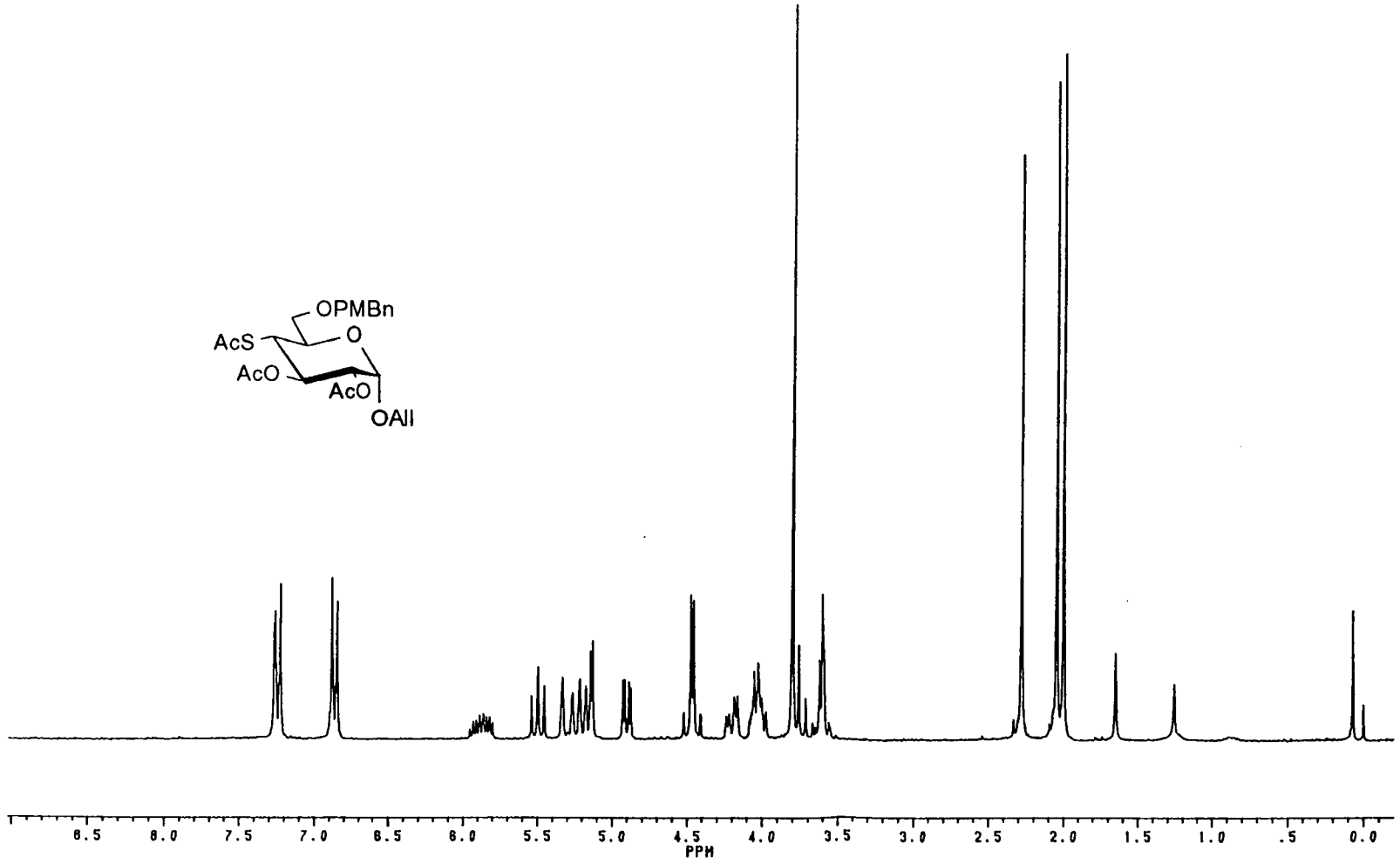
^{1}H NMR spectrum (250 MHz, $CDCl_3$) of allyl 4-*S*-acetyl-*2,3*-di-*O*-benzyl-6-*O*-*p*-methoxybenzyl-4-thio-α-D-galactopyranoside (**62**).



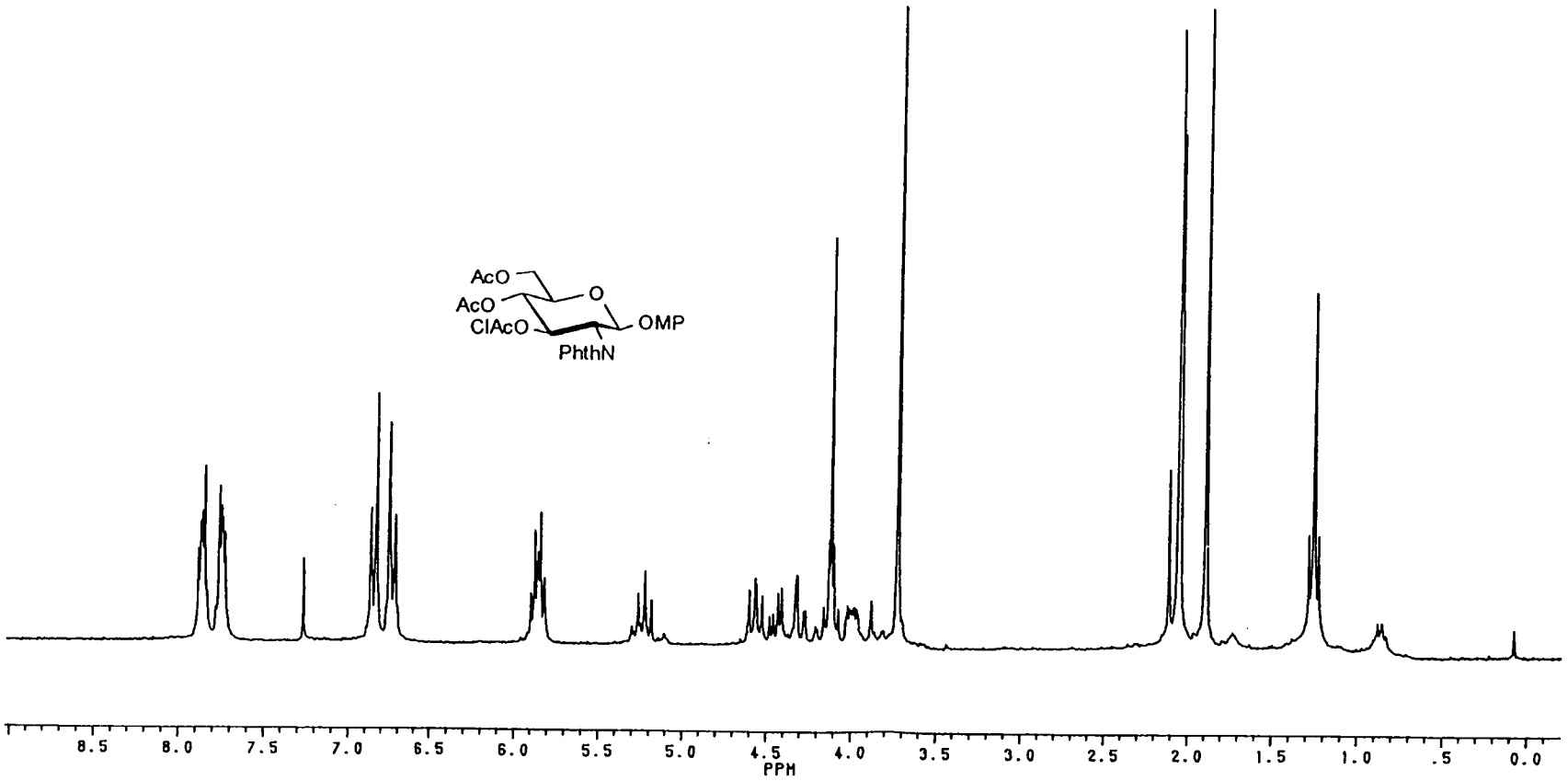
^{1}H NMR spectrum (250 MHz, $CDCl_3$) of allyl 2,3-di-*O*-benzyl-6-*O*-*p*-methoxybenzyl-4-thio-α-D-galactopyranoside (**63**).



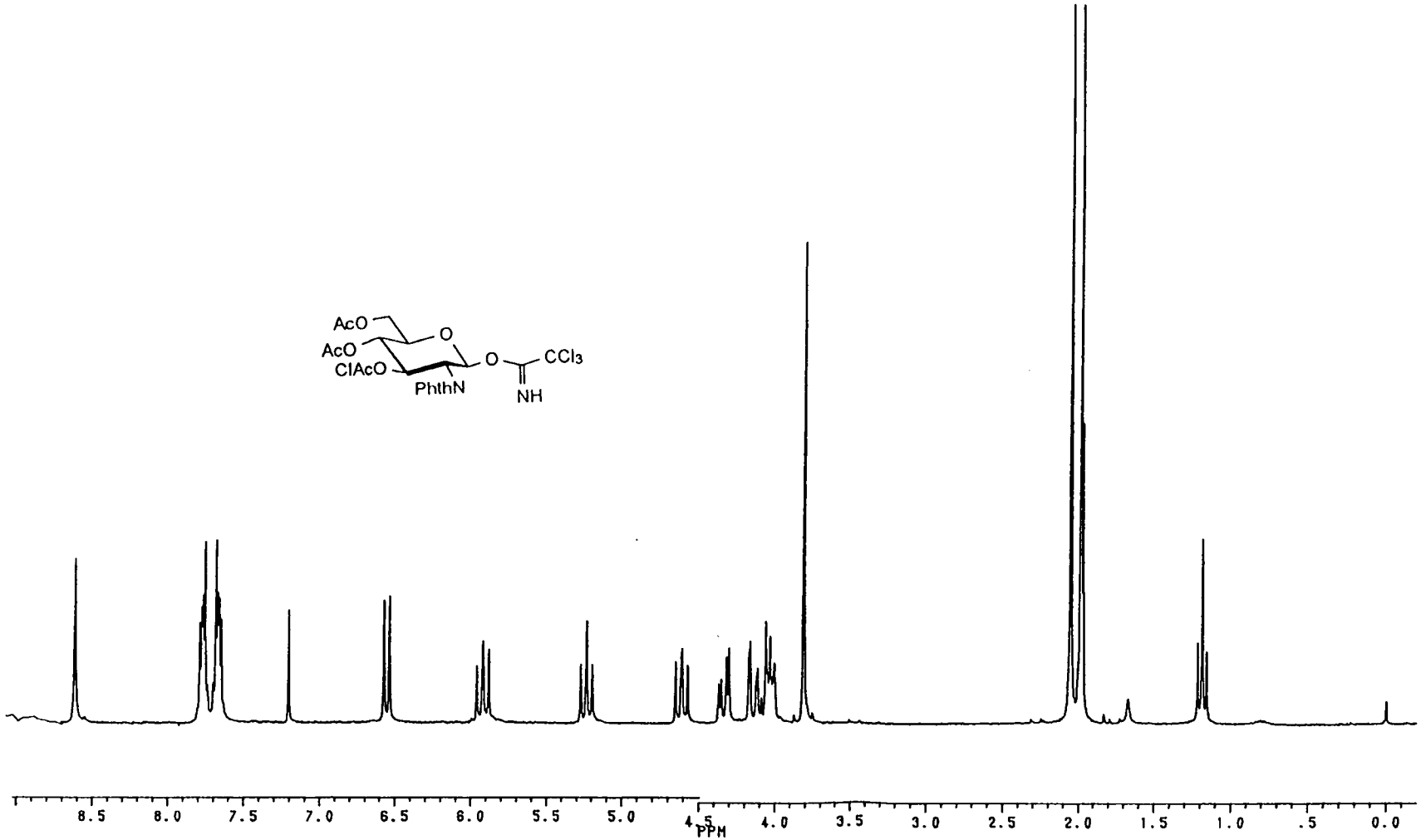
^{1}H NMR spectrum (250 MHz, $CDCl_3$) of allyl 4-*S*-(3-*O*-acetyl-4,6-di-*O*-benzyl-2-deoxy-2-phthalimido-β-D-glucopyranosyl)-2,3-di-*O*-benzyl-6-*O*-*p*-methoxybenzyl-4-thio-α-D-glucopyranoside (**57**).



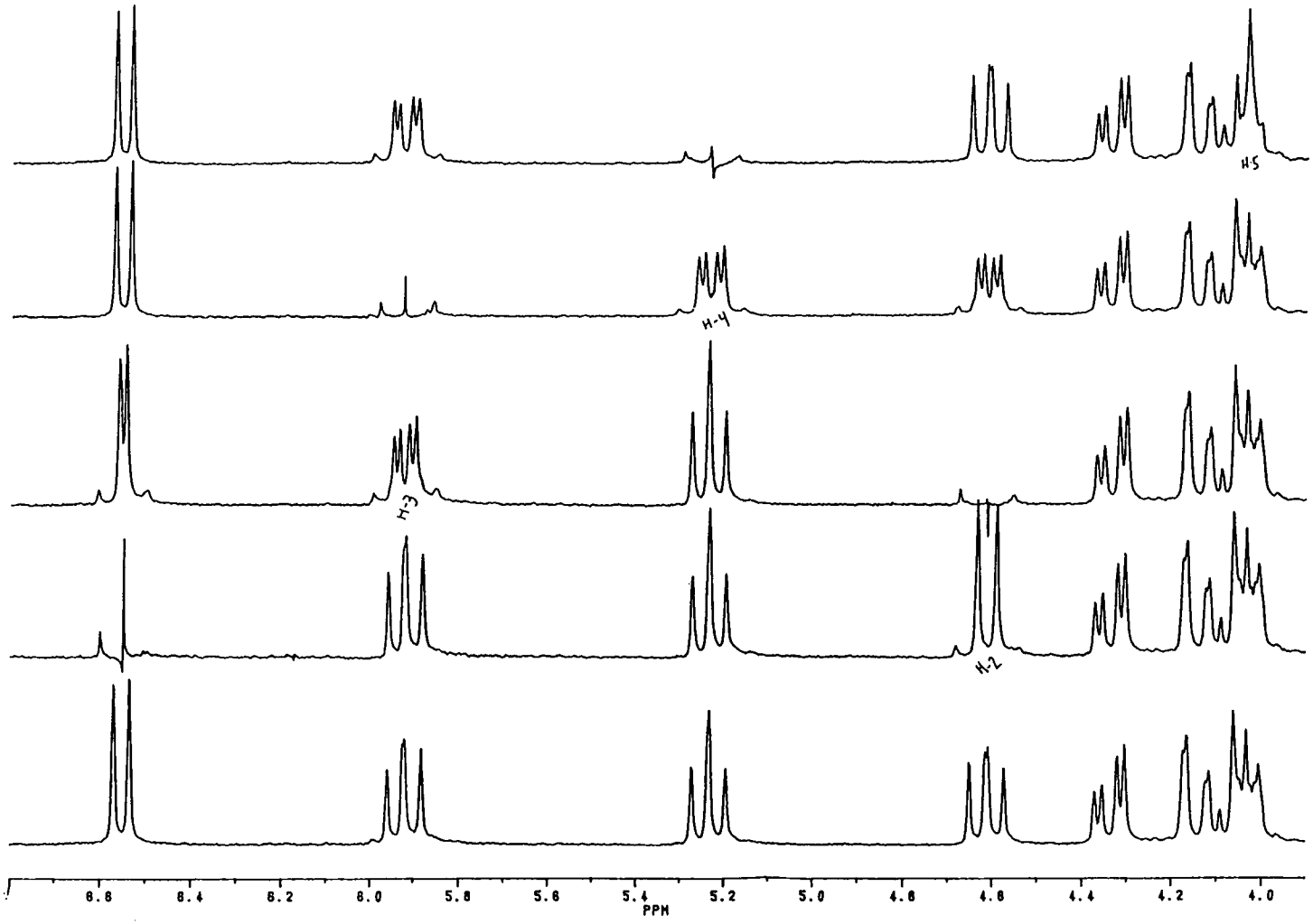
^{1}H NMR spectrum (250 MHz, $CDCl_3$) of allyl 2,3-di-*O*-acetyl-4-*S*-acetyl-6-*O*-*p*-methoxybenzyl-4-thio-α-D-galactopyranoside (**69**).



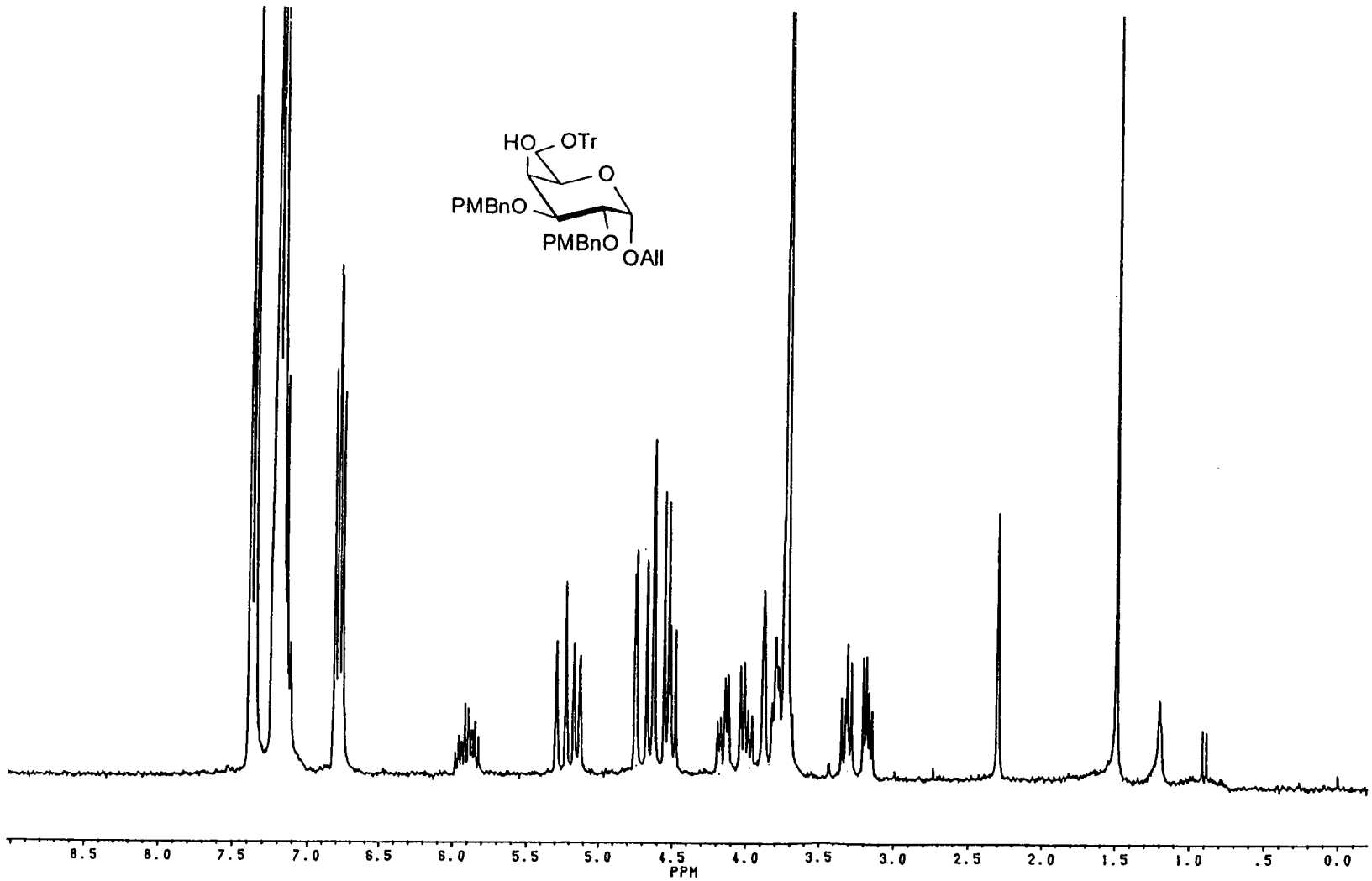
^{1}H NMR spectrum (250 MHz, $CDCl_3$) of *p*-methoxyphenyl 4,6-di-*O*-acetyl-3-*O*-chloroacetyl-2-deoxy-2-phthalimido-β-D-glucopyranoside (**66**).



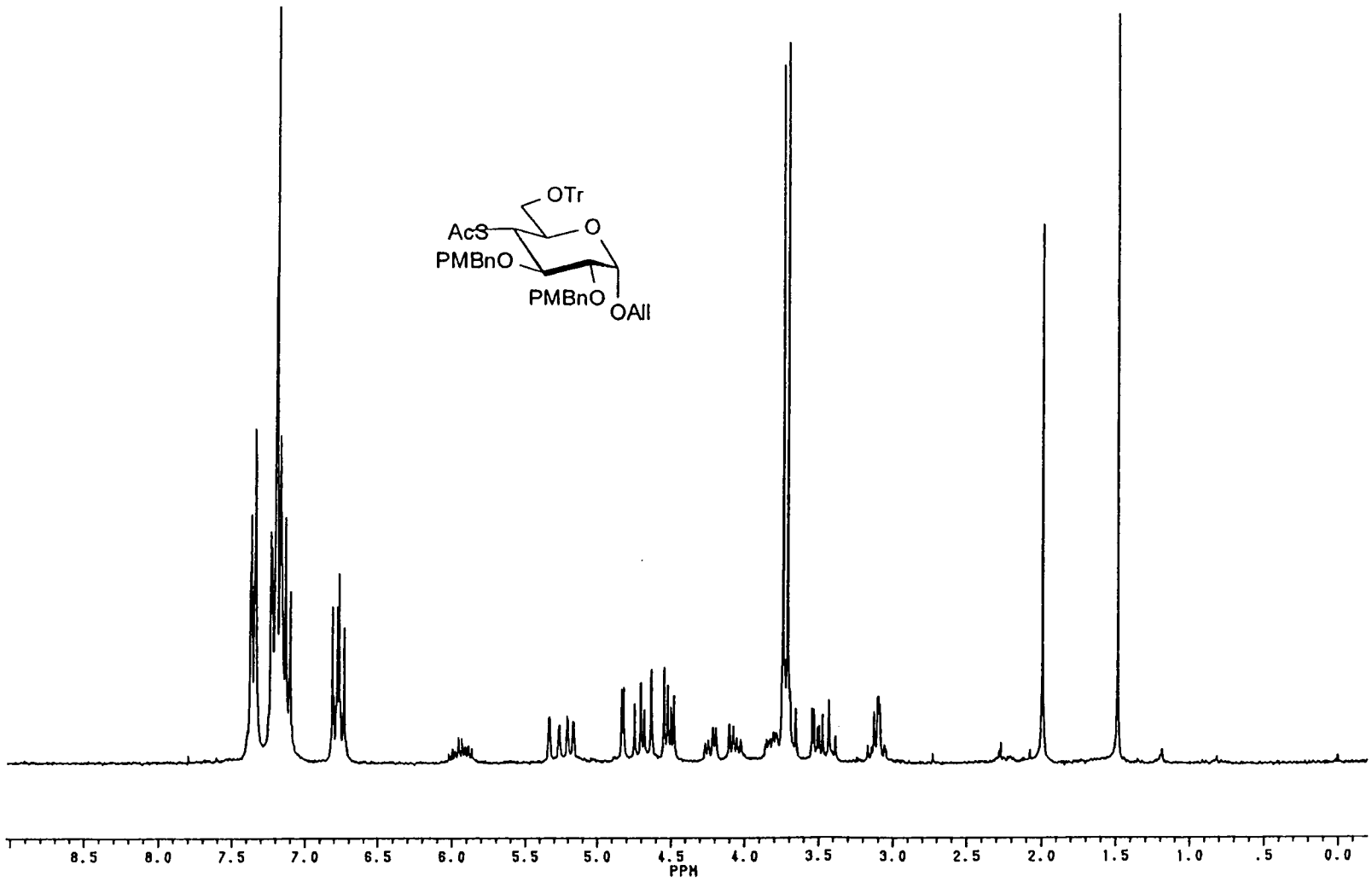
^{1}H NMR spectrum (250 MHz, $CDCl_3$) of 4,6-di-*O*-acetyl-3-*O*-chloroacetyl-2-deoxy-2-phthalimido-β-D-glucopyranosyl trichloroacetimidate (**67**).



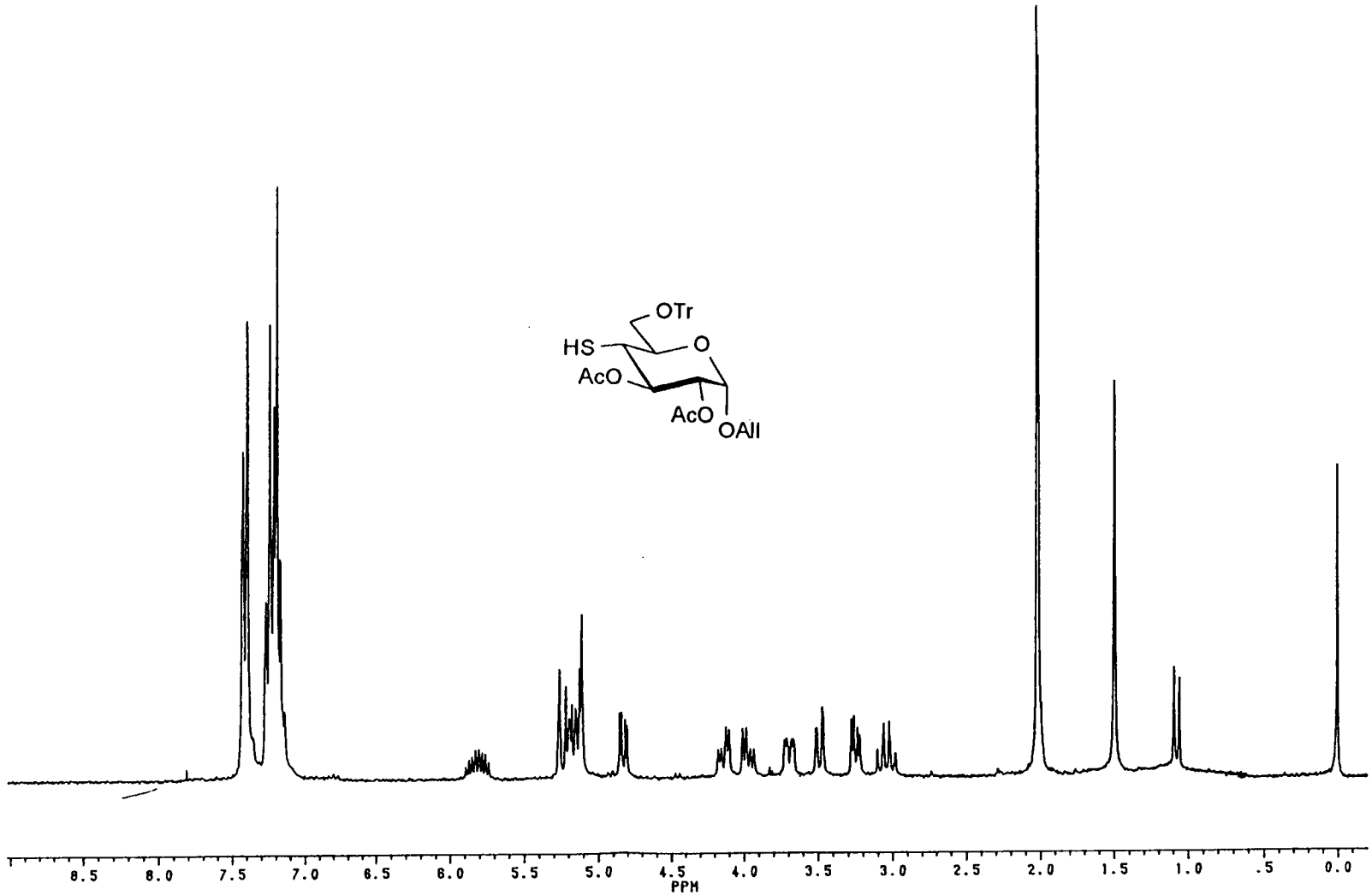
^{1}H NMR decoupling spectra (250 MHz, $CDCl_3$) of 4,6-di-*O*-acetyl-3-*O*-chloroacetyl-2-deoxy-2-phthalimido-β-D-glucopyranosyl trichloroacetimidate (**67**).



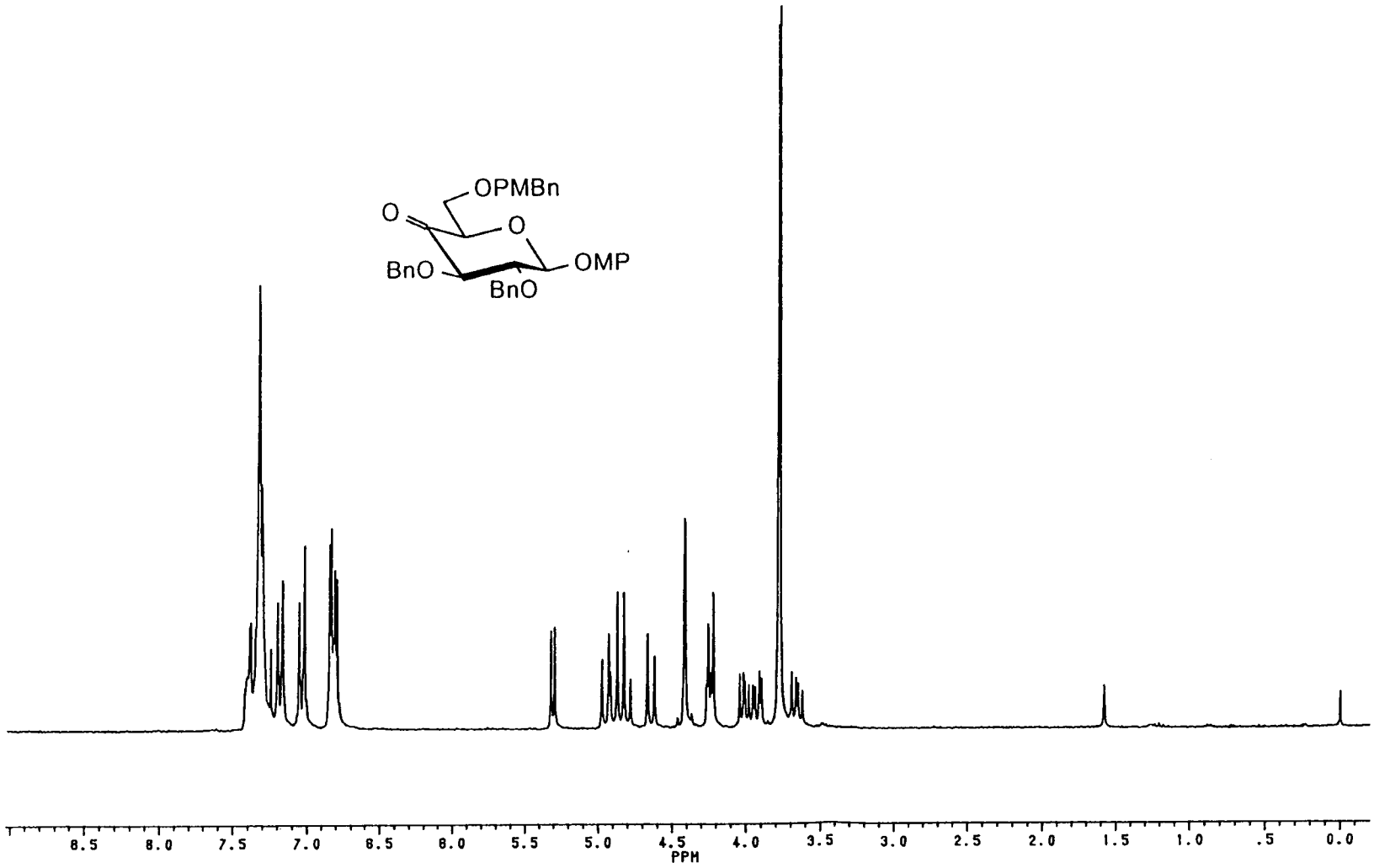
^{1}H NMR spectrum (250 MHz, $CDCl_3$) of allyl 2,3-di-*O*-*p*-methoxybenzyl-6-*O*-trityl-α-D-glucopyranoside (**71**).



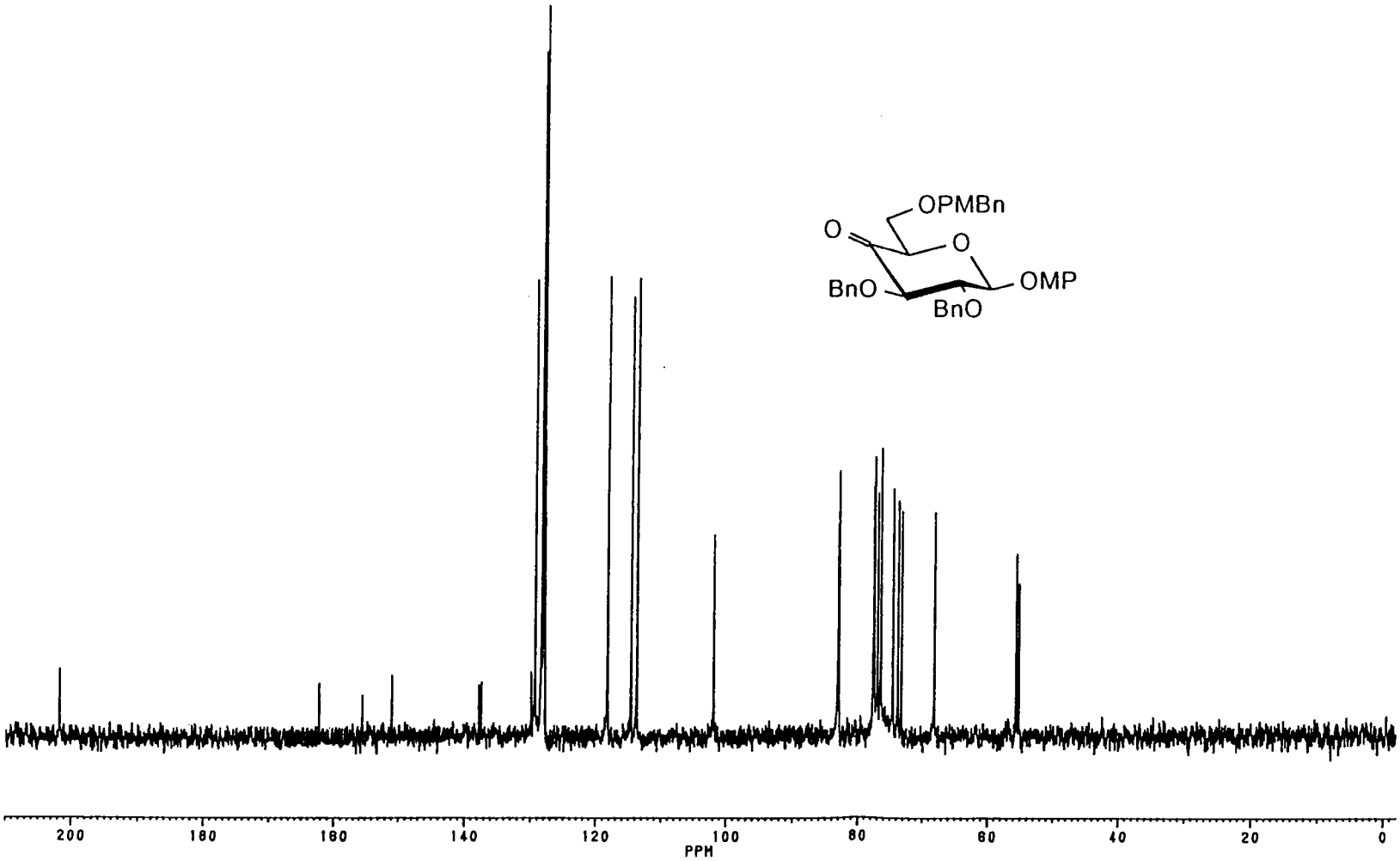
^{1}H NMR spectrum (250 MHz, $CDCl_3$) of allyl 4-*S*-acetyl-2,3-di-*O*-*p*-methoxybenzyl-4-thio-6-*O*-trityl-α-D-glucopyranoside (**72**).



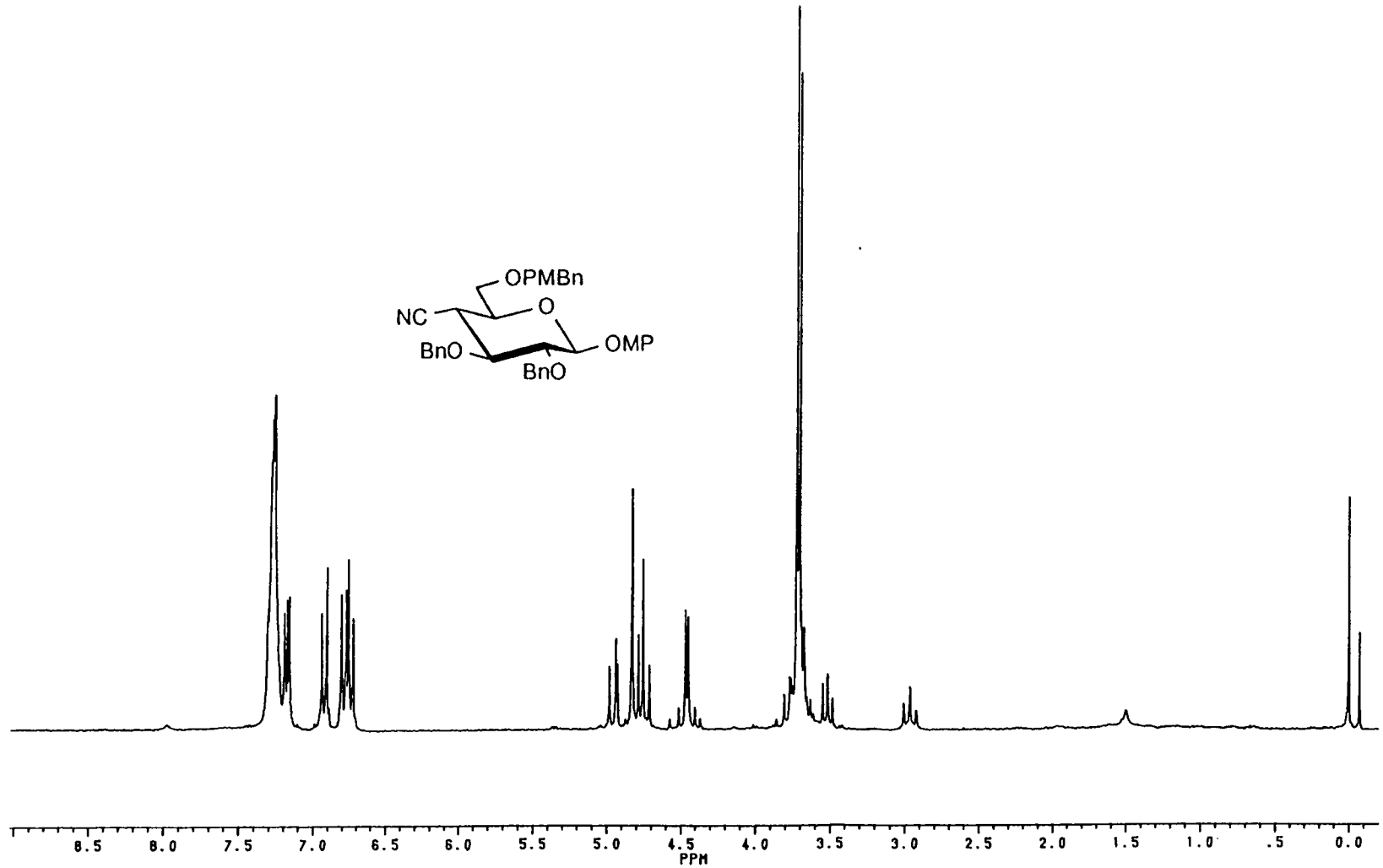
^{1}H NMR spectrum (250 MHz, $CDCl_3$) of allyl 2,3-di-*O*-acetyl-4-deoxy-4-thio-6-*O*-trityl-α-D-glucopyranoside (**69a**).



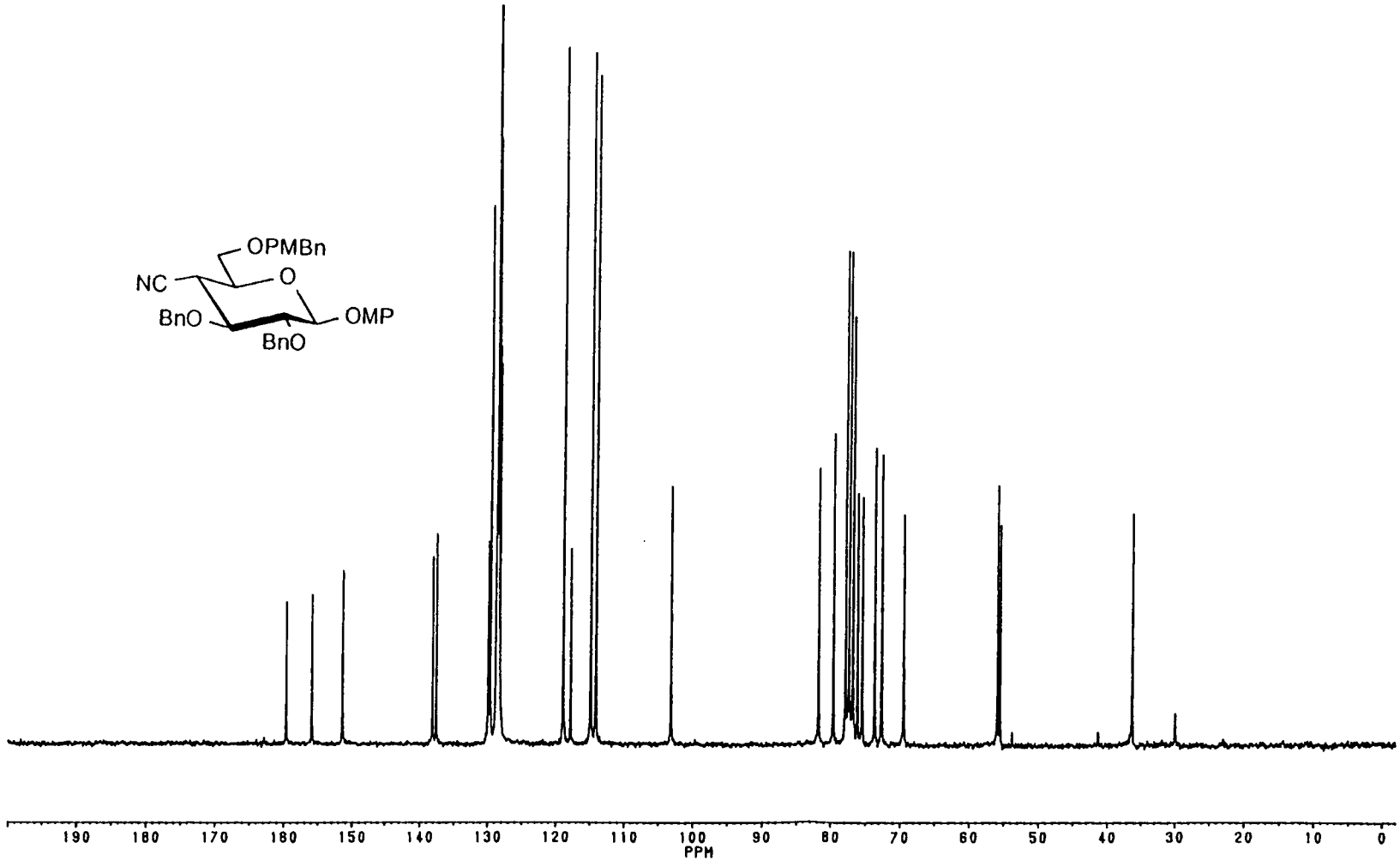
^{1}H NMR spectrum (250 MHz, $CDCl_3$) of *p*-methoxyphenyl *2,3*-di-*O*-benzyl-6-*O*-*p*-methoxybenzyl-β-D-*xylo*-hexopyranosid-4-ulose (77).



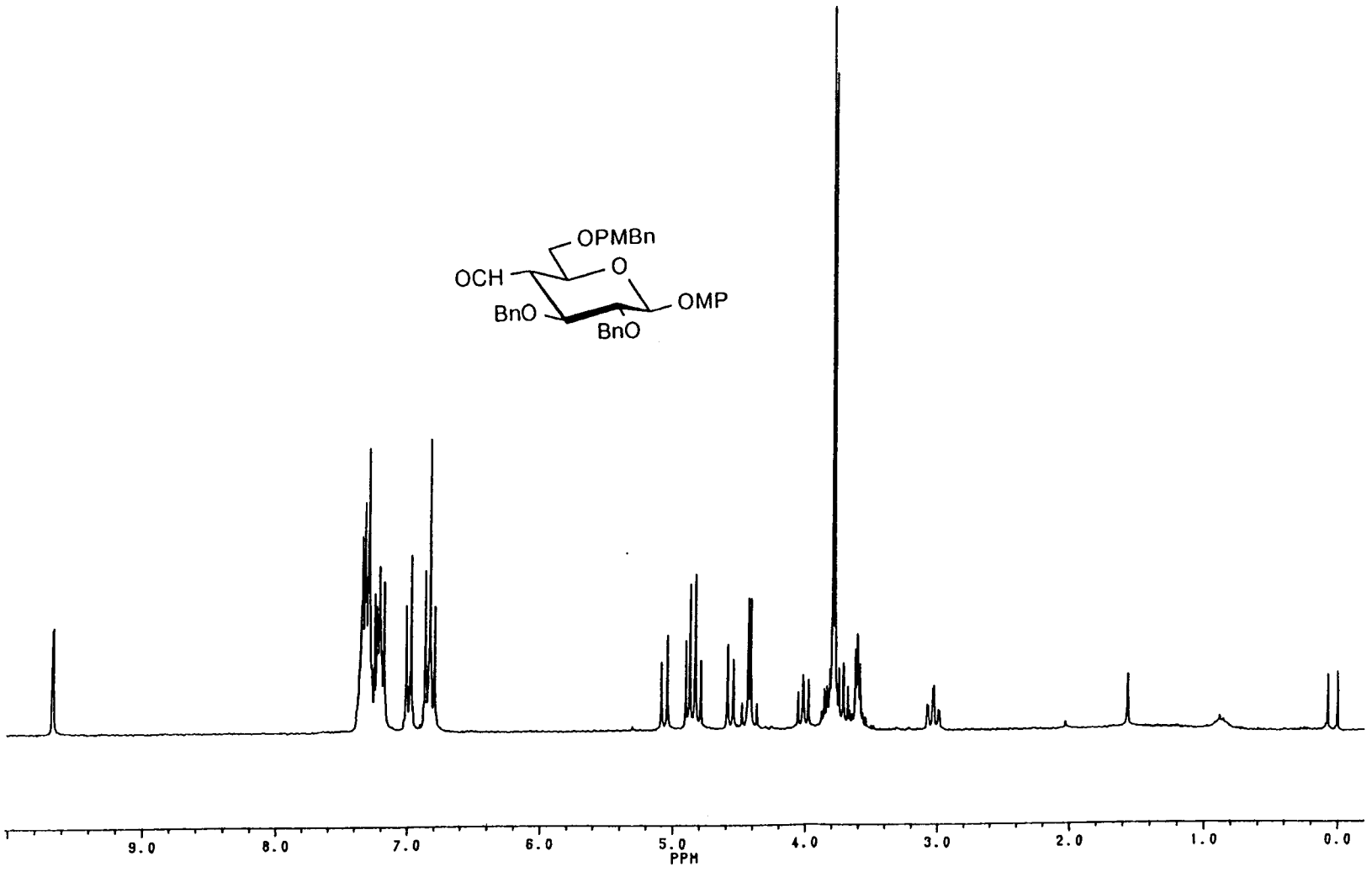
^{13}C NMR spectrum (62.5 MHz, $CDCl_3$) of *p*-methoxyphenyl *2,3*-di-*O*-benzyl-6-*O*-*p*-methoxybenzyl-β-D-*xylo*-hexopyranosid-4-ulose (77).



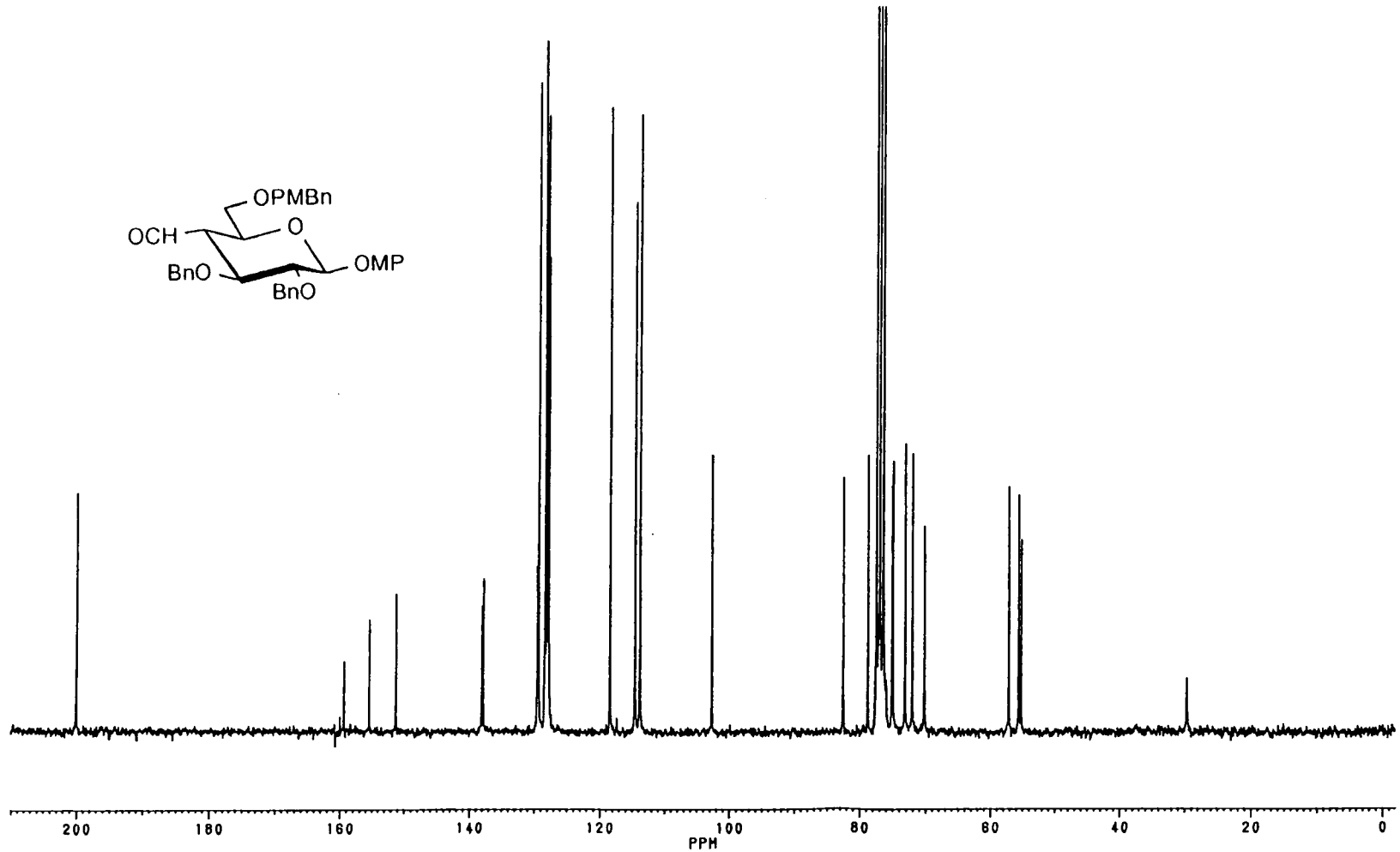
^{1}H NMR spectrum (250 MHz, $CDCl_3$) of *p*-methoxyphenyl 2,3-di-*O*-benzyl-4-*C*-cyano-4-deoxy-6-*O*-*p*-methoxybenzyl-β-D-glucopyranoside (**78**).



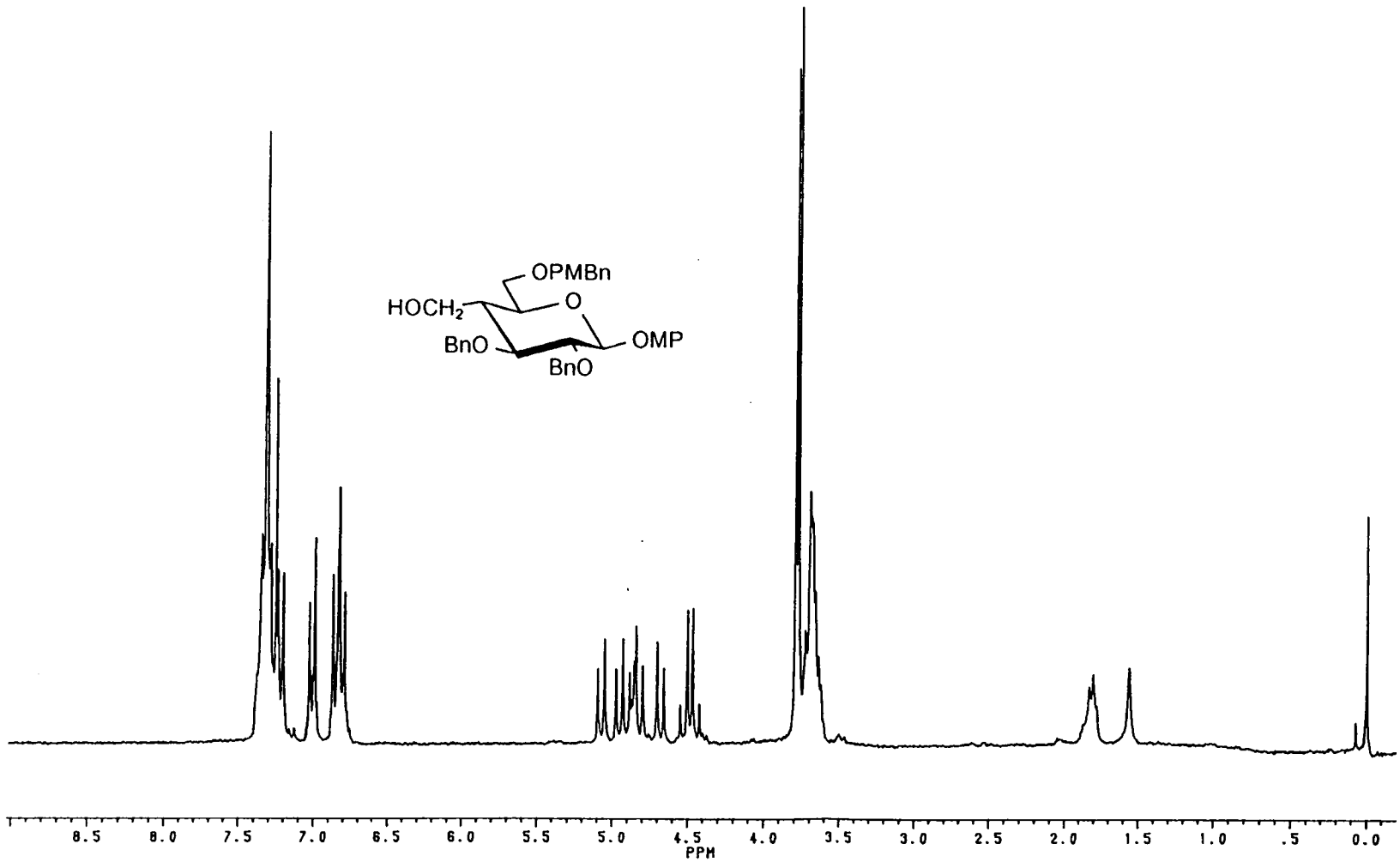
^{13}C NMR spectrum (62.5 MHz, $CDCl_3$) of *p*-methoxyphenyl 2,3-di-*O*-benzyl-4-*C*-cyano-4-deoxy-6-*O*-*p*-methoxybenzyl-β-D-glucopyranoside (**78**).



^{1}H NMR spectrum (250 MHz, $CDCl_3$) of *p*-methoxyphenyl 4-*C*-aldehydo-2,3-di-*O*-benzyl-4-deoxy-6-*O*-*p*-methoxybenzyl-β-D-glucopyranoside (**79**).



^{13}C NMR spectrum (62.5 MHz, $CDCl_3$) of *p*-methoxyphenyl 4-*C*-aldehydo-2,3-di-*O*-benzyl-4-deoxy-6-*O*-*p*-methoxybenzyl-β-D-glucopyranoside (**79**).



^{1}H NMR spectrum (250 MHz, $CDCl_3$) of *p*-methoxyphenyl 2,3-di-*O*-benzyl-4-deoxy-4-*C*-hydroxymethyl-6-*O*-*p*-methoxybenzyl-β-D-glucopyranoside (**80**).

VITA

Kenneth Price was born in Oak Ridge, Tennessee in 1965. After graduating from Farragut High School in 1983, he attended Furman University, where he graduated magna cum laude with a Bachelor's Degree in music, majoring in piano performance. From 1987-1990 he studied at the Yale School of Music with pianists Boris Berman and Claude Frank, and completed the Master's degree in piano performance. In 1992 he began graduate study in chemistry at the University of Tennessee, and joined the research group of Prof. David C. Baker, where he conducted research in organic synthesis and carbohydrate analysis. After completing his PhD at UTK in 1997, he accepted a position as Research Scientist in chemistry research and development at the Procter & Gamble Company in Cincinnati, Ohio.